

SIMULATION OF GROUND-WATER FLOW  
AND STREAM-AQUIFER RELATIONS IN THE  
VICINITY OF THE SAVANNAH RIVER SITE,  
GEORGIA AND SOUTH CAROLINA,  
PREDEVELOPMENT THROUGH 1992

By John S. Clarke and Christopher T. West

---

U.S. GEOLOGICAL SURVEY

Water-Resources Investigations Report 98-4062

Prepared in cooperation with the

U.S. DEPARTMENT OF ENERGY and the

GEORGIA DEPARTMENT OF NATURAL RESOURCES  
ENVIRONMENTAL PROTECTION DIVISION  
GEORGIA GEOLOGIC SURVEY



**U.S. DEPARTMENT OF THE INTERIOR**

**BRUCE BABBITT, Secretary**

**U.S. GEOLOGICAL SURVEY**

**Thomas J. Casadevall, Acting Director**

---

For additional information write to:

District Chief  
U.S. Geological Survey  
3039 Amwiler Road  
Peachtree Business Center, Suite 130  
Atlanta, GA 30360-2824

Copies of this report can be purchased from:

U.S. Geological Survey  
Branch of Information Services  
Denver Federal Center  
Box 25286  
Denver, CO 80225-0286

# CONTENTS

Abstract	1
Introduction	2
Purpose and scope	2
Description of study area	3
Previous investigations	3
Methods of study	7
Acknowledgments	7
Hydrogeology	8
Geologic setting	8
Hydrogeologic units	8
Floridan aquifer system	10
Dublin aquifer system	11
Midville aquifer system	11
Conceptualization of stream-aquifer flow system	12
Hydrologic budget	14
Predevelopment flow system	16
Modern-day (1987–92) flow system	16
Simulation of ground-water flow	18
Spatial and vertical discretization	20
Hydraulic characteristics	20
Boundary conditions	23
Pumpage	26
Model calibration	29
Steady-state simulation of predevelopment flow system	31
Simulated heads	31
Simulated water budget	33
Simulated ground-water recharge	39
Simulated ground-water discharge to streams	41
Simulated ground-water flow	43
Simulation of flow system, 1953–92	45
Testing of model for transient response to pumpage	45
Steady-state analysis of modern-day (1987–92) flow conditions	45
Simulated drawdown	55
Calibrated hydraulic properties	61
Trans-river flow beneath the Savannah River	74
Particle tracking analysis of advective ground-water flow	75
Westward trans-river flow	84
Eastward trans-river flow	84
Recharge areas to trans-river flow zones	85
Simulated time-of-travel	86
Trans-river flow, recharge areas, and time-of-travel at the Savannah River Site	88

Simulation of ground-water flow—Continued

Sensitivity analysis **88**

Limitations of digital simulation **90**

Limitations of particle tracking **100**

Summary and conclusions **100**

Selected References **104**

Appendix A. Mean-annual ground-water discharge to streams estimated using hydrograph separation and simulated ground-water discharge for predevelopment (prior to 1953) and modern-day (1987-92) conditions **114**

Appendix B. Estimated ground-water discharge to streams during 1954 and 1986 droughts, and simulated ground-water discharge for predevelopment (prior to 1953) and modern-day (1987-92) conditions **115**

Appendix C. Measured heads, simulated predevelopment (prior to 1953) and modern-day (1987-92) heads, and error criteria in wells used for model calibration **119**

## ILLUSTRATIONS

### PLATES

*[in pocket in back of report]*

- Plates 1-3. Maps showing:
1. Model grid and boundary conditions for the Upper Three Runs, Gordon, and Millers Pond aquifers
  2. Model grid and boundary conditions for the Dublin and Midville aquifers
  3. Estimated average potentiometric surface for the Upper Three Runs, Gordon, Dublin, and Midville aquifers

### FIGURES

- Figures 1a-2. Maps showing:
- 1a. Location of study area, Savannah River Site, well-cluster sites, and physiographic districts in Georgia and South Carolina **4**
  - 1b. Areal and local ground-water contamination at the Savannah River Site, South Carolina **5**
  2. Mean-annual runoff in Georgia part of study area, 1941-70; and locations of selected streamflow-gaging stations or periodic-measurement sites **6**
- Figure 3. Model layers, respective hydrogeologic units, and names applied to the P-21/P5R testhole at the Savannah River Site, South Carolina **9**
- Figures 4-6. Schematic diagrams of:
4. Conceptualized hydrogeologic framework and related ground-water flow in the vicinity of the Savannah River Site, Georgia, and South Carolina **13**
  5. Artesian water gap and related pattern of ground-water flow **14**
  6. Hydrogeologic framework, model layers, and boundary conditions for the Savannah River Site area ground-water model **22**
- Figure 7. Map showing locations where ground-water pumpage exceeded 1 million gallons per day during 1987-92, model grid and model boundary **27**
8. Boxplot showing difference between observed and simulated heads (residuals) for the predevelopment simulation **32**
- Figures 9-12. Maps showing simulated predevelopment potentiometric surface and observed heads for the:
9. Gordon aquifer (layer A2) **34**
  10. Millers Pond (layer A3) and upper Dublin (layer A4) aquifers **35**
  11. Lower Dublin (layer A5) and upper Midville (layer A6) aquifers **36**
  12. Lower Midville aquifer (layer A7) **37**
- Figure 13. Chart showing simulated predevelopment water budget by model layer **38**
14. Map showing simulated predevelopment recharge derived from leakage from the Upper Three Runs aquifer (layer A1) and from simulated recharge cells **40**
  15. Graph showing difference (residuals) between estimated ground-water discharge to streams for predevelopment simulation (excludes Savannah River) **42**
  16. Graph showing sensitivity of transient model to changes in storativity **46**
  17. Boxplot showing difference between observed and simulated heads (residuals) for the modern-day (1987-92) simulation **48**

## FIGURE—Continued

- Figures 18-20. Maps showing simulated modern-day (1987-92) potentiometric surface and observed heads for the:
- 18. Gordon (layer A2) and Millers Pond (layer A3) aquifers **49**
  - 19. Upper Dublin (layer A4) and lower Dublin (layer A5) aquifers **50**
  - 20. Upper Midville (layer A6) and lower Midville (layer A7) aquifers **51**
- Figure 21. Chart showing simulated modern-day (1987-92) water budget by model layer **53**
22. Graph showing difference (residuals) between estimated and simulated ground-water discharge to streams for modern-day (1987-92) simulation **54**
23. Simulated predevelopment and modern-day water budgets **55**
- Figures 24-26. Maps showing simulated drawdown, 1953-92, and locations of simulated pumpage and observation wells completed in the:
- 24. Gordon (layer A2) and Millers Pond (layer A3) aquifers **57**
  - 25. Upper Dublin (layer A4) and lower Dublin (layer A5) aquifers **58**
  - 26. Upper Midville (layer A6) and lower Midville (layer A7) aquifers **59**
- Figures 27-32. Graphs showing observed and simulated water levels in selected wells completed in the:
- 27. Gordon aquifer (layer A2) **60**
  - 28. Millers Pond aquifer (layer A3) **60**
  - 29. Upper Dublin aquifer (layer A4) **62**
  - 30. Lower Dublin aquifer (layer A5) **63**
  - 31. Upper Midville aquifer (layer A6) **64**
  - 32. Lower Midville aquifer (layer A7) **65**
- Figures 33-35. Maps showing calibrated transmissivity array and estimated values for the:
- 33. Gordon (layer A2) and Millers Pond (layer A3) aquifers **67**
  - 34. Upper Dublin (layer A4) and lower Dublin (layer A5) aquifers **68**
  - 35. Upper Midville (layer A6) and lower Midville (layer A7) aquifers **69**
- Figures 36-38. Maps showing calibrated leakance array and estimated values for the:
- 36. Gordon (layer C1) and Millers Pond (layer C2) confining units **71**
  - 37. Upper Dublin (layer C3) and (B) lower Dublin (layer C4) confining units **72**
  - 38. Upper Midville (layer C5) and lower Midville (layer C6) confining units **73**
- Figure 39. Schematic diagram showing possible ground-water and trans-river flow in the vicinity of the Savannah River **75**
40. Summary of simulated trans-river flow area by model layer for predevelopment and modern-day (1987-92) simulations **77**
- Figures 41-46. Maps showing simulated trans-river flow zones and associated recharge areas for the:
- 41. Gordon aquifer for predevelopment and modern-day (1987-92) conditions **78**
  - 42. Millers Pond aquifer for predevelopment and modern-day (1987-92) conditions **79**
  - 43. Upper Dublin aquifer for predevelopment and modern-day (1987-92) conditions **80**
  - 44. Lower Dublin aquifer for predevelopment and modern-day (1987-92) conditions **81**
  - 45. Upper Midville aquifer for predevelopment and modern-day (1987-92) conditions **82**
  - 46. Lower Midville aquifer for predevelopment and modern-day (1987-92) conditions **83**

## FIGURES—Continued

- Figure 47. Map showing simulated trans-river flow areas, associated recharge areas, and selected ground-water pathlines for the Gordon aquifer during the modern-day (1987-92) period, and ground-water contamination in the central part of the Savannah River Site **89**
- Figures 48-52. Graph showing sensitivity of simulated:
- 48. Ground-water discharge to the Savannah River to selected parameters **91**
  - 49. Ground-water levels to selected parameters **92**
  - 50. Westward trans-river flow area to changes in selected parameters **94**
  - 51. Westward trans-river flow zones to changes in selected parameters **96**
  - 52. Time-of-travel from recharge areas to westward trans-river flow zones to changes in selected parameters **98**

## TABLES

- Table
- 1. Estimated ground-water discharge to the Savannah River **15**
  - 2. Input requirements, sources of data, and calibration procedures for finite-difference ground-water flow model of Savannah River Site area **19**
  - 3. Ranges of field observations and estimates for transmissivity, storage coefficient, and confining unit leakance by hydrogeologic unit for ground-water flow model of Savannah River Site area **21**
  - 4. Ranges of estimates for riverbed conductance (CRIV) by hydrogeologic unit **25**
  - 5. Industrial and municipal ground-water pumping centers near the Savannah River Site and average annual ground-water withdrawal, 1987-92 **26**
  - 6. Simulated ground-water withdrawal by stress period **28**
  - 7. Calibration statistics for simulated heads for predevelopment conditions **32**
  - 8. Simulated predevelopment water budget **33**
  - 9. Observed and simulated predevelopment head at the P-21 and P-23 well-cluster sites **44**
  - 10. Calibration statistics for simulated heads for modern-day (1987-92) conditions **47**
  - 11. Simulated modern-day (1987-92) water budget **52**
  - 12. Simulated and estimated values for transmissivity **66**
  - 13. Simulated and estimated values for leakance **70**
  - 14. Ranges of simulated conductance (CRIV) by hydrogeologic unit **74**
  - 15. Simulated trans-river flow by layer for predevelopment (pre-1953) and modern-day (1987-92) conditions **76**
  - 16. Recharge areas to trans-river flow zones by layer for predevelopment (pre-1953) and modern-day (1987-92) conditions **85**
  - 17. Mean time-of-travel for water particles in trans-river flow zones for simulated predevelopment conditions **86**
  - 18. Mean time-of-travel for water particles in trans-river flow zones for simulated modern-day (1987-92) conditions **87**

# SIMULATION OF GROUND-WATER FLOW AND STREAM-AQUIFER RELATIONS IN THE VICINITY OF THE SAVANNAH RIVER SITE, GEORGIA AND SOUTH CAROLINA, PREDEVELOPMENT THROUGH 1992

by John S. Clarke and Christopher T. West

## ABSTRACT

Ground-water flow and stream-aquifer relations were simulated for seven aquifers in Coastal Plain sediments in the vicinity of the U.S. Department of Energy, Savannah River Site (SRS), in Georgia and South Carolina to evaluate the potential for ground water containing hazardous materials to migrate from the SRS into Georgia through aquifers underlying the Savannah River (trans-river flow). The work was completed as part of a cooperative study between the U.S. Geological Survey, the U.S. Department of Energy, and Georgia Department of Natural Resources. The U.S. Geological Survey three-dimensional finite-difference ground-water flow model, MODFLOW, was used to simulate ground-water flow in three aquifer systems containing seven discrete aquifers: (1) the Floridan aquifer system, consisting of the Upper Three Runs and Gordon aquifers in sediments of Eocene age; (2) the Dublin aquifer system, consisting of the Millers Pond, and upper and lower Dublin aquifers in sediments of Paleocene and Late Cretaceous age; and (3) the Midville aquifer system, consisting of the upper and lower Midville aquifers of sediments in Late Cretaceous age. Ground-water flow was simulated using a series of steady-state simulations of predevelopment (pre-1953) conditions and six pumping periods—1953–60, 1961–70, 1971–75, 1976–80, 1981–86, and 1987–92—results are presented for predevelopment (prior to 1953) and modern-day (1987–92) conditions.

Total simulated predevelopment inflow is 1,023 million gallons per day (Mgal/d), of which 76 percent is contributed by leakage from the Upper Three Runs aquifer. Over most of the study area, pumpage induced changes in ground-water levels, ground-water discharge

to streams, and water-budget components were small during 1953–92, and changes in aquifer storage were insignificant. Simulated drawdown between predevelopment and modern-day conditions is small (less than 7 feet) and of limited areal extent—the largest simulated declines occur in the upper and lower Dublin aquifers in the vicinity of the Sandoz plant site in South Carolina. These declines extend beneath the Savannah River and change the configuration of the simulated potentiometric surface and flow paths near the river.

Predevelopment and modern-day flowpaths were simulated near the Savannah River by using the U.S. Geological Survey particle-tracking code MODPATH. Eastward and westward zones of trans-river flow were identified in three principal areas as follows:

- zone 1—from the Fall Line southward to the confluence of Hollow Creek and the Savannah River;
- zone 2—from the zone 1 boundary southward to the southern border of the SRS (not including the Lower Three Runs Creek section); and
- zone 3—from the zone 2 boundary, southward into the northern part of Screven County, Ga. All zones for all model layers were located within or immediately adjacent to the Savannah River alluvial valley and most were located in the immediate vicinity of the Savannah River. Recharge areas for each of the zones of trans-river flow generally are in the vicinity of major interstream drainage divides.

Mean time-of-travel simulated for predevelopment conditions ranges from 300 to 24,000 years for westward trans-river flow zones; and from 550 to 41,000 years for eastward zones. Corresponding travel times under modern-day conditions range from 300 to 34,000 years for westward zones and from 580 to 31,000 years for eastward zones. Differences in travel times between predevelopment and modern-day simulations result from changes in hydraulic gradients due to ground-water pumpage that alter flow paths in the vicinity of the river.

Recharge to Georgia trans-river flow zones originating on the SRS was simulated for the Gordon and upper Dublin aquifers during predevelopment, and in the Gordon aquifer during 1987–92. During 1987–92, SRS recharge was simulated in 6 model cells covering a 2-square mile area, located away from areas of ground-water contamination. Simulated aquifer discharge from these sites occurs in a 1 square mile (mi<sup>2</sup>) marshy area immediately westward of the Savannah River that is distant from major pumping centers. Simulated time-of-travel from SRS recharge areas to westward trans-river flow zones ranged from about 90 years to 2,900 years.

## INTRODUCTION

The U.S. Department of Energy (DOE), Savannah River Site (SRS) near Aiken, South Carolina (figs. 1a, 1b), has manufactured nuclear materials for the National defense since the early 1950's. Various hazardous materials including radionuclides, volatile organic compounds, and heavy metals, are either disposed of or stored at several locations at the SRS. Contamination of ground water has been detected at several locations within the site (Clarke and West, 1997). Concern has been raised by State of Georgia officials regarding the possible migration of ground water contaminated with hazardous materials through aquifers underlying the Savannah River into Georgia.

The U.S. Geological Survey (USGS), in cooperation with the DOE and Georgia Department of Natural Resources (DNR) conducted a study during 1991–97 to describe ground-water flow and quality near the Savannah River, and to identify the potential for or possible occurrence of trans-river flow (trans-river flow study). Stream–aquifer relations were evaluated to determine the potential for ground-water movement beneath, or discharge into, the Savannah River. The objectives of the trans-river-flow study were to identify ground-water flow paths (particularly in the vicinity of the SRS area and the Savannah River), quantitatively describe ground-water flow (particularly ground-water

discharge to the Savannah River), and evaluate the hydraulic connection between the Savannah River and underlying aquifers in the vicinity of the SRS, Georgia and South Carolina. To help determine directions of ground-water flow in the SRS region, a digital ground-water flow model was developed for seven aquifers in Coastal Plain sediments.

## Purpose and Scope

This report is one in a series of reports that describe various aspects and characteristics of the geology, hydrogeology, and stream–aquifer relations in the vicinity of the Savannah River Site (see section on “Previous Investigations”). This report presents the results of the ground-water modeling part of the SRS trans-river flow study. Specifically, this report describes for predevelopment (prior to 1953) and modern-day (1987–92) conditions: (1) the general hydrogeology and conceptualized stream–aquifer flow; (2) the results of simulations of ground-water flow and stream–aquifer flow; and (3) simulated trans-river flow of ground-water under predevelopment and modern-day conditions. Trans-river flow is defined herein as ground water occurring on the opposite side of the Savannah River from where the ground-water recharged.

The study relied on data from published and unpublished sources. Recent and historical water-level measurements from 516 wells; and water analyses and hydraulic characteristics from selected existing wells were used in the study. This included water-level and water-quality data and hydraulic characteristics from 21 test wells constructed as a result of this study at five well-cluster sites in Georgia where data were sparse (fig. 1a—Millers Pond, TR-92-6, Girard, Brighams Landing, and Millhaven cluster sites). An inventory of existing wells was conducted to obtain additional data needed to define water chemistry and prepare potentiometric-surface maps, and to identify areas of major ground-water withdrawals. Aquifer tests were conducted and analyzed in 31 wells at 13 different locations. Eighteen auger borings were made to better define the shallow subsurface geology of the Savannah River alluvial valley. The study also utilized stream-stage data from 61 sites, precipitation data from four sites, and historical ground-water-use data.

## Description of Study Area

The 5,147-square mile (mi<sup>2</sup>) study area is located in the northern part of the Coastal Plain physiographic province of Georgia and South Carolina and includes the Savannah River Site and adjacent parts of Georgia and South Carolina (fig. 1a). In Georgia, the study area includes all or parts of Richmond, Burke, Screven, Jenkins, Jefferson, Glascock, McDuffie, Warren, and Columbia Counties. In South Carolina, the study area includes all or parts of Aiken, Barnwell, Allendale, Saluda, and Edgefield Counties.

The Fall Line, the boundary between the Piedmont and Coastal Plain, approximates the Inner Margin of Coastal Plain sediments (the contact between Coastal Plain sediments and Piedmont crystalline rocks) and forms the approximate northwestern limit of the study area. Generally, relief is greatest near the Fall Line and is progressively less toward the south and east. Altitudes range from about 650 feet (ft) above sea level near the Fall Line to less than 100 ft in the southern part of the study area and in the valleys of major streams such as the Savannah River or Brier Creek. Along the western bank of the Savannah River in southern Richmond County, and in most of Burke County, Ga., a steep bluff is present. Relief along this bluff is as much as 160 ft.

The Coastal Plain Province is moderately to well dissected by streams and is characterized by well-developed dendritic stream patterns. Streams that flow over the relatively softer Coastal Plain sediments develop wider floodplains and greater meander frequency than streams that flow over hard crystalline rocks of the Piedmont (Clark and Zisa, 1976). The floodplains near the principal rivers, such as the Savannah River, have a wide expanse of swamp bordering both sides of the channel. The Coastal Plain is subdivided into five physiographic divisions in the study area: the Coastal Terraces, Tifton Upland, Louisville Plateau, Aiken Plateau, and Fall Line Hills (fig. 1a) (see Clarke and West (1997) for a description of each of these features).

Silviculture and agriculture are the predominant land uses; and pine timber, cotton, and soybeans are the major crops in the study area. Kaolin is mined in parts of the study area. The largest cities in the study area are Augusta, Ga.—population 44,639 in 1990; and Aiken, S.C.—population 19,872 in 1990 (U.S. Department of Commerce, 1991). The SRS encompasses about 300 mi<sup>2</sup>, or 6 percent of the study area, and lies in parts of Aiken, Barnwell, and Allendale Counties, S.C. (figs. 1a, 1b).

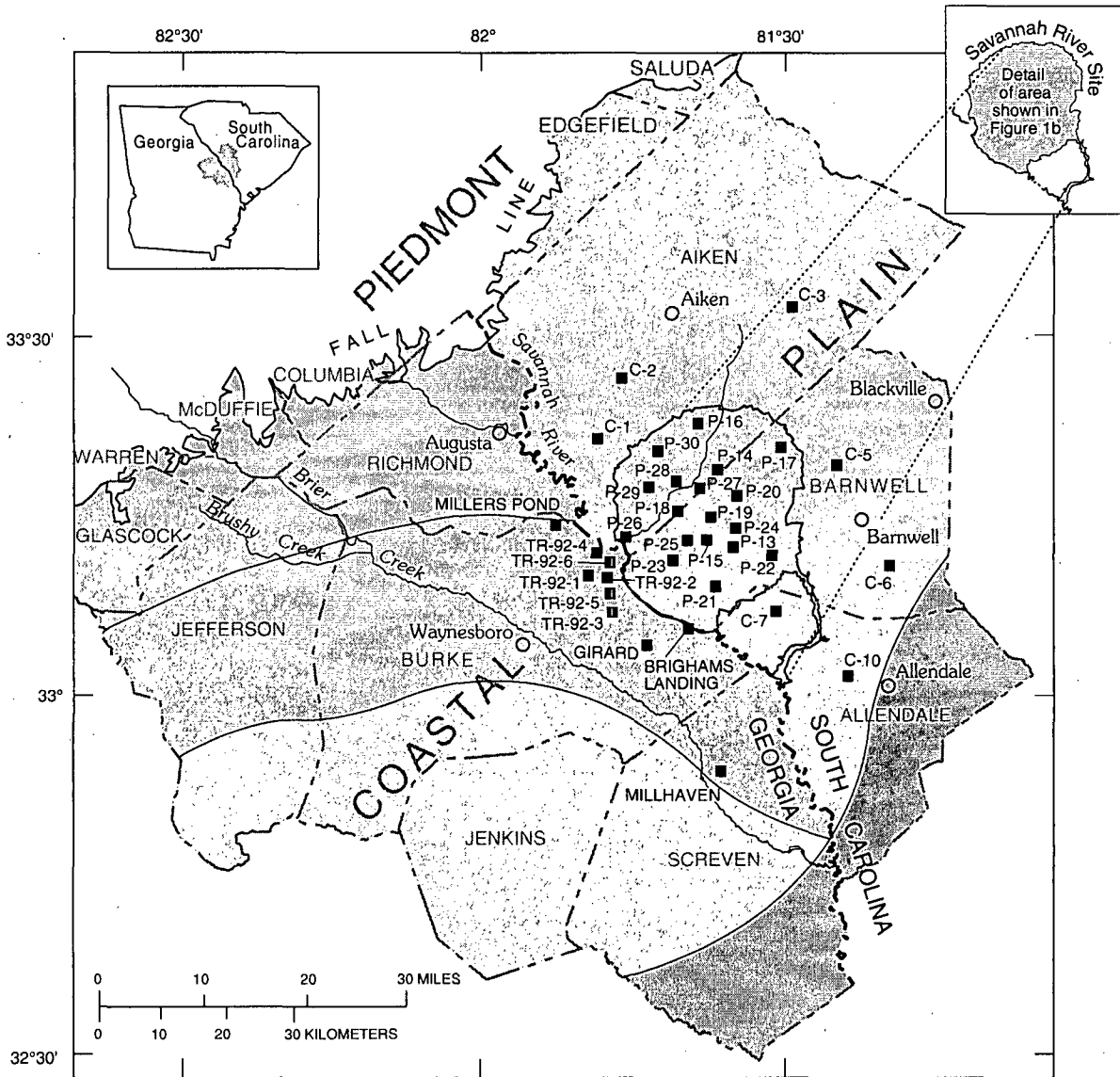
The study area is characterized by a relatively mild climate with warm, humid, summers and mild winters. Precipitation is highest during winter months when continental storm fronts from the west move through the area; and during July and August when thunderstorms are prevalent. Average-annual precipitation in the study area—for the period 1941-70—ranged from less than 44 inches in Richmond County, Ga., to more than 48 inches in southern Screven County, Ga., and Allendale County, S.C.

The Savannah River is the major surface-water drain in the study area and forms the State Line between Georgia and South Carolina (fig. 2). The river drains an area of about 10,580 mi<sup>2</sup> (of which, at least 1,140 mi<sup>2</sup> are located in the study area) and empties into the Atlantic Ocean near Savannah, Ga. During 1941-70, the mean-annual runoff in Georgia (fig. 2) ranged from less than 0.9 cubic feet per second per square mile [(ft<sup>3</sup>/sec)/mi<sup>2</sup>] of drainage area in southern Screven, Jenkins, Burke and Jefferson Counties, and in northern Richmond and Jefferson Counties; to more than 1.1 (ft<sup>3</sup>/sec)/mi<sup>2</sup> in eastern Richmond and Burke Counties (Faye and Mayer, 1990).

## Previous Investigations

This report is one in a series of reports describing results of the trans-river flow study. Other reports prepared for the study provide data and interpretations that support concepts of ground-water flow and stream-aquifer relations in the vicinity of SRS. These reports describe geology, hydrogeologic framework, hydrogeologic data, ground-water levels and estimated discharges, and previous ground-water modeling investigations; and are discussed by Clarke and West (1997).

Ground-water modeling investigations in the SRS area include Faye and Mayer (1997) and Aucott (1997), who conducted studies as part of the USGS Regional Aquifer System Analysis Program. Several ground-water flow models were developed as part of hydrogeologic investigations conducted at the SRS. These include Marine and Root (1975)—to evaluate flow in Cretaceous-age sediments (their "Tuscaloosa aquifer"); Parizek and Root (1986)—to evaluate ground-water velocity at the radioactive-waste-management facility; Looney and others (1990)—to evaluate flow at a proposed production-reactor site; Camp, Dresser, and McKee, Inc. (1992)—to evaluate flow at the nuclear-weapons-complex reconfiguration site; and HydroGeoLogic, Inc. (1992)—to evaluate flow and transport at the TNX area. Faye and Mayer (1990)



Base modified from U.S. Geological Survey State base maps

Physiographic districts from Cooke, 1936; and LaForge and others, 1925

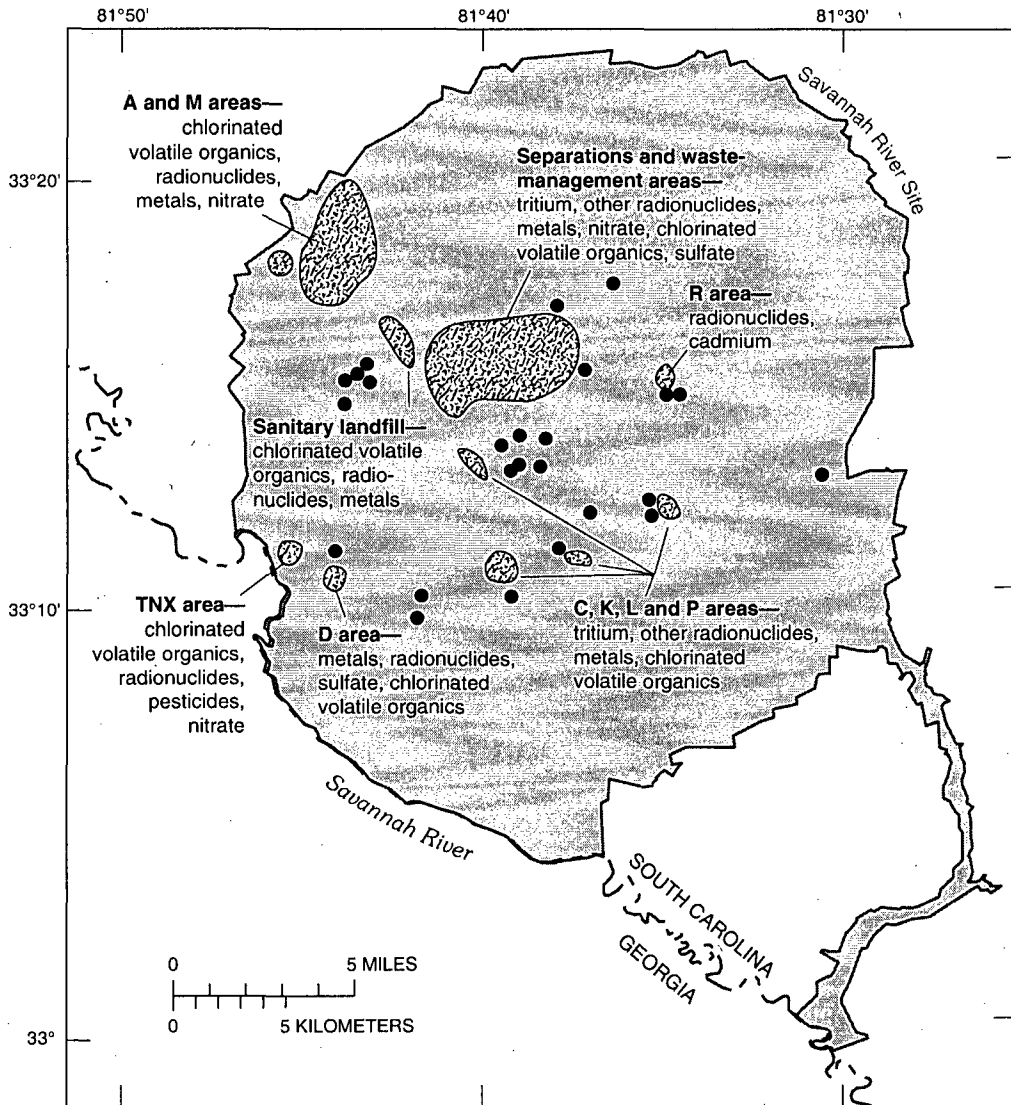
**EXPLANATION**

**PHYSIOGRAPHIC DISTRICT**

-  Fall Line Hills
-  Aiken Plateau
-  Louisville Plateau
-  Tifton Upland
-  Coastal Terraces

C-2 ■ WELL-CLUSTER SITE AND NAME

**Figure 1a.** Location of study area, Savannah River Site, well-cluster sites, and physiographic districts in Georgia and South Carolina.



**EXPLANATION**

CONTAMINATED SITES

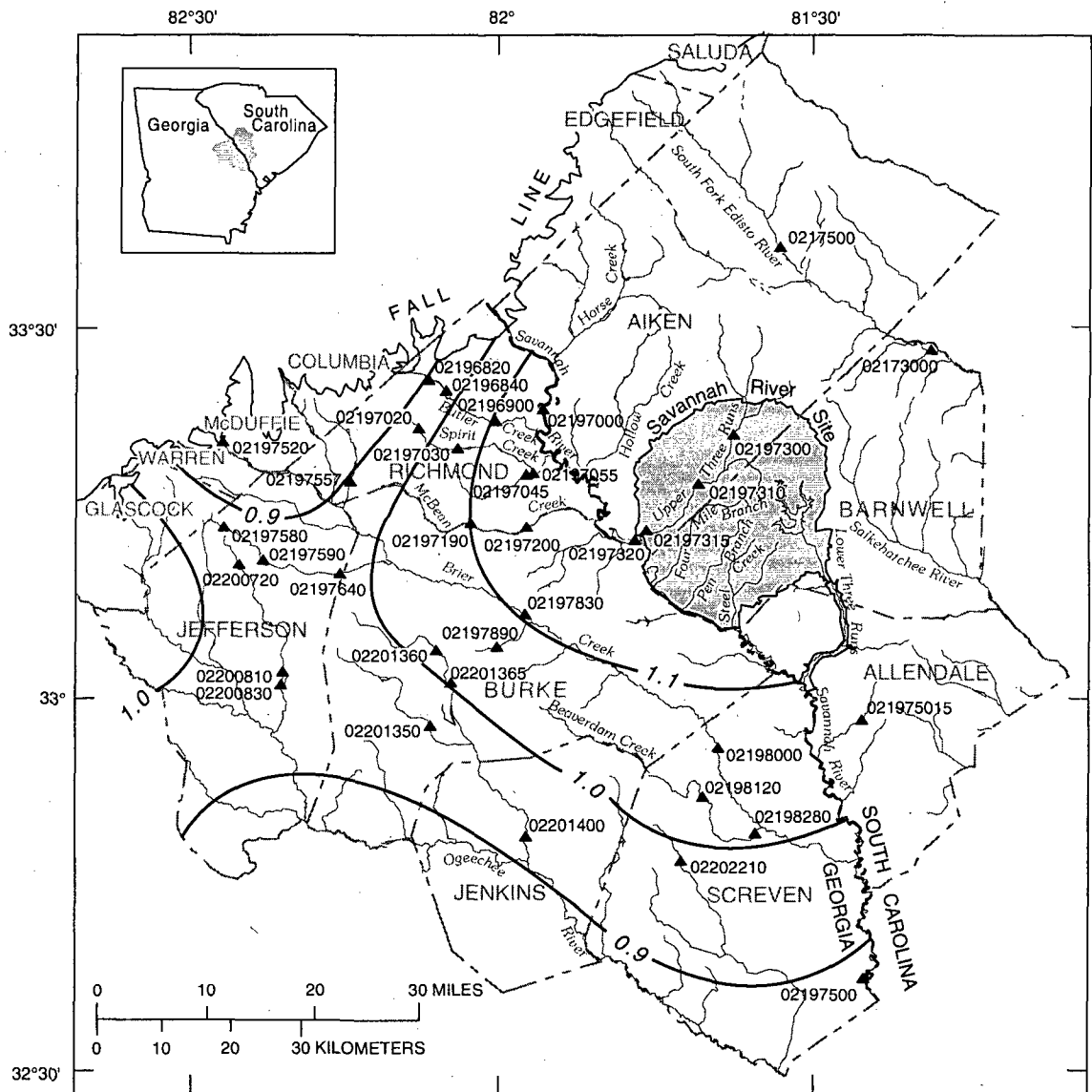


Areal contamination



Localized contamination

**Figure 1b.** Areal and local ground-water contamination at the Savannah River Site, South Carolina (modified from Westinghouse Savannah River Company, 1995).



Base modified from U.S. Geological Survey State base maps

**EXPLANATION**

- 1.0 — LINE OF EQUAL MEAN-ANNUAL RUNOFF, 1941-70—  
Interval 0.1 cubic foot per square mile of drainage area
- ▲ 02201400 / STREAMFLOW-GAGING STATION OR PERIODIC-MEASUREMENT SITE AND IDENTIFICATION NUMBER

**Figure 2.** Mean-annual runoff in Georgia part of study area, 1941-70; and locations of selected streamflow-gaging stations or periodic-measurement sites (modified from Faye and Mayer, 1990).

and Delaimi (1996) evaluated ground-water flow transverse to the Savannah River using cross-sectional-flow models.

### Methods of Study

Development of a ground-water flow model for the SRS area involved analysis of geologic, hydrologic, and water-quality data in order to develop a conceptual model of ground-water flow and stream-aquifer relations as a basis for simulation. Clarke and West (1997) described many of the data and interpretations required for simulation of ground-water flow. This included development of a conceptual model of stream-aquifer relations and ground-water flow, development of predevelopment potentiometric surfaces of major aquifers, assessment of water-level fluctuations and trends, tabulation of historical and modern-day ground-water pumpage, description of ground-water contribution to streamflow, and pertinent literature. Maps showing the average potentiometric surface of major aquifers during 1987-92 were constructed using data from 298 wells and streamflow-stage data at 62 sites. Because insufficient data are available to construct separate potentiometric-surface maps for the upper and lower Dublin aquifers, and for the upper and lower Midville aquifers, composite potentiometric-surface maps were constructed for the (1) Dublin aquifer system and the (2) Midville aquifer system (using procedures described in Clarke and West, 1997). Although the Millers Pond aquifer is part of the Dublin aquifer system, water-level data from this aquifer were not used to construct the composite map because of a high degree of hydraulic separation (and head differences) between the Millers Pond and the Dublin aquifers.

To better define hydraulic properties of aquifers and confining units in the SRS area, aquifer tests were conducted in selected wells by Clemson University, and selected core samples were analyzed by Core Laboratories, Inc. (New Orleans, La.), using a laboratory permeameter. These data were supplemented by data from published reports and by unpublished aquifer-test data that were analyzed by USGS. In addition, lateral hydraulic conductivity at selected sites was estimated from borehole resistivity logs using the methodology developed by Faye and Smith (1994). Snipes and others (1995a) provided a summary of aquifer tests conducted by Clemson University. Clarke and others (1994, 1996) and Leeth and others (1996) provided a listing of hydraulic properties of core samples.

A digital ground-water flow model was developed using the USGS MODFLOW computer code (McDonald and Harbaugh, 1988). The model was interfaced with a comprehensive geographic information system (GIS) data base to (1) spatially organize the types of data needed to conceptualize areally extensive ground-water flow; (2) facilitate testing and evaluation of various concepts of ground-water flow and stream-aquifer relations; (3) evaluate the effects of pumping on ground-water flow and stream-aquifer relations; and (4) delineate possible areas of trans-river flow near the Savannah River. Ground-water flowpaths under predevelopment (pre-1953) and modern-day (1987-92) conditions were simulated by using the USGS computer code MODPATH (Pollock, 1994).

### Acknowledgments

The authors extend their thanks to members of the SRS and USGS technical advisory groups established for the trans-river flow study. Without their help and guidance, completion of the study would have been more difficult and technically incomplete. Members of the SRS group, in alphabetical order, are: Rolf K. Aadland, Westinghouse Savannah River Company (WSRC); Adel Baker, Southeastern Technology Center; Bob Benson, South Carolina Department of Health and Environmental Control; Sally Benson, Clemson University; Constance Gawne, South Carolina Department of Natural Resources-Water Resources Division (DNR-WRD); Joe Gellici, SC DNR-WRD; Rex Hodges, Clemson University; Robert Logan, South Carolina Department of Health and Environmental Control; Chet Nichols, WSRC; Ralph Nichols, WSRC; Van Price, WSRC; Earl Shapiro, Georgia Geologic Survey; Dave Snipes, Clemson University; Joseph Summerour, Georgia Geologic Survey; Richard Strom, WSRC; and Tom J. Temples, DOE. Members of the USGS group, in alphabetical order, are Robert E. Faye, Arlen Harbaugh, Richard E. Krause, Gregory C. Mayer, David C. Prowell, and Lynn J. Torak.

Thanks are extended to Keith McFadden, Nancy Flexner, and Larry G. Harrelson (USGS) for help in developing and organizing the project data base. Michael F. Peck (USGS) provided help in development of the project data base and in the preparation of modern-day potentiometric surface maps. Fred Falls (USGS) developed the project hydrogeologic framework and collected samples for analysis of water-chemistry and isotopic composition. Joan Baum, DOE,

(formerly USGS,) assisted in the development of the hydrologic framework and project data base. The authors also are grateful to the various departments at the Savannah River Site for providing data, and to Clemson University for conducting and analyzing aquifer tests at several sites. Thanks also are extended to Carolyn A. Casteel, Caryl J. Wipperfurth, and James A. Tomberlin (USGS editorial and cartography staff); and to Bonnie Jean Turcott, a Volunteer for Science at the USGS for report preparation.

## HYDROGEOLOGY

Hydrogeology in the Coastal Plain Province in the vicinity of the SRS in Georgia and South Carolina is described in the following two sections of this report. General lithologies and ages of Coastal Plain sediments, depositional environments, and major structural features in the study area are described in the section "Geologic Setting." Hydrogeologic characteristics of the three aquifer systems—Floridan, Dublin, and Midville—and the relation of aquifers and confining units to corresponding model layers are given in the section "Hydrogeologic Units."

### Geologic Setting

Coastal Plain sediments in the study area consist of layers of sand, clay, and minor limestone that range in age from Late Cretaceous through Holocene. The northern limit of the strata and the contact between the Coastal Plain and Piedmont is marked by the Inner Coastal Plain Margin, approximated by the Fall Line (fig. 1a). The strata crop out in discontinuous belts that generally are parallel to the Fall Line. The strata dip and progressively thicken from the Fall Line to the southeast; estimated maximum thickness of these strata is 2,700 ft in the southern part of the study area (Wait and Davis, 1986). The sedimentary sequence unconformably overlies igneous and metamorphic rocks of Paleozoic age, and consolidated red beds of early Mesozoic age (Chowns and Williams, 1983).

The Coastal Plain deposits consist of fluvial, deltaic, and marine-coastal and shelf sediments (Prowell and others, 1985). Through time, the axes of deposition of the deltaic systems have changed due to differential tectonism and uplift in the Appalachian region (Prowell, 1988; D.C. Prowell, U.S. Geological Survey, oral commun., 1992). Numerous marine transgressions and regressions deposited, removed, and redistributed sediments (Colquhoun, 1981). In the updip part of the

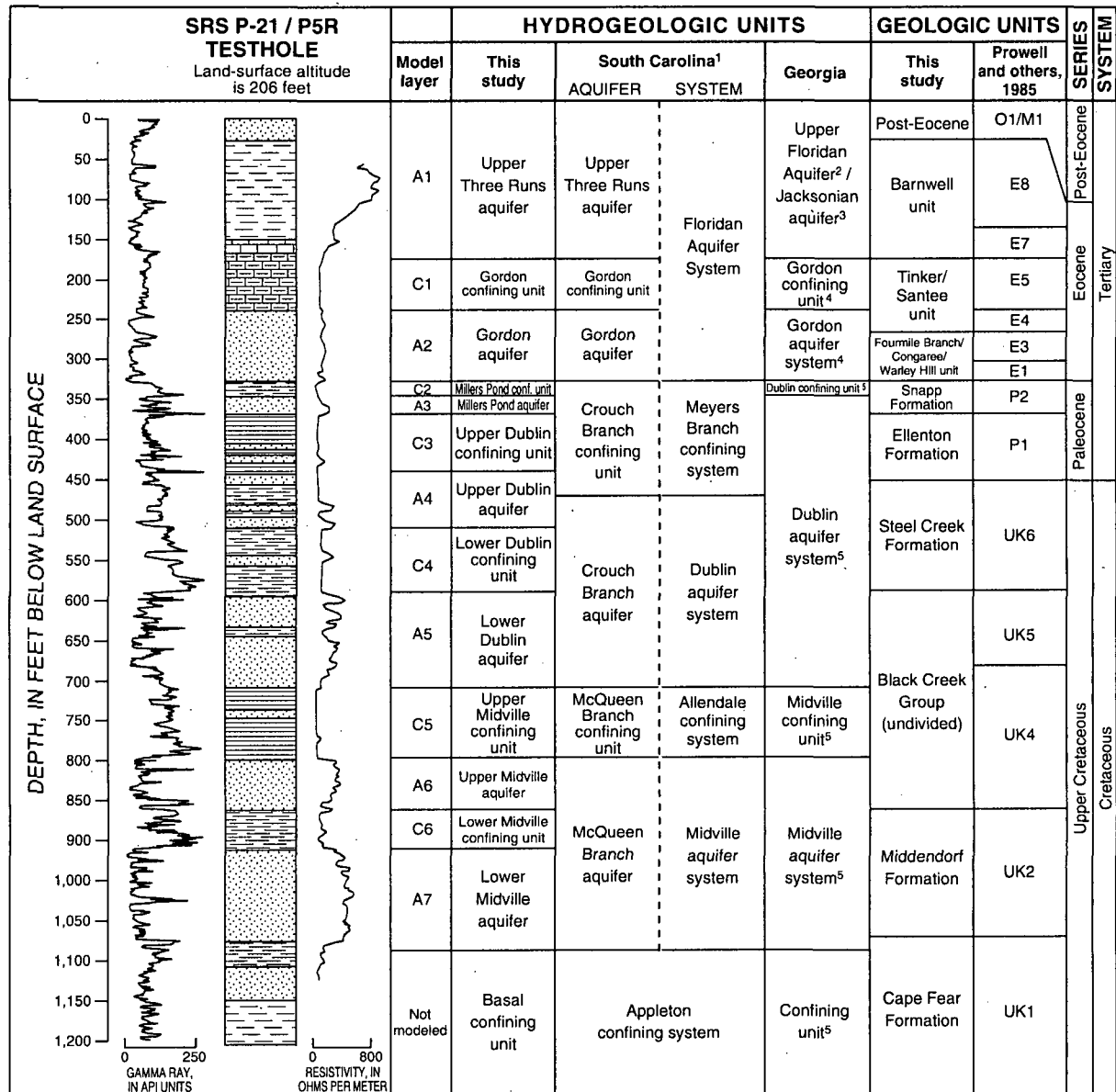
Coastal Plain in Aiken County, S.C., and Richmond County, Ga., the Coastal Plain predominantly consists of nonmarine siliciclastic sediments. Marine sediments are more abundant in the southern and southeastern parts of the study area than in the rest of the Coastal Plain and include carbonate-shelf deposits in some strata of Tertiary age.

The age and stratigraphic correlation of geologic units in the study area have been difficult to determine because fossil evidence is sparse, lithologies of vertically adjacent units commonly are similar, erosion has truncated units, and some units can be studied only in the subsurface. In addition, abrupt changes in lithology occur laterally and vertically. These changes, which juxtapose rocks characterized by different lithologic and hydrologic properties, may be due to abrupt changes in depositional environment, and may be complicated by erosional truncation or by faulting. Various stratigraphic and hydrogeologic nomenclatures have evolved for the area, in part as a result of the difficulties in correlation (fig. 3). See Falls and others (1997a, 1997b) for a complete description of geologic units in the study area.

Major structural features reported in the study area include the Belair Fault (Prowell and O'Connor, 1978), and the Pen Branch Fault (Price and others, 1991). The Belair Fault is a northeast-trending high-angle reverse fault with a maximum vertical displacement of 100 ft at the base of Coastal Plain strata (Prowell and O'Connor, 1978). The location of the Pen Branch Fault is coincident with the northwestern border of the Dunbarton early Mesozoic basin. The northeast-trending high-angle normal fault dips to the southeast and cuts strata of Cretaceous, Paleocene, and Eocene age. The fault is downthrown on the northwestern side, and maximum displacement ranges from 100 ft at the base of Coastal Plain strata to 30 ft at the top of the Eocene Dry Branch Formation (Price and others, 1991).

### Hydrogeologic Units

Previous investigators in Georgia (Miller, 1986; Brooks and others, 1985; Clarke and others, 1985) and South Carolina (Logan and Euler, 1989; Bledsoe and others, 1990; Aadland and others, 1995) defined three principal aquifer systems near SRS. In descending order, these aquifer systems are: (1) the Floridan aquifer system, originally defined by Miller (1986) and later redefined by Aadland and others (1995)—comprised largely of calcareous sand and limestone of Eocene age;



<sup>1</sup> Aadland and others, 1992, 1995

<sup>2</sup> Krause and Randolph, 1989;

Aadland and others, 1995

<sup>3</sup> Vincent, 1982

<sup>4</sup> Brooks and others, 1985

<sup>5</sup> Clarke and others, 1985

**EXPLANATION**

- [Pattern] SAND
- [Pattern] MARL
- [Pattern] CLAYEY SAND
- [Pattern] MASSIVE CLAY
- [Pattern] LIMESTONE
- [Pattern] LAMINATED CLAY

MODEL LAYER—A, simulated aquifer;  
C, simulated confining unit

**Figure 3.** Model layers, respective hydrogeologic units, and names applied to the P-21/P5R testhole at the Savannah River Site, South Carolina (modified from Falls and others, 1997a, b).

(2) the Dublin aquifer system (Clarke and others, 1985)—comprised of sand of Paleocene and Late Cretaceous age; and (3) the Midville aquifer system (Clarke and others, 1985)—comprised of sand of Late Cretaceous age. Although this subdivision was suitable for most regional-scale hydrogeologic studies, greater subdivision of units was required to define vertical hydraulic heterogeneity for detailed investigations of ground-water flow near the Savannah River. Accordingly, the three aquifer systems were divided into seven aquifers:

- the Floridan aquifer system was subdivided into the Upper Three Runs aquifer and the Gordon aquifer (Aadland and others, 1995);
- the Dublin aquifer system was subdivided into the Millers Pond aquifer, the upper Dublin aquifer and the lower Dublin aquifer (Falls and others, 1997a, 1997b); and
- the Midville aquifer system was subdivided into the upper Midville aquifer and the lower Midville aquifer (Falls and others, 1997a, 1997b).

A comparison of hydrogeologic units and names applied to the P-21/P5R well-cluster site at the SRS and their relation to model layers A1-A7 and C1-C6 is shown in figure 3. A detailed description of the hydrogeologic framework employed during the trans-river flow study—including areal extent, thickness, and hydraulic properties of hydrogeologic units—is provided by Falls and others (1997a, 1997b).

The aquifers are separated and confined by layers of clay and silt that become progressively sandy and discontinuous in updip areas. The aquifer systems coalesce where the confining units become sandy. Clarke and others (1985, 1994) described the coalescence of the Dublin and Midville aquifer systems in the northern part of the study area (Dublin-Midville aquifer system), and suggested that the Gordon aquifer might also coalesce with these units in updip areas. Similar coalescence of aquifer units at SRS was identified by Aadland and Bledsoe (1990), Aadland and others (1995), and Faye and Mayer (1997).

#### *Floridan Aquifer System*

The Floridan aquifer system is comprised of the largely carbonate Upper and Lower Floridan aquifers, and extends into the southern part of the study area

(Miller, 1986). In updip areas, terrigenous sediments of Eocene are hydraulically connected to the Upper and Lower Floridan aquifers. To account for this connection, Krause and Randolph (1989) included these updip equivalents in their simulation of ground-water flow in the Floridan aquifer system. Updip equivalents of the Upper Floridan aquifer have been referred to in the study area as the Jacksonian aquifer (Vincent, 1982) and the Upper Three Runs aquifer (Aadland and others, 1992, 1995; Summerour and others, 1994). Updip equivalents of the Lower Floridan aquifer have been referred to as the Gordon aquifer system (Brooks and others, 1985) and the Gordon aquifer (Aadland and others, 1992, 1995; Summerour and others, 1994). Aadland and others (1995) extended the Floridan aquifer system into the northern part of the study area, where it consists of the Upper Three Runs and Gordon aquifers.

The Upper Three Runs aquifer (model layer A1) is comprised of all sediments between land surface and the top of the Gordon confining unit, and includes lithostratigraphic equivalents of the Upper Floridan, Jacksonian, and Upper Three Runs aquifers. This aquifer consists of sand, calcareous sand, and limestone of the Barnwell unit and younger post-Eocene sediments, and includes the more-permeable upper layers of the Tinker/Santee unit.

In parts of the study area, the Upper Three Runs aquifer consists of several water-bearing zones characterized by different degrees of hydraulic separation (Clarke and West, 1997). The largest head differences occur in the vicinity of topographic highs, which are areas of recharge containing downward hydraulic gradients. In the vicinity of sandy ridges, the geologic sediments that comprise the Upper Three Runs aquifer may be unsaturated because the water table is situated beneath the base of the equivalent sediments (Clarke and West, 1997).

The Gordon confining unit (model layer C1) underlies the Upper Three Runs aquifer and separates it from the Gordon aquifer. The unit consists of clay and marl of the Tinker/Santee unit.

The Gordon aquifer (model layer A2) is equivalent to the Gordon aquifer system as defined in Georgia by Brooks and others (1985), and the Gordon aquifer as correlated in South Carolina by Aadland and others (1992). The aquifer consists of sand and calcareous sand of the Fourmile Branch/Congaree/Warley Hill unit and, in downdip areas, the lower part of the Tinker/Santee unit. In Barnwell, Allendale, Burke, Jenkins and Screven Counties, the base of the Gordon aquifer is defined by

the top of the Millers Pond confining unit. Where the Millers Pond confining unit is absent (Aiken, Richmond, and northern Jefferson Counties), the Gordon and Millers Pond aquifers coalesce and the base of the aquifer is defined by the top of the upper Dublin confining unit.

In parts of the study area, the Gordon aquifer consists of three water-bearing zones showing some degree of hydraulic separation (Clarke and West, 1997). Head differences between the three zones are minimal (generally less than 1.6 ft), with the exception of aquifer recharge or discharge areas where pronounced vertical gradients occur (Clarke and West, 1997). Near the Pen Branch Fault in the central part of the SRS, water levels in the Gordon aquifer at the P-19 well-cluster site are anomalously high, producing a mound in the potentiometric surface.

#### *Dublin Aquifer System*

The Dublin aquifer system in east-central Georgia was defined by Clarke and others (1985) as comprising sediments of Paleocene and Late Cretaceous age. Near the Savannah River, Clarke and others (1985) described local confining units that divided the aquifer system into an upper aquifer in Paleocene sediments and a lower aquifer in Cretaceous sediments. In South Carolina, Aadland and others (1992) redefined the Dublin to consist of Cretaceous sediments of the Crouch Branch aquifer and the overlying Paleocene sediments as the Crouch Branch confining unit of the Meyers Branch confining system.

The Dublin aquifer system in this study is divided into three aquifers—separated by confining units—that are informally named the Millers Pond, upper Dublin, and lower Dublin aquifers (fig. 3). This separation was based on data collected at well-cluster sites that indicated differences in hydraulic head and water chemistry, and little drawdown response to pumpage of adjacent zones (Clarke and others, 1994).

The Millers Pond confining unit (model layer C2) is equivalent to the confining unit at the top of the Dublin aquifer system originally defined by Clarke and others (1985) and separates the Gordon aquifer from the Millers Pond aquifer. The unit consists of massive, white clay of the Snapp Formation of Paleocene age.

The Millers Pond aquifer (model layer A3) was named for sediments penetrated at the Millers Pond site in northern Burke County, Ga., and consists of fine-to-very coarse-grained sand of the Snapp Formation that is

equivalent to the upper “Paleocene-age” aquifer of Clarke and others (1985). This interval was identified as early Eocene (Harris and Zullo, 1990) and late Paleocene age (P2) (Prowell and others, 1985) in previous studies.

The upper Dublin confining unit (model layer C3) separates the Millers Pond and the upper Dublin aquifers and consists of laminated, black clay of the Ellenton Formation. The upper Dublin aquifer (model layer A4) includes the basal sand of the Ellenton Formation and the moderately to very poorly sorted sand and sandy clay of the Steel Creek Formation (fig. 3). The lower Dublin confining unit (model layer C4) separates the upper Dublin and the lower Dublin aquifers and is characterized by a white clay and silty clay interpreted as the top of the Black Creek Group in this study. The lower Dublin aquifer (model layer A5) comprises the well-sorted to moderately sorted sand in the upper part of the Black Creek Group. Because of minimal hydraulic separation (and associated head differences) between the upper and lower Dublin aquifers, it is likely that direction and rates of groundwater flow in the two aquifers are similar (Clarke and West, 1997). Head differences between the upper and lower Dublin aquifers range from 0.03 to 6.18 ft, and between the Millers Pond and upper Dublin aquifers range from 0.3 to 31.82 ft. Head differences tend to be least where lateral flow in an aquifer is dominant and greatest in the vicinity of ground-water recharge and discharge areas, associated with large vertical components of flow.

#### *Midville Aquifer System*

The Midville aquifer system of Clarke and others (1985) is divided into the upper and lower Midville aquifers (fig. 3). The upper Midville confining unit (model layer C5) comprises the clay-dominated central part of the Black Creek Group and corresponds to the confining unit between the Dublin and Midville aquifer systems defined by Clarke and others (1985). The upper Midville aquifer (model layer A6) consists of sand and clay from the lower part of the Black Creek Group. The lower Midville confining unit (model layer C6) separates the upper and lower Midville aquifers and consists of clay at the top of the Middendorf Formation. The lower Midville aquifer (model layer A7) contains sand from the Middendorf Formation and locally includes a porous, permeable sand interval at the top of the Cape Fear Formation. Because of minimal hydraulic separation (and associated head differences) between the upper and lower Midville aquifers (0.1 to 9.57 ft),

ground-water flow directions and rates probably are similar in the two aquifers. Head differences tend to be least where lateral flow is dominant and greatest in the vicinity of major aquifer recharge and discharge areas, characterized by large vertical components of flow.

In the northern parts of the study area, the basal confining unit of the Midville aquifer system consists of either crystalline rock or saprolite. In the southern parts of the study area, the basal confining unit consists of low-permeability sediments of the Cape Fear Formation that are equivalent to the Appleton confining system of Aadland and others (1992).

### CONCEPTUALIZATION OF STREAM-AQUIFER FLOW SYSTEM

In the study area, the ground-water and surface-water systems interact dynamically. Possible ground-water-flow conditions in the Savannah River area near the SRS are diagrammed in figure 4. The Savannah River serves as the major hydrologic drain in the SRS area with its floodplain considered to represent the same or nearly the same hydrologic condition as the river (Clarke and West, 1997). As the paleo-Savannah River channel meandered and eroded through the uppermost confining units and was subsequently filled with permeable sediments, greater hydraulic connection between the alluvium and underlying hydrogeologic units resulted. Because the alluvium is much more permeable than the underlying aquifers and confining beds, and hydraulic head in the alluvium is nearly the same as river stage; the river floodplain acts as a hydrologic "sink" into which ground water and surface runoff from surrounding and underlying units discharges.

Each of the seven aquifers was incised by the paleo-Savannah River channel and covered with an infill of permeable alluvium, allowing direct hydraulic interconnection between the aquifers and the river (Clarke and West, 1997). This hydraulic connection allows water in confined aquifers to discharge into the river—by way of the alluvium—and may induce ground-water flow in an updip or upriver direction (fig. 5).

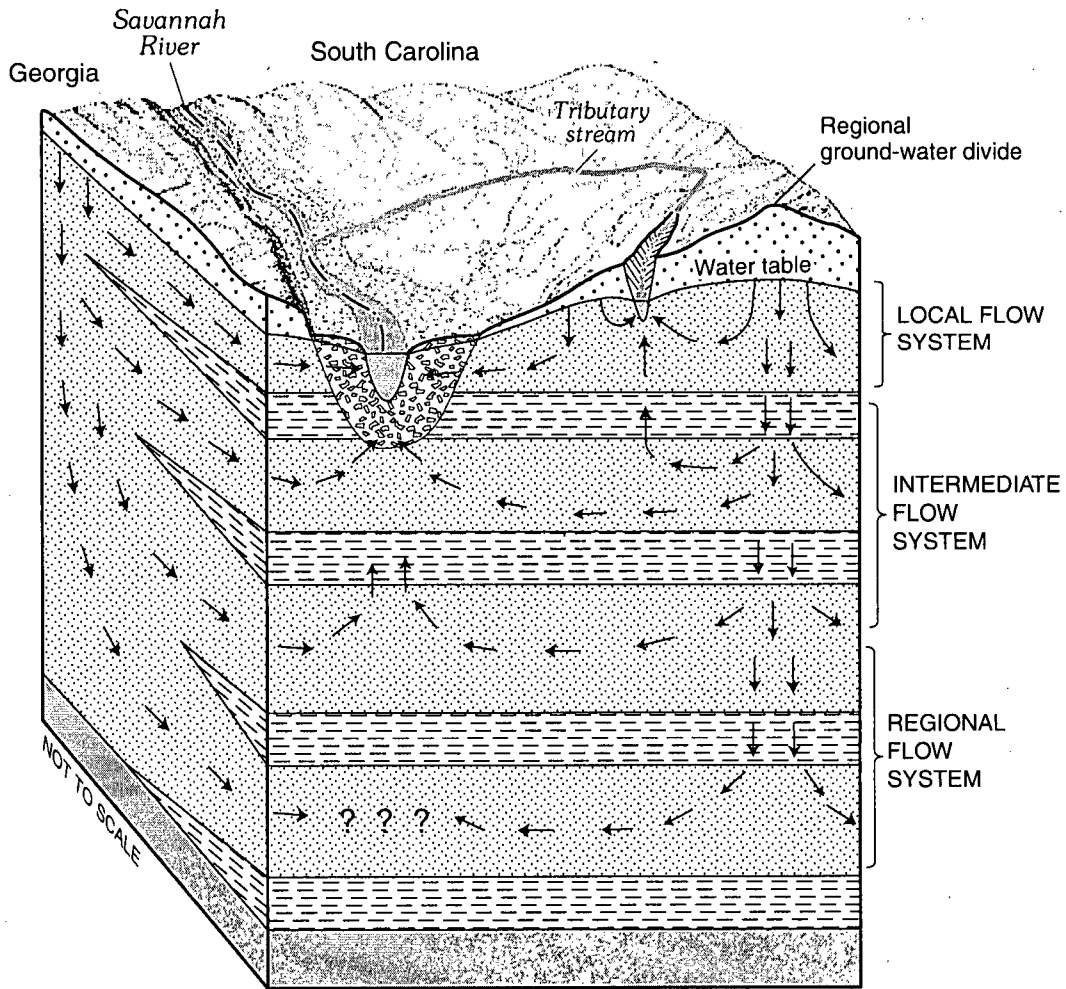
Direct substantial hydraulic connection between confined aquifers and the Savannah River can be inferred from potentiometric-surface maps that show ground-water discharge areas along the Savannah River valley as lows or depressions in the potentiometric surface (Clarke and West, 1997). Ground water flows toward the depressions from all directions; however, downstream from the depressions, the influence of the river on the aquifers becomes progressively diminished,

and ground water resumes its southeastward flow. In these downstream areas, a ground-water divide or "saddle" (Siple, 1960, 1967), in the potentiometric surface occurs symmetrical to the river and separates upstream from downstream ground-water flow (fig. 5).

Trans-river flow is a term that describes a condition whereby ground water originating on one side of a river migrates to the other side of the river through confined aquifers that underlie the river. Although some ground water could discharge into the river floodplain or alluvium on the opposite side of the river from its point of origin, this flow likely would return to the river. Return flow would occur because a slight hydraulic gradient exists toward the river along the floodplain. Flow lines on potentiometric-surface maps of the confined Dublin and Midville aquifer systems suggest possible occurrences of trans-river flow for a short distance into Georgia prior to discharge into the Savannah River (Clarke and West, 1997). However, similar flow lines on maps for the Upper Three Runs and Gordon aquifers do not indicate this occurrence.

The flow mechanisms of the surface-water and ground-water systems in the study area are vastly different—streams exhibit swift open-channel flow, and aquifers exhibit slow porous-media flow (Atkins and others, 1996). Streamflow is comprised of two major components—overland or surface runoff and baseflow. Streamflow is assumed to be sustained entirely by baseflow during extended periods of drought. Baseflow in streams is comprised of contributions from the local, intermediate, and regional ground-water flow regimes (fig. 4) (Faye and Mayer, 1990). Local ground-water flow is characterized by relatively shallow and short flowpaths that extend from a topographic high (recharge area) to an adjacent topographic low (discharge area). Intermediate flow regimes include at least one local flow regime between their respective points of recharge and discharge and intermediate regime flowpaths are somewhat longer and deeper than local flowpaths. Regional or deep flowpaths begin at or near a major ground-water divide and terminate at a regional drain, such as the Savannah River.

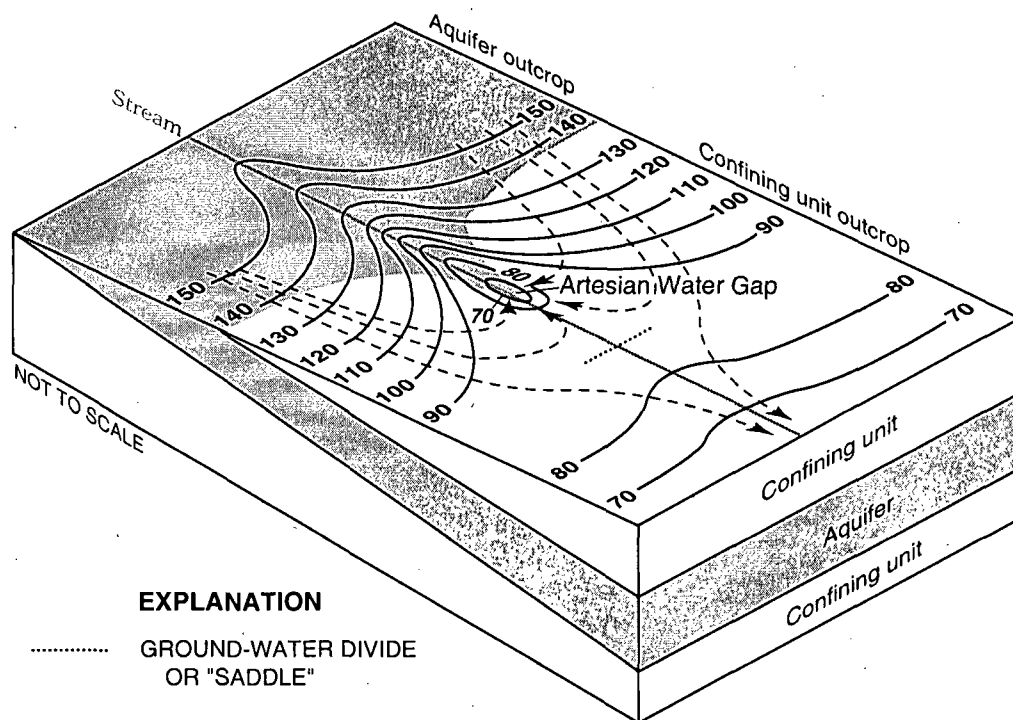
Ground-water recharge is provided by precipitation, much of which is discharged from the local and intermediate flow regime into small streams. Some water is discharged from the intermediate flow regimes to major tributaries of the Savannah River and some discharges directly to the Savannah River valley. A small percentage of total recharge in highland areas infiltrates through clayey confining units and enters the



**EXPLANATION**

- |  |  |  |
|--|--|--|
| AQUIFER  |  |  ALLUVIUM                     |
|  Unsaturated zone |  |  CONFINING UNIT               |
|  Saturated zone   |  |  PRE-CRETACEOUS BASEMENT ROCK |
- DIRECTION OF GROUND-WATER FLOW—Queried where unknown

**Figure 4.** Conceptualized hydrogeologic framework and related ground-water flow in the vicinity of the Savannah River Site, Georgia and South Carolina (modified from Atkins and others, 1996).



#### EXPLANATION

- ..... GROUND-WATER DIVIDE OR "SADDLE"
- 70 — POTENTIOMETRIC CONTOUR—  
Shows altitude at which water level would have stood in tightly cased wells.  
Contour interval 10 feet. Datum is sea level
- > DIRECTION OF GROUND-WATER FLOW

**Figure 5.** Schematic diagram of artesian water gap and related pattern of ground-water flow (modified from LeGrand and Pettyjohn, 1981; Clarke and West, 1997).

deeper regional flow regime. Water from the regional flow regime is discharged almost entirely to the Savannah River valley; the remainder of the regional flow moves southeastward (down-dip) out of the study area. The Upper Three Runs aquifer is unconfined to semiconfined throughout most of the study area, and most ground-water flow in that aquifer is local flow. Ground-water flow in the deeper, confined aquifers is characterized by local flow near outcrop areas to the north that transforms to intermediate and regional flow down-dip (southeastward) where the aquifers are deeply buried.

Generally, the vertical distribution of hydraulic head in the ground-water flow system is related to topographic location. In the vicinity of a major ground-water divide, head decreases with depth—probably to

the base of the regional flow system. In the vicinity of a regional drain, such as the Savannah River, head increases with depth.

#### Hydrologic Budget

A hydrologic budget of ground-water flow was developed as an aid to model calibration. Ground-water recharge is provided by precipitation that ranges from 44 to 48 in/yr. Under steady-state conditions, ground water discharges to streams by an amount equal to ground-water recharge minus the sum of pumpage, recharge to deeper layers, and subsurface flow out of study area. The percent contribution from the local, intermediate, and regional flow regimes to ground-water discharge varies based largely on (1) stream order, (2) aquifer thickness, and (3) degree of confinement. In general, regional drains such as the Savannah River, receive a larger

contribution of water from the regional-flow regime than do tributary streams. Tributary streams generally receive most of their flow from the intermediate and local flow regimes. Discharge from the regional flow regime may occur to the downstream reaches of large streams tributary to the Savannah River. According to Faye and Mayer (1990), the lower the tributary-stream order, the greater the relative contribution from the local-flow regime. Under wet-climatic conditions, the contribution from the local-flow regime is considerably higher than under dry climatic conditions, when local flow may be negligible.

Estimates of mean-annual ground-water discharge to streams (baseflow) determined using hydrograph-separation methods are considered to approximate a large percentage of the long-term average recharge to the local, intermediate, and regional components of the ground-water-flow system. Estimates of ground-water discharge to selected streams (see locations, fig. 2) based on hydrograph separation are listed in Appendix A, and—based on drought streamflow during 1954 and 1986—are listed in Appendix B.

Estimates of mean-annual ground-water discharge in the Savannah River basin—covering about 35 percent of the actively simulated model area—range from 10.8 to 19.8 in/yr with an average of 14.5 in/yr (table 1). These estimates are based on the gain in ground-water discharge (streamflow) between the Augusta gage (02197000), located near the Fall Line, and Millhaven gage (02197500), located near the southern boundary of the model area (fig. 2). Of the estimated average 14.5 inches recharge:

- 47 percent (6.8 inches) enters the local flow system;
- 40 percent (5.8 inches) enters the intermediate flow system; and
- 13 percent (1.9 inches) enters the regional flow system (Clarke and West, 1997).

**Table 1. Estimated ground-water discharge to the Savannah River**

[Source of data—F, Faye and Mayer, 1990; A, Aucott, Meadows, and Patterson, 1987; table from Clarke and West, 1997

Date	Streamflow		Net gain in streamflow (estimated ground-water discharge)		Source of data	Remarks
	Savannah River at Augusta, Ga. (02197000) (cubic feet per second)	Savannah River at Burtons Ferry Bridge, near Millhaven, Ga. (02197500) (cubic feet per second)	cubic feet per second	inches per year		
Water year 1941 <sup>1/</sup>	2,430	<sup>2/</sup> 3,340	<sup>1/</sup> 910	10.8	F	dry year
Water year 1942 <sup>1</sup>	2,840	<sup>2/</sup> 3,930	<sup>1/</sup> 1,090	13.0	F	average year
Water year 1949 <sup>1/</sup>	5,370	<sup>2/</sup> 7,040	<sup>1/</sup> 1,670	19.8	F	wet year
Mean of 1941, 1942 and 1949 water years <sup>1/</sup>	3,550	<sup>2/</sup> 4,770	<sup>1/</sup> 1,220	14.5	F	mean of dry, average, and wet years
October 1941	2,320	2,980	660	7.8	F	mean monthly measurements during dry period, including tributary inflow
9/24/68-10/7/68	6,720	6,940	220	2.6	A	synoptic measurements during dry period, excluding tributary inflow

<sup>1/</sup>Mean annual discharge.

<sup>2/</sup>Equals the sum of the reported net-annual discharge gain during the given water year between the Savannah River gages at Augusta and Millhaven, Ga.; and corresponding ground-water discharge computed by hydrograph separation at Augusta, Ga.

### **Predevelopment Flow System**

In general, the period prior to major construction and production at the Savannah River Site (late 1952) is representative of predevelopment, steady-state conditions in the study area (Clarke and West, 1997). Prior to 1952, ground-water withdrawals were small and limited to widely scattered pumping centers such as Augusta, Ga., and Barnwell and Allendale, S.C. In late 1952, large water withdrawals began at SRS, and water-level declines in several aquifers were observed in scattered areas.

Under predevelopment conditions, the ground-water flow regime was in a state of dynamic equilibrium—long-term recharge equalled long-term discharge—and no change in aquifer storage took place. Ground-water-level fluctuations largely were seasonal. Clarke and West (1997) reported that during 1992, seasonal ground-water-level fluctuations in the study area generally were 4 ft or less, with scattered larger changes near areas of ground-water pumpage. Seasonal changes during the predevelopment period probably were of similar magnitude.

The configuration of the potentiometric surfaces, developed by Clarke and West (1997), indicate that ground-water flow is influenced by surface topography and streams throughout the study area for the largely unconfined Upper Three Runs aquifer and in northern areas where the confined Gordon aquifer, and Dublin and Midville aquifer systems are at or near land surface (plates 1-3). For each of the seven aquifers, major surface-water drains include the Savannah River, South Fork of the Edisto River, Brier Creek, and Upper Three Runs Creek. Major ground-water divides are present near interstream drainage divides and include the area between the Ogeechee River and Brier Creek in Georgia, and the area between the South Fork of the Edisto River and Salkehatchie River in South Carolina.

### **Modern-Day (1987–92) Flow System**

The modern-day flow system is assumed to be represented by average hydrologic conditions during 1987–92, a period of relatively steady ground-water levels, invariable climatic conditions, and pumping stresses. Water levels in the seven aquifers generally fluctuated about 5 ft or less during this period.

In most aquifers, ground-water flow directions, recharge and discharge areas, and hydrologic boundaries during 1987–92 remained largely unchanged from the predevelopment period as indicated by the modern-day potentiometric-surface maps (plate 3a, 3b, 3c, 3d).

Water levels in the seven principal aquifers over most of the study area showed little long-term change from predevelopment to modern-day conditions (Clarke and West, 1997). Siple (1967) described the continuing contemporaneity of potentiometric conditions in the SRS area based on comparison of measurements made in 1954, with measurements made in 1960 and 1963. Contemporaneity also was observed in the present study—evaluation of water-level data from 283 wells having 10 or more years of record prior to 1993—indicates that water levels generally have changed little over time, although isolated areas of water-level change did occur in parts of the study area (Clarke and West, 1997). These changes could be the result of seasonal or long-term changes in precipitation, pumpage, or of combinations or effects of these changes, such as increased rates of vertical leakage. Most changes are less than 15 ft, with larger changes limited to pumping centers at the SRS; south of the SRS; and in the Augusta, Ga., area. Clarke and West (1997) provide a detailed discussion of ground-water-level fluctuations and long-term trends in the vicinity of the SRS.

The configuration of the potentiometric surface of the Upper Three Runs aquifer remained largely unchanged from predevelopment (plate 1b) to 1987–92 (plate 3a). Evaluation of data from 200 wells indicates that long-term water-level changes in the Upper Three Runs aquifer ranged mostly from -17 to +18 ft, and that larger changes ranging from -44 ft to +43 ft, occur in areas influenced by pumpage (Clarke and West, 1997). Water-level declines in excess of 15 ft occurred in scattered wells located in northern Jefferson, northern Burke and southern Screven Counties, Ga.; and at SRS, in Aiken and Barnwell Counties, S.C. Water-level declines of 5 to 15 ft were widespread in much of Screven County, Ga., probably the result of irrigation pumpage in the area. Water-level rises in excess of 15 ft occurred in southern Jefferson, Screven, and eastern Burke Counties, Ga.; in the northern part of SRS in Aiken and Barnwell Counties, S.C.; and east of SRS in central Barnwell County, S.C. These water-level changes caused no apparent shift in the position of ground-water divides or recharge and discharge areas for the Upper Three Runs aquifer. In the central part of the SRS, however, the areal extent of a large potentiometric high noted under predevelopment conditions (as indicated by the closed 260- and 300-ft contours) (plate 3a) decreased because of water-level declines in that area. Because pumpage from the Upper Three Runs aquifer is small in this area, this water-level decline suggests leakage to underlying units where pumping occurs.

The configuration of the potentiometric surface of the Gordon aquifer remained largely unchanged from predevelopment (plate 1c) to 1987-92 (plate 3b). Evaluation of data from 28 wells completed in the Gordon aquifer indicates that maximum long-term water-level changes mostly were between -18 and +13 ft (Clarke and West, 1997). Water-level declines in excess of 5 ft occurred in northern Jenkins County, northeastern Burke County, southern Jefferson County, eastern Barnwell County, eastern Burke County, and in the northern part of the SRS in Aiken County. Water-level rises of more than 5 ft occurred in Jenkins, Screven, Barnwell, and Aiken Counties. Each of the changes in excess of 5 ft occurred near supply wells completed in the Gordon aquifer. These water-level changes caused no apparent shift in the position of ground-water divides or recharge and discharge areas for the Gordon aquifer over most of the area. In eastern Barnwell County at the town of Blackville, a small cone of depression developed because of increased pumpage that resulted in a water-level decline of about 38 ft (Clarke and West, 1997).

In the Dublin aquifer system, water-level changes in the upper and lower Dublin aquifers resulted in some changes to the configuration of the composite potentiometric surface for the two aquifers (plates 2a, 2b, and 3c). Although there are no long-term data available for the Millers Pond aquifer, maximum observed long-term water-level changes in 11 wells completed in the upper Dublin aquifer mostly ranged from -22 to +15 ft, and in 8 wells completed in the lower Dublin aquifer mostly ranged from -14 to +4 ft (Clarke and West, 1997). Water-level declines in excess of 5 ft occurred near supply wells in south-central Jefferson County, central Burke County, southwestern Richmond County, southwestern Screven County, southern Allendale County; and in the northern part of the SRS in southwestern Aiken County. These water-level declines changed the configuration of the potentiometric surface near the river in the southern part of the area. In that area, the ground-water divide or "saddle" that occurred between the 160-ft contours on the predevelopment map (plate 2a, 2b) changed position and occurs over a wider area between the 140-ft contours that cross the river in an upstream and downstream direction (plate 3c). Away from the river, a general shifting of contours northward is evident on the map and is indicative of some water-level decline. Despite these changes, the position of major ground-water divides are largely unchanged from predevelopment conditions.

In local areas, water-level declines in some wells in the upper and lower Midville aquifers changed the configuration of the 1987-92 composite potentiometric surface (plate 3d) from predevelopment (plate 2c, 2d). Long-term water-level data for the upper Midville aquifer are sparse; maximum observed water-level fluctuations prior to 1993 were +16 ft in one Georgia well, and -4 ft in one South Carolina well (Clarke and West, 1997). In the lower Midville aquifer, the maximum observed water-level change prior to 1993 in 34 wells mostly was between -40 and +8 ft. Water-level declines in excess of 5 ft occurred near supply wells in Richmond, Aiken, and Barnwell Counties. The largest and most widespread water-level declines occurred in eastern Richmond County near the Savannah River alluvial valley, where declines of as much as 59 ft occurred (Clarke and West, 1997). In this area, the size of the 100 ft closed contour representing a depression in the potentiometric surface expanded slightly, and contours west of the alluvial valley shifted slightly northwestward, indicating water-level decline. In the southern part of the study area, near the Savannah River, the 180-ft contour expanded eastward and southward in response to increased ground-water withdrawal and associated water-level decline in the Midville aquifer system in northwest Allendale County, S.C.

Hydrograph-separation estimates of mean-annual ground-water-discharge rates during 1987-92 were compared to estimates for the entire period of record (including 1987-92) to determine any variation from long-term average conditions (Appendix A). Comparison of area-weighted estimates (in/yr) for the two periods indicate that ground-water contribution to streamflow at most sites was nearly the same for both periods.

Estimated ground-water discharge during 1987-92 was slightly lower than the period of record in the upper reach of Upper Three Runs Creek and about 40 percent lower in middle reach of Brier Creek between streamflow gages 02197830 and 02198000 (see locations, fig. 2). Lower flows in Brier Creek during 1987-92 than during the period of record may be the result of measurement error or variations in the discharge measurements used to compute the means, or by one or more of the following factors, each of which can reduce the amount of local ground-water flow available to discharge into the creek:

- larger surface-water withdrawals from the creek;
- increased ground-water withdrawals from the surficial Upper Three Runs aquifer, which reduced the amount of local ground-water flow available to discharge into the creek;
- changes in agricultural crop patterns that increased the amount of evapotranspiration; or
- a combination of measurement errors and the previous three factors.

### SIMULATION OF GROUND-WATER FLOW

Ground-water flow was simulated using the USGS three-dimensional finite-difference ground-water-flow model program, MODFLOW (McDonald and Harbaugh, 1988). The quasi-three-dimensional approach assumed that (1) within aquifers, flow is essentially parallel to the structural trends of the aquifer (nearly horizontal); (2) the vertical component of flow between aquifers is controlled by the vertical hydraulic gradient and conductivity, thickness of the confining unit, and by the aquifers; and (3) horizontal flow and storage change within the confining units are minor compared to corresponding rates in aquifers.

MODFLOW solves the governing partial-differential equation for movement of ground water of constant density through a porous medium

$$\frac{\partial}{\partial x} \left( K_{xx} \frac{\partial h}{\partial x} \right) + \frac{\partial}{\partial y} \left( K_{yy} \frac{\partial h}{\partial y} \right) + \frac{\partial}{\partial z} \left( K_{zz} \frac{\partial h}{\partial z} \right) - W = S_s \frac{\partial h}{\partial t} \quad (1)$$

where

$x$ ,  $y$ , and  $z$  are cartesian coordinates aligned along the major axes of aquifer hydraulic conductivity  $K_{xx}$ ,  $K_{yy}$ , and  $K_{zz}$  [ $LT^{-1}$ ];

$h$  is hydraulic head [ $L$ ];

$W$  is a volumetric flow rate per unit volume used to represent sources and sinks [ $T^{-1}$ ]

$S_s$  is the specific storage of the porous material [ $L^{-1}$ ];

$L$  and  $T$  represent dimensions in length and time, respectively.

The model is represented as a three-dimensional matrix of discrete nodes centered in grid cells. For each grid cell, a finite-difference equation is formulated that constitutes an approximation of equation (1). These approximations are assembled into a set of simultaneous finite-difference equations that are solved by using an iterative solution technique.

The ground-water flow model was designed to simulate steady-state conditions. After large-scale pumpage began in late 1952, ground-water levels declined in some areas and quantities of discharge to streams and springs were reduced. To assess whether these changes in pumpage produced a transient response in the ground-water flow system, a series of sensitivity tests were conducted (see section, "Testing of model for transient response to pumping"). These tests indicate that the flow system during 1953-92 was acting under steady-state conditions—that is, the aquifers equilibrated rapidly to the new condition with virtually no contribution from aquifer storage.

Input requirements for simulating ground-water flow varies depending on the type of simulation (table 2). Steady-state simulations require input of hydraulic characteristics of aquifers and confining units, boundary conditions, and ground-water pumpage (if any). Transient simulations require the same input parameters as steady-state simulations, but also require time-step parameters and arrays of storage characteristics of the aquifers, expressed as storage coefficient for confined aquifers. Input requirements, sources of data, and calibration procedures for the SRS model for both steady-state and transient simulations are listed in table 2.

**Table 2.** Input requirements, sources of data, and calibration procedures for finite-difference ground-water flow model of Savannah River Site area

[Units: ft<sup>3</sup>/d, cubic foot per day; ft<sup>2</sup>/d, square foot per day; (ft/d)/ft, foot per day per foot of thickness; ft/d, foot per day; ft, foot; —, dimensionless]

Input parameter	Required model input		Units	Source(s) of data	Calibration procedure
	Steady state	Transient			
<b>Hydraulic properties</b>					
Transmissivity	Yes	Yes	ft <sup>2</sup> /d	derived from field data and estimated by multiplying aquifer thickness by median lateral hydraulic conductivity derived from aquifer tests, specific-capacity estimates, and electrical resistivity estimates	adjusted based on head residuals in well network and observed drawdown response and simulated ground-water budget
Vertical leakance	Yes	Yes	(ft/d)/ft	estimated from confining-unit-thickness maps and limited vertical hydraulic-conductivity data	adjusted based on head residuals in well network, on the direction and magnitude of vertical flux simulated between vertically adjacent units, on simulated river fluxes, and on simulated drawdown response
Riverbed conductance	Yes	Yes	ft <sup>2</sup> /d	estimated from aquifer and confining-unit-thickness maps, and limited vertical hydraulic conductivity data	adjusted based on head residuals in well network, on the direction and magnitude of vertical flux simulated between vertically adjacent units, on simulated river fluxes, and on simulated drawdown response
Storage coefficient	No	Yes	—	estimated from limited aquifer-test data. Mean of aquifer-test values for layer assigned to entire layer	adjusted based on simulated drawdown response
<b>Boundary conditions</b>					
Specified head of source/sink layer	Yes	Yes	ft	derived from digitized potentiometric surface map of Upper Three Runs aquifer (Clarke and West, 1997)	adjusted based on head residuals in well network, on the direction and magnitude of vertical flux simulated between vertically adjacent units, on simulated river fluxes, and on simulated drawdown response
River head	Yes	Yes	ft	derived from digitized potentiometric-surface map of Upper Three Runs aquifer (Clarke and West, 1997), and from U.S. Geological Survey (1989) Digital Line Graph hypsography (topographic relief) file	adjusted based on head residuals in well network, on the direction and magnitude of vertical flux simulated between vertically adjacent units, on simulated river fluxes, and on simulated drawdown response
Lateral specified head boundary of active model layers 2-7	Yes	Yes	ft	derived from digitized potentiometric surface maps of Gordon, upper and lower Dublin, and upper and lower Midville aquifers (Clarke and West, 1997)	adjusted based on head residuals in well network and on simulated river fluxes
Recharge	Yes	Yes	ft/d	derived from estimated average-recharge rate of 14.5 in/yr for Savannah River basin (Faye and Mayer, 1990)	adjusted based on head residuals in well network and on simulated river fluxes. Values kept at 20 in/yr or less based on maximum estimated value of 19.8 in/yr by Faye and Mayer (1990)
<b>Stresses</b>					
Ground-water pumpage	<sup>1/</sup> Yes	Yes	ft <sup>3</sup> /d	derived from historical and modern water-use reports (Clarke and West, 1997)	adjusted based on simulated drawdown response; maximum adjustment 25 percent prior to 1980; 10 percent 1980-92

<sup>1/</sup>Pumpage is not required for predevelopment steady-state model, but is required for steady-state simulation of stress periods during 1953-92.

## Spatial and Vertical Discretization

The finite-difference technique employed by MODFLOW requires that a simulated area be divided into discrete blocks or cells. The finite-difference grid for the SRS model was designed with consideration of the hydrogeologic framework, conceptualized stream-aquifer flow, and orientation of the Savannah River. The grid was aligned nearly parallel to the Savannah River—regional dip of hydrogeologic units—and orientation of a regional ground-water flow model of Coastal Plain aquifers developed by Faye and Mayer (1997). Total grid area encompasses about 4,455 mi<sup>2</sup>, of which about 3,250 mi<sup>2</sup> is actively simulated. The grid consists of 130 rows and 102 columns with a variable-grid spacing ranging in size from 0.33 mi x 0.33 mi, to 2.0 mi x 2.5 mi (plates 1, 2). Smaller grid sizes were utilized near the Savannah River and near aquifer outcrop areas which are characterized by high relief and steep gradients. Larger grid sizes were utilized in areas distant from the Savannah River or from aquifer outcrop areas. Typically, large grid sizes were used where hydrogeologic units were not well defined as centrally in the study area, and the level of accuracy was not critical to the simulation of ground-water flow and stream-aquifer relations.

The flow model was vertically discretized into seven layers (A1–A7) that are separated to varying degrees by six confining units. Model layers and corresponding field and calibrated values of hydraulic properties for the 13 simulated hydrogeologic units are listed in table 3; a schematic diagram showing conceptualization of model layers and boundary conditions is shown in figure 6.

## Hydraulic Characteristics

Transmissivity—product of lateral hydraulic conductivity and aquifer thickness—describes water-transmitting characteristics of aquifers. Mean transmissivity values are highest for the lower Midville aquifer (8,900 feet squared per day (ft<sup>2</sup>/d) and lowest for the Millers Pond aquifer (1,020 ft<sup>2</sup>/d) (table 3). Initial transmissivity values were assigned to the model using field observations, where available; and in areas of sparse data coverage, aquifer thickness was multiplied by the median value of lateral hydraulic conductivity derived or estimated from aquifer tests, specific capacity, and borehole-resistivity data.

Storage coefficient—product of specific storage of an aquifer or confining unit and the unit's thickness—defines storage characteristics of aquifers and confining units. Values listed in table 3 were determined from limited multiple-well aquifer tests conducted in the study area and are available only for the Gordon (A2),

upper Dublin (A4), and lower Midville (A7) aquifers. Storage coefficient is not used for steady-state simulations, but was required for testing the model under transient conditions (see section, "Testing of model for transient response to pumpage").

Leakance—a measure of the vertical water-transmitting capabilities of aquifers and confining units—is described by the equation (McDonald and Harbaugh, 1988):

$$L = \frac{1}{\frac{1}{2\Delta z_u} + \frac{1}{2\Delta z_l} + \frac{1}{\Delta z_c}} \left( \frac{1}{Kz_u} + \frac{1}{Kz_l} + \frac{1}{Kz_c} \right) \quad (2)$$

where

- $L$  is the leakance [ $T^{-1}$ ];
- $\Delta z_u$  is the thickness of the upper aquifer [L];
- $\Delta z_c$  is the thickness of the intervening confining unit [L];
- $\Delta z_l$  is the thickness of the lower aquifer [L];
- $kz_u$  is the vertical hydraulic conductivity of the upper aquifer [ $LT^{-1}$ ];
- $kz_c$  is the vertical hydraulic conductivity of the intervening confining unit [ $LT^{-1}$ ];
- $kz_l$  is the vertical hydraulic conductivity of the lower aquifer [ $LT^{-1}$ ].

In most of the study area, values of  $kz_c$  are much smaller than values of either  $kz_u$  or  $kz_l$ ; and thus, the movement of water is restricted primarily by the  $kz_c$  term of equation (2). Based on this observation, initial leakance values were assigned on the basis of thickness variations of confining units. Where units were thick—generally in downgradient areas to the south—low leakance values were assigned; where units were thin—generally in upgradient areas to the north—higher leakance values were assigned. Estimates of leakance listed in table 3 were derived at selected sites by multiplying the thickness of confining units by the vertical hydraulic conductivity of the confining unit derived from permeameter tests or estimated from grain-size analyses of core. The mean of these leakance values is lowest for the lower Midville confining unit (C6) ( $1.0 \times 10^{-5}$  feet per day per foot thickness (ft/d)/ft), and highest in the Gordon confining unit (C1) ( $2.1 \times 10^{-3}$  (ft/d)/ft). The derivation of leakance values solely from confining unit properties probably is appropriate for most aquifer layers; however, low permeability layers within the Upper Three Runs aquifer (A1) probably influence leakance values to a greater degree than in other aquifers. These low permeability layers may result in low leakance values assigned to the Gordon confining unit in upgradient areas, even where the lithostratigraphic equivalent of the confining unit is absent.

**Table 3.** Ranges of field observations and estimates for transmissivity, storage coefficient, and confining unit leakance by hydrogeologic unit for ground-water flow model of Savannah River Site area  
 [Units: ft<sup>2</sup>/d, square foot per day; (ft/d)/ft, foot per day per foot thickness; —, no value]

Hydrogeologic unit	Layer number		Transmissivity (ft <sup>2</sup> /d) <sup>1/</sup>			Storage coefficient <sup>2/</sup>			Estimated leakance (ft/d)/ft <sup>3/</sup>				
	Number	Number	Minimum	Maximum	Mean	Number	Minimum	Maximum	Mean	Number	Minimum	Maximum	Mean
Upper Three Runs aquife <sup>4/</sup>	A1	8	500	9,500	3,260	—	—	—	—	—	—	—	—
Gordon confining unit	C1	—	—	—	—	—	—	—	—	6	4.7 x 10 <sup>-6</sup>	1.2 x 10 <sup>-2</sup>	2.1 x 10 <sup>-3</sup>
Gordon aquifer	A2	18	180	12,200	4,460	2	3.0 x 10 <sup>-4</sup>	3.7 x 10 <sup>-4</sup>	3.4 x 10 <sup>-4</sup>	—	—	—	—
Millers Pond confining unit	C2	—	—	—	—	—	—	—	—	—	—	—	—
Millers Pond aquifer	A3	10	195	2,000	1,020	—	—	—	—	—	—	—	—
Upper Dublin confining unit	C3	—	—	—	—	—	—	—	—	9	1.8 x 10 <sup>-6</sup>	1.6 x 10 <sup>-3</sup>	3.6 x 10 <sup>-4</sup>
Upper Dublin aquifer	A4	17	555	25,200	5,830	2	4.2 x 10 <sup>-4</sup>	4.4 x 10 <sup>-4</sup>	4.3 x 10 <sup>-4</sup>	—	—	—	—
Lower Dublin confining unit	C4	—	—	—	—	—	—	—	—	1	2.4 x 10 <sup>-5</sup>	2.4 x 10 <sup>-5</sup>	2.4 x 10 <sup>-5</sup>
Lower Dublin aquifer	A5	21	40	8,900	3,940	—	—	—	—	—	—	—	—
Upper Midville confining unit	C5	—	—	—	—	—	—	—	—	11	6.7 x 10 <sup>-7</sup>	3.9 x 10 <sup>-4</sup>	7.6 x 10 <sup>-5</sup>
Upper Midville aquifer	A6	15	1,300	5,430	2,760	—	—	—	—	—	—	—	—
Lower Midville confining unit	C6	—	—	—	—	—	—	—	—	1	1.0 x 10 <sup>-5</sup>	1.0 x 10 <sup>-5</sup>	1.0 x 10 <sup>-5</sup>
Lower Midville aquifer	A7	37	800	25,500	8,900	6	7.1 x 10 <sup>-5</sup>	1.3 x 10 <sup>-4</sup>	1.1 x 10 <sup>-4</sup>	—	—	—	—

<sup>1/</sup>Determined from aquifer tests and estimated from specific-capacity data and from hydraulic-conductivity estimates derived from borehole resistivity logs and aquifer thickness.

<sup>2/</sup>Determined from multiple well-aquifer tests.

<sup>3/</sup>Estimated by dividing the vertical hydraulic conductivity of confining unit by the thickness of the confining unit.

<sup>4/</sup>Source/sink layer for gound-water flow model.

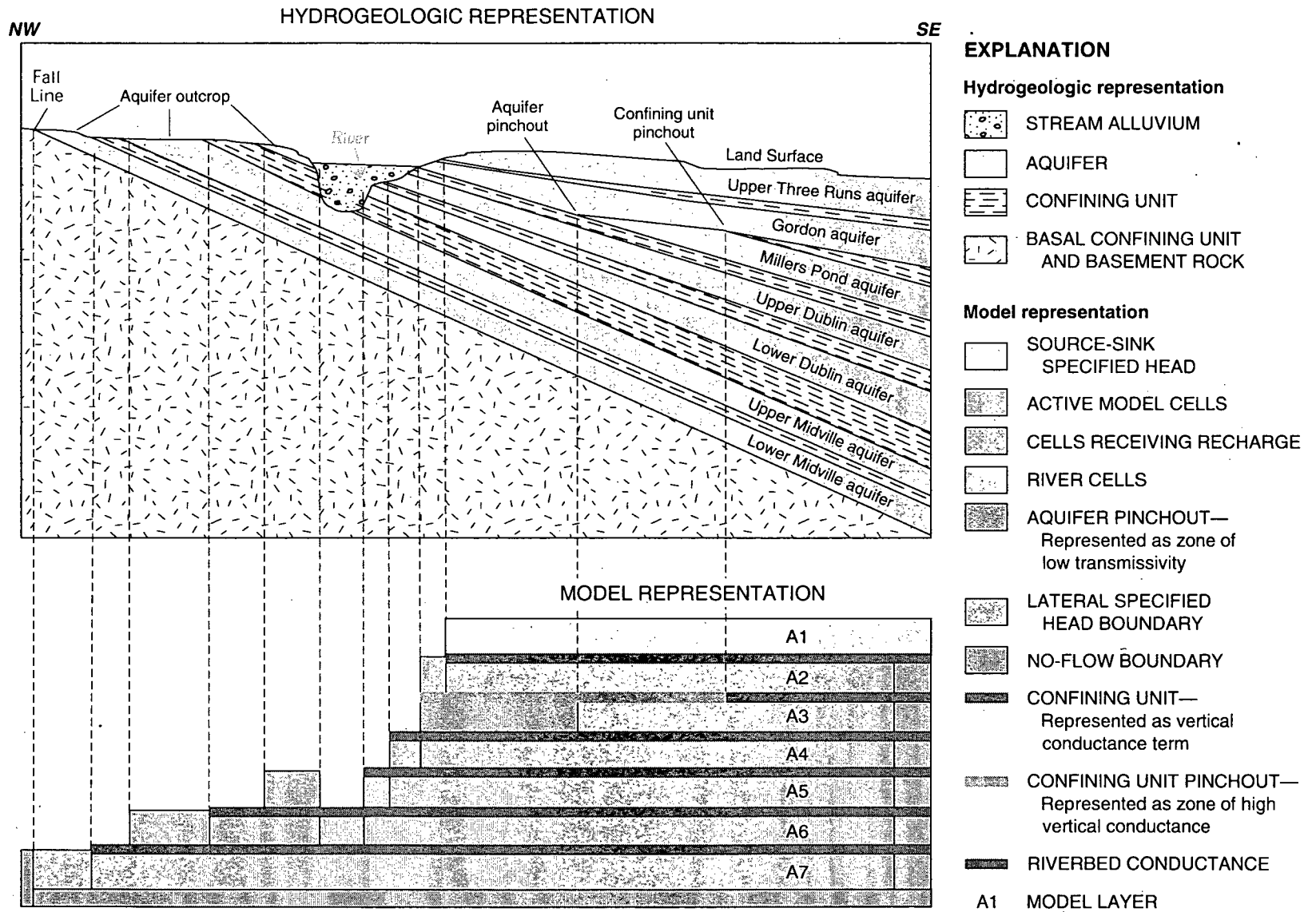


**Figure 6.** Schematic diagram showing hydrogeologic framework, model layers, and boundary conditions for the Savannah River Site area ground-water model.

Simulated vertical flow between model layers was controlled by varying the leakance between layers. Because several of the aquifers and confining units are discontinuous (pinch out) in the study area, hydraulic properties were adjusted to simulate the absence of the unit:

- where an aquifer pinches out, a very low initial value of transmissivity was assigned ( $0.9 \text{ ft}^2/\text{d}$ ) to restrict the potential for lateral flow; and
- where a confining unit pinches out, a very high initial value of leakance was assigned ( $0.9 \text{ (ft/d)/ft}$ ) to permit transfer of vertical flow between aquifers.

### Boundary Conditions

Lateral boundary conditions for the ground-water flow model were selected to coincide as closely as possible with assumed no-flow boundaries or ground-water divides. A schematic diagram of model layers and boundary conditions is shown in figure 6. Maps showing boundary conditions for each of the seven aquifer layers are shown in plates 1 and 2.

The lower most model boundary represents no-flow conditions and corresponds to the contact between the base of the lower Midville aquifer and the underlying basal confining unit; in updip (northern) areas, where the basal confining unit is absent, this boundary corresponds to the contact between Coastal Plain sediments and underlying crystalline rocks or low-permeability sedimentary rocks of Paleozoic or Mesozoic age.

The uppermost boundary corresponds to the estimated water-table or potentiometric head represented by the Upper Three Runs aquifer (layer A1) and is a source/sink layer assigned specified heads throughout its extent. Head values assigned to the source/sink layer were derived from the estimated predevelopment potentiometric surface of the Upper Three Runs aquifer (Clarke and West, 1997), which is representative of head at the base of the aquifers. The upper source/sink layer (A1) corresponds to the Upper Three Runs aquifer and was assigned specified heads throughout its extent. Water in the Upper Three Runs aquifer occurs under both water-table and confined conditions in the study area (Clarke and West,

1997). Because the Upper Three Runs aquifer is sparsely utilized as a water source over most of the study area, the head distribution shown in plate 1a is considered constant throughout the steady-state and transient simulations. Clarke and West (1997) reported that during 1992, seasonal ground-water-level fluctuations in the Upper Three Runs aquifer generally were 5 ft or less, with scattered larger changes near areas of ground-water withdrawal. An evaluation of records from 200 wells indicates that long-term water-level changes in the Upper Three Runs aquifer mostly were plus-or-minus ( $\pm$ ) 10 ft, with slightly greater water-level changes in scattered areas influenced by pumping.

Southwestern and northeastern model boundaries generally correspond to ground-water divides in each layer—the southwestern ground-water divide occurs between the Ogeechee River and Brier Creek, and the northeastern ground-water divide occurs between the South Fork of the Edisto River and the Savannah River (plates 1, 2). Because natural hydrologic boundaries are not present near the southeastern limits of the model, the southeastern boundary and parts of the northwestern and northeastern boundaries for each layer were designated as specified head. Head values for these areas were derived from potentiometric maps (Clarke and West, 1997). The sensitivity of simulated heads to the position of these specified-head boundaries was tested and is described later in the “Sensitivity Analysis” section.

West of the Savannah River, the northwestern model boundary generally coincides with either (1) a no-flow boundary near the approximate contact between Coastal Plain sediments and crystalline rocks of the Piedmont at the Fall Line; (2) a no-flow boundary along Rocky Creek in Richmond County, Ga., which incises the basal (lower Midville) aquifer, and probably intercepts all or most ground water flowing to the southeast; or (3) a specified-head boundary in an area where natural-flow boundaries are not present. East of the Savannah River, the northwestern model boundary consists of (1) Horse Creek in Aiken County, S.C., which incises the basal (lower Midville) aquifer and probably acts as a no-flow boundary; or (2) a specified-head boundary east of Horse Creek in an area where natural flow boundaries are not present.

## Recharge and Discharge

The SRS ground-water flow model simulates both recharge to and discharge from the ground-water system. Local-, intermediate-, and regional-flow regimes were simulated, depending on model-cell size and topography—flow from all three regimes probably was simulated in the smaller model cells; whereas, only flow from the intermediate and regional regimes was simulated in large-model cells. This variation is due to the relatively short local flow paths to nearby streams; small cell sizes make simulation of cell-to-cell flow in the local-flow regime more likely.

Areas of ground-water recharge and discharge are influenced by the distribution of hydrogeologic unit areas of outcrop and the subsurface extent of units underlying stream alluvium (plates 1 and 2). Recharge areas generally correspond to interstream divides of high elevation, whereas discharge areas generally correspond to stream valleys of low elevation. Recharge was simulated by specifying recharge rates in designated recharge cells for outcropping aquifers (layers A2 through A7), and by model-calculated downward vertical flux from the source/sink layer (A1). A uniform value of 14.5 in/yr, representing the long-term average ground-water discharge to the Savannah River in the study area initially was applied to recharge cells in the model. (See section, "Hydrologic Budget" and table 1).

Throughout most of the study area, sediments comprising the Upper Three Runs aquifer (layer A1) onlap underlying units, and the outcrop areas of active model layers (layers A2 through A7) are limited mostly to deeply incised stream valleys (fig. 6). In the Savannah River alluvial valley, incision by the ancient Savannah River has exposed a wide band of deep aquifers (layers A4-A6) that underlie the highly permeable stream alluvium, and are in direct or nearly direct hydraulic connection with the river. Away from stream valleys, the area of exposed aquifers is considerably smaller; thus, there is little direct recharge from precipitation. Because of the limited area of exposed sediments, most recharge to the deep aquifers occurs as leakage from the source/sink layer (A1) through the Gordon confining unit.

The SRS model simulates ground-water discharge to major streams from the intermediate- and regional-flow systems; and in areas of finer grid resolution, some discharge from the local-flow system. Streams selected for simulation were designated based on whether or not

the stream had a pronounced effect on the potentiometric surfaces of aquifers, and on the degree of incisement into deeper units (A2-A7).

Ground-water discharge to streams in layers A2-A7 was simulated by using (1) river cells in areas where the aquifers are directly exposed or occur immediately beneath stream alluvium; and (2) specified-head boundaries acting as sinks in the source/sink layer (A1) in areas where the aquifers are not incised by streams (plates 1 and 2). Streams in the source-sink layer that were simulated by the SRS model are plotted on figure 2 and are indicated by reaches between streamflow-gaging stations that are listed in table 1 and Appendices A and B.

Ground-water discharge at river cells is computed in MODFLOW using the relationship:

$$Q_{riv} = \frac{KLW}{M}(HRIV - HCELL) \quad (3)$$

where

$Q_{riv}$  is the flow between the stream and aquifer [ $L^3T^{-1}$ ];

$K$  is the vertical hydraulic conductivity of the streambed [ $LT^{-1}$ ];

$L$  is the length of the stream reach in model node [ $L$ ];

$W$  is the average stream width in model node [ $L$ ];

$M$  is the streambed thickness [ $L$ ];

$HRIV$  is the altitude of stream stage [ $L$ ]; and

$HCELL$  is the simulated head in aquifer [ $L$ ].

The term  $(KLW/M)$  also is referred to as the streambed conductance ( $CRIV$ ).

Rates of ground-water discharge to streams are largely controlled by the vertical hydraulic conductivity of hydrogeologic units directly underlying the streams. Because of the regional structural dip of sediments, aquifers and confining units alternate beneath the river, resulting in significant variations in aquifer discharge along the river's course. Ground-water discharge is highest in areas where aquifers directly underlie the river and lowest where confining units underlie the river. To capture these variations in the simulation,  $CRIV$  values were varied according to hydrogeologic units directly

under streams. The streambed (alluvial) hydraulic conductivities are higher than the vertical hydraulic conductivity of the underlying aquifers and confining units, and water entering the streambed is considered to discharge unimpeded to rivers. Therefore, the streambed conductance (CRIV) was used as a surrogate to simulate the vertical conductance of aquifers or confining units in contact with rivers, by calculating CRIV from vertical hydraulic conductivity data of the underlying aquifers or confining units, and by using underlying confining unit thickness or one-half underlying aquifer thickness in lieu of streambed thickness (M).

CRIV was estimated from limited vertical hydraulic conductivity and thickness data for aquifers and confining units, and using the geometric specifications for streams and underlying units in an individual cell. The width (W) of streams within individual cells was considered to include both the width of the stream and the extent of alluvial deposits. As such, the width of

major streams often is greater than the width of one cell. For example, in the Savannah River valley, alluvial deposits extend to a width of as much as 7 mi, and include as many as 22 cells across the valley. Stream widths were computed using a GIS to: (1) determine the percentage area covered by stream alluvium as indicated on digitized geologic maps (Prowell, 1994; Hetrick, 1992); and (2) determine the extent of stream floodplain as indicated by digitized elevation contours (U.S. Geological Survey, 1989). Thickness values (M) were derived from published hydrogeologic unit maps (Falls and others, 1997a, 1997b). The altitude of stream stage (HRIV) was estimated from digitized elevation contours (U.S. Geological Survey, 1989) using a GIS, and from limited well data in the Savannah River floodplain. A GIS was used to determine the length (L) of stream reaches within individual model cells. Initial estimates of CRIV used in the model are listed in table 4.

**Table 4.** Ranges of estimates for riverbed conductance (CRIV) by hydrogeologic unit

[units: ft<sup>2</sup>/d, square foot per day]

Hydrogeologic unit	Layer number	Number of values	Streambed conductivity (ft <sup>2</sup> /d)		
			Minimum	Maximum	Mean
Gordon confining unit	C1	244	0.1	1,600	140
Gordon aquifer	A2	443	240	1.6x10 <sup>+6</sup>	81,000
Millers Pond confining unit	C2	42	1,400	31,000	13,000
Millers Pond aquifer	A3	58	28,000	1.0x10 <sup>+6</sup>	121,000
Upper Dublin confining unit	C3	62	2.3	6,100	1,200
Upper Dublin aquifer	A4	207	8.6	648,000	44,000
Lower Dublin confining unit	C4	113	1.0	6,100	720
Lower Dublin aquifer	A5	176	550	1.6x10 <sup>+6</sup>	95,000
Upper Midville confining unit	C5	88	140	207,000	25,000
Upper Midville aquifer	A6	57	1,400	2.5x10 <sup>+6</sup>	294,000
Lower Midville confining unit	C6	61	0.6	6,100	790
Lower Midville aquifer	A7	108	95	406,000	85,000

## Pumpage

The locations of ground-water pumping centers and amounts of water withdrawn from these centers may significantly affect ground-water levels and stream-aquifer relations in the study area. Changes in pumping rates and the addition of new pumping centers may alter the configuration of potentiometric surfaces, reverse ground-water-flow directions, and increase seasonal and long-term water-level fluctuations in the aquifers. Major

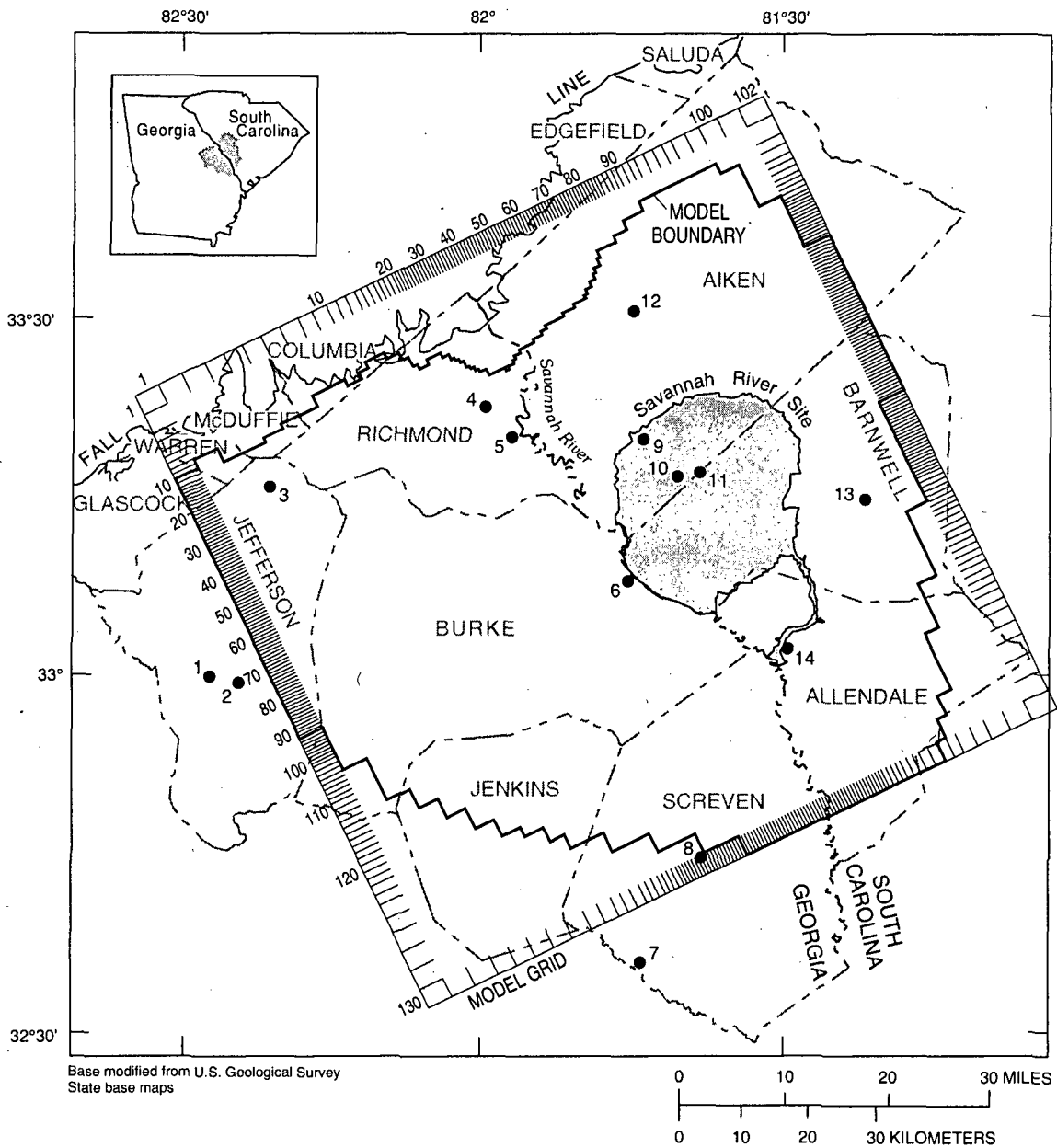
municipal and industrial pumping centers were categorized as those exceeding 1 million gallons per day (Mgal/d) during 1987–92 (table 5; fig. 7). Major pumping centers located adjacent to the Savannah River include—Plant Vogtle nuclear power station (site 6), Richmond County water system (site 4), and Olin Corporation (site 5) in Georgia; and Sandoz Corporation (site 14) and the SRS (sites 9, 10, and 11) in South Carolina.

**Table 5.** Industrial and municipal ground-water pumping centers near the Savannah River Site and average annual ground-water withdrawal, 1987–92

[limited to pumping centers withdrawing 1 million gallons per day or greater; (from Clarke and West, 1997)]

Site number	County	Site name	Type of water use	Average withdrawal during 1987-92 <sup>1/</sup> (million gallons per day)	Aquifer
<b>Georgia</b>					
1	Jefferson	J.P. Stevens, Inc.	industrial	1.40	Gordon
2	Jefferson	City of Louisville	public supply	1.37	upper Dublin
3	Jefferson	Anglo-American Clay Company	industrial	2.0	upper Dublin, lower Dublin, upper Midville, lower Midville
4	Richmond	Richmond County Water System	public supply	11.94	upper Midville, lower Midville
5	Richmond	Olin Corporation	industrial	1.08	upper Midville, lower Midville
6	Burke	Plant Vogtle Nuclear Power Station	industrial	2.41	lower Dublin, upper Midville, lower Midville
7	Screven	King Finishing Company	industrial	2.22	lower Dublin
8	Screven	City of Sylvania	public supply	1.09	Upper Three Runs
<b>South Carolina</b>					
9	Aiken	Savannah River Site A/M area	industrial	2.46	lower Dublin, upper Midville, lower Midville
10	Aiken	Savannah River Site F- area	industrial	2.01	Gordon, upper Dublin, upper Midville, lower Midville
11	Aiken and Barnwell	Savannah River Site H-area	industrial	2.27	Gordon, upper Dublin, upper Midville, lower Midville
12	Aiken	City of Aiken	public supply	1.44	lower Dublin, upper Midville, lower Midville
13	Barnwell	Barnwell Mills, Inc.	industrial	1.23	Gordon
14	Allendale	Sandoz, Inc.	industrial	1.53	upper Dublin, lower Dublin

<sup>1/</sup>Data from U.S. Geological Survey Water-Use-Data System.



**EXPLANATION**

- <sup>7</sup> GROUND-WATER PUMPING CENTER THAT WITHDREW GREATER THAN 1 MILLION GALLONS PER DAY—  
Number is site identification listed in table 5

**Figure 7.** Locations where ground-water pumpage exceeded 1 million gallons per day during 1987–92 (modified from Clarke and West, 1997), model grid and model boundary.

To simulate changes in the ground-water flow system over time, ground-water pumpage was discretized into six stress periods (table 6) based mostly on pumping trends at the SRS (Clarke and West, 1997):

- 1953–60, a period of increased pumpage at SRS;
- 1961–70, a period of relatively steady pumpage at SRS;
- 1971–75, a period of decreased pumpage at SRS;
- 1976–80, a period of increased irrigation pumpage in the southern part of the study area and relatively steady pumpage at SRS;
- 1981–86, a period of increased pumpage at SRS and Plant Vogtle; and

- 1987–92, a period of decreased pumpage at SRS and Plant Vogtle.

These six periods are not necessarily the same as the pumping trends for the entire study area shown in table 6. Ground-water flow during each stress period was simulated using six consecutive steady-state simulations (one for each stress period). Reported water-use data for industry and public supply probably has an error margin of 25 percent prior to 1980, and 10 percent during 1980–92 (R.R. Pierce, U.S. Geological Survey, oral commun., 1997). Irrigation withdrawal has an unknown margin of error, but probably exceeds 25 percent. Total pumpage in the model area increased from 11.5 Mgal/d during 1953–60, to 52.6 Mgal/d during 1987–92 (table 6).

**Table 6.** Simulated ground-water withdrawal by stress period  
[<, less than]

Stress period	Years	Withdrawal rate by model layer and aquifer, in million gallons per day						Total
		Layer A2, Gordon aquifer	Layer A3, Millers Pond aquifer	Layer A4, upper Dublin aquifer	Layer A5, lower Dublin aquifer	Layer A6, upper Midville aquifer	Layer A7, lower Midville aquifer	
1	1953-60	1.8	<0.1	0.7	3.8	1.9	3.3	11.5
2	1961-70	2.3	1.0	0.6	5.8	3.0	10.2	22.9
3	1971-75	4.2	1.4	0.8	6.7	3.6	21.4	38.1
4	1976-80	4.7	1.4	2.4	9.2	4.1	29.8	51.6
5	1981-86	9.4	2.5	4.4	8.8	5.7	20.6	51.4
6	1987-92	9.9	2.0	3.8	9.5	6.6	20.8	52.6

## Model Calibration

Model calibration is the ability of the computed results to simulate measurements, data, and/or other observations with an acceptable level of error. Calibration generally is accomplished by adjusting input values of hydraulic properties and boundary conditions within plausible limits until calibration criteria are achieved. Input data adjusted during model calibration and calibration procedures are listed in table 2.

The SRS ground-water flow model was calibrated by: (1) attempting to match potentiometric heads; and (2) approximating discharge from the ground-water flow system to major streams. Other factors considered during model calibration included: (1) matching simulation results to the conceptual model of the stream-aquifer system, including areal distributions of recharge and discharge areas; (2) adhering to the geologic and hydrogeologic framework as defined by Falls and others (1997a, 1997b); (3) maintaining "realistic" values of hydraulic properties as defined by field data; and (4) maintaining "realistic" values of estimated aquifer recharge in recharge cells and in cells supplied by leakage from the source/sink layer (A1).

The model was calibrated using the following procedures:

- model initially was calibrated to predevelopment conditions using head and streamflow-discharge data;
- hydraulic-characteristics arrays derived from calibration of the predevelopment period were used as initial conditions to simulate modern-day conditions;
- additional stresses provided by simulated pumpage during modern-day conditions allowed additional refinement of the aquifer characteristics; and
- modified characteristics then were used to refine calibration of predevelopment conditions.

This iterative process continued until the model was calibrated for both predevelopment and modern-day conditions.

Hydrologic properties adjusted during model calibration were vertical leakance, riverbed conductance, and transmissivity. Vertical leakance and riverbed conductance were adjusted during calibration more than transmissivity.

Boundary conditions adjusted during calibration consisted of head in the source/sink layer (A1); head along lateral boundaries in layers A2–A7; river stage; and recharge. Values of head in layers A1–A7 were adjusted within reasonable limits, based on observed head variations in observation wells (Clarke and West, 1997). Similarly, values of river head were adjusted within limits as determined from potentiometric maps and topographic contours. Recharge values in recharge cells and in cells supplied by leakage from the source/sink layer (A1), were constrained to be less than 20 in/yr (the maximum estimated value for the Savannah River basin as determined from hydrograph separation).

For the steady-state simulations, potentiometric heads utilized for calibration were selected as follows:

- for the predevelopment (pre-1953) period—the maximum water level in a given well in areas unaffected by pumpage was used to evaluate calibration because the predevelopment period represents the highest potentiometric surface of the aquifers (Clarke and West, 1997); and
- for the modern-day (1987–92) period—the average head in a given well was used to evaluate calibration. Because there was little water-level change attributed to pumpage during this period, use of the average head should reduce the influence of seasonal fluctuation of head on calibration results.

Wells used for model calibration, and observed and simulated heads, are listed in Appendix C. Well-construction data, ground-water levels, location, and other pertinent information for wells utilized for model calibration are provided in Harrelson and others (1997).

When multiple-head observations occurred within a single model cell, the average measured head was used for calibration and was counted as one observation for statistical comparisons. This prevented the statistics from being skewed toward areas of high data density, such as the extensively monitored waste sites located on the SRS, or well fields in the Augusta, Ga., area. The largest number of multiple-observation cells were in the Gordon aquifer (layer A2) (79 cells), followed by the lower Midville aquifer (layer A7) (20 cells). In cells containing multiple head observations, the variation of head was small, as measured water levels in 90 percent of the cells were within 10 ft of the corresponding mean value for the cell. Thus, the mean head of the cell probably is an appropriate representation for comparison with simulated values. The maximum

variation of measured heads in multiple-observation cells was within 27 ft of the mean. Such a large variation may indicate data error, large lateral hydraulic gradients, or a combination of these.

Improvement in the quality of the steady-state simulations between successive model runs was evaluated by comparisons by layer, and for the entire model of the following:

- residuals (differences) between observed head and simulated head; and the mean, root-mean-square (RMS), and standard deviation (SD) of the residuals;
- percentage of wells whose residual met established calibration criteria (see following section); and
- estimated rate of ground-water discharge to simulated discharge for selected stream reaches.

The mean of the residuals indicates whether the mean difference between computed and observed water levels is positive or negative in magnitude. The RMS is the square root of the average deviation of the residuals from zero. The following equations were used to compute the statistics:

$$\text{Mean of residuals} = \frac{1}{N} \sum_{i=1}^N (h_s - h_m) \quad (4)$$

where

$N$  is the number of measured water levels within the model area;

$h_s$  is the simulated water level at the center of the cell in which a water level was measured; and

$h_m$  is the measured water level.

$$RMS = \frac{1}{N} \sqrt{\sum_{i=1}^N (h_s - h_m)^2} \quad (5)$$

$$SD = \sqrt{\frac{1}{N-1} \sum_{i=1}^N (h_s - h_m)^2} \quad (6)$$

Simulated ground-water discharge to major streams in the area was compared with estimated values. Simulated ground-water discharge consisted of: (1) fluxes exiting through cells where MODFLOW's river package is active; and (2) fluxes entering the source/sink

layer (A1) within the stream's drainage area. This simulated discharge was summed using the MODFLOW postprocessor ZONEBUDGET (Harbaugh, 1990).

Simulated head and ground-water discharge from a calibrated ground-water model may depart from field measured values, even after a diligent calibration effort. This discrepancy (model error) may be caused by: (1) simplification of the conceptual model by the digital model; (2) difficulty in obtaining sufficient data to account for all of the spatial variation in hydraulic properties throughout the model area; (3) seasonal fluctuations and measurement error in ground-water level and streamflow-discharge data; (4) errors associated with topographic location of observation wells; and (5) errors due to cell size. Quantification of model errors associated with factors 1 and 2 is not possible; however, estimation of errors for factors 3, 4 and 5 is possible.

Based on reported ranges of fluctuations (Clarke and West, 1997), seasonal fluctuations in ground-water levels (factor 3) probably are about 5 ft. Error associated with estimates of ground-water discharge to streams are difficult to quantify; however, ranges of error can be inferred from the accuracy of the streamflow-discharge measurements used to estimate ground-water discharge to streams. According to Faye and Mayer (1990), estimates of streamflow based on stage-discharge relations probably are accurate to within 10 percent; estimates of streamflow based on discharge measurements probably are accurate to within 5 percent. Because two streamflow gages generally are involved in computation of the gain (or loss) of water along a given stream reach, these error percentages are multiplied by a factor of two. Thus, estimates of ground-water discharge based on hydrograph separation have an associated error margin of at least 20 percent, and at least 10 percent based on drought streamflow. The error associated with hydrograph-separation estimates are difficult to confirm and are of unknown confidence (Mayer and Jones, 1996). Ground-water-discharge estimates based on drought-streamflow measurements (discharge measurements) are considered to represent minimum values because of reduced recharge to an aquifer during a drought. Because the steady-state ground-water model simulates long-term-average conditions—characterized by higher ground-water discharge and recharge rates than occurred during drought conditions—one calibration goal was to maintain ground-water discharge at rates above estimates derived from drought streamflow. Measured

variation of measured heads in multiple-observation cells was within 27 ft of the mean. Such a large variation may indicate data error, large lateral hydraulic gradients, or a combination of these.

Improvement in the quality of the steady-state simulations between successive model runs was evaluated by comparisons by layer, and for the entire model of the following:

- residuals (differences) between observed head and simulated head; and the mean, root-mean-square (RMS), and standard deviation (SD) of the residuals;
- percentage of wells whose residual met established calibration criteria (see following section); and
- estimated rate of ground-water discharge to simulated discharge for selected stream reaches.

The mean of the residuals indicates whether the mean difference between computed and observed water levels is positive or negative in magnitude. The RMS is the square root of the average deviation of the residuals from zero. The following equations were used to compute the statistics:

$$\text{Mean of residuals} = \frac{1}{N} \sum_{i=1}^N (h_s - h_m) \quad (4)$$

where

$N$  is the number of measured water levels within the model area;

$h_s$  is the simulated water level at the center of the cell in which a water level was measured; and

$h_m$  is the measured water level.

$$RMS = \frac{1}{N} \sqrt{\sum_{i=1}^N (h_s - h_m)^2} \quad (5)$$

$$SD = \sqrt{\frac{1}{N-1} \sum_{i=1}^N (h_s - h_m)^2} \quad (6)$$

Simulated ground-water discharge to major streams in the area was compared with estimated values. Simulated ground-water discharge consisted of: (1) fluxes exiting through cells where MODFLOW's river package is active; and (2) fluxes entering the source/sink

layer (A1) within the stream's drainage area. This simulated discharge was summed using the MODFLOW postprocessor ZONEBUDGET (Harbaugh, 1990).

Simulated head and ground-water discharge from a calibrated ground-water model may depart from field measured values, even after a diligent calibration effort. This discrepancy (model error) may be caused by: (1) simplification of the conceptual model by the digital model; (2) difficulty in obtaining sufficient data to account for all of the spatial variation in hydraulic properties throughout the model area; (3) seasonal fluctuations and measurement error in ground-water level and streamflow-discharge data; (4) errors associated with topographic location of observation wells; and (5) errors due to cell size. Quantification of model errors associated with factors 1 and 2 is not possible; however, estimation of errors for factors 3, 4 and 5 is possible.

Based on reported ranges of fluctuations (Clarke and West, 1997), seasonal fluctuations in ground-water levels (factor 3) probably are about 5 ft. Error associated with estimates of ground-water discharge to streams are difficult to quantify; however, ranges of error can be inferred from the accuracy of the streamflow-discharge measurements used to estimate ground-water discharge to streams. According to Faye and Mayer (1990), estimates of streamflow based on stage-discharge relations probably are accurate to within 10 percent; estimates of streamflow based on discharge measurements probably are accurate to within 5 percent. Because two streamflow gages generally are involved in computation of the gain (or loss) of water along a given stream reach, these error percentages are multiplied by a factor of two. Thus, estimates of ground-water discharge based on hydrograph separation have an associated error margin of at least 20 percent, and at least 10 percent based on drought streamflow. The error associated with hydrograph-separation estimates are difficult to confirm and are of unknown confidence (Mayer and Jones, 1996). Ground-water-discharge estimates based on drought-streamflow measurements (discharge measurements) are considered to represent minimum values because of reduced recharge to an aquifer during a drought. Because the steady-state ground-water model simulates long-term-average conditions—characterized by higher ground-water discharge and recharge rates than occurred during drought conditions—one calibration goal was to maintain ground-water discharge at rates above estimates derived from drought streamflow. Measured

and simulated values of ground-water discharge for the predevelopment and modern-day steady-state periods are listed in Appendices A and B.

Errors associated with topographical location (factor 4) may occur because the water level in a well is computed relative to the land-surface elevation. Errors in land-surface elevations were introduced into water-level measurements when wells were located on topographic maps. These errors, combined with water-level measurement errors, are assumed to be 5 ft.

Errors associated with cell size (factor 5) occur because the simulated head represents the value at the center of a cell; whereas, the field-measured head could be located anywhere within a cell. This error was determined by calculating the difference in hydraulic head across a cell based on potentiometric surfaces. Errors resulting from cell size are greater where cell sizes are large (generally along the outer margins of the model), and where topographic or hydraulic gradients are steep. Typically, larger grid sizes were used in areas where hydrogeologic units were not as well defined and the level of simulation accuracy was not as critical.

Calibration criteria was established for each cell in model layers 2–7 to account for head errors associated with topographic location, seasonal fluctuation, and cell size:

$$EC = T + S + \frac{1}{2}H \quad (7)$$

where

- EC* is the error criteria in feet;
- T* is the land-surface altitude and water-level measurement error (5 ft);
- S* is the seasonal water-level fluctuation, assumed to equal 5 ft; and
- H* is the difference in hydraulic head across a cell based on potentiometric surface maps, in feet.

The *H* term in equation (7) was computed using a geographic information system to determine the head variation across a cell based on digitized maps of potentiometric surfaces by Clarke and West (1997).

A simulated head was considered calibrated when its residual was within the established calibration criteria. Although the RMS of residuals for a given layer may be relatively poor (high), the percent of matched heads based on the calibration criteria may still be relatively high. This apparent discrepancy results because the percent of matched heads maybe the same regardless of

the magnitude of the residuals. For example, if 7 of 10 heads matched the calibration criteria, the percentage matched would be 70 percent, regardless of whether the RMS of residuals was 15 or 50 ft. Measured and simulated values of hydraulic head for the predevelopment and modern-day periods, together with established calibration criteria, are listed in Appendix C.

### Steady-State Simulation of Predevelopment Flow System

Within the study area, long-term water levels and ground-water discharge from aquifers to rivers and streams showed little change during predevelopment (pre-1953) and modern-day periods (1987–92). Therefore, rates and directions of ground-water flow, and stream–aquifer relations can be evaluated using a steady-state ground-water flow model based on modification of equation (1):

$$\frac{\partial}{\partial x} \left( K_{xx} \frac{\partial h}{\partial x} \right) + \frac{\partial}{\partial y} \left( K_{yy} \frac{\partial h}{\partial y} \right) + \frac{\partial}{\partial z} \left( K_{zz} \frac{\partial h}{\partial z} \right) - W = 0 \quad (8)$$

The assumption made to apply this approach is water is not contributed to the ground-water system from ground-water storage; and thus, from equation (1)  $S \frac{\partial h}{\partial y} = 0$ . Ground-water storage contribution to the flow system was found to be insignificant during detailed testing following calibration of the predevelopment model (see section “Testing of model for transient response to pumpage”).

The predevelopment model was calibrated using observed-head data at 462 model cells (Appendix C); and ground-water discharge along 36 reaches of selected streams (see locations, fig. 2; and Appendix A and B). The calibrated model matched established error criteria for heads in 90 percent of the cells where observations were available, and simulated ground-water discharge was within 50 percent of estimated values for the selected stream reaches. Simulated ground-water flow directions and distribution of recharge and discharge are consistent with the conceptual model within most of the model area.

#### Simulated heads

Simulated heads for predevelopment conditions show an excellent match with observed values and conform to established error criteria. Summary statistics for simulated heads are listed in table 7 and Appendix C, and are plotted on figure 8. In each layer, 88 percent or greater of measured values were matched. The boxplot

shown in figure 8 indicates that 80 percent of all residuals are within about 12 ft of observed values. The RMS of residuals for all layers is 10.7 ft, ranging from 8.2 ft in the upper Dublin aquifer (A4) to 11.9 ft in the Gordon aquifer (A2) (table 7). The mean of residuals indicates whether or not simulated heads are positively

or negatively skewed. For all layers, the mean of residuals is 0.2, with no individual layer exceeding the mean by more than 3.2 ft. Three of seven layers have mean values within 0.5 and -0.5 ft. These values indicate there is little or no overall positive or negative bias for simulated heads in any layer.

**Table 7.** Calibration statistics for simulated heads for predevelopment conditions

Aquifer	Model layer	Number of observations	Percentage of heads matched <sup>1/</sup>	Root mean square of residuals (feet)	Mean of residuals (feet)	Standard deviation of residuals (feet)
Gordon	A2	178	89.3	11.9	-0.4	11.9
Millers Pond	A3	13	92.3	8.3	3.2	8.0
Upper Dublin	A4	78	89.7	8.2	0.4	8.2
Lower Dublin	A5	69	88.4	9.7	0.3	9.8
Upper Midville	A6	38	89.5	11.5	-2.6	11.3
Lower Midville	A7	86	93.0	10.8	2.2	10.6
All layers		462	90.0	10.7	0.2	10.7

<sup>1/</sup>When compared with established error criteria, EC, for each grid cell.

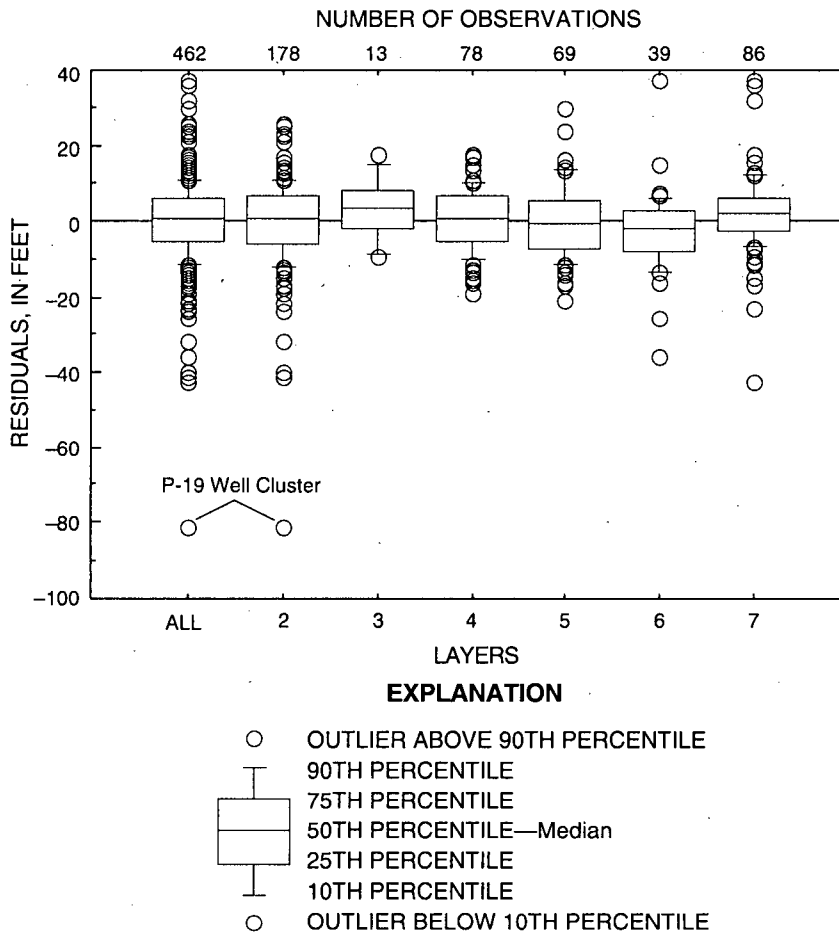


**Figure 8.** Difference between observed and simulated heads (residuals) for the predevelopment simulation.

Simulated predevelopment potentiometric-surface maps compare favorably to the configuration of interpreted potentiometric surface maps (Clarke and West, 1997), depicting many similar features including the potentiometric depression centered around the Savannah River and the ground-water divide or "saddle" located downriver of the depression (figs. 9-12). The simulated surfaces generally show flow patterns similar to interpreted maps in the vicinity of major streams; however, near some small streams and in areas of large, elongated cells along the perimeter of the model, simulated contours do not depict as pronounced a response to streams as do the interpreted potentiometric surface maps.

The distribution of simulated potentiometric-surface contours and observed heads show some areal trends that reflect model accuracy and the magnitude of water-level residuals (figs. 9-12). The area of smallest percentage of matched heads and the largest residuals of all locations is in the northwestern part of the model area. In this area, cell sizes are large and elongated, data that characterize hydraulic properties are sparse, and observed-head data largely are based on historical records. Thus, this area contains less reliable hydrological information than other parts of the study area.

In the bottom four layers (A4-A7), similar patterns of matched heads and residuals are evident: (1) south of Upper Three Runs Creek, residuals were mostly positive but of low magnitude and (2) near the Aiken-Barnwell County line and Savannah River, residuals were negative, with some heads outside of established error criteria. Negative residuals in this area may indicate that the model is simulating too much discharge to the river or is not simulating enough flow from recharge areas.

In layer A2, residuals near Upper Three Runs Creek and near the Savannah River adjacent to the SRS largely are positive, but mostly are within established error criteria. These positive residuals may indicate the model is not simulating enough discharge into the overlying stream from layer A2, or is simulating too much leakage into layer A2 from underlying units.

In the vicinity of the Pen Branch Fault and the P-19 well cluster, simulated head values for layer A2 are considerably lower than observed values from well BW-395, with a residual of -81.1 ft (Appendix C). The model was unable to match head in layer A2 in this area because (1) the water-level measurement in well BW-395 may not be representative of head in layer A2 because of problems with well construction or measurement error, or (2) of a possible localized hydraulic connection between layers A1 (Upper Three Runs) and A2 (Gordon) in the vicinity of the Pen Branch Fault. Clarke and West (1997) reported that aquifer interconnection between the two aquifers in this area may have resulted in higher head in the Gordon Aquifer than in adjacent areas.

#### Simulated water budget

The simulated predevelopment-water budget includes the following components of inflow and outflow to the ground-water flow system: (1) recharge; (2) inflow across lateral boundaries; (3) discharge to streams; and (4) outflow across lateral boundaries (table 8 and fig. 13).

**Table 8.** Simulated predevelopment water budget  
[—, not applicable]

Aquifer	Model layer	Inflow, in million gallons per day			Outflow, in million gallons per day		
		Recharge	Inflow across lateral boundaries	Total	Outflow across lateral boundaries	Discharge to streams	Total
Upper Three Runs	<sup>1/</sup> A1	<sup>2/</sup> 773	—	773	—	<sup>3/</sup> 506	506
Gordon	A2	53	5	58	2.8	230	233
Millers Pond	A3	0	2.9	2.9	0.7	8.4	9.1
Upper Dublin	A4	11.5	3.5	15	2.5	47.8	50.3
Lower Dublin	A5	45.4	4.5	49.9	4.7	92.8	97.5
Upper Midville	A6	25	18.8	43.8	12	58.6	70.6
Lower Midville	A7	18.1	62	80.1	11.4	45.1	56.5
All layers		926	96.7	1,023	34.1	988.7	1,023

<sup>1/</sup>Inactive, source/sink layer.

<sup>2/</sup>Simulated recharge derived from vertical leakage from specified head cells in source/sink layer to underlying units.

<sup>3/</sup>Simulated discharge derived from vertical leakage from underlying units to specified-head cells in source/sink layer.

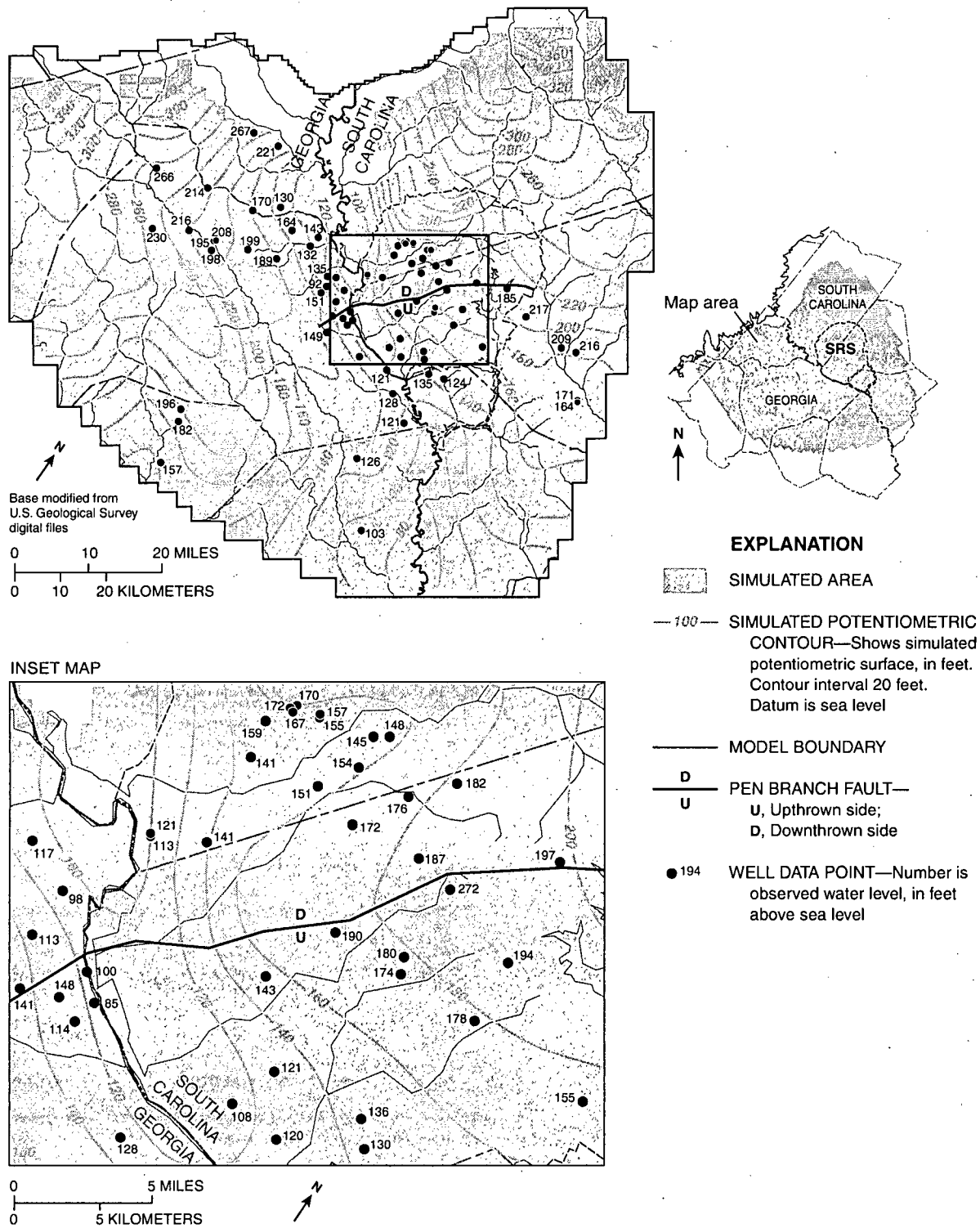
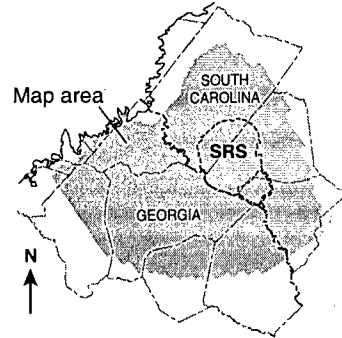
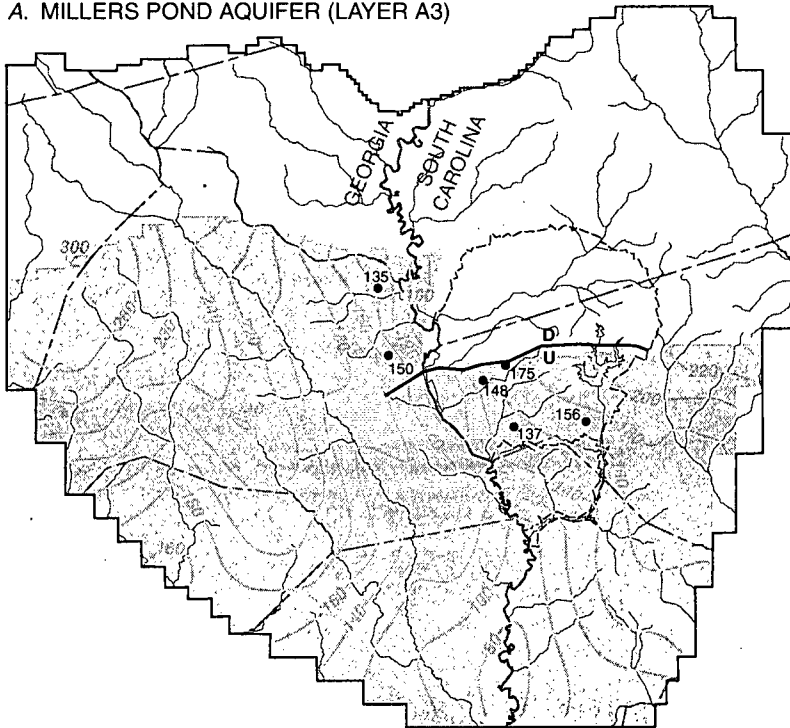


**Figure 9.** Simulated predevelopment potentiometric surface and observed heads for the Gordon aquifer (layer A2).

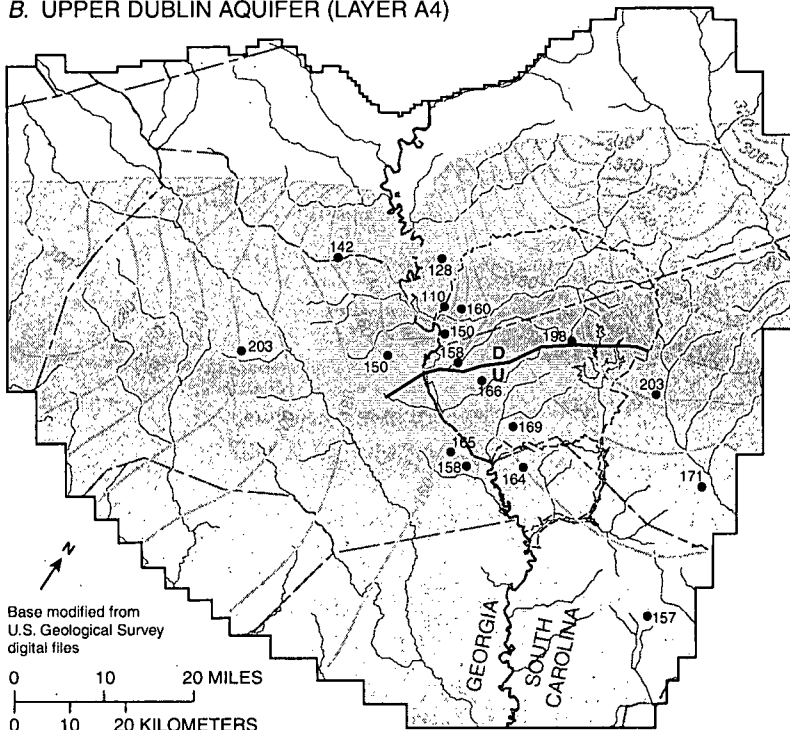
A. MILLERS POND AQUIFER (LAYER A3)



EXPLANATION

- SIMULATED AREA
- 100 SIMULATED POTENTIOMETRIC CONTOUR—Shows simulated potentiometric surface, in feet. Contour interval 20 feet. Datum is sea level
- MODEL BOUNDARY
- PEN BRANCH FAULT—  
U, Upthrown side;  
D, Downthrown side
- 203 / WELL DATA POINT—Number is observed water level, in feet above sea level

B. UPPER DUBLIN AQUIFER (LAYER A4)

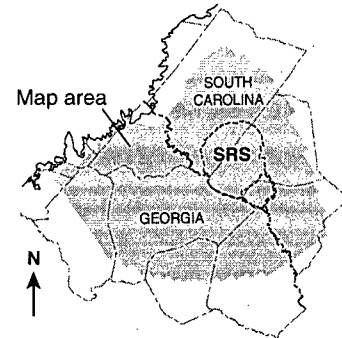
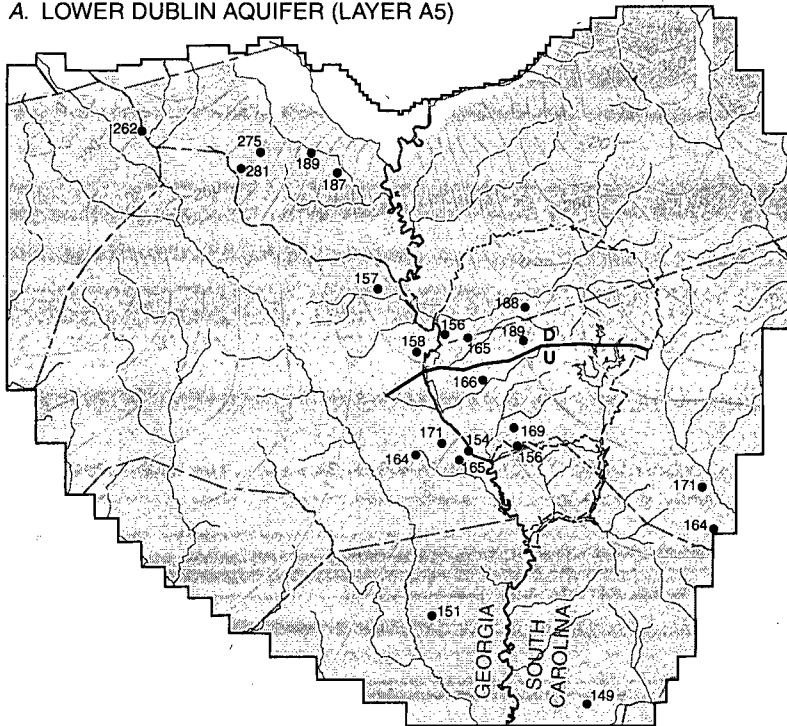


Base modified from  
U.S. Geological Survey  
digital files

0 10 20 MILES  
0 10 20 KILOMETERS

**Figure 10.** Simulated predevelopment potentiometric surface and observed heads for the (A) Millers Pond (layer A3) and (B) upper Dublin (layer A4) aquifers.

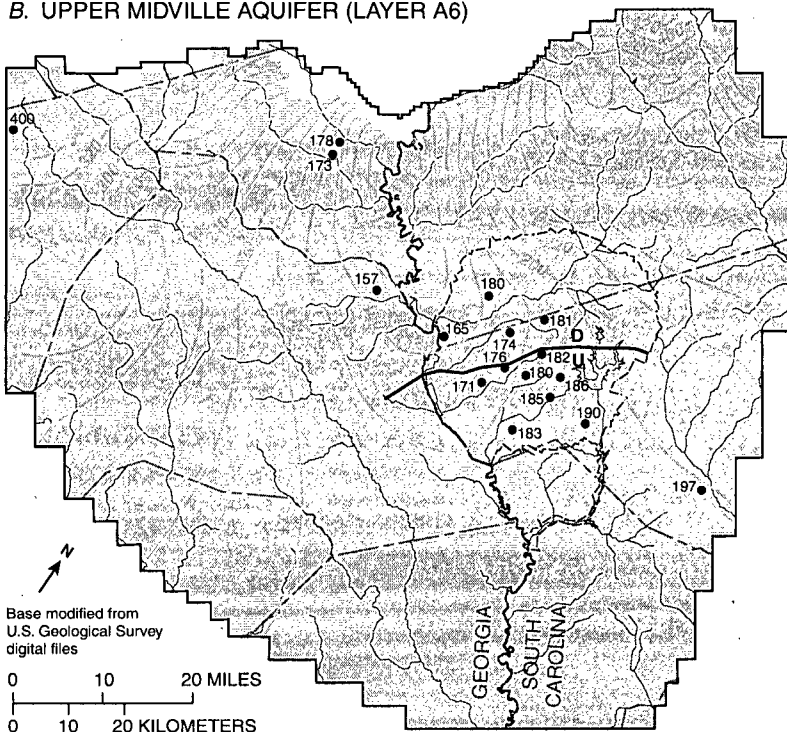
A. LOWER DUBLIN AQUIFER (LAYER A5)



EXPLANATION

-  SIMULATED AREA
-  100 SIMULATED POTENTIOMETRIC CONTOUR—Shows simulated potentiometric surface, in feet. Contour interval 20 feet. Datum is sea level
-  MODEL BOUNDARY
-  PEN BRANCH FAULT—  
U, Upthrown side;  
D, Downthrown side
-  197 WELL DATA POINT—Number is observed water level, in feet above sea level

B. UPPER MIDVILLE AQUIFER (LAYER A6)



Base modified from  
U.S. Geological Survey  
digital files

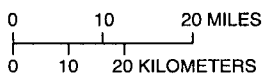
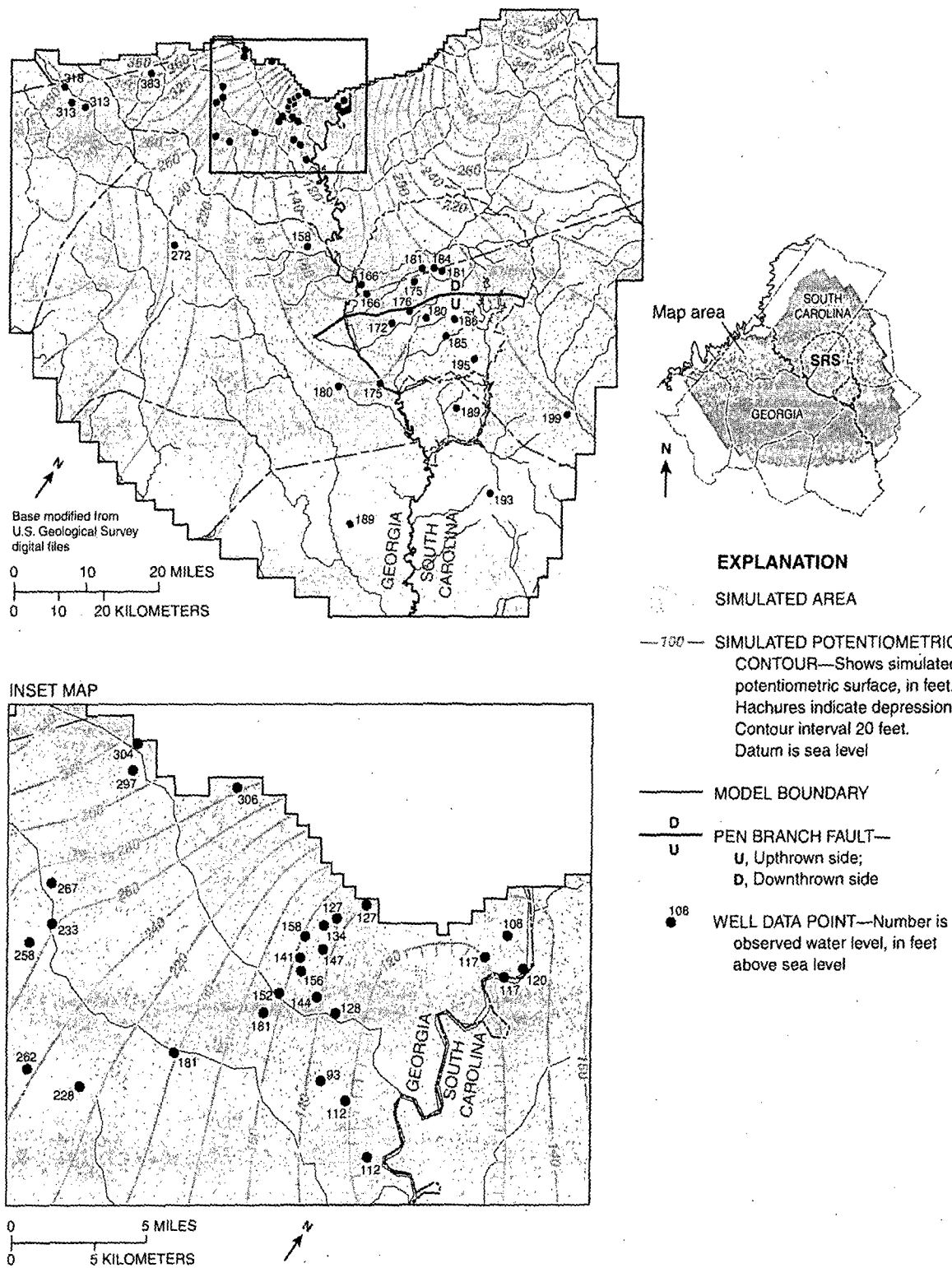
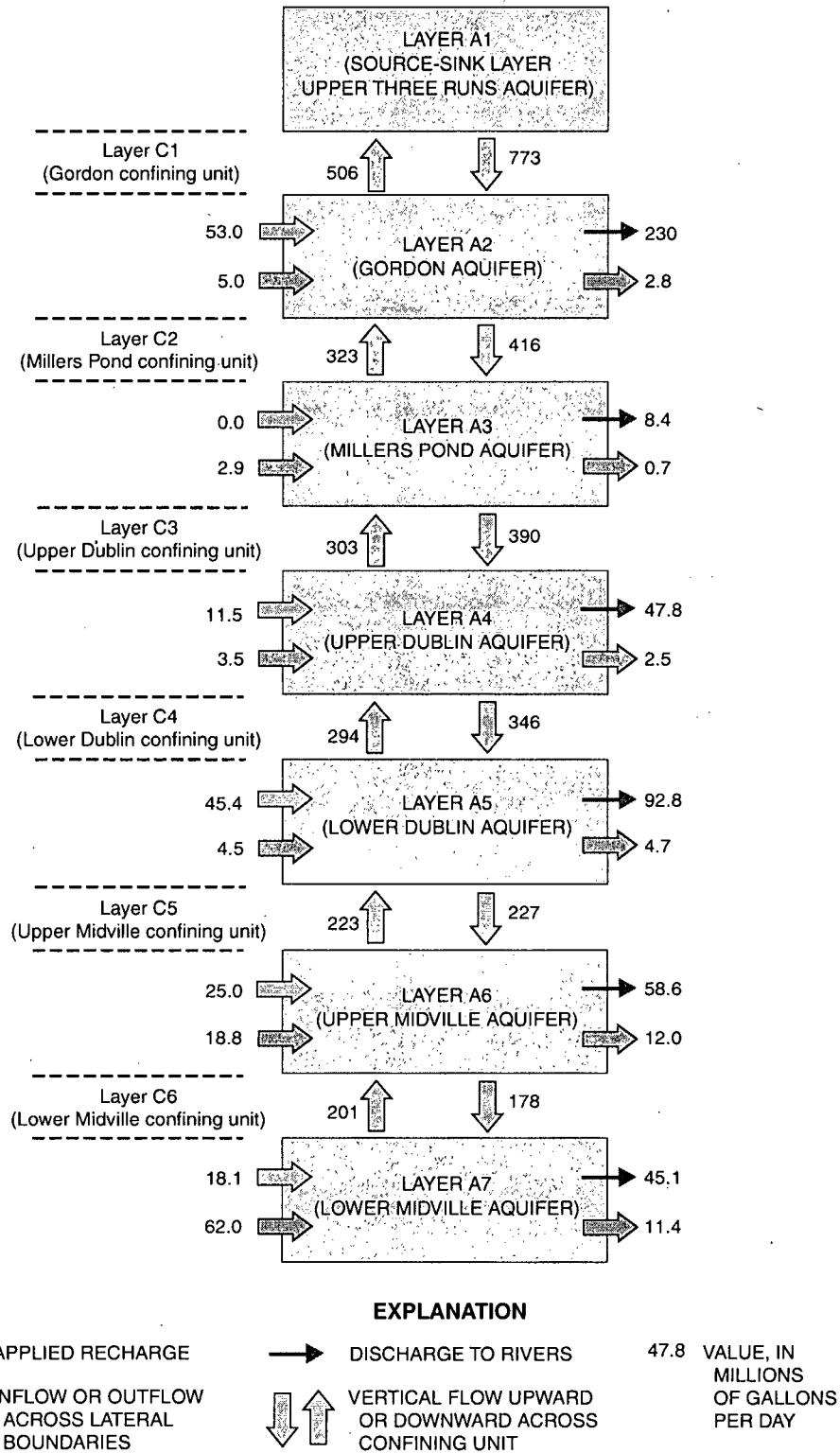


Figure 11. Simulated predevelopment potentiometric surface and observed heads for the (A) lower Dublin (layer A5) and (B) upper Midville (layer A6) aquifers.



**Figure 12.** Simulated predevelopment potentiometric surface and observed heads for the lower Midville aquifer (layer A7).



**Figure 13.** Simulated predevelopment water budget by model layer.

Of the total simulated inflow of 1,023 Mgal/d, 76 percent is contributed by leakage from constant-head cells in the source-sink layer (A1), 15 percent is contributed by direct recharge to layers A2–A7, and 9 percent is contributed as inflow from lateral specified-head boundaries in layers A2–A7. Direct recharge of aquifer sediments by precipitation contributes only a small percentage of inflow because the area of exposed-aquifer sediments is small, and mostly limited to stream valleys that typically are ground-water-discharge areas. In layer A3, for example, outcrops of aquifer sediments are not mapped in areas favorable for recharge and thus, no recharge was computed for the unit. Because direct recharge of aquifers by precipitation is limited to a small percentage of the study area, vertical leakage from layer A1 is the largest contributor to ground-water inflow. Most of the leakage from A1 occurs in interstream areas of relatively higher land-surface altitudes, where vertical-head gradients are downward. The smallest contribution to inflow is from lateral specified-head boundaries, with most of the water entering through the deepest unit (layer A7). For A7, about one-half of the water is from the northwestern-model boundary and one-half is from the northeastern-model boundary. Water entering the northeastern-model boundary possibly represents regional flow from a recharge zone outside of the simulated area. Water entering the northwestern boundary possibly represents regional flow from recharge areas between the model boundary and the Fall Line, with a possible small contribution from fractured crystalline rocks of the Piedmont Province.

Of the total 1,023 Mgal/d outflow, ground-water discharge to streams accounts for 97 percent of the outflow, with only 3 percent attributed to outflow at lateral specified-head boundaries. Ground-water discharge to streams is equally divided between simulated river cells in layers A2–A7, and streams simulated as areas of low specified head in the source-sink layer (A1). Of the total simulated stream discharge, 988 Mgal/d, flow to the Savannah River accounts for 43 percent; Brier Creek, 28 percent; and Upper Three Runs Creek, 8 percent.

#### *Simulated Ground-Water Recharge*

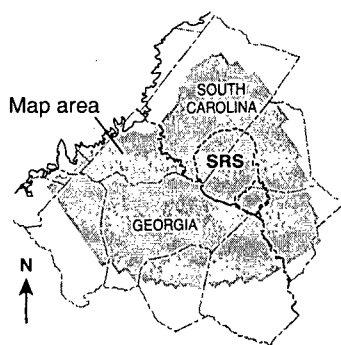
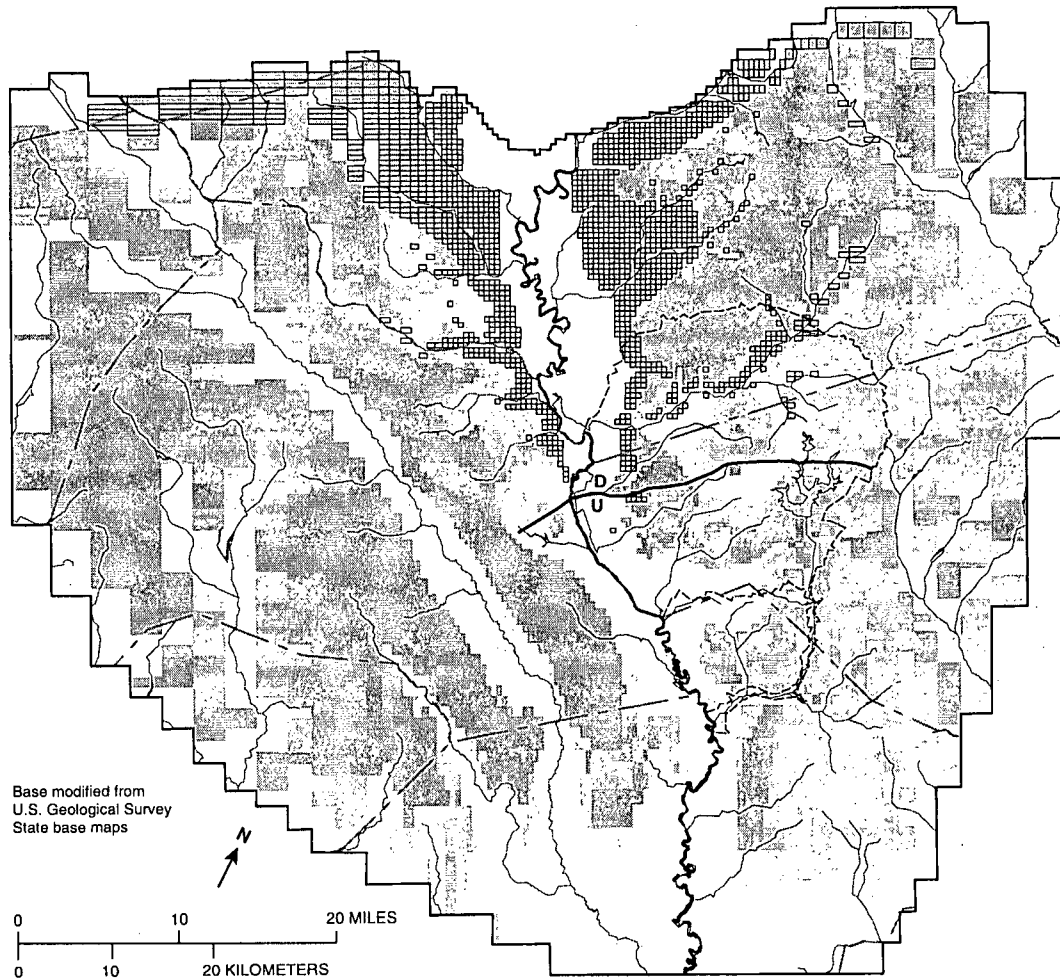
Ground-water recharge was simulated by using specified recharge rates in cells located in aquifer-outcrop areas (layers A2–A7), and with model-calculated downward vertical flux from the source/sink layer (A1). Goals during calibration included maintaining consistency with the conceptual model of

the flow system, and “realistic” values of estimated aquifer recharge in recharge cells and in cells supplied by leakage from the source/sink layer (A1). To maintain consistency with the conceptual model, no recharge was simulated in stream valleys (where discharge occurs) or in selected urban areas where land surface is impervious. Further, values assigned to recharge cells or calculated from layer A1 (vertical flux) did not exceed 20 in/yr (the maximum estimated value for the Savannah River basin; table 1). Values of vertical flux from layer A1 were maintained below 20 in/yr by adjusting, within realistic limits, values of vertical conductance and specified heads in A1.

The total simulated recharge to the ground-water system is 926 Mgal/d (table 8), calculated by summing values assigned to recharge cells and values computed as vertical flux from layer A1. This is equivalent to an average of about 6 in/yr over the entire model area. Calibrated recharge values for recharge cells range from 8 in/yr where confining units crop out, to 16 in/yr where aquifers crop out. The calculated recharge from layer A1 ranges from about 0 to 19.6 in/yr, with a mean of about 8.7 in/yr. Ninety percent of the values calculated from layer A1 are less than 18 in/yr, and 75 percent are less than 15 in/yr.

Most recharge to the simulated ground-water system was provided by leakage from layer A1, with a comparatively smaller amount derived from recharge cells. A map showing simulated recharge based on vertical leakage from layer A1 and on values assigned to designated recharge cells (fig. 14) indicates that the highest rates of recharge generally are in the vicinity of interstream drainage divides. Recharge rates generally are higher in Georgia (15–20 in/yr) and areas of recharge extend further southward than in South Carolina. The relatively high recharge in Georgia is due, in part, to relatively higher vertical leakance of the Gordon confining unit (C1) in Georgia than in South Carolina (see section, “Calibrated Hydraulic Properties”).

Low recharge rates (less than 0.5 in/yr) occur in the central and southern parts of the SRS, and near the Savannah River in central Burke County; and probably are related to the relatively low vertical leakance of the Gordon confining unit (C1) in those areas. The low recharge rates (less than 0.5 in/yr) in parts of the SRS are much lower than values utilized in several previous modeling investigations (10–18 in/yr) at the SRS (Robert Hiergesell, Westinghouse Savannah River Company, written commun., 1998). The difference in recharge



### EXPLANATION

SIMULATED GROUND-WATER RECHARGE, IN INCHES PER YEAR—Derived from leakage from Upper Three Runs aquifer and from simulated recharge cells. Designated recharge cells are boxed

□ SIMULATED GROUND-WATER DISCHARGE

— MODEL BOUNDARY

$\frac{D}{U}$  PEN BRANCH FAULT—  
U, Upthrown side;  
D, Downthrown side

Less than 1

1 to 2.5

2.5 to 5

5 to 10

10 to 15

15 to 20

**Figure 14.** Simulated predevelopment recharge derived from leakage from the Upper Three Runs aquifer (layer A1) and from simulated recharge cells.

rates may be due to differences in modeling approach and scale. The SRS investigations actively simulated local flow in the surficial Upper Three Runs aquifer, whereas the current investigation designated this layer as a source-sink layer and simulated flow of a more regional nature. The active simulation of local flow in the Upper Three Runs aquifer in the onsite models required larger recharge rates to maintain lateral flow and discharge to streams. The more regional extent of the USGS model included a larger component of lateral flow than did the onsite SRS models, and required less vertical influx of water (recharge) to achieve calibration of heads and fluxes.

In parts of the study area, such as western Burke County, simulated leakage from layer A1 suggests the occurrence of losing streams. Although such flow conditions are possible during drought conditions, it is unlikely that they are representative of long-term average conditions, and are rather a problem associated with insufficient resolution of source-sink heads due to model cell size.

#### *Simulated Ground-Water Discharge to Streams*

Ground-water discharge to streams simulated for predevelopment conditions to estimated values determined from hydrograph separation and drought-streamflow measurements (Appendices A, B; fig. 15). Estimated ground-water discharge determined from drought-streamflow measurements during 1954 and 1986 (Appendix B) is considered to represent an anomalously low value that is not representative of long-term conditions, and is thus, considered a lower bound for calibration of simulated discharges. Ground-water discharge to streams estimated from hydrograph separation for the period of record (Appendix A) is considered to be more representative of long-term average conditions, but also includes a larger contribution from the local-flow regime than do estimates derived from drought streamflows. Thus, values derived from hydrograph separation are considered an upper bound for calibration of simulated discharges, although simulated values should be closer in magnitude to these estimates. As described earlier, estimates derived from hydrograph separation have an associated error of at least 20 percent; estimates derived from drought streamflow have an associated error of at least 10 percent. A graphical representation of the difference between simulated and estimated ground-water discharge (residuals) based on drought streamflow and hydrograph separation is shown in figure 15.

Comparison of estimated and simulated ground-water discharge residuals for drought streamflow (fig. 15; Appendix B) indicate that 10 of 11 simulated discharges are greater than the corresponding 1986 drought streamflow values, and that 23 of 29 residuals are above the lower 50-percent error line for the 1954 drought streamflow values. Of the 6 residuals below the lower 50-percent error line, three of the reaches—(between sites: 02197580 and 02197590; stream headwaters and 02200720; and 02198120 and 02198280)—are located near the southwestern boundary of the model where cells are large and elongated and the influence of boundary conditions may account for much of the simulation error (see locations, fig. 2). The remaining three reaches—(between sites: stream headwaters and 02197560; stream headwaters and 02197890; and stream headwaters and 02201360)—are located in small basins, and are simulated by relatively large cell sizes that are unable to accurately characterize local flow in shallow aquifers.

Comparison of residuals between simulated ground-water discharge and estimates based on hydrograph separation for the period of record indicate that simulated discharges are generally lower and within 50 percent of estimated values (fig. 15, Appendix A). Ground-water discharge to the three major streams in the area—the Savannah River, Upper Three Runs Creek, and Brier Creek—were considered matched by the model. Simulated ground-water discharge for these three streams accounts for about three-fourths of the ground-water discharge in the study area.

Ground-water discharge to the Savannah River is simulated by using both specified heads in the source—sink layer (A1) and the MODFLOW river package in areas where deeper layers were incised by the paleo-Savannah River channel. Where specified heads were used, ground-water discharge was largely influenced by the leakance value beneath the source/sink layer and by specified heads in the stream valley. Simulated ground-water discharge from all layers to the Savannah River is about 651 ft<sup>3</sup>/s, within the range of reported estimates for the Savannah River (table 1). The simulated value is very close to the estimated discharge of 660 ft<sup>3</sup>/s, based on the gain in streamflow between gages at Augusta and Millhaven, Ga., during a dry period in October 1941 (table 1, fig. 2). One reason for the simulated discharge being low is that the model does not fully simulate the local flow regime.

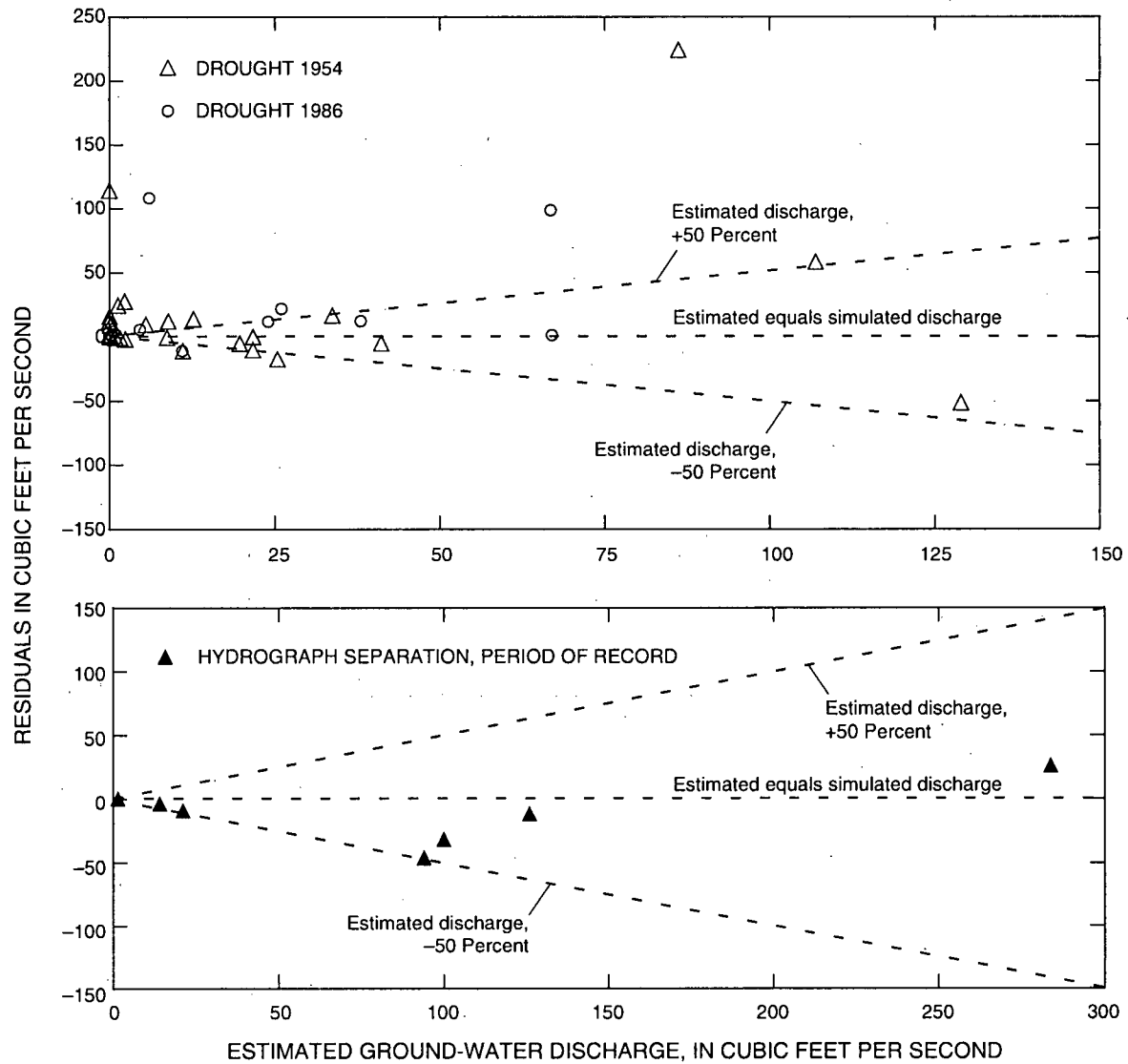


**Figure 15.** Difference (residuals) between estimated ground-water discharge to streams for predevelopment simulation (excludes Savannah River).

Upper Three Runs Creek is simulated entirely by using the MODFLOW river package in areas where aquifer layers are incised by the stream. Simulated ground-water discharge was compared with values estimated using hydrograph separation and drought streamflow data for three stream reaches of Upper Three Runs Creek. All simulated values are higher than drought-streamflow estimates for 1986 (Appendix B), but are lower than hydrograph-separation estimates (Appendix A); simulated values for two of the three reaches are within 50 percent of the estimated value.

Brier Creek predominantly is simulated by specified heads in the source/sink layer (A1)—a limited number of river cells are located within the northern part of the model area. Simulated ground-water discharge for three stream reaches of Brier Creek were compared to values estimated using hydrograph separation and drought-streamflow data. Simulated values are all higher than drought-streamflow estimates for 1954 and 1986 (Appendix B), and are within about 10 percent of hydrograph-separation estimates (Appendix A). Elongated model cells in the Brier Creek area may contribute to some of the high simulated discharge values.

Ground-water discharge in the Savannah River alluvial valley is controlled largely by the subsurface extent of aquifers and confining units beneath the river. In general, simulated discharge to the alluvial sediments varies according to the underlying unit. In areas where aquifers directly underlay alluvial sediments, rates of ground-water discharge are high; where confining units underlay alluvial sediments, rates of discharge are low. This is consistent with the observed gain in stream discharge that occurred in the area where the Gordon aquifer underlies the river alluvium (G.G. Patterson, U.S. Geological Survey, written commun., 1992).

#### *Simulated ground-water flow*

The predevelopment simulation matches the conceptual model of ground-water flow in the SRS area. Features depicted by both the conceptual model and the predevelopment simulation include:

(1) *The Savannah River serves as the major drain for the hydrologic system. The present-day floodplain represents the same or nearly the same hydraulic condition as the river, acting as a hydrologic "sink" into which ground water discharges from surrounding and underlying units.* Simulated potentiometric contours indicate that potentiometric lows or depressions for layers A1-A7 (figs. 9-12) are coincident with the area of the Savannah River floodplain. This supports the concept of a hydrologic sink. The simulated hydrologic budget supports the concept of the Savannah River as the major drain in the hydrologic system and accounts for 43 percent of the total simulated ground-water discharge, with the second highest percentage (28 percent) attributed to discharge to Brier Creek.

(2) *In the Savannah River alluvial valley, hydraulic interconnection between aquifers and Savannah River alluvium results in the development of a depression in the potentiometric surface that is symmetrical to the river valley. This ground-water flows in an updip or upriver direction resulting in the development of a ground-water divide, or "saddle" that occurs symmetrically to the river and separates upstream from downstream components of ground-water flow.* Maps of the simulated potentiometric surface for layers A2-A7 (figs. 9-12), show a good match to the conceptual model and interpreted maps constructed by Clarke and West (1997). Simulated surfaces indicate that the Savannah River valley is a line sink of ground-water discharge, separated by a ground-water divide or "saddle" into an upriver depression or discharge zone and a downriver, less pronounced, discharge zone. Flow in the vicinity of

the saddle is poorly defined by observation because of low gradients, but can be downriver or upriver toward the two discharge zones or across the river through a confined aquifer. Low vertical conductance of the Gordon confining unit (C1) might be a contributing factor to saddle development. Calibrated values of vertical conductance for the Gordon confining unit are low in the vicinity of the saddle, and probably account for decreased ground-water discharge from deeper aquifers (A2-A7) into the Savannah River in that area. Because of this restriction to vertical flow, water from these deeper aquifers moves laterally along gradients, either upriver toward the area where the aquifer is in hydraulic contact with the river alluvium (upriver discharge zone), or downriver where the vertical conductance of C1 is greater, allowing more discharge into the river (downriver discharge zone).

(3) *Most recharge water is discharged from the shallow-local and intermediate-flow systems into streams with a smaller percentage infiltrating through clayey confining units into the deeper regional-flow system.* The simulated hydrologic budget (table 8; fig. 13) indicates that the total simulated vertical flux (combined upward and downward leakage) between adjacent layers diminishes with depth, from about 1,279 Mgal/d between layers A1 and A2, to about 379 Mgal/d between layers A6 and A7 (fig. 13). Simulated vertical flux is highest in the shallow-flow system (as indicated by fluxes from specified heads in layer A1), which contributes 76 percent of total ground-water inflow and accounts for 50 percent of total ground-water outflow. The simulated vertical flux between layers A1 and A2 (source/sink contribution to ground-water discharge), combined with discharge to rivers from layer A2, accounts for about 74 percent of the total simulated ground-water discharge. This percent contribution is near the estimated 87 percent contribution of the local and intermediate-flow regimes to Savannah River flow (see section, "Hydrologic Budget"), suggesting that the upper two model layers contain the local- and intermediate-flow regimes. The simulated contribution to total system ground-water outflow is considerably less in deep layers (A3-A7) than in shallow layers, ranging from less than 1 percent in A3, to 9 percent in layer A5. Similarly, the simulated contribution to ground-water inflow (recharge and lateral boundaries) is low in layers A2-A7, ranging from less than 1 percent in A3, to 9 percent in A7. Layer A3 contributes the lowest percentage to ground-water inflow and outflow of all layers, probably because the

aquifer: (1) is thin and discontinuous; (2) pinches out in the subsurface, does not crop out, and, thus, cannot receive direct recharge by precipitation; and (3) has the smallest area of subsurface extent of any of the seven layers beneath the Savannah River alluvial valley. The small subsurface areal extent of layer A3 also limits discharge of ground water.

(4) *Ground-water flow in the Upper Three Runs aquifer (A1) mostly is part of the local-flow regimes; flow in deeper aquifers (A2-A7) is characterized by some local flow near outcrop areas to the north that transforms to intermediate and regional flow downdip (southeastward) where the aquifers are deeply buried.* Although layer A1 was simulated using specified heads, the simulated potentiometric-surface maps for layers A2-A7 (figs. 9-12), indicate a more pronounced connection to streams in northern parts of the area (indicative of local flow regime), that diminishes toward the southern parts of the study area. In general, the simulated potentiometric surfaces show more pronounced interaction with larger intermediate flow regime streams such as the Upper Three Runs Creek, Brier Creek, and Lower Three Runs Creek. In the downdip part of the study area, the intermediate streams connection with the aquifers diminishes and the Savannah River is the only stream with significant hydraulic connection to the aquifers.

(5) *The vertical distribution of hydraulic head in the stream-aquifer system generally is related to topographic location—in the vicinity of a major ground-*

*water divide, head decreases with depth; whereas—in the vicinity of a regional drain, such as the Savannah River, head increases with depth.* Simulated heads and vertical fluxes support the conceptual model over much of the area, indicating upward vertical gradients beneath major streams, and downward vertical gradients beneath upland areas, such as ground-water divides.

Although the relationship described in number 5 (above) holds true over much of the study area, in parts of the area, head data indicate that the Gordon (layer A2), Millers Pond (layer A3), and lower Dublin aquifers (layer A5) are apparent hydraulic “sinks”; whereby the hydraulic head is higher in overlying and underlying units (Clarke and West, 1997). This phenomenon also is evident in the predevelopment simulation as shown by head data at the P-21 and P-23 well-cluster sites on the SRS (table 9). At these well-cluster sites, both simulated and observed heads indicate the Gordon aquifer (A2) is an apparent hydrologic sink. At the P-23 well-cluster, the Gordon and Millers Pond aquifers (A3) have identical simulated heads; and thus, the layers were simulated as a hydrologic sink. Possible reasons for the occurrence of anomalously low heads (“sink” condition) were described by Clarke and West (1997), and include (1) subsurface pinchout of the aquifer which influences flow patterns in the stream-aquifer system; (2) hydraulic connection of the aquifer to river alluvium, which facilitates high ground-water discharge that lowers heads; and (3) water-level declines as a result of pumpage.

**Table 9.** Observed and simulated predevelopment head at the P-21 and P-23 well-cluster sites

[shaded values represent lowest value at site (potential hydrologic sink); —, not measured]

Aquifer	Layer	Head, in feet above sea level			
		P-21		P-23	
		Observed	Simulated	Observed	Simulated
Upper Three Runs	A1	161.4	<sup>1</sup> 161.9	147.3	<sup>1</sup> 173.7
Gordon	A2	135.8	144.3	142.6	156.3
Millers Pond	A3	136.6	151.1	147.9	156.3
Upper Dublin	A4	168.8	165.0	166.0	165.1
Lower Dublin	A5	168.8	165.0	<sup>2</sup> 167.9	166.0
Upper Midville	A6	183.1	183.0	171.4	174.2
Lower Midville	A7	—	183.0	172.0	174.2

<sup>1</sup>Represents average head in simulated specified-head cell. May differ from observed value due to large horizontal gradients within cell.

<sup>2</sup>Average of wells BW-377 and BW-412.

## Simulation of Flow System, 1953–92

To simulate changes to the ground-water flow system after the initiation of large-scale pumpage in late 1952, the model was first tested for transient response to changes in pumpage. It then was used to simulate a series of six steady-state pumping periods: 1953–60, 1961–70, 1971–75, 1976–80, 1981–86, and 1987–92 (table 6).

### *Testing of model for transient response to pumpage*

Simulation of stresses on the ground-water flow system can be made using either a steady-state or transient simulation (table 2). Steady-state simulations require input of hydraulic characteristics of aquifers and confining units, boundary conditions, and ground-water pumpage (if any). Transient simulations require the same input parameters as steady-state simulations, but also require time-step parameters and arrays of storage characteristics of the aquifers, expressed as storage coefficient for confined aquifers. Because transient simulations are more complex and require a large amount of computer storage space for additional data arrays and model output, the flow system was tested to determine if transient simulation was required.

Clarke and West (1997) suggested that during the period 1953–92, the ground-water flow system in the study area generally was under steady-state conditions as indicated by little change in hydraulic head or ground-water discharge to streams. To test this hypothesis, the calibrated steady-state model was tested for transient response to 1953–92 ground-water pumpage. This was accomplished by incorporating storage coefficient and pumpage arrays representing six pumping periods into the model (transient model), and then evaluating the overall model budget and sensitivity of the model to storage. Mean values of storage coefficient are listed in table 3 and range from  $1.1 \times 10^{-4}$  to  $4.3 \times 10^{-4}$ . These mean values were assigned as uniform initial values in the ground-water model for their respective layers. Where storage coefficient data were unavailable, the mean value from an adjacent unit was assigned (on the basis of similar depositional environment and lithology). The response of simulated heads to storage during the final stress period (1987–92) was tested by multiplying values of storage coefficient by factors of 0.001 to 1,000 (fig. 16). Plots of changes in the percent of matched heads, RMS of residuals, and mean of residuals, indicate that the model is insensitive

to changes in storage. The contribution of water from storage to the model budget was negligible during the beginning of the stress periods, and at the end of the simulation it accounted for less than  $1 \times 10^{-5}$  percent of the total budget.

Additional indication of steady-state conditions during 1953–92 was given by the rate of head stabilization during each stress period. At the beginning of each stress period, heads showed an almost instantaneous stabilization, suggesting that the prevalence of steady-state conditions were achieved immediately following a change in pumpage.

As a further test of steady-state conditions, two additional stress periods (7 and 8) were added to the simulation, each representing 10 years and assigned the same quantity of pumpage as the sixth stress period representing 1987–92 conditions. During these two additional stress periods, simulated heads did not change from those simulated for the sixth stress period, and the contribution from storage remained negligible, indicating the transient-model had reached a steady-state condition. An additional test of simulated transient response was accomplished by doubling the pumpage applied during stress periods 6 through 8. Results were similar to the previous tests. The contribution from storage was less than  $1.3 \times 10^{-5}$  percent, indicating that doubling of pumpage did not produce a substantial transient response.

In summary, test results indicate that transient response to changes in pumpage are short term and that the model results are insensitive to changes in storage. Thus, model simulations of 1953–92 conditions were accomplished using steady-state assumptions.

### *Steady-state analysis of modern-day (1987–92) flow conditions*

Because the calibrated model showed virtually no transient response to pumpage, a series of steady-state simulations were utilized to characterize changes in head for 6 stress periods, representing pumping conditions during 1953–92 (table 6). Calibration results for the sixth stress period (1987–92), herein referred to as modern-day, are presented in this section; results for the other 5 stress periods are presented in the section, "Simulated Drawdown." Sensitivity of the calibrated modern-day model to hydraulic properties, boundary conditions, and stresses are presented in the section "Sensitivity Analysis."

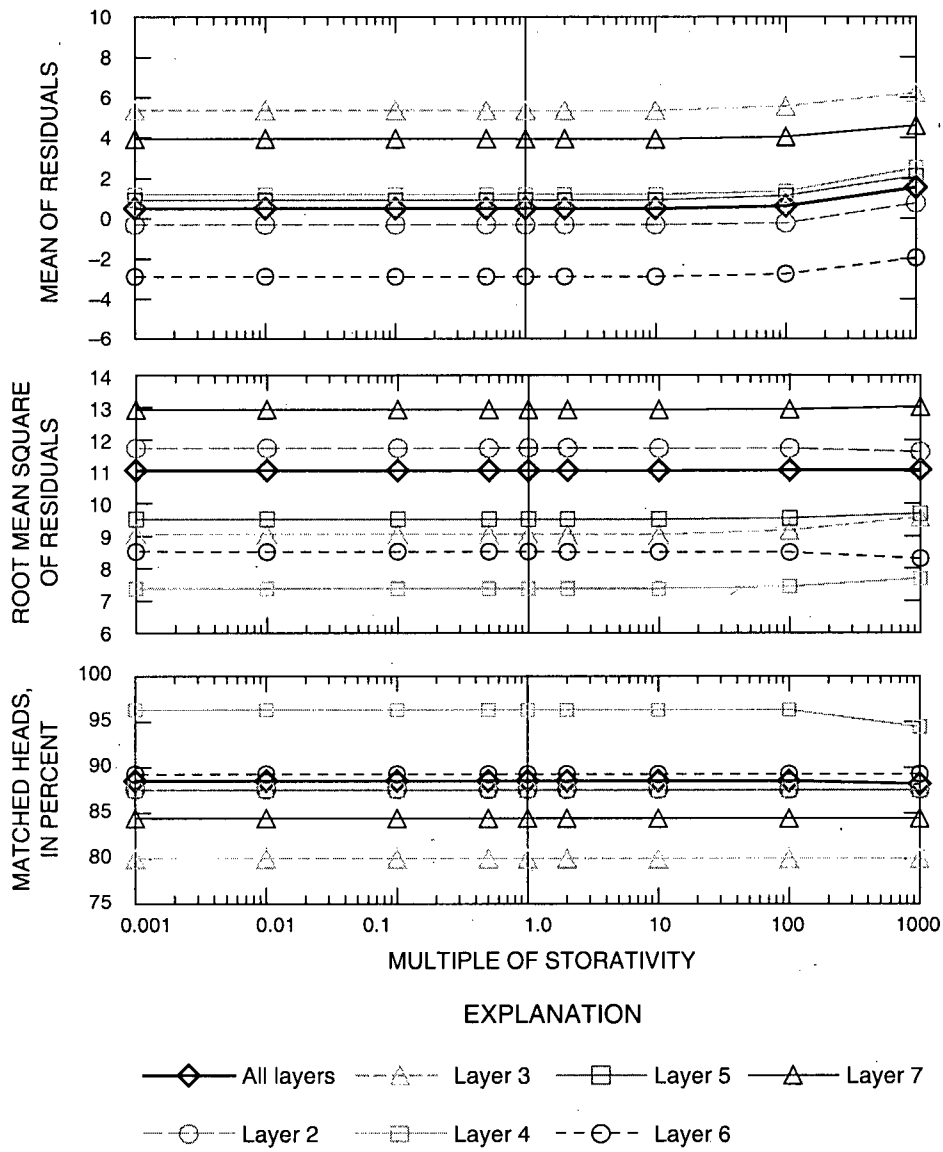


**Figure 16.** Sensitivity of transient model to changes in storativity.

The model was calibrated to modern-day conditions using the average observed head during 1987–92 at 313 model cells (Appendix C; table 10); and by comparing simulated and estimated ground-water discharge along 36 reaches of selected streams (see locations, fig. 2; and Appendices A and B). For the modern-day period, the model matched established error criteria for heads in 88.2 percent of the cells where observations were available, and simulated ground-water discharge was within 50 percent of estimated values for selected stream reaches. Simulated ground-water flow directions and the distribution and quantity of recharge and discharge are consistent with the conceptual model over most of the model area.

As was the case for predevelopment conditions, simulated heads for the modern-day period show an excellent match to established error criteria for observed heads, ranging from 80 percent matched in layer A3, to 96.3 percent matched in layer A4. Summary statistics for simulated heads for the modern-day period are listed in table 10 and Appendix C, and are plotted graphically on figure 17. Eighty percent of the residuals are within about 12 feet of observed values (fig. 17). As was the case for the predevelopment period, the largest residual (-77 ft) occurs at well BW-395 in the vicinity of the Pen Branch Fault at the P-19 well-cluster (Appendix C). The model was unable to match head in layer A2 in this area

because (1) the water-level measurement in well BW-395 may not have been representative of head in layer A2 because of problems with well construction or measurement error, or (2) of a possible localized hydraulic connection between layers A1 (Upper Three Runs) and A2 (Gordon) in the vicinity of the Pen Branch Fault.

In most layers, the percentage of matched heads, and RMS of residuals for the modern-day period was about the same as for the predevelopment period (tables 7 and 10). In layers A3, A4, and A7, however, the percentage of matched heads was lower than for the predevelopment period. This is probably because: (1) the modern-day water levels are considerably more influenced by pumping than predevelopment levels; (2) the difference between cell area and the area represented by the radius of influence of the actual pumping well or wells; or (3) problems associated with simulation of drawdown, such as errors in confining unit leakance or pumpage arrays. The mean of residuals for the modern-day period showed a slight positive skew for all layers except A2 and A6 (table 10). This positive skew may indicate that the full magnitude of drawdown response to pumpage was not fully simulated by the model.

**Table 10.** Calibration statistics for simulated heads for modern-day (1987–92) conditions  
[—, not applicable].

Aquifer	Model layer	Number of observations	Percentage of heads matched <sup>1/</sup>	Root mean square of residuals	Mean of residuals	Standard deviation of residuals
Gordon	A2	136	88.2	11.5	-0.1	11.5
Millers Pond	A3	10	80.0	9.0	5.4	7.7
Upper Dublin	A4	54	96.3	7.4	1.2	7.3
Lower Dublin	A5	40	87.5	9.5	1.0	9.6
Upper Midville	A6	28	89.3	8.5	-2.8	8.2
Lower Midville	A7	45	84.4	13.2	4.1	12.7
All layers		313	88.8	10.6	0.8	10.6

<sup>1/</sup>When compared to established error criteria.

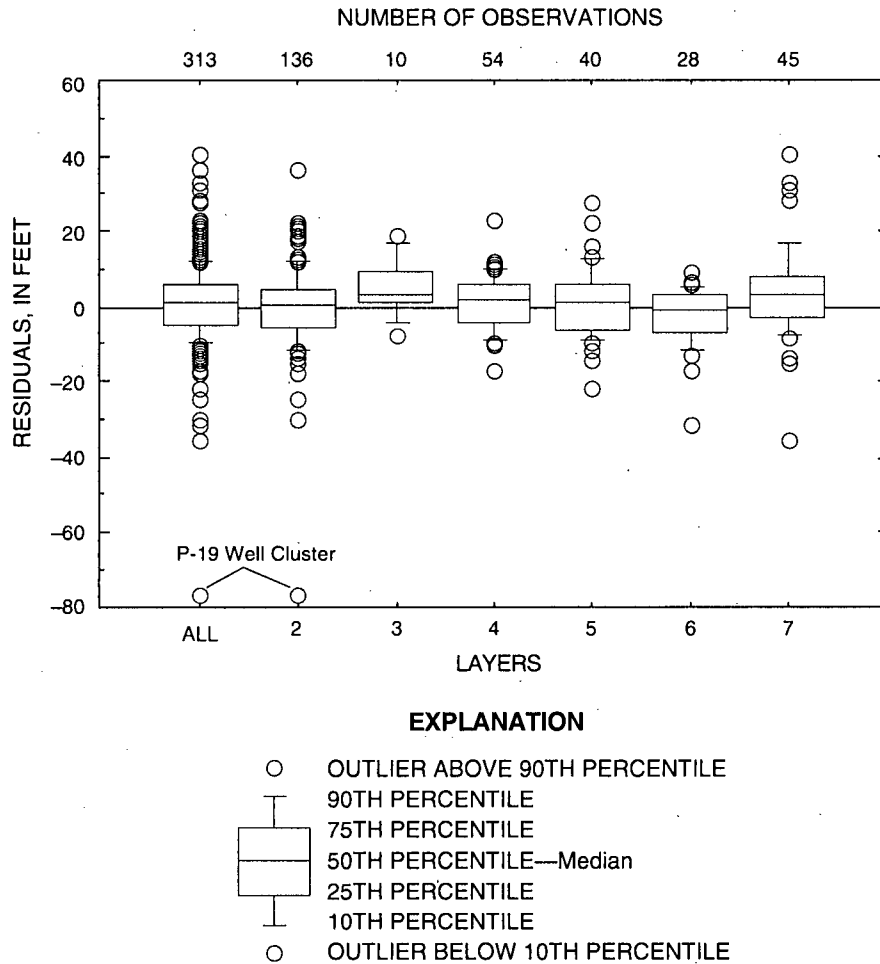


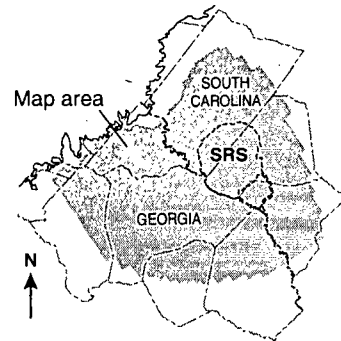
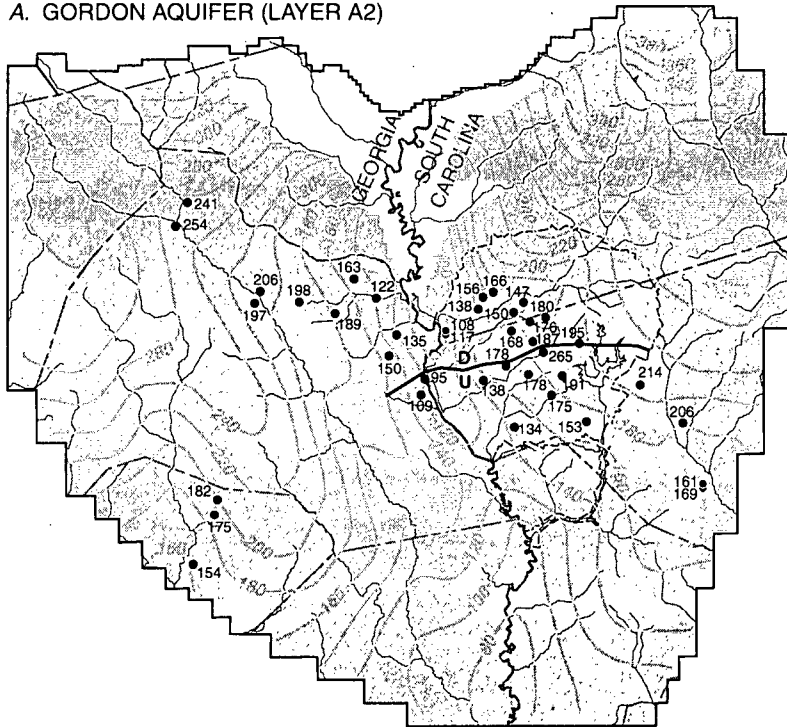
**Figure 17.** Difference between observed and simulated heads (residuals) for the modern-day (1987–92) simulation.

Maps of the simulated predevelopment potentiometric surface for the modern-day period compare favorably to the interpreted configuration of the potentiometric-surface maps representing average conditions during 1987–92 (see plate 3). Maps showing simulated potentiometric surfaces and observed heads for layers A2 through A7 are shown in figures 18–20. In general, these surfaces are similar to simulated and interpreted potentiometric-surface maps for predevelopment conditions; however, in layers A4 and A5 (upper and lower Dublin aquifers) the configuration of the maps in the vicinity of the Savannah River changed (fig. 19). In this area, the potentiometric “saddle” feature has disappeared, as evidenced by the position of the 160-ft contour, which is no longer subdivided into an upstream

discharge zone and a downstream discharge zone. Water-level declines in layers A4 and A5 in the vicinity of the “saddle” feature resulted in collapse of the ground-water divide in that area, and changed the configuration of the potentiometric surface.

The distribution of matched heads and residuals for the modern-day period is similar to the distribution of computed heads and residuals for the predevelopment period, as indicated by comparing simulated contours and observed heads shown on figures 18–20. Although head comparisons are fewer for the modern-day period than for the predevelopment period, the northwestern part of the simulated area for the modern-day period is the area of the lowest percentage of matched heads and is the area of highest residuals.

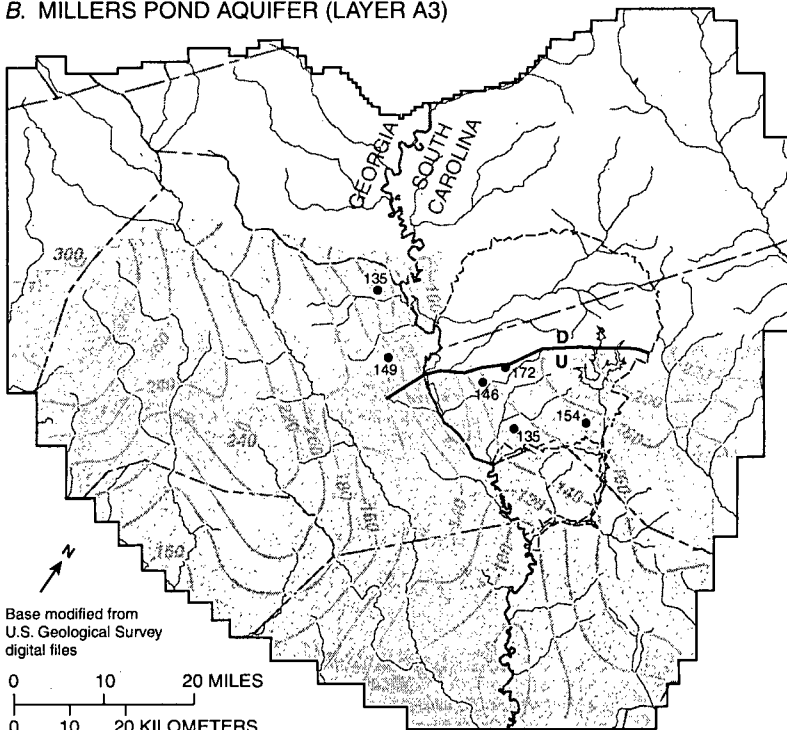
A. GORDON AQUIFER (LAYER A2)



EXPLANATION

-  SIMULATED AREA
-  SIMULATED POTENTIOMETRIC CONTOUR—Shows simulated potentiometric surface, in feet. Contour interval 20 feet. Datum is sea level
-  MODEL BOUNDARY
-  PEN BRANCH FAULT—  
U, Upthrown side;  
D, Downthrown side
-  WELL DATA POINT—Number is observed water level, in feet above sea level

B. MILLERS POND AQUIFER (LAYER A3)



Base modified from  
U.S. Geological Survey  
digital files

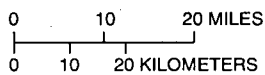
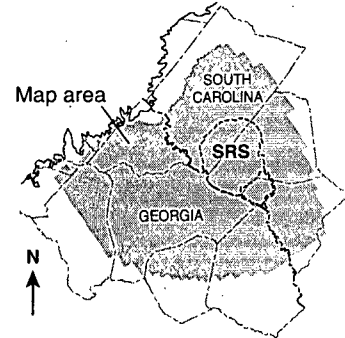
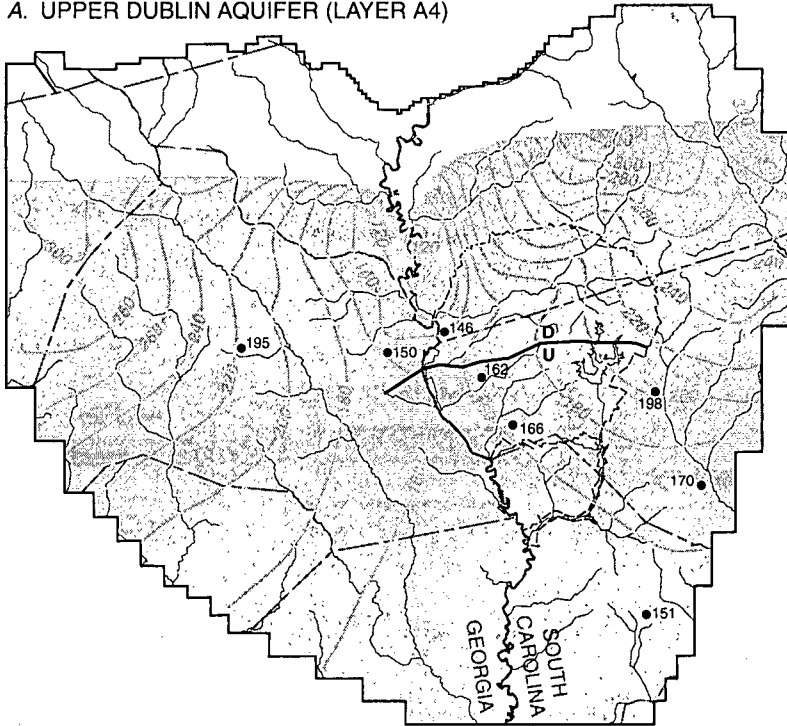


**Figure 18.** Simulated modern-day (1987–92) potentiometric surface and observed heads for the (A) Gordon (layer A2) and (B) Millers Pond (layer A3) aquifers.

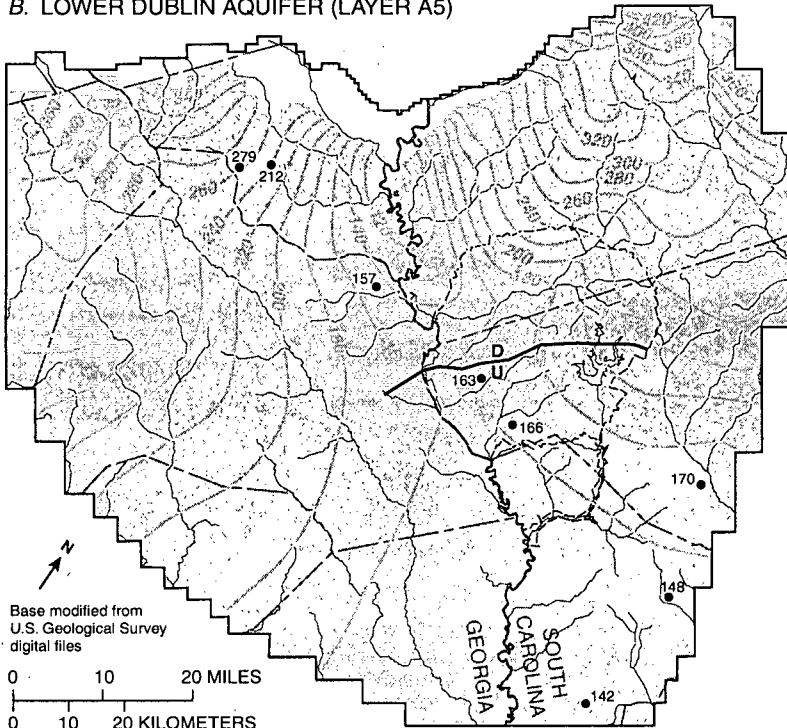
A. UPPER DUBLIN AQUIFER (LAYER A4)



EXPLANATION

- SIMULATED AREA
- SIMULATED POTENTIOMETRIC CONTOUR—Shows simulated potentiometric surface, in feet. Contour interval 20 feet. Datum is sea level
- MODEL BOUNDARY
- PEN BRANCH FAULT—  
U, Upthrown side;  
D, Downthrown side
- WELL DATA POINT—Number is observed water level, in feet above sea level

B. LOWER DUBLIN AQUIFER (LAYER A5)



Base modified from U.S. Geological Survey digital files

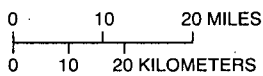
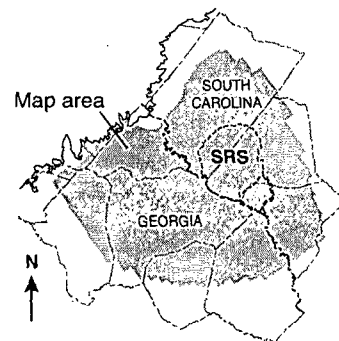
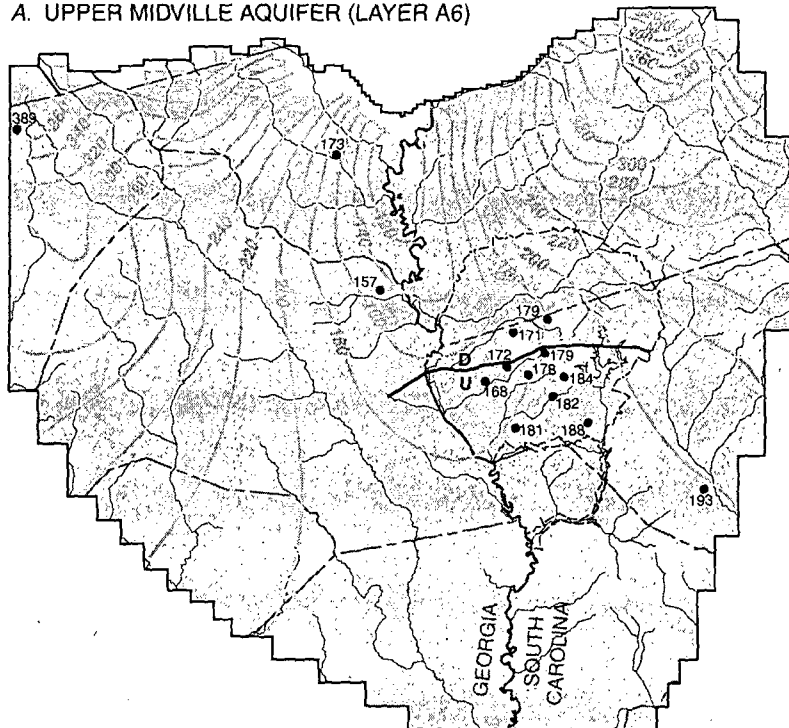


Figure 19. Simulated modern-day (1987–92) potentiometric surface and observed heads for the (A) upper Dublin (layer A4) and (B) lower Dublin (layer A5) aquifers.

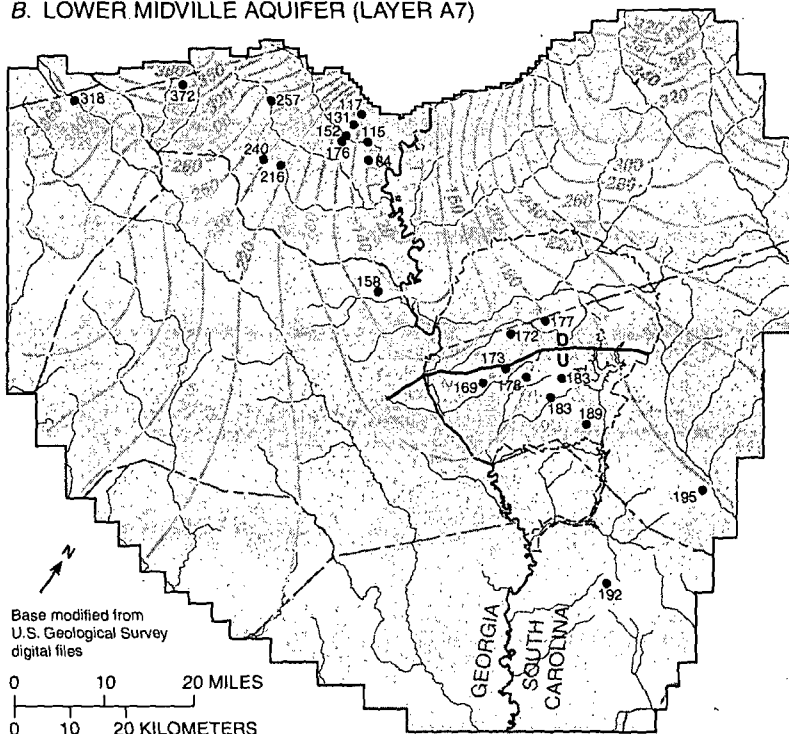
A. UPPER MIDVILLE AQUIFER (LAYER A6)



EXPLANATION

-  SIMULATED AREA
-  SIMULATED POTENTIOMETRIC CONTOUR—Shows simulated potentiometric surface, in feet. Hachures indicate depression. Contour interval 20 feet. Datum is sea level
-  MODEL BOUNDARY
-  PEN BRANCH FAULT—  
U, Upthrown side;  
D, Downthrown side
-  WELL DATA POINT—Number is observed water level, in feet above sea level

B. LOWER MIDVILLE AQUIFER (LAYER A7)



Base modified from U.S. Geological Survey digital files

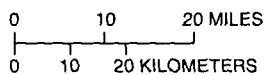


Figure 20. Simulated modern-day (1987–92) potentiometric surface and observed heads for the (A) upper Midville (layer A6) and (B) lower Midville (layer A7) aquifers.

In the Augusta, Ga., area, the simulated head in layer A7 in the vicinity of a small depression in the estimated potentiometric surface (see 100-ft contour, plate 3), shows a poor match to observed heads with head residuals as large as +33 ft. Possible reasons for the poor match include: (1) error in the pumpage data set; (2) insufficient transmissivity data; (3) insufficient grid resolution to simulate drawdown near the well; (4) measurements not depicting average water-level values in a model cell; (5) inaccurate leakance; or (6) a combination of these factors. In an attempt to improve calibration results in this area, the transmissivity was reduced 10–20 percent, which produced a slight reduction in the positive residuals, but still did not meet error criteria. Similarly, increasing pumpage arrays in the area within an error margin of 10 percent, produced insignificant reductions in residuals.

The water budget for the modern-day period shows a distribution of flow similar to the predevelopment period, with the exception that outflow from the

modern-day simulation includes ground-water pumpage. The simulated water budget for the modern-day period is summarized in table 11 and illustrated in figure 21. Of the total simulated inflow of 1,041 Mgal/d, 76 percent is contributed by leakage from specified-head cells in the source-sink layer (A1), 15 percent is contributed by direct areal-recharge to layers A2-A7, and 9 percent is contributed as lateral inflow from specified-head boundaries in layers A2-A7. Of the total 1,042.0 Mgal/d outflow, ground-water discharge to streams accounted for 92 percent, lateral outflow at specified-head boundaries accounted for 3 percent, and discharge to wells accounted for 5 percent of the water leaving the model. Ground-water pumpage accounted for about a 3 percent reduction in stream discharge for the modern-day period. Clarke and West (1997) reported a decrease in ground-water discharge between predevelopment and modern-day conditions in the vicinity of Brier Creek, and suggested that this decrease could be attributed to changes in pumpage near the stream.

**Table 11.** Simulated modern-day (1987–92) water budget

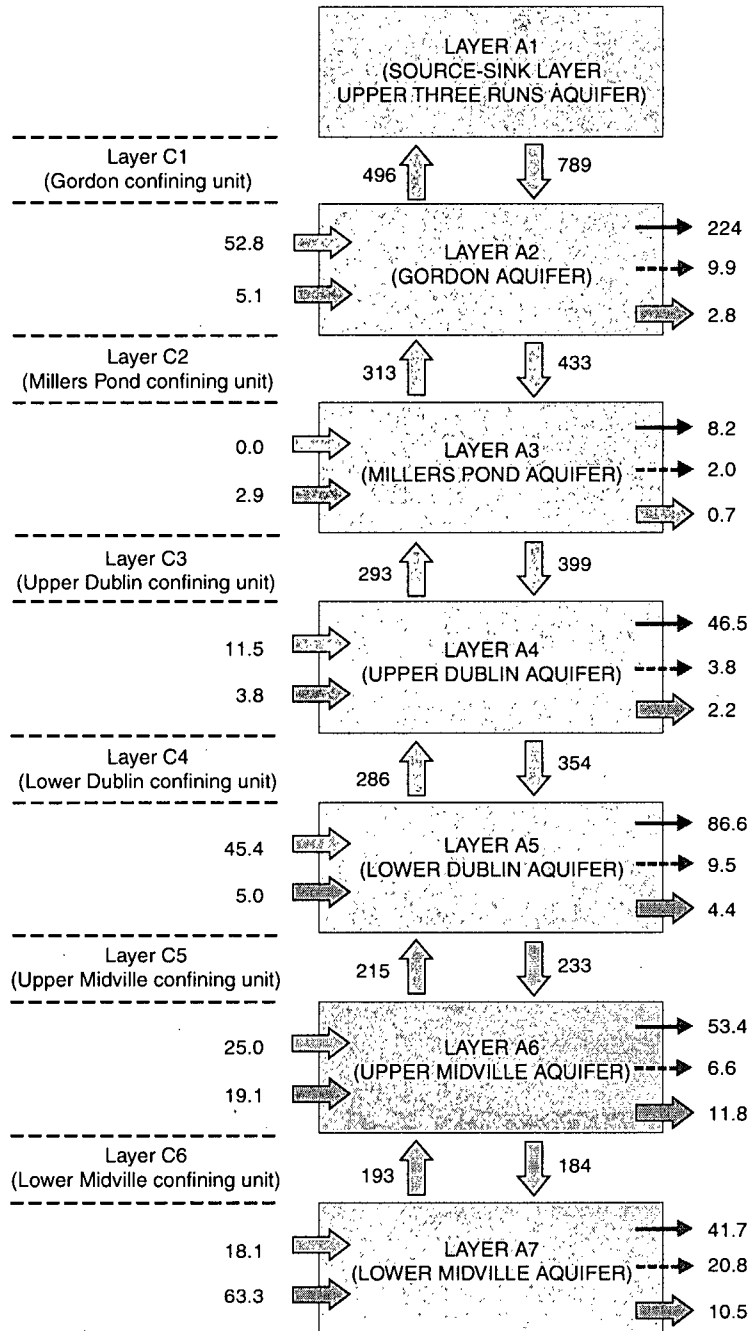
[—, not applicable]

Aquifer	Model layer	Inflow, in million gallons per day			Outflow, in million gallons per day			
		Recharge	Inflow across lateral boundaries	Total	Outflow across lateral boundaries	Discharge to stream boundaries	Discharge to wells	Total
Upper Three Runs	<sup>1/</sup> A1	<sup>2/</sup> 788.6	—	788.6	—	<sup>3/</sup> 496.5	—	496.5
Gordon	A2	52.8	5.1	57.9	2.8	224.1	9.9	236.8
Millers Pond	A3	0	2.9	2.9	0.7	8.2	2	10.9
Upper Dublin	A4	11.5	3.8	15.3	2.2	46.5	3.8	52.5
Lower Dublin	A5	45.4	5	50.4	4.4	86.6	9.5	100.5
Upper Midville	A6	25	19.1	44.1	11.8	53.4	6.6	71.8
Lower Midville	A7	18.1	63.3	81.4	10.5	41.7	20.8	73
All layers		941.4	99.2	1,040.6	32.4	957	52.6	1,041.5

<sup>1/</sup>Inactive, source/sink layer.

<sup>2/</sup>Simulated recharge derived from vertical leakage from specified head cells in source/sink layer into underlying units.

<sup>3/</sup>Simulated discharge derived from vertical leakage from underlying units into specified head cells in source/sink layer.



**EXPLANATION**

- APPLIED RECHARGE
- INFLOW OR OUTFLOW ACROSS LATERAL BOUNDARIES
- DISCHARGE TO RIVERS
- DISCHARGE TO PUMPING
- VERTICAL FLOW UPWARD OR DOWNWARD ACROSS CONFINING UNIT
- 0.3 VALUE, IN MILLIONS OF GALLONS PER DAY

**Figure 21.** Simulated modern-day (1987–92) water budget by model layer.

Simulated ground-water discharge to streams for the modern-day period compares favorably to estimated values determined from hydrograph separation and drought streamflow (fig. 22; Appendices A and B). A graphical comparison of estimated to simulated ground-water discharge for the modern-day period, plotted as residuals together with 50-percent error ranges is shown in figure 22. Comparison of simulated ground-water discharge for the modern-day period to estimates based on hydrograph separation of drought streamflow (fig. 22, Appendix B) indicates results nearly identical to those obtained for the predevelopment period (fig. 15), with slightly lower

simulated discharge to streams for the modern-day period. Comparison of simulated ground-water discharge to baseflow rates values estimated using hydrograph separation for the period 1987-92 along six stream reaches indicates that all simulated discharges are within 50 percent of estimated values, and only one simulated value is greater than the hydrograph separated estimate (fig. 22, Appendix A). Estimated baseflow rates of the six stream reaches during 1987-92, were either the same, or slightly lower than values computed for entire the period of record. This decrease in discharge also is simulated for the modern-day period.

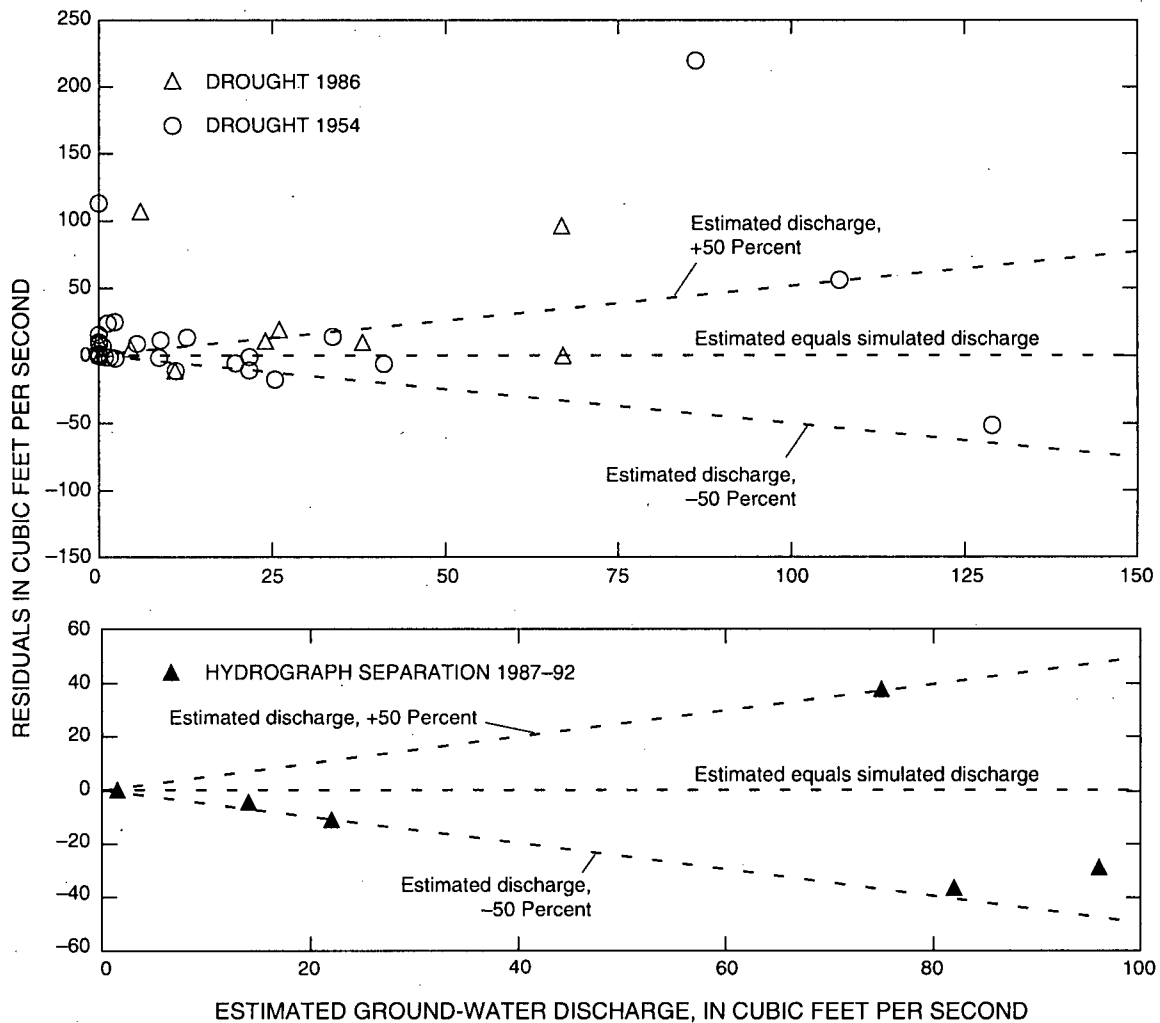


**Figure 22.** Difference (residuals) between estimated and simulated ground-water discharge to streams for modern-day (1987-92) simulation.

*Simulated drawdown*

A series of steady-state simulations were utilized to characterize changes in head for six stress periods during 1953–92 (table 6). To evaluate effects of ground-water pumpage on ground-water flow during 1953–92: (1) water budgets and ground-water discharge for the calibrated model under predevelopment and modern-day conditions were compared; (2) drawdown between predevelopment and modern-day conditions was computed and mapped; and (3) simulated water levels were plotted at the end of each stress period and compared with hydrographs of water-level trends. In some areas, overall trends were matched despite significant differences between observed and simulated head values (residuals). Observed water-level variations within a stress period probably are due to variations in precipitation and pumping that are beyond the temporal resolution of the model.

Over most of the study area, changes in ground-water levels, ground-water discharge to streams, and water-budget components, attributed to ground-water pumpage, were small during 1953–92. In some areas, simulation results did not match the magnitude of

observed drawdowns; however, most water-level trends were matched. The addition of pumped wells accounted for only minor changes to the simulated modern-day water budget compared to the simulated predevelopment water budget (fig. 23). The 52.6 Mgal/d of water withdrawn by wells during 1987–92, accounted for: (1) 5 percent of the total ground-water outflow for the modern-day period; (2) about a 3-percent decrease in ground-water discharge to streams; (3) about a 2-percent increase in downward leakage from layer A1 (representing aquifer recharge); and (4) minor changes to ground-water inflow or outflow along lateral boundaries for the modern-day period. Contributions to ground-water withdrawals are provided mostly by intercepted recharge prior to discharge into streams (62 percent), with the remainder provided by increased leakage from layer A1 (30 percent) and changes in lateral flux (7 percent). As described previously, changes in ground-water storage accounted for an insignificant contribution (less than  $1 \times 10^{-5}$  percent) to the total modern-day water budget, so steady-state simulation was utilized to evaluate flow conditions during 1953–92.

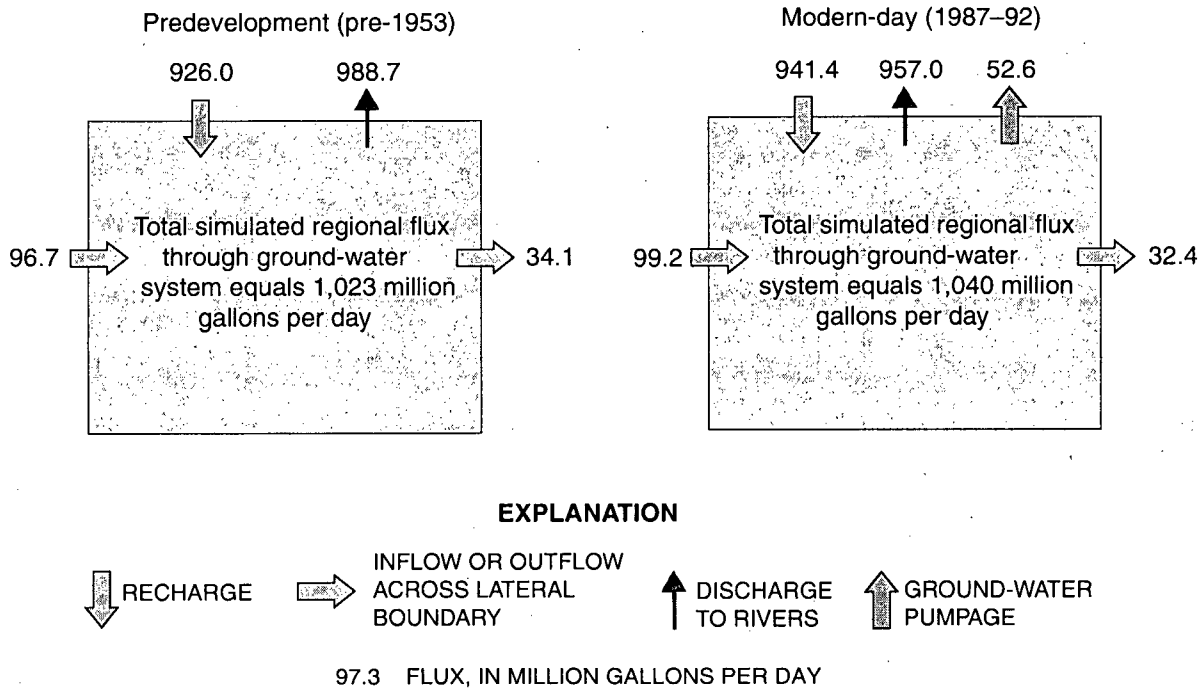


**Figure 23.** Simulated predevelopment and modern-day water budgets.

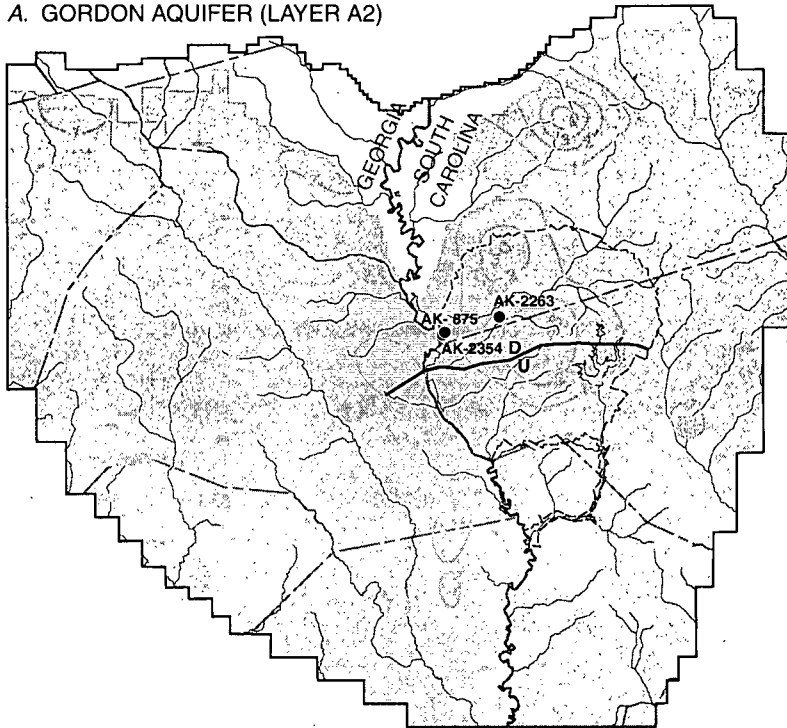
Maps showing simulated water-level declines (or drawdown) from predevelopment to modern-day conditions indicate small drawdown (less than 7 ft) of limited areal extent (figs. 24–26) due to pumpage. Most drawdown in South Carolina occurred in the vicinity of pumping centers at the cities of Aiken (site 12) and Barnwell (site 13), the A/M area at the SRS (site 9), and Sandoz, Inc. (site 14) (see figure 7 for locations; table 5 lists rates). In Georgia, most drawdown occurred in the Augusta area (sites 4 and 5), at Plant Vogtle (site 6), and in the vicinity of kaolin-mining operations in northern Jefferson County (site 3). The largest simulated declines (about 7 ft) occurred in layers A4 and A5 in the vicinity of the Sandoz site in South Carolina (fig. 25). However, the magnitude of water-level declines was insufficient to depict cones of depression on maps of the simulated modern-day potentiometric surface (figs. 18–20), at the contour interval (20 ft) presented in this report.

In layer A2, simulated pumpage of 9.9 Mgal/d during 1987–92 (table 6) resulted in minor changes in the simulated predevelopment water budget and little water-level change. Simulated inflows and outflows remained largely the same, with about a 2-percent decrease in ground-water discharge to streams (table 11; fig. 21). Declines of 1–3 ft were observed in the vicinity of the SRS, 1–4 ft in the vicinity of Aiken, S.C., and 1 ft in northern Jefferson County, Ga. (fig. 24). These declines occurred even though only minor (if any) pumpage from the aquifer occurred in these areas. Increased leakage due to pumpage in underlying units may account for some of the simulated decline. Comparison of simulated predevelopment and modern-day water budget indicates downward leakage between layers A2 and A3 increased about 10.7 Mgal/d in the modern-day simulation from predevelopment conditions (figs. 13, 21), which probably accounts for the simulated declines in layer A2 (fig. 24). Although long-term water-level data for layer A2 are sparse, some indication of long-term trends can be discerned from water-level data at wells AK-875, AK-2263, and AK-2354 (fig. 27). In each of the three wells, little, if any, changes were observed, matching the simulated trend in the area. Although the overall trend was matched, the difference between observed and simulated head (residual) at well AK-875 was large (about 30 ft), reflecting a steep head gradient that is not completely resolved by the model grid array.

In layer A3, simulated pumpage of 2 Mgal/d during 1987–92 (table 6) resulted in minor changes in the simulated predevelopment water budget and little water-level change. Simulated inflows and outflows remained largely the same, with about a 2-percent decrease in ground-water discharge to streams (table 11, fig. 21). Simulated drawdown of 1–2 ft was limited to scattered areas, the largest of which occurred at the SRS (fig. 24). As was the case for layer A2, long-term water-level data for layer A3 are sparse. Water-level data from wells BW-407, BW-414, and BW-403 on the SRS (fig. 28) during 1985–92 showed no apparent trend, consistent with the simulated water levels in the area. However, head residuals at wells BW-407 and BW-403 were large (about 15–20 ft), reflecting the steep head gradients across grid cells.

In layers A4 and A5, simulated pumpage of 3.8 Mgal/d in layer A4, and 9.4 Mgal/d in layer A5 during 1987–92 (table 6) produced small changes compared to the predevelopment water budget but caused more pronounced drawdown than in overlying layers. The most significant change to the simulated water budget occurred in layer A4—a 9-percent increase in ground-water inflow at lateral boundaries, accompanied by a 12-percent reduction in ground-water outflow at lateral-flow boundaries (table 11, fig. 21). In layer A5, discharge to streams decreased by about 7 percent, while lateral-boundary inflow decreased by 11 percent and outflow decreased by about 6 percent. Changes in the flow rate along lateral boundaries are likely due to water-level declines that changed head gradient or reversed the direction of ground-water flow. Simulated water-level declines in layers A4 and A5 were of the highest magnitude and covered the largest area of any of the layers (fig. 25). Because layers A4 and A5 are highly interconnected, water-level declines in the two aquifers are similar. Water-level declines of 1 ft or more cover a large area that includes the SRS, Sandoz, and Plant Vogtle pumping centers (fig. 7, table 5), with the largest declines in the vicinity of Sandoz (7 ft). The effects of Sandoz pumpage from layers A4 and A5 on overlying or underlying units are not evident, suggesting that confining units above A4 and below A5 are sufficiently impermeable to inhibit significant leakage at modern-day pumping rates.

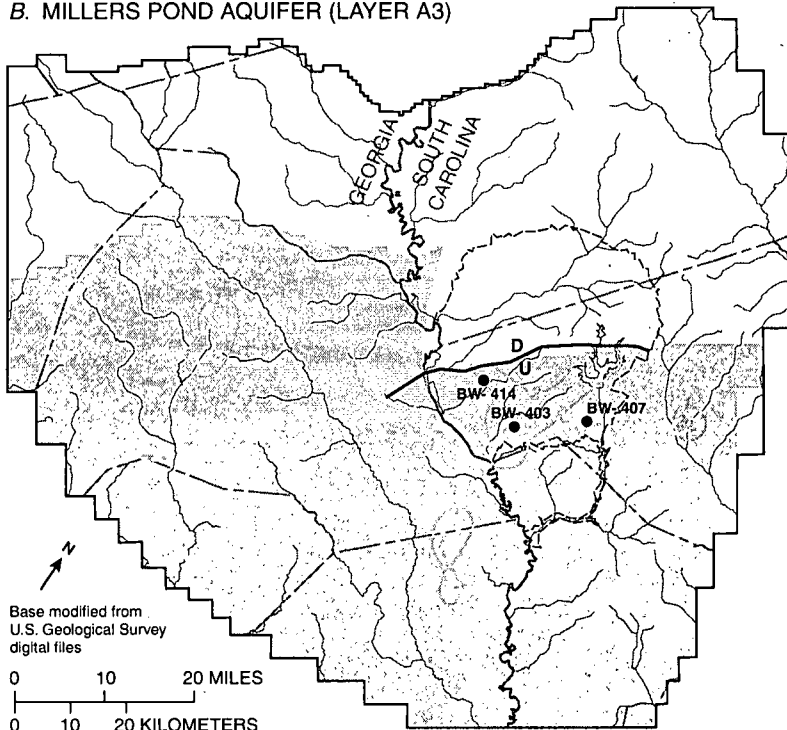
A. GORDON AQUIFER (LAYER A2)



EXPLANATION

- SIMULATED AREA
- SIMULATED PUMPAGE
- SIMULATED DRAWDOWN—  
Interval 1 foot
- MODEL BOUNDARY
- PEN BRANCH FAULT—  
U, Upthrown side;  
D, Downthrown side
- BW-407 OBSERVATION WELL—  
Number is well identification

B. MILLERS POND AQUIFER (LAYER A3)



Base modified from  
U.S. Geological Survey  
digital files

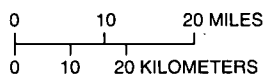
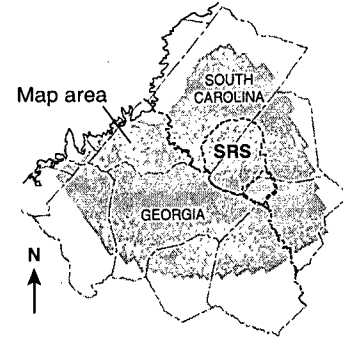
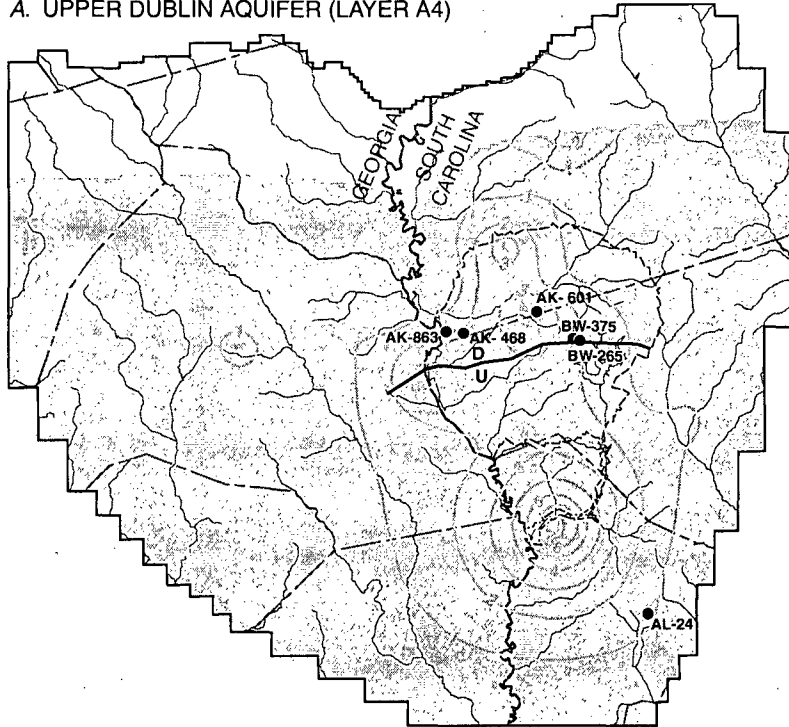


**Figure 24.** Simulated drawdown, 1953–92, and locations of simulated pumpage and observation wells completed in the (A) Gordon (layer A2) and (B) Millers Pond (layer A3) aquifers.

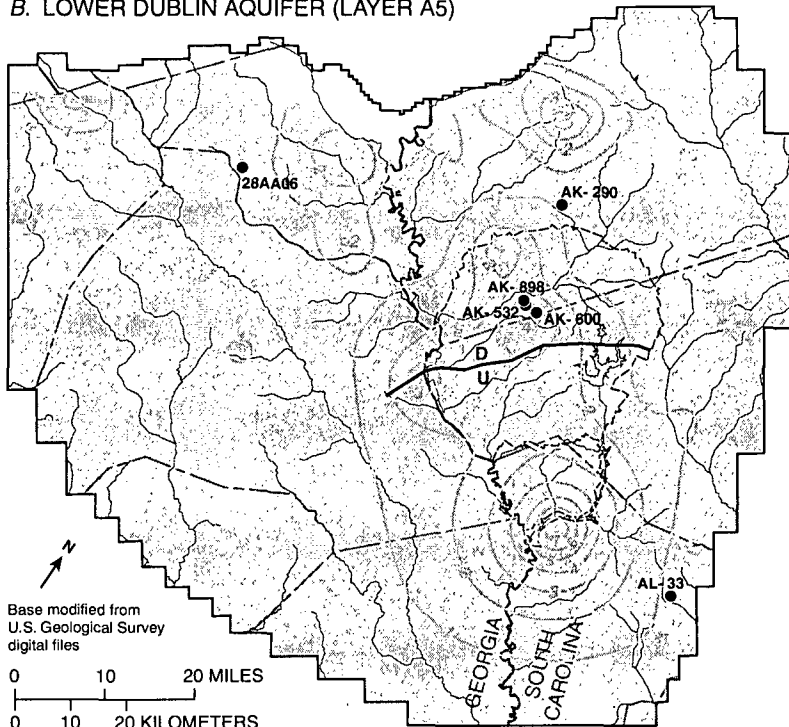
A. UPPER DUBLIN AQUIFER (LAYER A4)



EXPLANATION

-  SIMULATED AREA
-  SIMULATED PUMPAGE
-  SIMULATED DRAWDOWN—  
Interval 1 foot
-  MODEL BOUNDARY
-  PEN BRANCH FAULT—  
U, Upthrown side;  
D, Downthrown side
-  AK-290 OBSERVATION WELL—  
Number is well identification

B. LOWER DUBLIN AQUIFER (LAYER A5)



Base modified from  
U.S. Geological Survey  
digital files

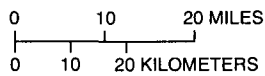
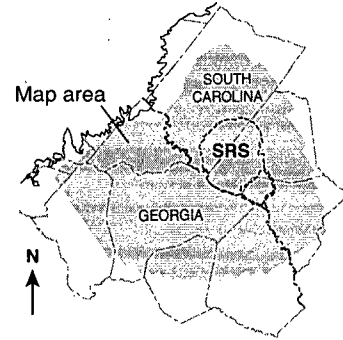
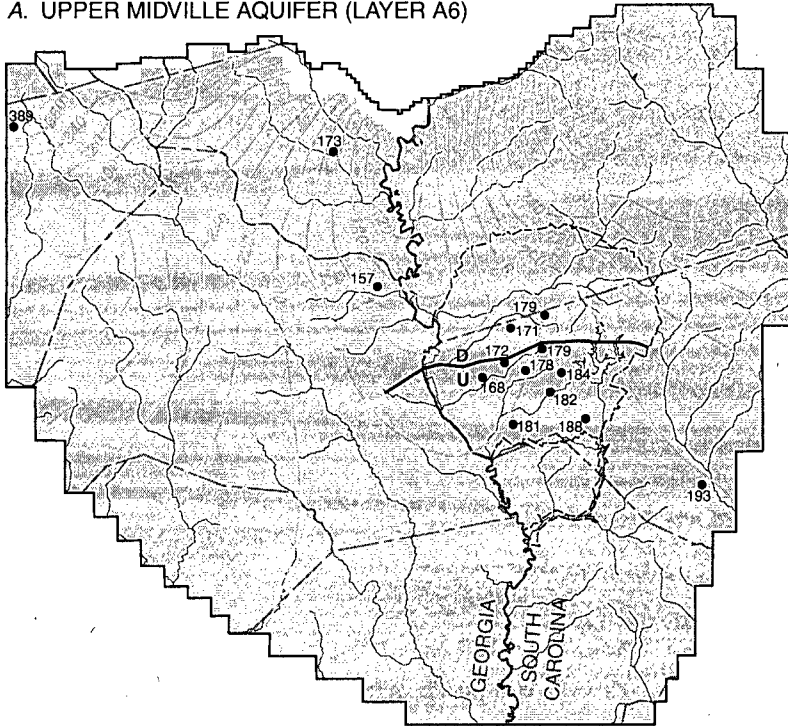


**Figure 25.** Simulated drawdown, 1953–92, and locations of simulated pumpage and observation wells completed in the (A) upper Dublin (layer A4) and (B) lower Dublin (layer A5) aquifers.

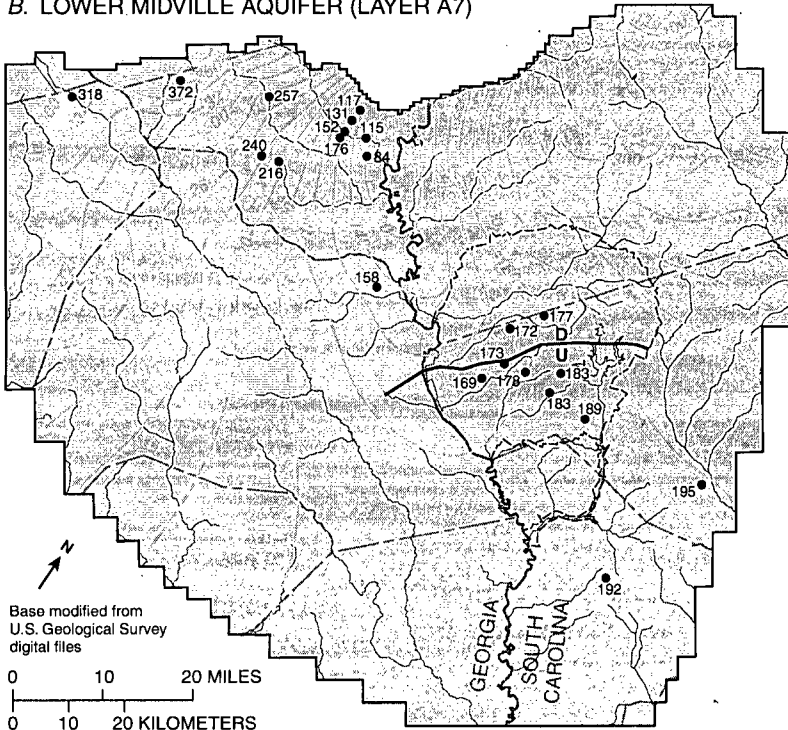
A. UPPER MIDVILLE AQUIFER (LAYER A6)



EXPLANATION

-  SIMULATED AREA
-  SIMULATED POTENTIOMETRIC CONTOUR—Shows simulated potentiometric surface, in feet. Hachures indicate depression. Contour interval 20 feet. Datum is sea level
-  MODEL BOUNDARY
-  PEN BRANCH FAULT—  
U, Upthrown side;  
D, Downthrown side
-  WELL DATA POINT—Number is observed water level, in feet above sea level

B. LOWER MIDVILLE AQUIFER (LAYER A7)



Base modified from U.S. Geological Survey digital files

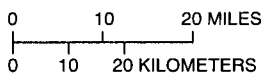
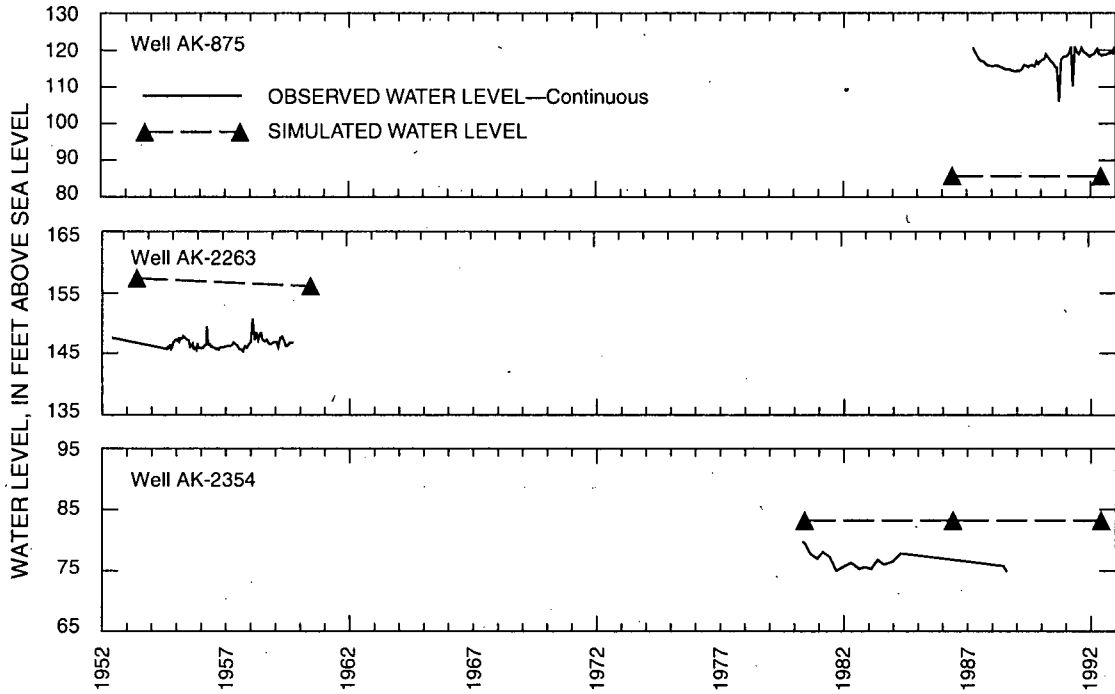
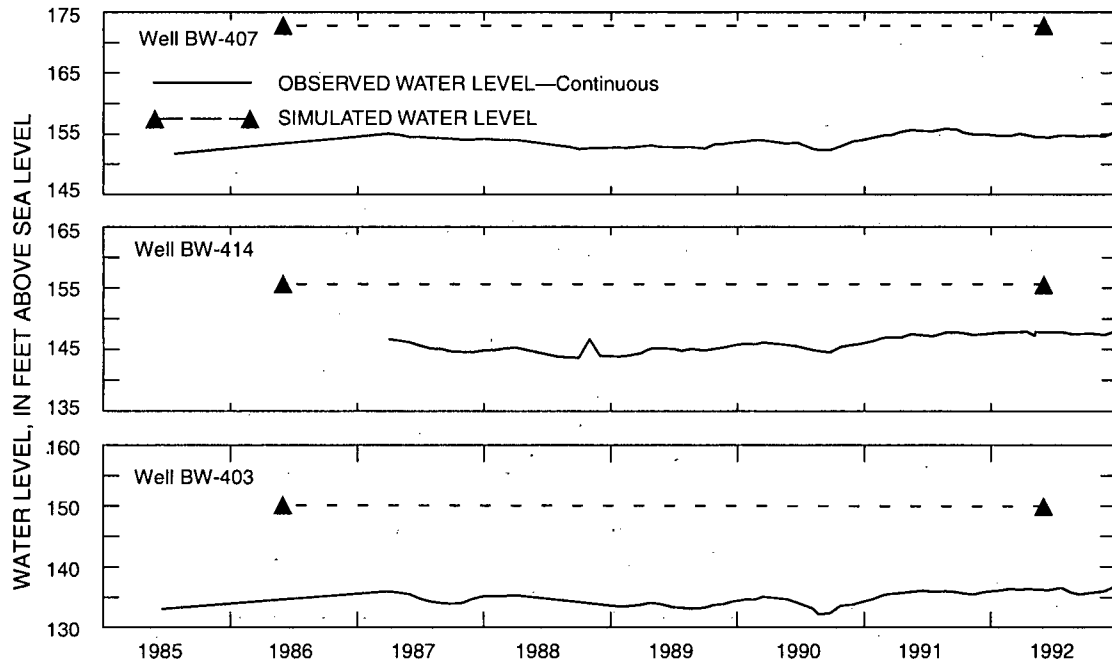


Figure 20. Simulated modern-day (1987–92) potentiometric surface and observed heads for the (A) upper Midville (layer A6) and (B) lower Midville (layer A7) aquifers.



**Figure 27.** Graph showing observed and simulated water levels in selected wells completed in the Gordon aquifer (layer A2). (Well locations shown in figure 24A; modified from Clarke and West, 1997.)



**Figure 28.** Graph showing observed and simulated water levels in selected wells completed in the Millers Pond aquifer (layer A3). (Well locations shown in figure 24B; modified from Clarke and West, 1997.)

Simulated water-level declines in layers A4 and A5 extend beneath the Savannah River, resulting in a change in the configuration of simulated potentiometric surface near the river (fig. 19). In this area, the potentiometric "saddle" feature has disappeared, as evidenced by the position of the 160-ft contour, which is no longer subdivided into upstream and downstream discharge zones.

In the northernmost part of the study area, simulated drawdown in layer A4 is less than that in layer A5, largely because layer A5 extends farther northward in the study area than layer A4 (fig. 25). In these northern areas, water levels in A5 are influenced by pumpage and by leakage to underlying units. Simulated water-level declines in layer A5, in the Augusta and northern Jefferson County, Ga., areas were 1–2 ft; and in the Aiken, S.C., area were 1–4 ft.

In general, simulated water-level trends in layers A4 and A5 show a good match to water-level trends in observation wells (figs. 29, 30). Although head residuals at wells AK-863 (fig. 29), 28AA06 and AK-532 (fig. 30) were relatively large (about 15 ft), simulated water levels still matched observed trends. During 1952–75 water levels in well AK-468 showed little change, and then declined about 13 ft during 1975–88 (fig. 29). Although the lack of water-level trend during 1952–75 was simulated by the model, the decline during 1975–88 was not. This discrepancy may be the result of inaccurate pumpage data or insufficient resolution of hydraulic properties in the area.

In layers A6 and A7, simulated pumpage of 6.6 Mgal/d in layer A6, and 20.8 Mgal/d in layer A7 during 1987–92 (table 6), produced only minor changes from the simulated predevelopment water budget, and drawdown of as much as 5 ft. The most significant change to the simulated predevelopment water budget was a reduction in the amount of ground-water discharge to streams—9 percent in layer A6 and about 8 percent in layer A7; and a reduction in ground-water outflow along lateral boundaries—about 2 percent in layer A6 and 8 percent in layer A7 (table 11; fig. 21). Simulated drawdown in layers A6 and A7 (fig. 26) was similar due to the high degree of hydraulic connection of the layers. Drawdown greater than 1 ft covered a large area that included pumping sites on both sides of the Savannah River—Plant Vogtle in Georgia, and the SRS and

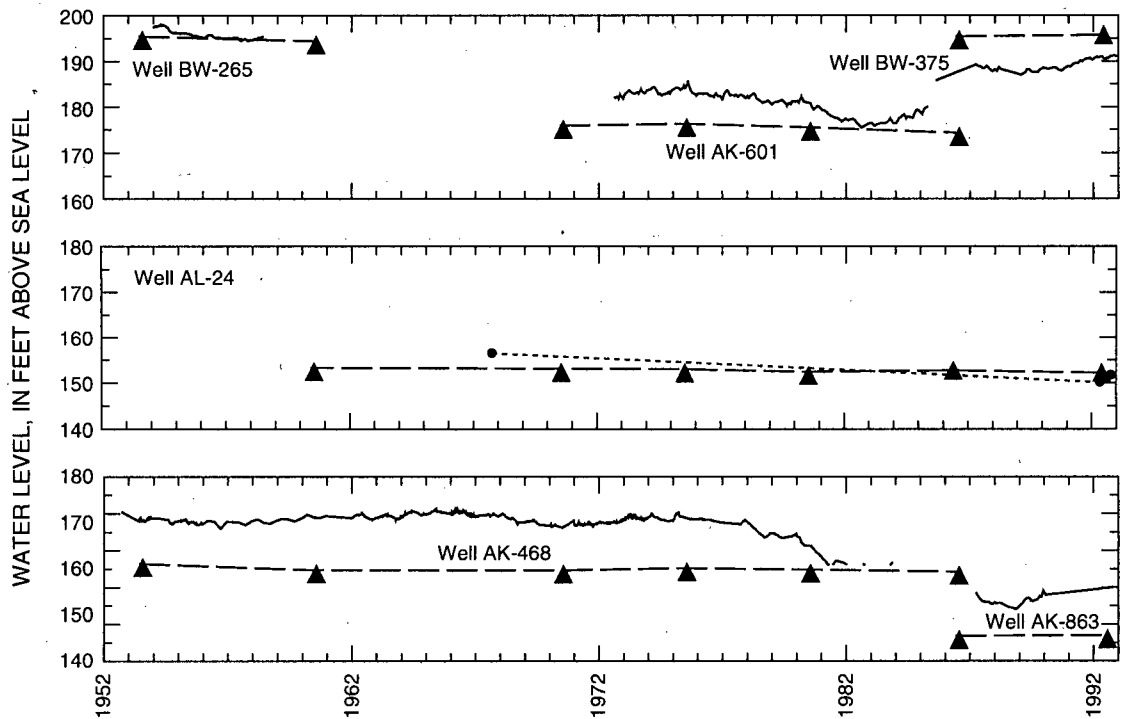
Aiken in South Carolina. Maximum simulated drawdown in this area was about 5 ft near the A/M area at SRS (site 9), 4 ft at Aiken (site 12), and 3 ft at Plant Vogtle (site 6) (see locations, fig. 7). Declines of 1 to 5 ft were simulated in the Richmond County, Ga., area, in response to pumpage at the Richmond County wellfield (site 4) and Olin Corp. (site 5). Despite these simulated declines, the configuration of the simulated modern-day potentiometric surface for layers A6 and A7 (fig. 20) remained largely unchanged from predevelopment conditions.

In general, simulated water-level trends in layers A6 and A7 show a good match to water-level trends in observation wells (figs. 31 and 32). In layer A6, simulated water-level trends for wells BW-382, BW-383, BW-44, and AK-864 (fig. 31), agree well with observed values, with the exception of some fluctuations observed in BW-44 in the middle of stress period 2 (1961–70). In layer A7, simulated water-level trends in wells BW-274, AK-582, BW-316, BW-430, and 30AA02 (fig. 32) also are in good agreement with observed trends.

Although most simulated water-level trends in layer A7 agree well with observations, trends in several wells showed a poor match. Simulated water-levels in layer A7 in well AK-183 (fig. 32) initially showed a good match to observed drawdown during the first stress period (1953–60), but a water-level recovery during the latter part of the stress period was not simulated by the model. In wells 29AA08 and 29BB01, simulated water levels also showed a poor match to observed trends. These discrepancies may be the result of inaccurate pumpage data, insufficient resolution of hydraulic properties in the area, or error introduced by the proximity of the well to a lateral model boundary.

### Calibrated Hydraulic Properties

The predevelopment and modern-day periods were calibrated, in part, by adjusting values of transmissivity, vertical conductance, and riverbed conductance. Most adjustments were made to the vertical conductance and riverbed conductance arrays, which have the poorest data coverage.



**EXPLANATION**

- OBSERVED WATER LEVEL—Continuous
- - - - • OBSERVED WATER LEVEL—Periodic
- ▲- - - - ▲ SIMULATED WATER LEVEL

**Figure 29.** Observed and simulated water levels in selected wells completed in the upper Dublin aquifer (layer A4). (Well locations shown in figure 25A; modified from Clarke and West, 1997).

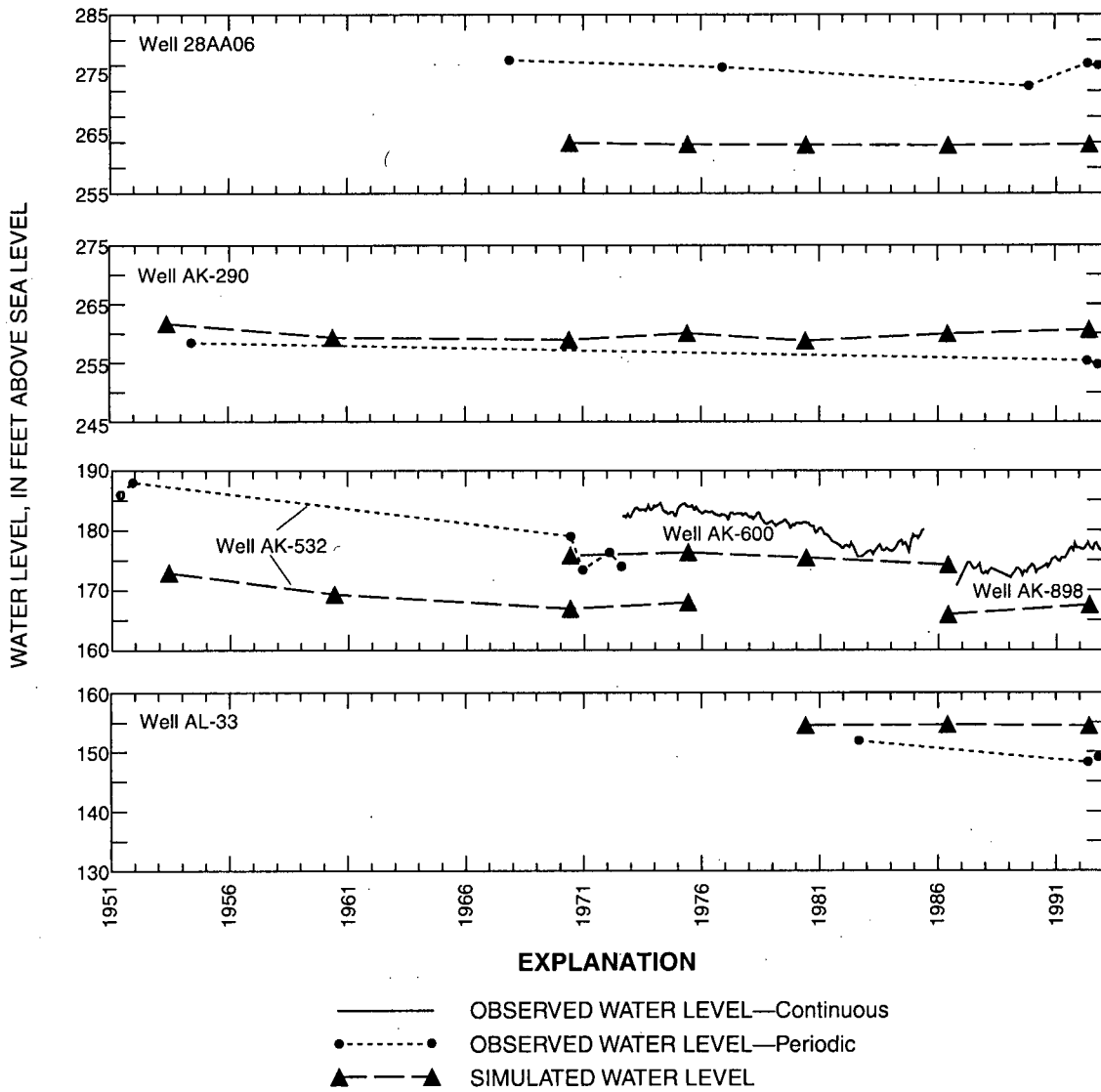


**Figure 30.** Observed and simulated water levels in selected wells completed in the lower Dublin aquifer (layer A5). (Well locations shown in figure 25B; modified from Clarke and West, 1997).

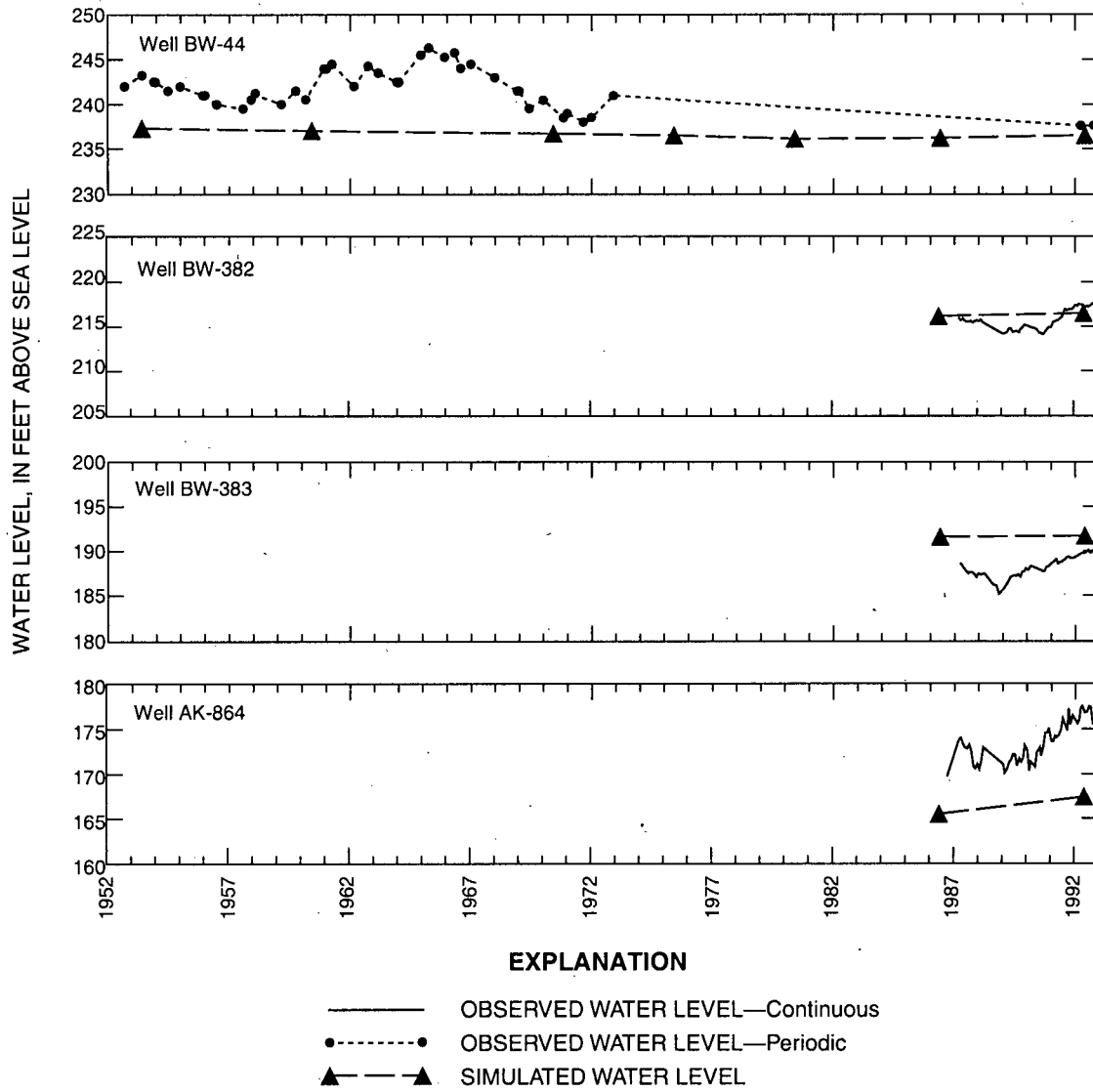
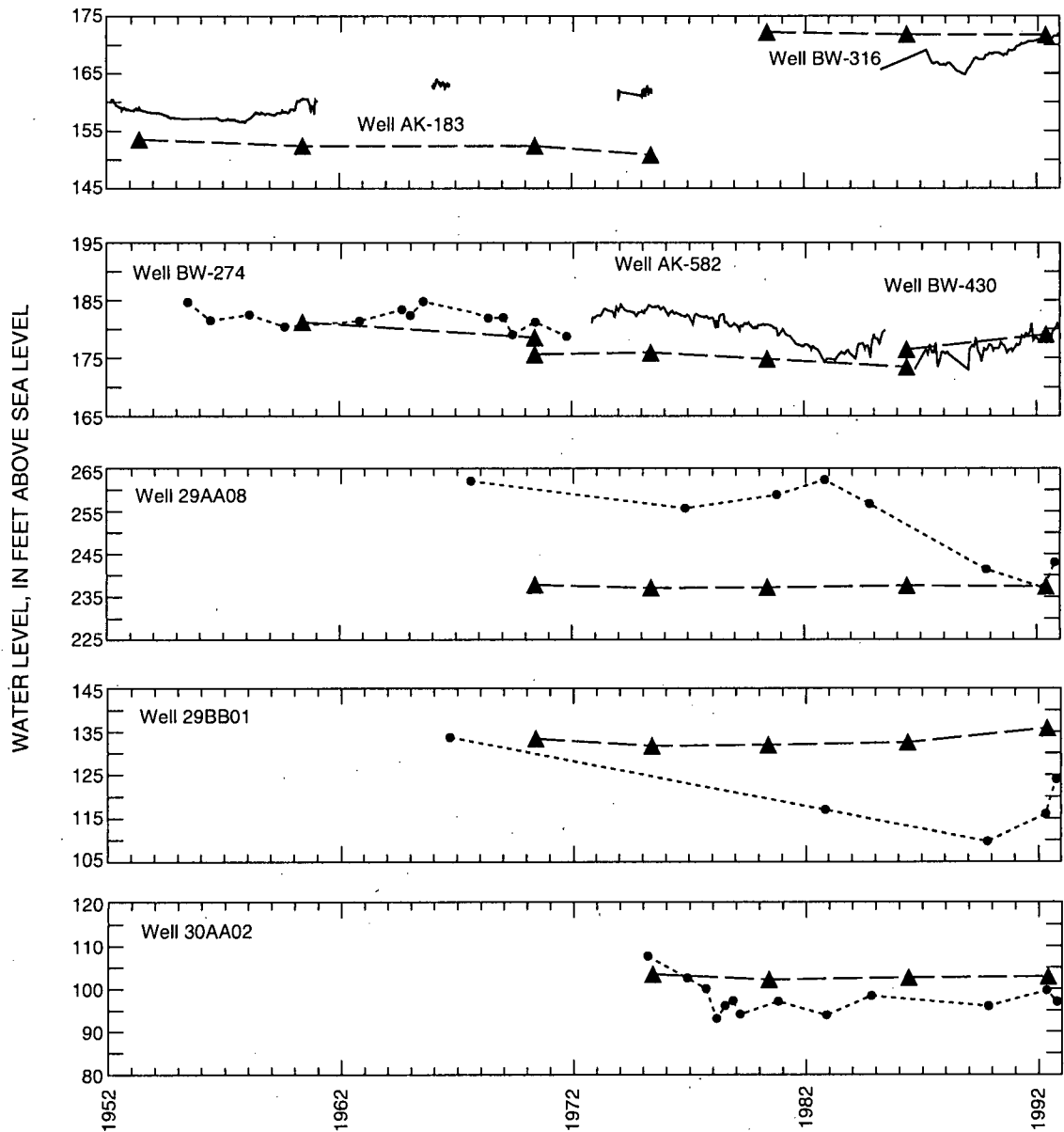


**Figure 31.** Observed and simulated water levels in selected wells completed in the upper Midville aquifer (layer A6). (Well locations shown in figure 26A; modified from Clarke and West, 1997).



**EXPLANATION**

- OBSERVED WATER LEVEL—Continuous
- OBSERVED WATER LEVEL—Periodic
- ▲—▲ SIMULATED WATER LEVEL

**Figure 32.** Observed and simulated water levels in selected wells completed in the lower Midville aquifer (layer A7). (Well locations shown in figure 26B; modified from Clarke and West, 1997).

The area-weighted mean of the calibrated transmissivity ranged from 1,310 ft<sup>2</sup>/d in layer A3 to 19,020 ft<sup>2</sup>/d in layer A7 (table 12). Calibrated mean transmissivity generally was higher than the mean of estimates based on field data. Maps of model-derived transmissivity, together with field observations and estimates for layers A2–A7, are shown in figures 33–35; ranges of calibrated and estimated based on field data values are listed in table 12. Calibrated transmissivity generally is high toward the southern part of the study area, where aquifers are thick; and low along the northern part of the study area, where aquifers are thin. In layer A3, a zone of relatively high transmissivity occurs in the central part of the study area (2,500 to 5,000 ft<sup>2</sup>/d), with low transmissivity in the southern part of the study area (fig. 33). In layers A4 and A5, a zone of high transmissivity (greater than 20,000 ft<sup>2</sup>/d) occurs along the southern side of the Pen Branch Fault (fig. 34). In layer A7, a zone of high transmissivity (10,000 to 15,000 ft<sup>2</sup>/d) occurs near the Savannah River and Fall Line (fig. 35), in an area where aquifer sediments are relatively thin. These high transmissivities may be related to increased permeability of sediments having coarse grain sizes near their source area.

In layers A2, A5, and A7, the area-weighted mean simulated transmissivity is approximately twice the mean of that estimated based on field data (table 13). Possible causes of this discrepancy are the heterogeneity of the aquifer sediments; or estimates based on tests conducted in wells that only partially penetrated the aquifer, and were thus, not representative of the entire aquifer thickness. In addition, because transmissivity data were not available over large parts of the study area, comparisons are biased toward the relatively smaller areas of data coverage.

Area-weighted means of model-derived leakance values range from  $1.7 \times 10^{-4}$  (ft/d)/ft in layer C1, to  $1.9 \times 10^{-2}$  (ft/d)/ft in layer C2 (table 13). Model-derived values were compared to estimates of leakance determined from core data at selected sites (table 13). Mean calibrated leakance values were within an order of magnitude of estimated values for all layers except C4 and C6, which were within 2 orders of magnitude. Reasons for these large differences include: (1) the few laboratory-derived conductance values probably are not representative of the confining unit at the site the cores were obtained; and (2) the values probably do not represent large areas of the confining unit.

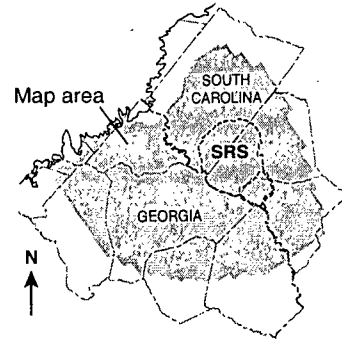
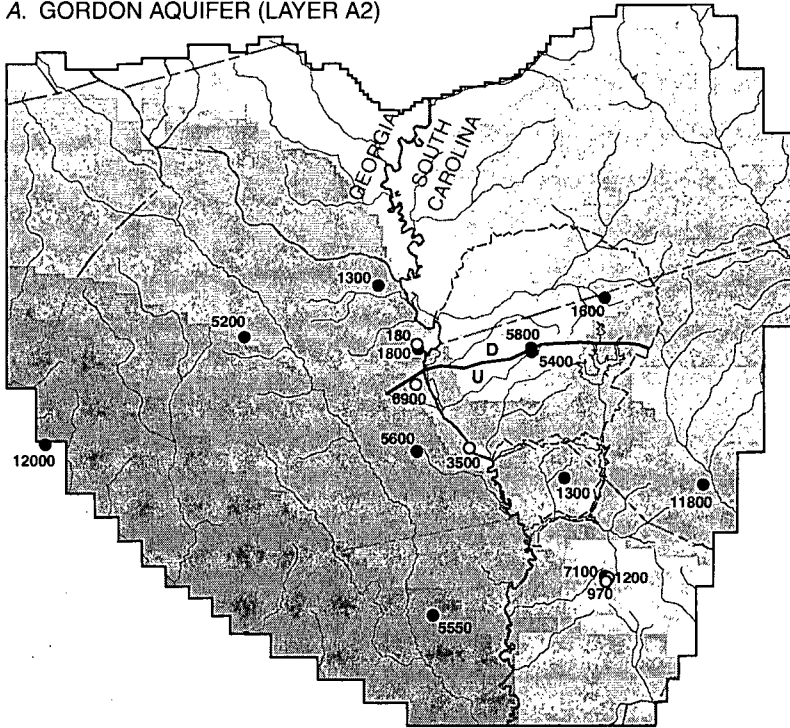
**Table 12.** Simulated and estimated values for transmissivity

Aquifer	Layer number	Transmissivity, in feet squared per day						
		<sup>1</sup> Estimated based on field data				Simulated		
		Number of values	Minimum	Maximum	Mean	Minimum	Maximum	Mean <sup>2</sup>
Gordon aquifer	A2	18	180	12,200	4,500	100	24,760	10,350
Millers Pond aquifer	A3	10	195	2,000	1,000	10	3,900	1,310
Upper Dublin aquifer	A4	17	555	25,200	5,830	10	20,000	7,220
Lower Dublin aquifer	A5	21	40	8,900	3,940	10	25,500	10,030
Upper Midville aquifer	A6	15	1,300	5,430	2,760	10	12,390	6,270
Lower Midville aquifer	A7	37	800	25,500	8,900	515	34,395	19,020

<sup>1</sup>Determined from aquifer tests and estimated from specific-capacity data and from borehole-resistivity logs.

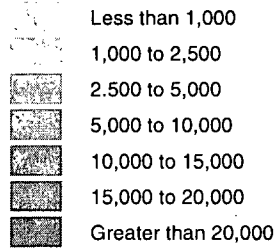
<sup>2</sup>Mean value weighted according to cell areas.

A. GORDON AQUIFER (LAYER A2)



EXPLANATION

CALIBRATED TRANSMISSIVITY,  
IN FEET SQUARED PER DAY



INACTIVE CELLS

MODEL BOUNDARY

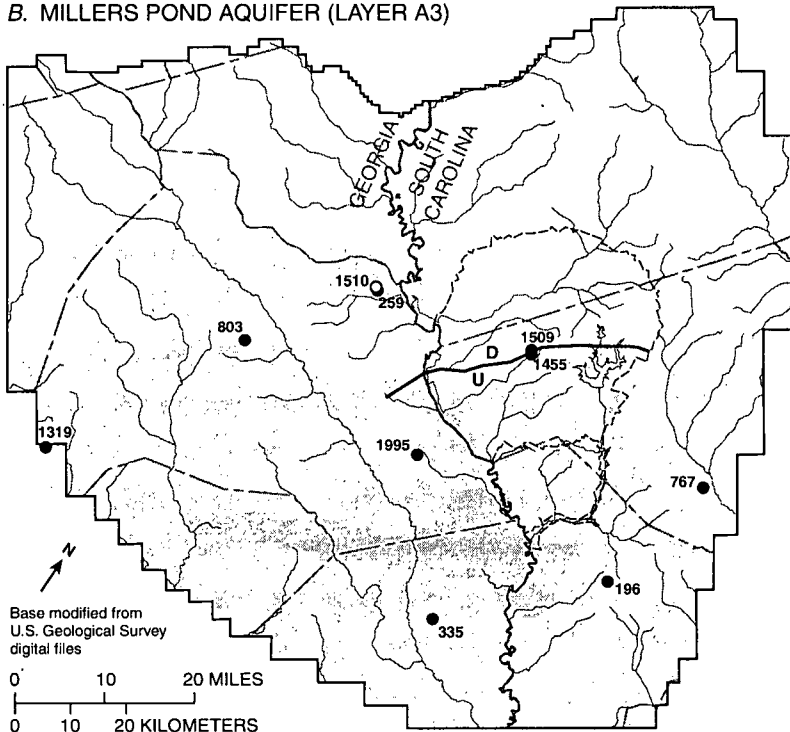
PEN BRANCH FAULT—  
U, Upthrown side;  
D, Downthrown side

WELL— Number is estimated  
transmissivity, in feet squared  
per day, determined from:

1510 Aquifer test or specific capacity

767 Resistivity logs

B. MILLERS POND AQUIFER (LAYER A3)



Base modified from  
U.S. Geological Survey  
digital files

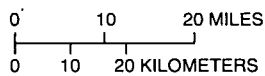
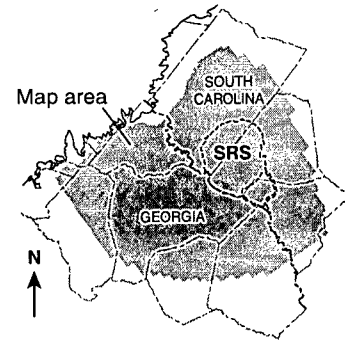
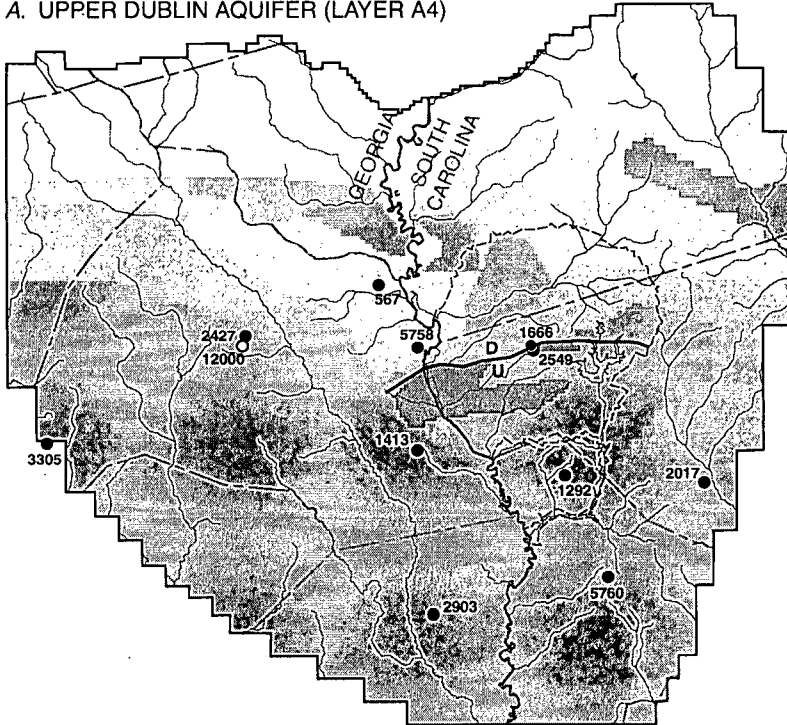


**Figure 33.** Calibrated transmissivity array and estimated values for the (A) Gordon (layer A2) and (B) Millers Pond (layer A3) aquifers.

A. UPPER DUBLIN AQUIFER (LAYER A4)



EXPLANATION

CALIBRATED TRANSMISSIVITY, IN FEET SQUARED PER DAY

- Less than 1,000
- 1,000 to 2,500
- 2,500 to 5,000
- 5,000 to 10,000
- 10,000 to 15,000
- 15,000 to 20,000
- Greater than 20,000

INACTIVE CELLS

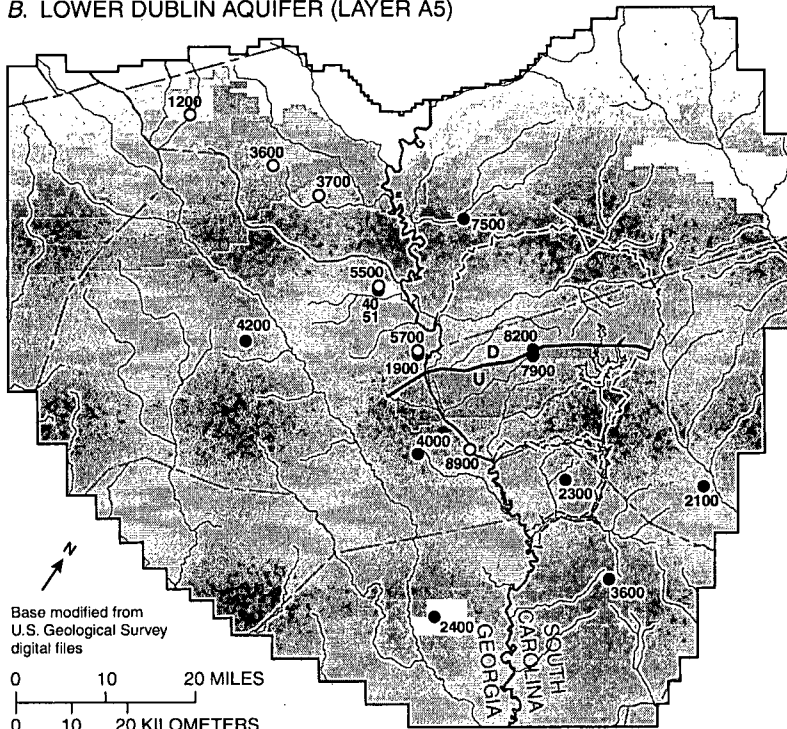
MODEL BOUNDARY

PEN BRANCH FAULT—  
U, Uphrown side;  
D, Downthrown side

WELL— Number is estimated transmissivity, in feet squared per day, determined from:

- 8900 Aquifer test or specific capacity
- 2100 Resistivity logs

B. LOWER DUBLIN AQUIFER (LAYER A5)



Base modified from U.S. Geological Survey digital files

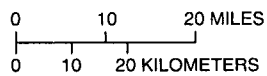
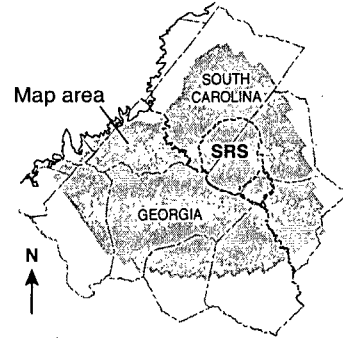
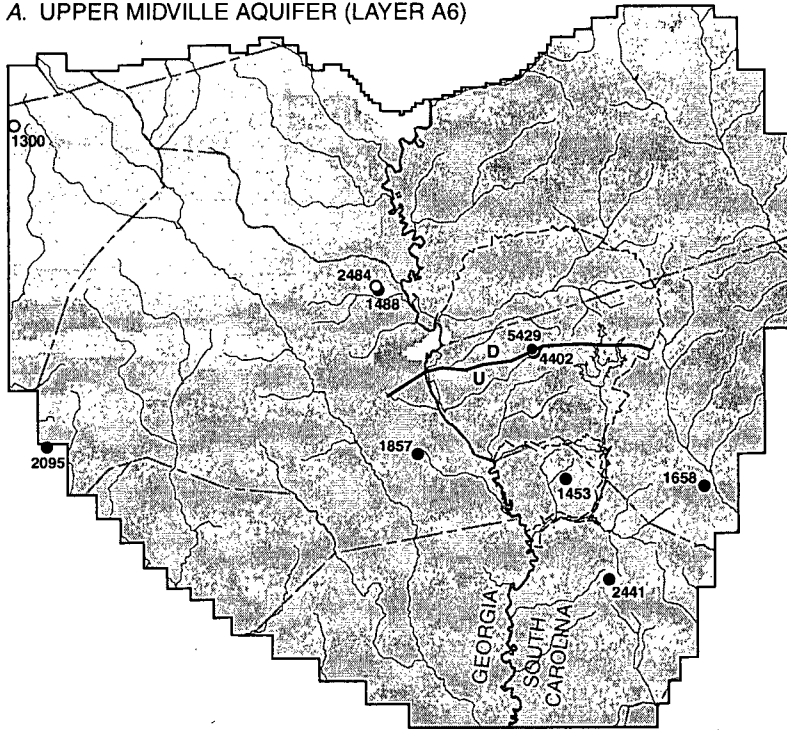


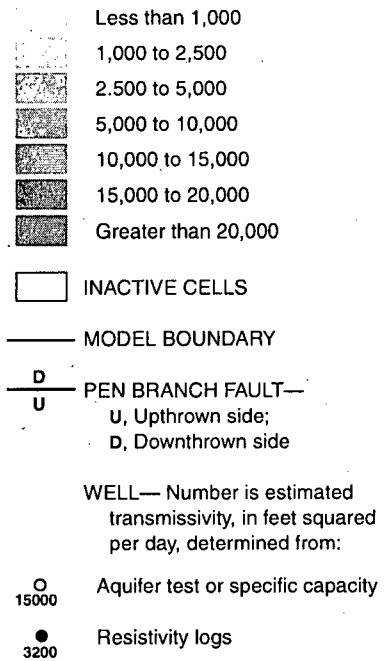
Figure 34. Calibrated transmissivity array and estimated values for the (A) upper Dublin (layer A4) and (B) lower Dublin (layer A5) aquifers.

A. UPPER MIDVILLE AQUIFER (LAYER A6)



**EXPLANATION**

CALIBRATED TRANSMISSIVITY,  
IN FEET SQUARED PER DAY



B. LOWER MIDVILLE AQUIFER (LAYER A7)

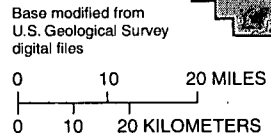
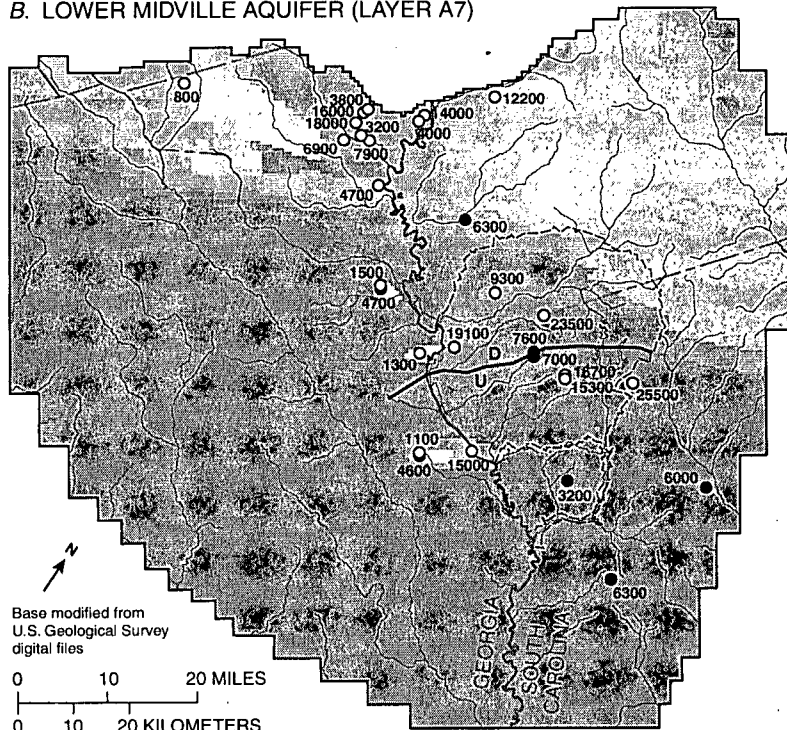


**Figure 35.** Calibrated transmissivity array and estimated values for the (A) upper Midville (layer A6) and (B) lower Midville (layer A7) aquifers.

**Table 13.** Simulated and estimated values for leakance

[—, not measured]

Hydrogeologic unit	Layer number	Leakance, in feet per day per foot of confining unit thickness <sup>1/</sup>						
		<sup>2/</sup> Estimated leakance			Simulated			
		Number of values	Minimum	Maximum	Mean	Minimum	Maximum	Mean <sup>3/</sup>
Gordon confining unit	C1	6	$4.7 \times 10^{-6}$	$1.2 \times 10^{-2}$	$2.1 \times 10^{-3}$	$9.0 \times 10^{-8}$	$1.3 \times 10^{-3}$	$1.7 \times 10^{-4}$
Millers Pond confining unit	C2	—	—	—	—	$3.9 \times 10^{-6}$	$8.7 \times 10^{-1}$	$1.9 \times 10^{-2}$
Upper Dublin confining unit	C3	9	$1.8 \times 10^{-6}$	$1.6 \times 10^{-3}$	$3.6 \times 10^{-4}$	$1.2 \times 10^{-6}$	$7.3 \times 10^{-3}$	$1.2 \times 10^{-3}$
Lower Dublin confining unit	C4	1	$2.4 \times 10^{-5}$	$2.4 \times 10^{-5}$	$2.4 \times 10^{-5}$	$3.0 \times 10^{-7}$	$6.5 \times 10^{-3}$	$6.6 \times 10^{-3}$
Upper Midville confining unit	C5	11	$6.7 \times 10^{-7}$	$3.4 \times 10^{-4}$	$7.6 \times 10^{-5}$	$2.1 \times 10^{-7}$	$1.0 \times 10^{-1}$	$9.7 \times 10^{-4}$
Lower Midville confining unit	C6	1	$1.0 \times 10^{-5}$	$1.0 \times 10^{-5}$	$1.0 \times 10^{-5}$	$7.7 \times 10^{-5}$	$3.6 \times 10^{-1}$	$9.0 \times 10^{-3}$

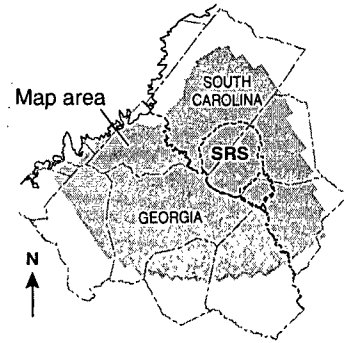
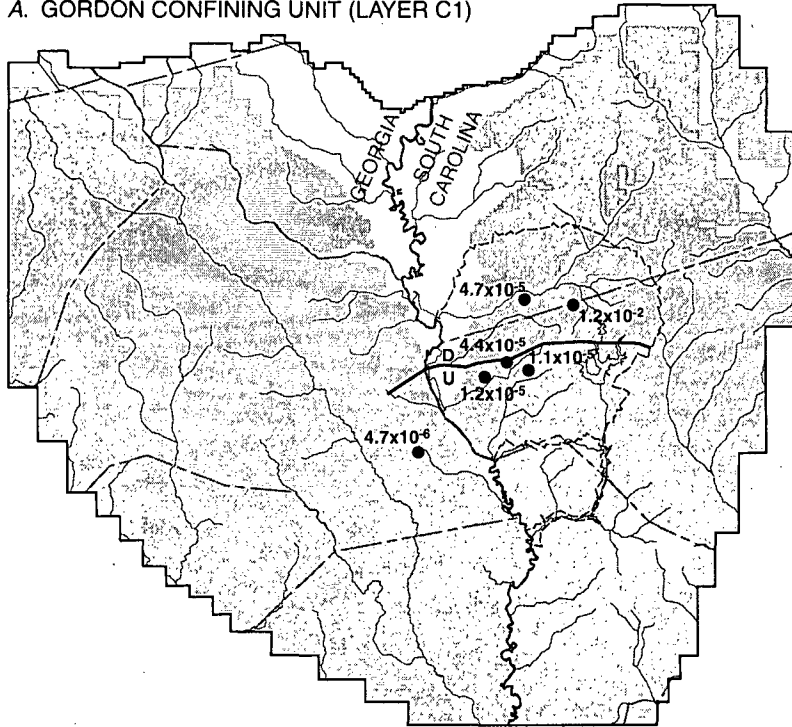
<sup>1/</sup>Includes low permeability layers within aquifer layers.<sup>2/</sup>Estimated by dividing the vertical hydraulic conductivity of confining unit by the thickness of the confining unit.<sup>3/</sup>Mean value weighted according to cell area.

Leakance values were adjusted during calibration to regulate the flow of water between the model layer and overlying and underlying layers or to overlying streams. These include adjustments to values in layer C1 in order to maintain “realistic” rates of recharge (less than 20 inches per year). Calibrated leakance values for layers C1-C6 are shown in figures 36–38. In general, the areal distribution of model-derived leakance conforms to initial estimates based on thickness variations of confining units. Low leakance values in updip areas are evident in layers C1 (fig. 36) and C6 (fig. 38) in much of the northern part of the study area, and in layers C3 and C4 between Upper Three Runs Creek and Hollow Creek (fig. 37). Elsewhere, leakance beneath major streams was adjusted in order to regulate ground-water discharge into the stream. A zone of high leakance is evident in layer C2 beneath Brier Creek and Lower Three Runs Creek (fig. 36). Conversely, a zone of low leakance is evident beneath the Savannah River in layer

C4 (fig. 37). Variations in leakance values may be related to changes in the depositional environment of sediments, changes in thickness due to erosion, or the presence of low permeability units within aquifers. Increased leakance near streams may be related to reduced thickness of confining units as a result of erosion during periods when stream base levels were lower than at present.

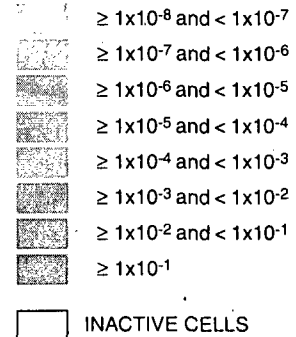
Values of riverbed conductance were adjusted during calibration: (1) to regulate the amount of ground-water discharge to a stream; and (2) to control aquifer head. The area-weighted mean of calibrated riverbed conductance for areas where aquifers are in hydraulic connection with stream alluvium ranges from about 1,720 to 11,200 ft<sup>2</sup>/d; whereas, the area-weighted mean of riverbed conductance for areas where confining units are in hydraulic connection with stream alluvium ranges from about 1,420 to 6,320 ft<sup>2</sup>/d (table 14).

A. GORDON CONFINING UNIT (LAYER C1)



**EXPLANATION**

CALIBRATED LEAKANCE,  
IN FEET PER DAY PER  
FOOT OF THICKNESS—  
≥, greater than or equal to;  
<, less than

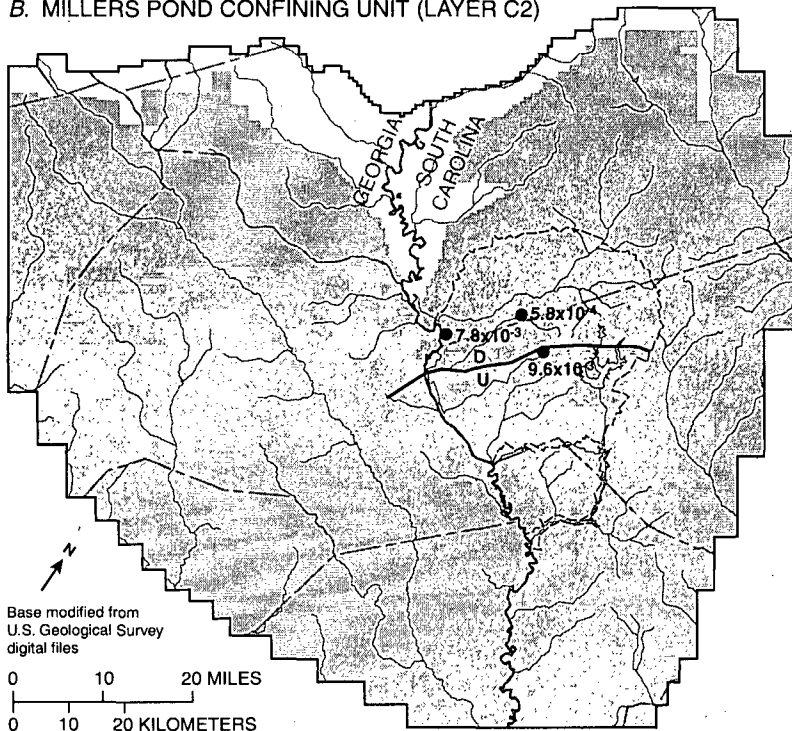


— MODEL BOUNDARY

PEN BRANCH FAULT—  
U, Upthrown side;  
D, Downthrown side

WELL— Number is leakance,  
in feet per day per foot of  
thickness, estimated by  
dividing vertical hydraulic  
conductivity by confining  
unit thickness

B. MILLERS POND CONFINING UNIT (LAYER C2)



Base modified from  
U.S. Geological Survey  
digital files

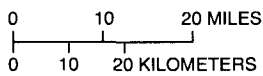
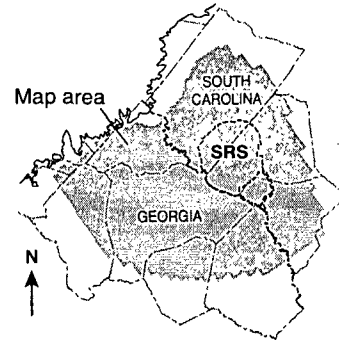
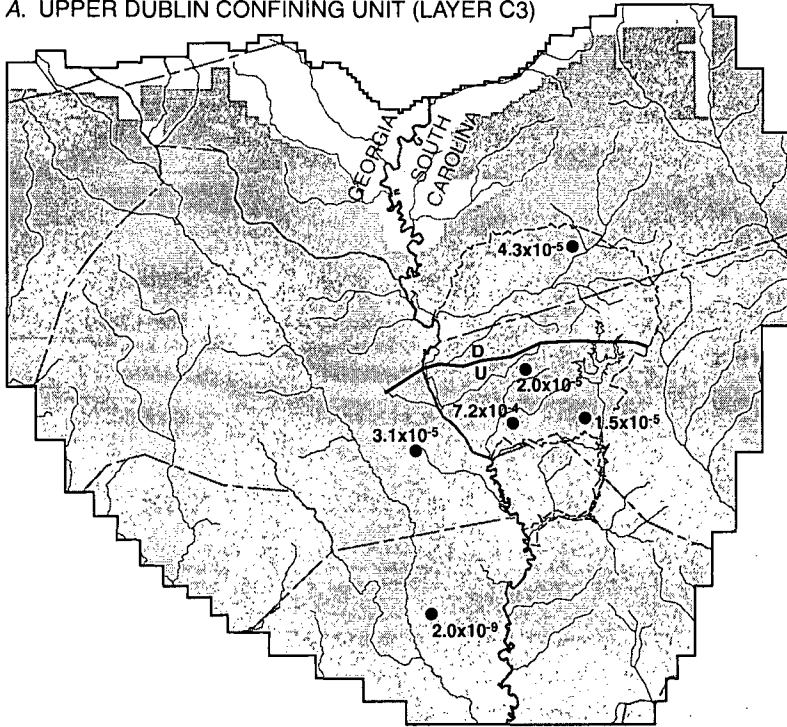


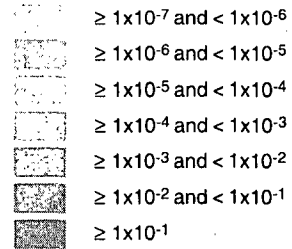
**Figure 36.** Calibrated leakance array and estimated values for the (A) Gordon (layer C1) and (B) Millers Pond (layer C2) confining units.

A. UPPER DUBLIN CONFINING UNIT (LAYER C3)



EXPLANATION

CALIBRATED LEAKANCE,  
IN FEET PER DAY PER  
FOOT OF THICKNESS—  
≥, greater than or equal to;  
<, less than



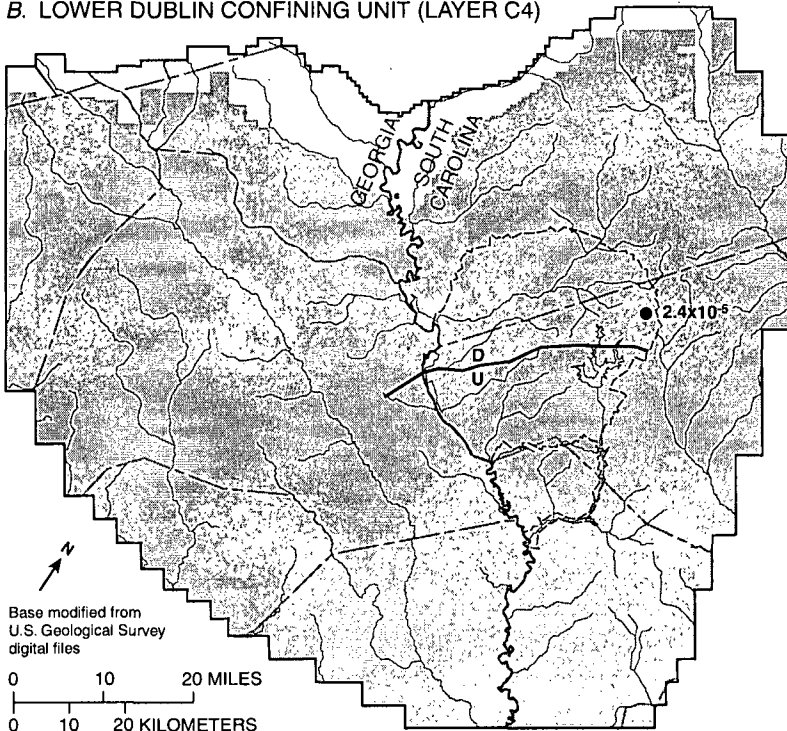
INACTIVE CELLS

MODEL BOUNDARY

PEN BRANCH FAULT—  
U, Upthrown side;  
D, Downthrown side

● 2.4x10<sup>-5</sup> WELL— Number is leakance,  
in feet per day per foot of  
thickness, estimated by  
dividing vertical hydraulic  
conductivity by confining  
unit thickness

B. LOWER DUBLIN CONFINING UNIT (LAYER C4)



Base modified from  
U.S. Geological Survey  
digital files

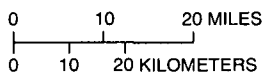
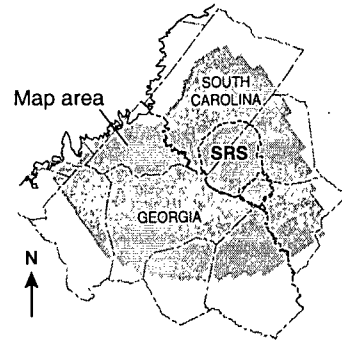
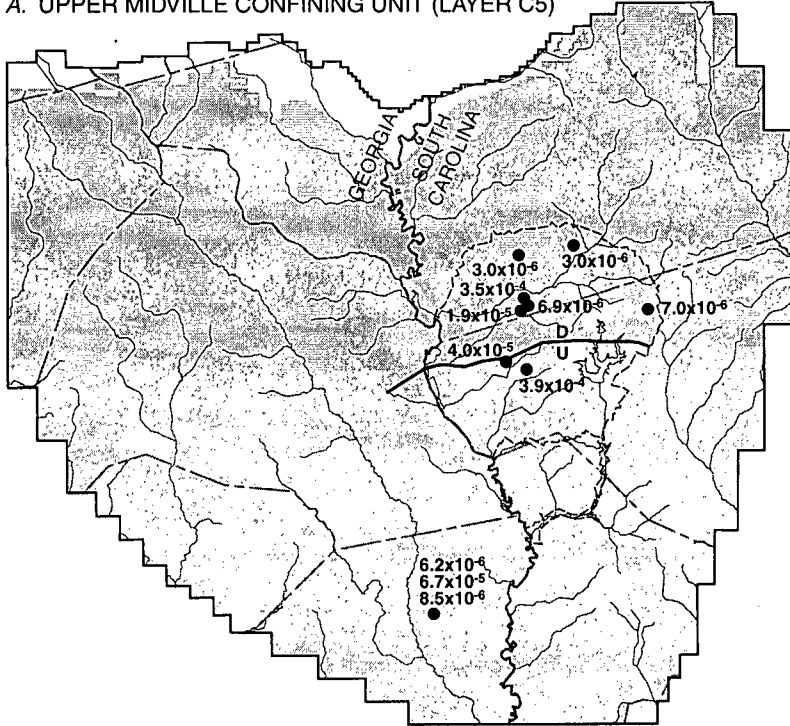


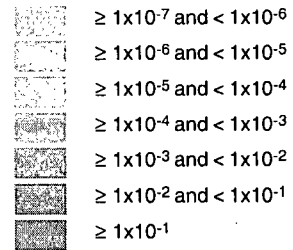
Figure 37. Calibrated leakance array and estimated values for the (A) upper Dublin (layer C3) and (B) lower Dublin (layer C4) confining units.

A. UPPER MIDVILLE CONFINING UNIT (LAYER C5)



EXPLANATION

CALIBRATED LEAKANCE,  
IN FEET PER DAY PER  
FOOT OF THICKNESS—  
≥, greater than or equal to;  
<, less than



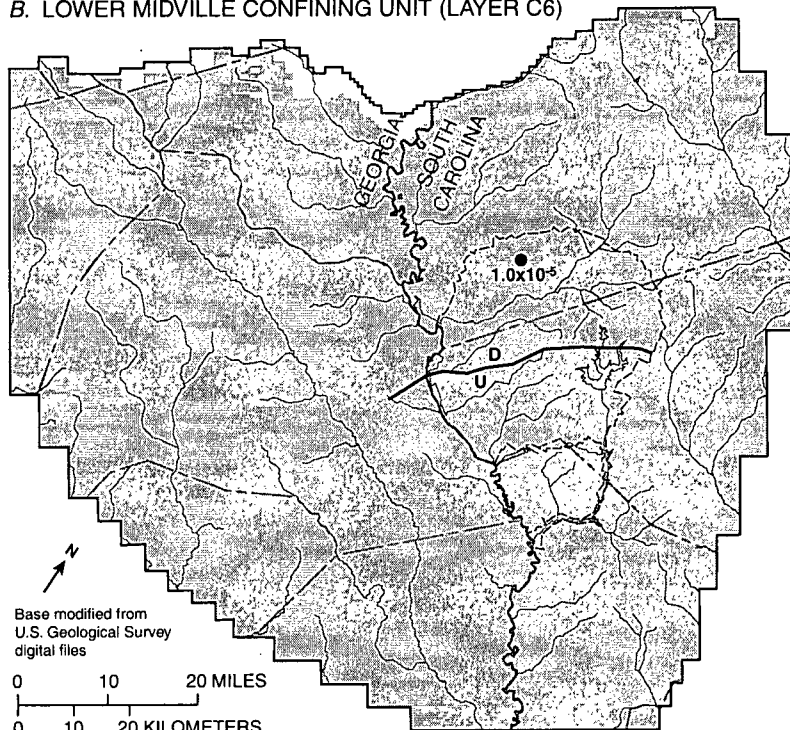
INACTIVE CELLS

MODEL BOUNDARY

PEN BRANCH FAULT—  
U, Upthrown side;  
D, Downthrown side

WELL— Number is leakance,  
in feet per day per foot of  
thickness, estimated by  
dividing vertical hydraulic  
conductivity by confining  
unit thickness

B. LOWER MIDVILLE CONFINING UNIT (LAYER C6)



Base modified from  
U.S. Geological Survey  
digital files



Figure 38. Calibrated leakance array and estimated values for the (A) upper Midville (layer C5) and (B) lower Midville (layer C6) confining units.

**Table 14.** Ranges of simulated conductance (CRIV) by hydrogeologic unit

Hydrogeologic unit	Layer number	Simulated streambed conductivity, in feet squared per day			
		Number of values	Minimum	Maximum	Mean <sup>1/</sup>
Gordon confining unit	C1	244	7.8	30,400	6,320
Gordon aquifer	A2	443	15	110,800	11,200
Millers Pond confining unit	C2	42	66	26,300	1,420
Millers Pond aquifer	A3	58	323	3,000	2,500
Upper Dublin confining unit	C3	62	31	42,400	2,330
Upper Dublin aquifer	A4	207	30	4,320	2,410
Lower Dublin confining unit	C4	122	8.6	85,600	3,680
Lower Dublin aquifer	A5	177	216	110,500	3,900
Upper Midville confining unit	C5	91	8.6	36,400	9,320
Upper Midville aquifer	A6	58	2,290	11,000	7,350
Lower Midville confining unit	C6	62	8.6	11,000	3,580
Lower Midville aquifer	A7	107	7.8	406,080	1,720

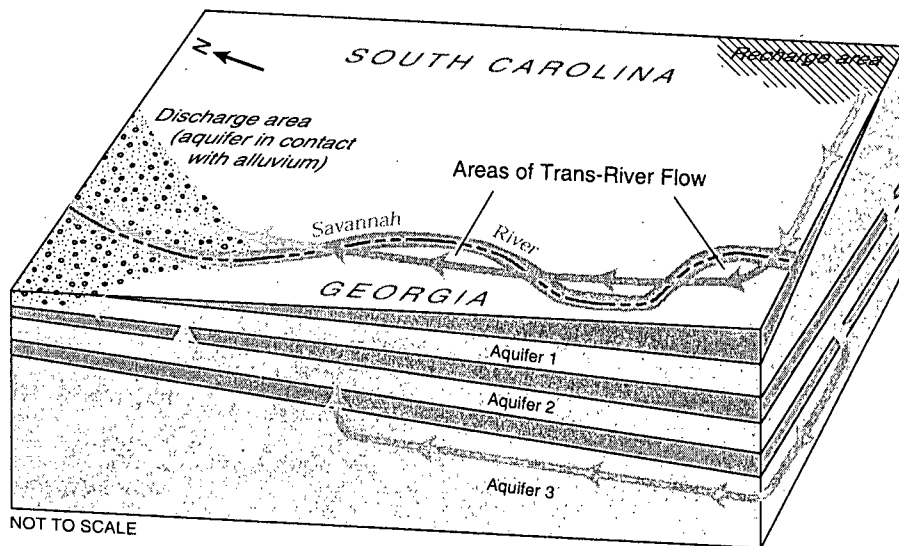
<sup>1/</sup>Mean value weighted according to cell areas.

### Trans-River Flow Beneath the Savannah River

Trans-river flow is a term that describes a condition where ground water originating on one side of a river flows beneath the river to the other side (Clarke and West, 1997). Natural factors controlling trans-river flow include: (1) vertical and horizontal hydraulic conductivity of aquifers and confining units; (2) thickness and areal extent of confining units; and (3) hydraulic gradient. In addition to natural factors, trans-river flow may be induced by ground-water withdrawal. The hydraulic gradient and the corresponding trans-river flow may be altered by ground-water withdrawal, particularly by pumping centers (fig. 7) located near the river. Pumped wells on one side of the river could induce the flow of ground water from the other side, thus altering the natural pattern of ground-water discharge into the river and adjacent alluvial valley. For the study area a potential for trans-river flow occurs in areas where aquifers are well separated hydraulically from the Savannah River (fig. 39). Although the principal objective of the trans-river flow study was to determine trans-river flow from the SRS into Georgia, ground-

water flow from Georgia to South Carolina is also presented in this report to provide a balanced overview of flow conditions in the study area.

Potentiometric-surface maps can be used to delineate lateral-flow directions, and thus give an indication of the possibility of trans-river ground-water flow (plates 1 and 2). Clarke and West (1997) presented a detailed evaluation of ground-water flow near the Savannah River, based on predevelopment potentiometric-surface maps interpreted from field data. That report indicated the possible occurrence of trans-river flow for a short distance into Georgia in the Dublin and Midville aquifer systems, prior to discharge to the Savannah River alluvial valley. Potentiometric-surface maps for the Upper Three Runs aquifer and Gordon aquifers did not indicate the possible occurrence of trans-river flow (Clarke and West, 1997). The configuration of modern-day potentiometric surfaces for each of the aquifers (plate 3) is not appreciably different from predevelopment conditions, and thus, directions of ground-water flow, including trans-river flow, generally are little changed for both flow conditions.



**EXPLANATION**

- |   |                |   |
|---|----------------|---|
|  | ALLUVIUM       | <b>GROUND-WATER FLOW</b>  |
|  | AQUIFER        |  Aquifer 1 |
|  | CONFINING UNIT |  Aquifer 2 |
|   |                |  Aquifer 3 |

**Figure 39.** Schematic diagram showing possible ground-water and trans-river flow in the vicinity of the Savannah River.

*Particle tracking analysis of advective ground-water flow*

Because ground-water flow in the vicinity of the Savannah River is characterized by large vertical gradients and nearly flat lateral gradients, flow directions derived from incomplete data and interpreted potentiometric-surface maps are imprecise and highly generalized. To better characterize the three-dimensional nature of ground-water flow near the Savannah River, the USGS particle-tracking code MODPATH (Pollock, 1994) was used to simulate flow paths during predevelopment and modern-day conditions.

MODPATH computes particle locations and travel times in three dimensions based on advective flow in a uniformly porous medium. MODPATH can track particles forward in time and space in the direction of ground-water flow, or backward toward recharge areas. The cell-by-cell flow terms from the calibrated steady-state MODFLOW simulations for predevelopment and 1987–92 were used as input to MODPATH. Results are based on steady-state simulations, and are subject to the

same errors and limitations as the model (See sections, “Limitations of Digital Simulation” and “Limitations of Particle Tracking.”)

To evaluate the occurrence of trans-river flow, particles of water in each active model layer (layers A2–A7) were ‘seeded’ along a 6-mi-wide corridor extending 3 mi into Georgia and 3 mi into South Carolina, along the entire course of the Savannah River in the model area. Within each model cell, five particles were placed centrally from the bottom to the top in increments of one-quarter of the total aquifer thickness. These particles were backtracked to determine their point of entry into the ground-water flow system (recharge areas). Model cells containing one or more particles that entered the flow system from the opposite side of the river, were mapped as areas of eastward or westward trans-river flow. It is important to note that greater vertical and horizontal saturation of particles in individual model cells (more than five particles) would likely result in delineation of larger contributing (recharge) areas. Such resolution would be required to determine the source of water to an individual well; however, that is beyond the scope of this study.

For each model cell, there are potentially five particles that might enter the flow system on the opposite side of the river. If only one particle enters on the opposite side of the river, there is less likelihood that a well installed in the cell area would capture water from the opposite side of the river, compared to a cell where all five particles entered on the other side of the river. Areas of trans-river flow are summarized in table 15 and figure 40, and are mapped in figures 41–47.

Westward and eastward trans-river flow occurs in three principal zones along the Savannah River:

- zone 1—from the Fall Line southward to the confluence of Hollow Creek and the Savannah River;
- zone 2—from the zone 1 southern boundary southward to the southern border of the SRS (not including the Lower Three Runs Creek section); and
- zone 3—from the zone 2 southern boundary, southward into the northern half of Screven County, Ga.

All trans-river flow zones for all model layers were located within or immediately adjacent to the Savannah River alluvial valley, and most were located in the immediate vicinity of the Savannah River.

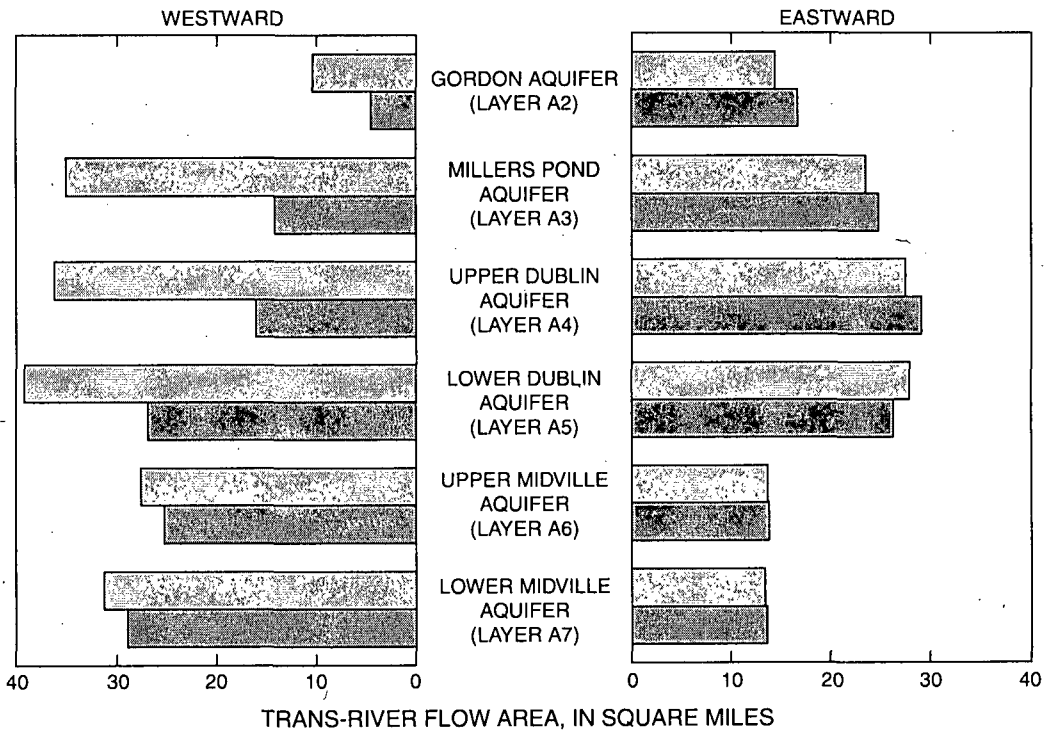
Because of changing meander patterns of the Savannah River, it is possible for a single flowpath to cross from one side of the river to the other several times prior to its ultimate discharge into the alluvial valley (fig. 39). This is demonstrated by different positions of trans-river flow zones shown on the maps. For example, in layer A2 (fig. 41), westward trans-river flow occurs along the same general flowpath in northern Screven and southern Burke Counties.

Areas of westward trans-river flow during predevelopment are larger than or equal to areas of eastward trans-river flow for all layers except A2, which contains larger eastward flow than westward (table 15, fig. 40). During modern-day conditions, the largest area of trans-river flow in layers A3 and A4 shifts from west to east, reflecting changes in hydraulic gradients due to pumpage. Although no major pumping centers are located in any of the predevelopment or modern-day trans-river flow zones, several are located in close proximity to these zones (sites 5, 6, and 14, fig. 7). Changes in pumpage at these sites could influence hydraulic gradients near the river and the occurrence of trans-river flow.

**Table 15.** Simulated trans-river flow by layer for predevelopment (pre-1953) and modern-day (1987–92) conditions

[mi<sup>2</sup>, square miles]

Model layer	Trans-river flow							
	Predevelopment conditions (pre-1953)				Modern-day conditions (1987–92)			
	Number of cells	Area (mi <sup>2</sup> )	Number of particles	Percentage of total trans-river particles in affected cells	Number of cells	Area (mi <sup>2</sup> )	Number of particles	Percentage of total trans-river particles in affected cells
<b>Westward trans-river flow</b>								
A2	38	10.4	95	50	21	4.5	71	68
A3	123	35.1	321	52	55	14.2	139	51
A4	131	36.3	616	94	65	16.1	299	92
A5	156	39.3	629	81	120	26.9	396	66
A6	130	27.6	648	100	122	25.3	603	99
A7	163	31.3	814	100	155	30	774	100
<b>Eastward trans-river flow</b>								
A2	124	14.8	529	85	123	16.7	532	87
A3	192	23.5	851	89	184	24.8	825	90
A4	203	27.5	969	95	197	29.1	942	96
A5	208	27.9	871	84	198	26.3	851	86
A6	123	13.7	603	98	124	13.8	608	98
A7	121	13.4	603	100	122	13.6	609	100

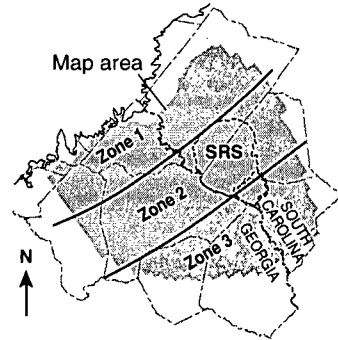
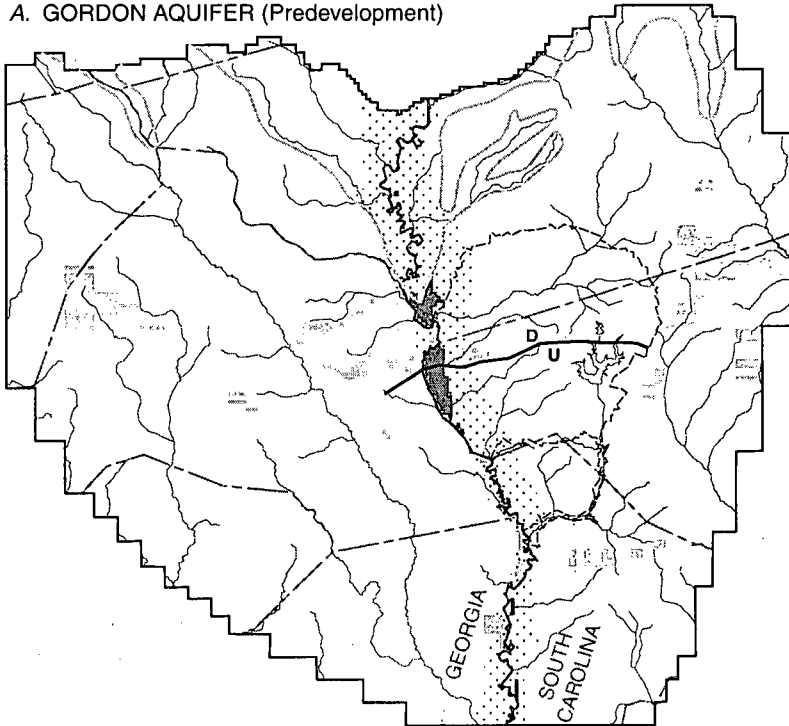


**EXPLANATION**

PREDEVELOPMENT
     
 
 MODERN DAY

**Figure 40.** Summary of simulated trans-river flow area by model layer for predevelopment and modern-day (1987–92) simulations.

A. GORDON AQUIFER (Predevelopment)



**EXPLANATION**

TRANS-RIVER FLOW

 Western, from South Carolina to Georgia

 Eastern, from Georgia to South Carolina

 RECHARGE AREA FOR TRANS-RIVER FLOW ZONES

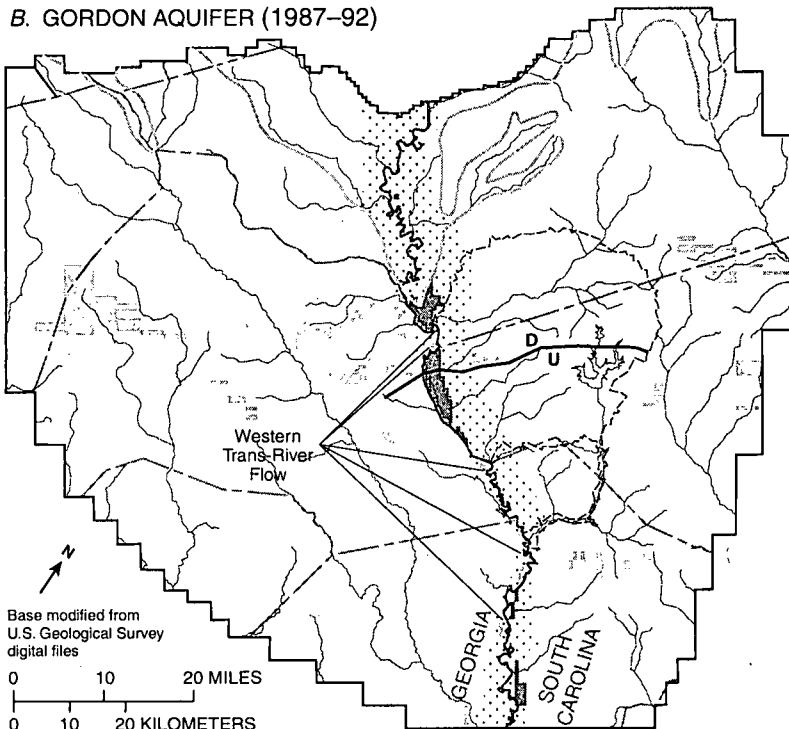
 SAVANNAH RIVER ALLUVIAL VALLEY

 APPROXIMATE NORTHERN EXTENT OF AQUIFER

 MODEL BOUNDARY

 PEN BRANCH FAULT—  
U, Upthrown side;  
D, Downthrown side

B. GORDON AQUIFER (1987–92)



Base modified from U.S. Geological Survey digital files

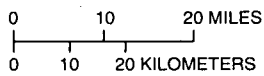
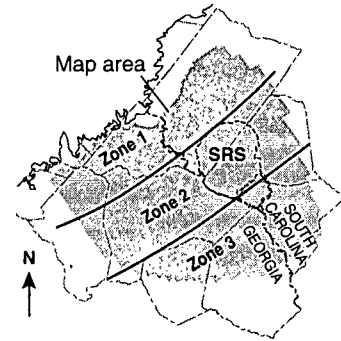
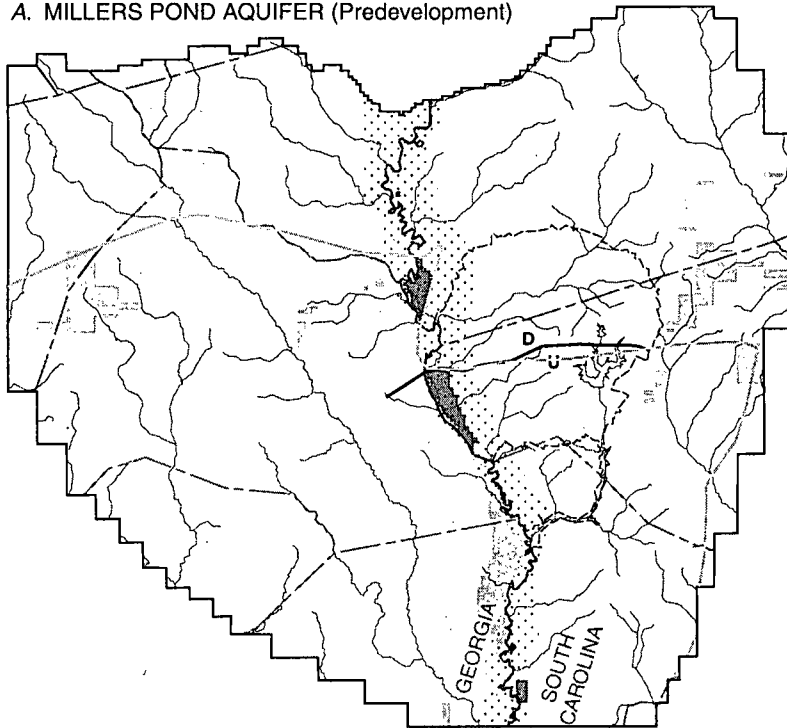


**Figure 41.** Simulated trans-river flow zones and associated recharge areas for the Gordon aquifer for (A) predevelopment and (B) modern-day (1987–92) conditions.

A. MILLERS POND AQUIFER (Predevelopment)



EXPLANATION

TRANS-RIVER FLOW

Western, from South Carolina to Georgia

Eastern, from Georgia to South Carolina

RECHARGE AREA FOR TRANS-RIVER FLOW ZONES

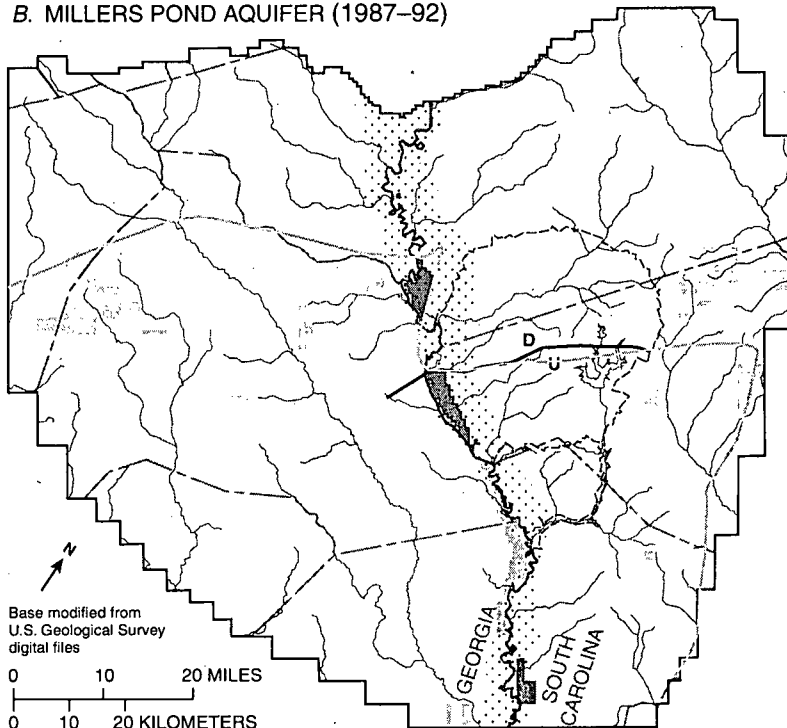
SAVANNAH RIVER ALLUVIAL VALLEY

APPROXIMATE NORTHERN EXTENT OF AQUIFER

MODEL BOUNDARY

PEN BRANCH FAULT—  
U, Upthrown side;  
D, Downthrown side

B. MILLERS POND AQUIFER (1987–92)



Base modified from  
U.S. Geological Survey  
digital files

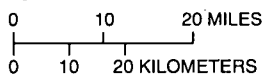
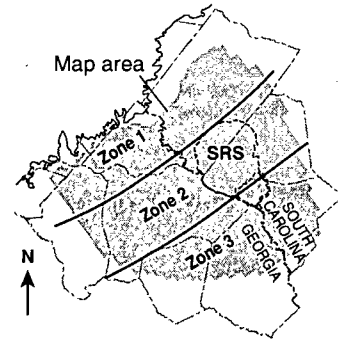
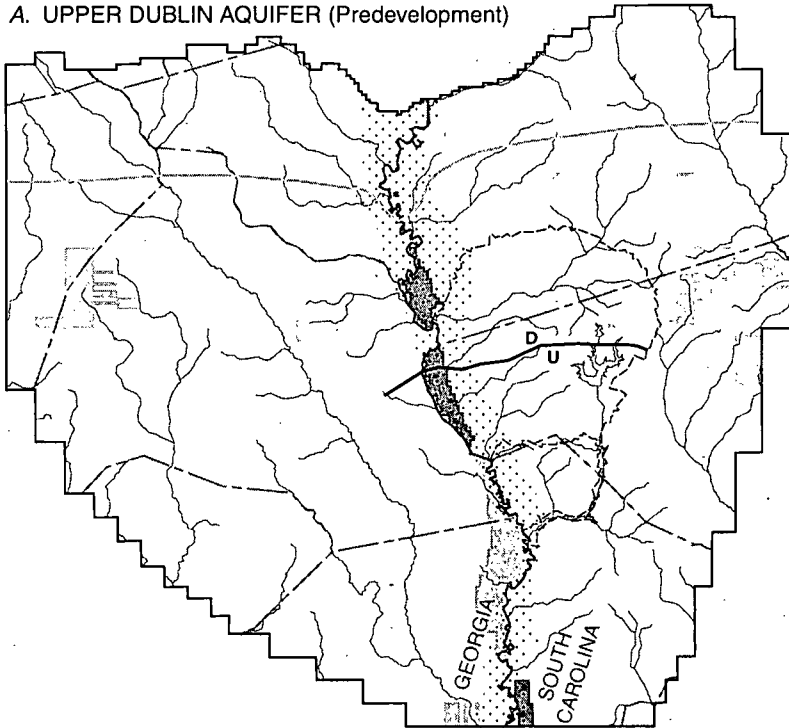


**Figure 42.** Simulated trans-river flow zones and associated recharge areas for the Millers Pond aquifer for (A) predevelopment and (B) modern-day (1987–92) conditions.

A. UPPER DUBLIN AQUIFER (Predevelopment)



**EXPLANATION**

TRANS-RIVER FLOW

 Western, from South Carolina to Georgia

 Eastern, from Georgia to South Carolina

RECHARGE AREA FOR TRANS-RIVER FLOW ZONES

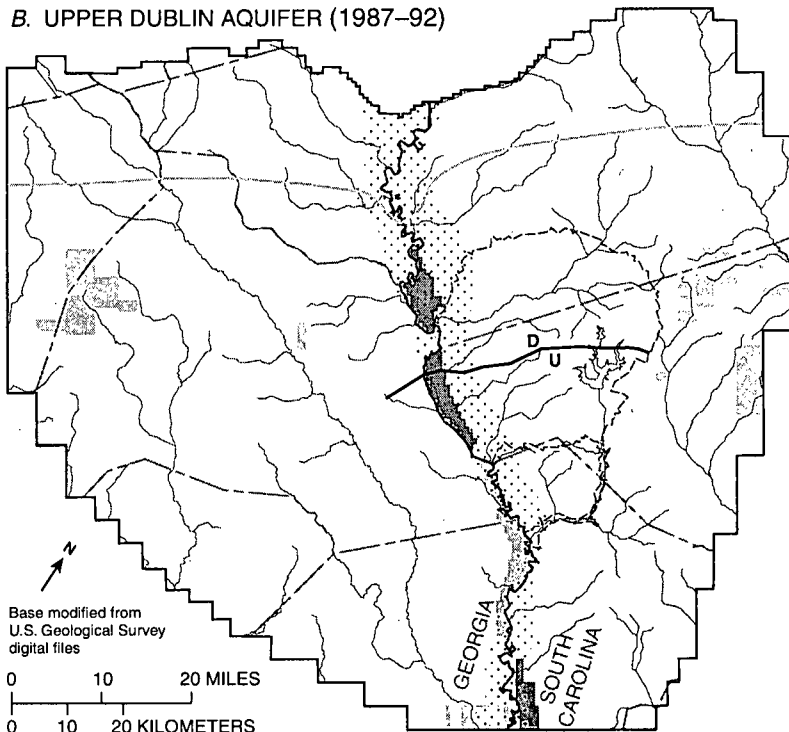
 SAVANNAH RIVER ALLUVIAL VALLEY

 APPROXIMATE NORTHERN EXTENT OF AQUIFER

 MODEL BOUNDARY

 PEN BRANCH FAULT—  
U, Upthrown side;  
D, Downthrown side

B. UPPER DUBLIN AQUIFER (1987-92)



Base modified from U.S. Geological Survey digital files

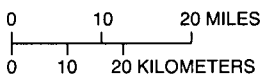
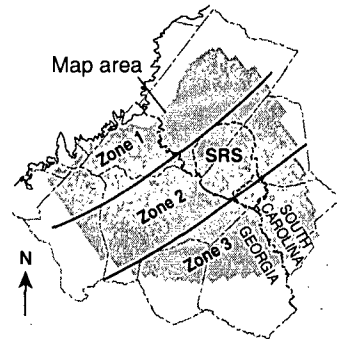
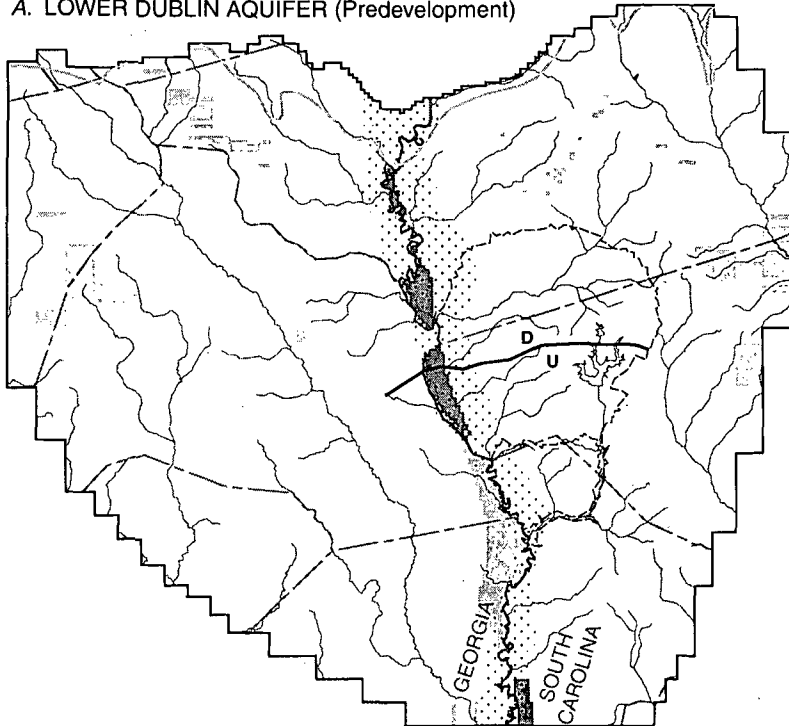
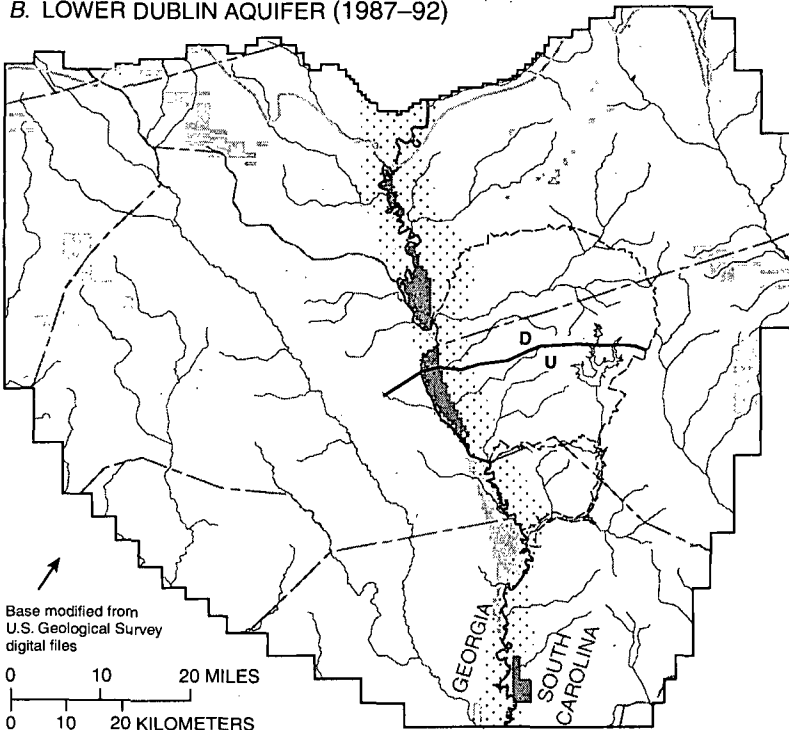


**Figure 43.** Simulated trans-river flow zones and associated recharge areas for the upper Dublin aquifer for (A) predevelopment and (B) modern-day (1987-92) conditions.

A. LOWER DUBLIN AQUIFER (Predevelopment)



B. LOWER DUBLIN AQUIFER (1987-92)



EXPLANATION

TRANS-RIVER FLOW

Western, from South Carolina to Georgia

Eastern, from Georgia to South Carolina

RECHARGE AREA FOR TRANS-RIVER FLOW ZONES

SAVANNAH RIVER ALLUVIAL VALLEY

APPROXIMATE NORTHERN EXTENT OF AQUIFER

MODEL BOUNDARY

PEN BRANCH FAULT—  
U, Upthrown side;  
D, Downthrown side

Base modified from U.S. Geological Survey digital files

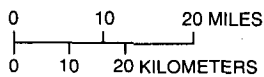
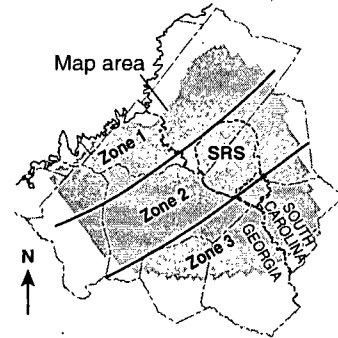
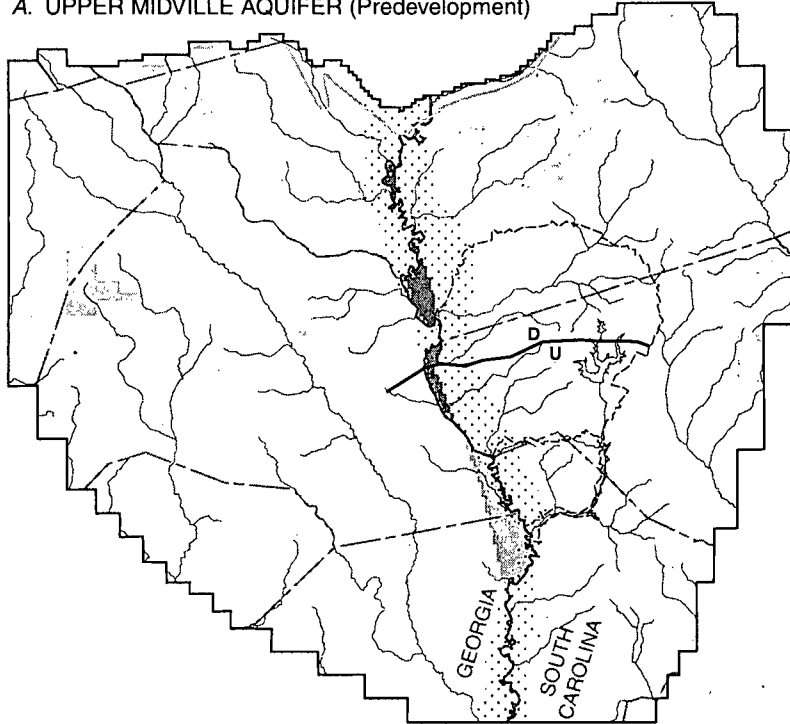


Figure 44. Simulated trans-river flow zones and associated recharge areas for the lower Dublin aquifer for (A) predevelopment and (B) modern-day (1987-92) conditions.

A. UPPER MIDVILLE AQUIFER (Predevelopment)



**EXPLANATION**

**TRANS-RIVER FLOW**

Western, from South Carolina to Georgia

Eastern, from Georgia to South Carolina

**RECHARGE AREA FOR TRANS-RIVER FLOW ZONES**

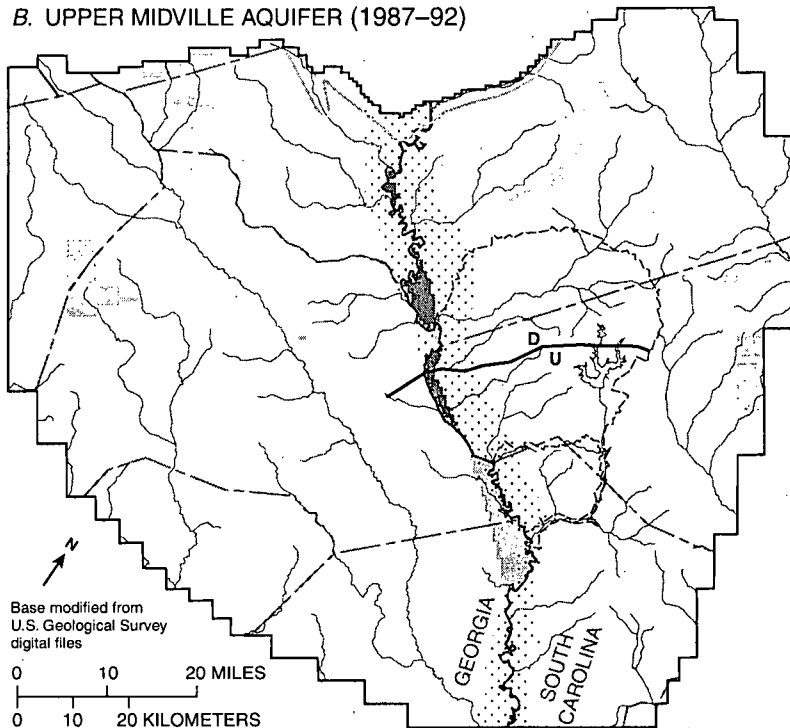
SAVANNAH RIVER ALLUVIAL VALLEY

**APPROXIMATE NORTHERN EXTENT OF AQUIFER**

MODEL BOUNDARY

PEN BRANCH FAULT—  
U, Upthrown side;  
D, Downthrown side

B. UPPER MIDVILLE AQUIFER (1987–92)

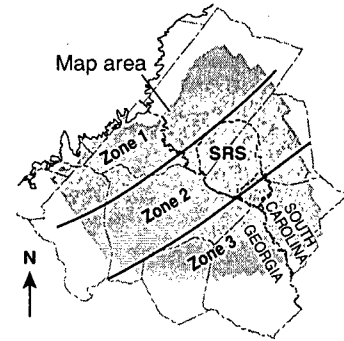
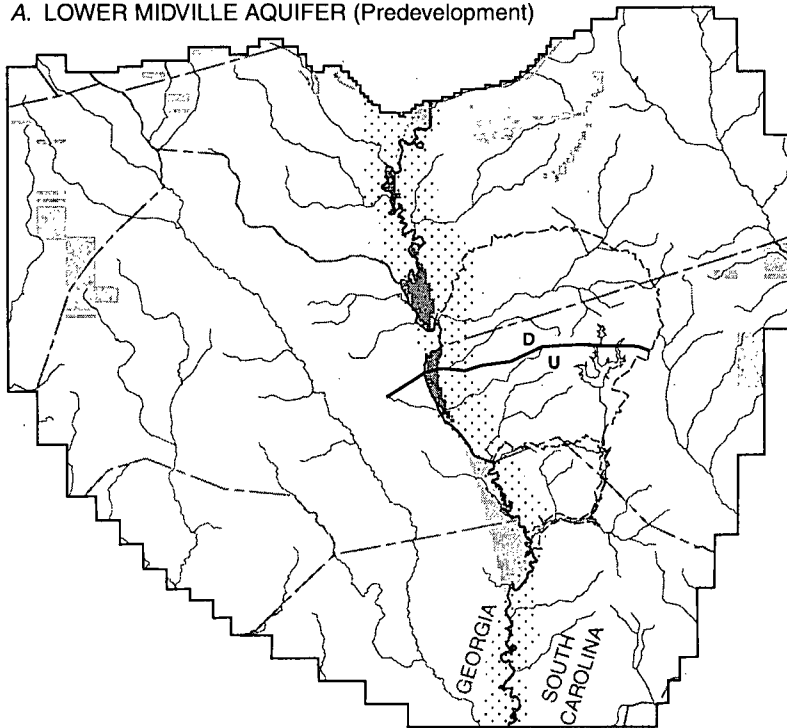


Base modified from  
U.S. Geological Survey  
digital files

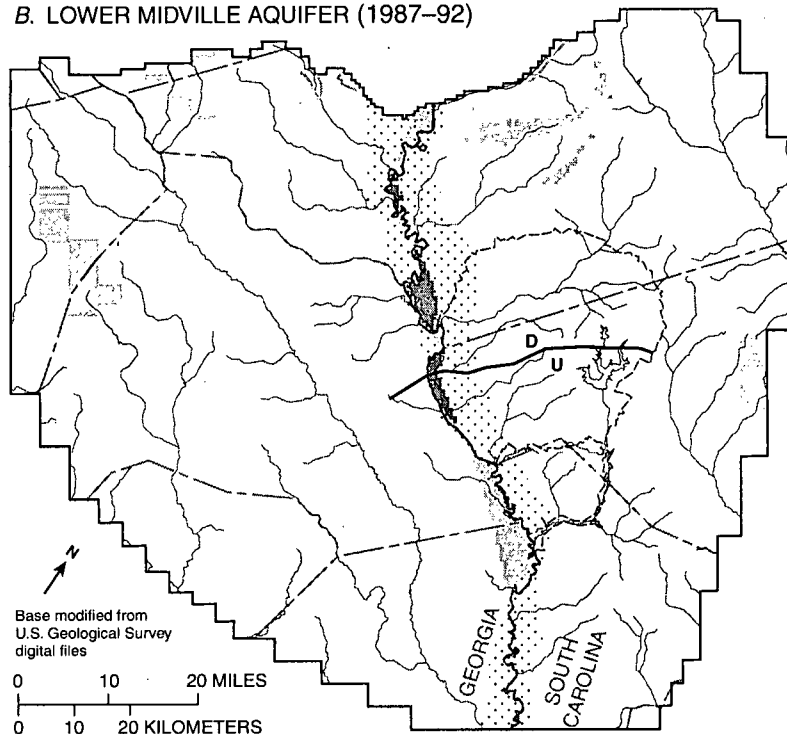
0 10 20 MILES  
0 10 20 KILOMETERS

**Figure 45.** Simulated trans-river flow zones and associated recharge areas for the upper Midville aquifer for (A) predevelopment and (B) modern-day (1987–92) conditions.

A. LOWER MIDVILLE AQUIFER (Predevelopment)



B. LOWER MIDVILLE AQUIFER (1987-92)



- TRANS-RIVER FLOW**
- Western, from South Carolina to Georgia
- Eastern, from Georgia to South Carolina
- RECHARGE AREA FOR TRANS-RIVER FLOW ZONES
- SAVANNAH RIVER ALLUVIAL VALLEY
- APPROXIMATE NORTHERN EXTENT OF AQUIFER
- MODEL BOUNDARY
- PEN BRANCH FAULT—  
U, Upthrown side;  
D, Downthrown side

Base modified from U.S. Geological Survey digital files

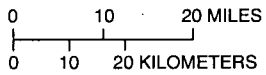


**Figure 46.** Simulated trans-river flow zones and associated recharge areas for the lower Midville aquifer for (A) predevelopment and (B) modern-day (1987-92) conditions.

### *Westward Trans-River Flow*

MODPATH analysis indicates that during predevelopment, westward trans-river flow (toward Georgia) occurs in model layers A2–A7; the largest affected areas occur in layers A3–A5 (Dublin aquifer system); the smallest occur in layer A2 (Gordon aquifer) (table 15, figs. 40–46). For each layer, the largest area of westward trans-river flow occurs in zone 3, where the Savannah River meanders eastward and is separated hydraulically from the aquifers. Other areas of westward trans-river flow include zone 1 in layers A4–A7; and zone 2 in layers A2–A7.

As a further evaluation of westward trans-river flow, the percentage of particles in the westward trans-river flow areas that enter the flow system on the eastern side of the river was computed (table 15). With the exception of layers A2 and A3, at least 80 percent of particles in trans-river flow zones originated from the opposite side of the river during predevelopment. One-hundred percent of the particles in trans-river flow zones for layers A6 and A7 originated on the opposite side of the river. In the trans-river flow zones for layers A2 and A3, the percentage of particles originating on the opposite side of the river was only 50 to 52 percent. Because of this low percentage, wells pumping in the trans-river flow zones of layers A2 and A3 would have a lesser likelihood of intercepting water from the eastern side of the river than would wells pumping in the trans-river flow zones for layers A4–A7.

During modern-day conditions, simulated westward trans-river flow zones are smaller in area than under simulated predevelopment conditions (fig. 40; table 15), but generally are in the same locations. In layers A2–A5, the area of westward trans-river flow decreased by 32 to 60 percent; whereas, the percentage area in layers A6 and A7 decreased by only 7–8 percent (table 15; fig. 40). The decrease in westward trans-river flow area during the modern-day simulation probably results from water-level declines and associated changes in hydraulic gradient due to ground-water pumping. Maps showing drawdown between the predevelopment and modern-day simulations indicate that drawdown in South Carolina generally is greater than in Georgia for layers A2–A5 (figs. 24–26), which shifts hydraulic gradients slightly toward South Carolina, and thus, reduces the area of westward trans-river flow. This is particularly evident in layers A4 and A5, in the area of zone 3 near the Burke-Screven County line. At this location pumpage at Sandoz (site 14, fig. 7) resulted in

drawdown that extended into Georgia (fig. 25) and modified the configuration of the modern-day potentiometric surfaces (plate 3, fig. 19).

The percentage of particles originating from the opposite side of the river for the modern-day simulation generally is the same or slightly lower than under predevelopment conditions (table 15). In layer A2, however, the percentage of particles increased to 68 percent, while the trans-river flow zone decreased in area to 4.5 mi<sup>2</sup>. The increased percentage of particles originating from the opposite side of the river in the modern-day simulation coupled with the decrease in area of trans-river flow, probably indicates that flow paths in the modern-day simulation are more concentrated in areas closer to the river. Even though the percentage of particles from the opposite side of the river has increased, wells pumping in the trans-river-flow zone of layer A2 would have a lesser likelihood of intercepting water from the eastern side of the river than would wells pumping in the trans-river flow zone layers A4–A7.

### *Eastward Trans-River Flow*

During predevelopment, eastward trans-river flow (toward South Carolina) occurs in model layers A2–A7, with the largest affected areas occurring in layers A3–A5 (figs. 40–46). For each layer, the largest area of eastward trans-river flow occurs in zone 2, where the Savannah River meanders westward and is hydraulically separated from the aquifers. Other areas of eastward trans-river flow include zone 1 in layers A5–A7; and zone 3 in layers A2–A5.

As a further evaluation of eastward trans-river flow, the percentage of particles in the eastward trans-river flow areas that enter the flow system on the western side of the river was computed (table 15). The percentage of particles originating from the opposite side of the river for all layers during predevelopment was at least 84 percent, indicating that most flow in these zones originated on the western side of the river.

Areas of eastward trans-river flow generally occur in the same locations during the modern-day simulation as in predevelopment (figs. 41–46). Under modern-day conditions, simulated eastward trans-river flow zones are the same or slightly larger in area than the zones represented by predevelopment simulations in all layers except A5, which is slightly smaller (fig. 40, table 15). The percentage of particles in eastward trans-river flow zones that originate from the opposite side of the river for the modern-day simulation generally is unchanged from the predevelopment simulation (table 15).

### Recharge Areas to Trans-River Flow Zones

Particles of water from trans-river flow zones were backtracked to their origin (recharge area) on the opposite side of the river using MODPATH (figs. 41–47). Recharge areas to trans-river flow zones occur in both the uppermost unit and at lateral specified-head boundaries. Most recharge enters the water table along topographically high interstream areas, flows downward and laterally through one or more hydrogeologic units, and then flows upward and laterally through one or more hydrogeologic units to discharge into the Savannah River alluvial valley (fig. 39).

In South Carolina, recharge to westward trans-river flow zones (located in Georgia) occurred in similar locations for the predevelopment and modern-day simulations, mostly in the vicinity of interstream drainage divides (figs. 41–46):

- zone 1—northwest and southeast of Hollow Creek, and near Aiken, S.C.;
- zone 2—between the South Fork of the Edisto River and the Salkehatchee River; and

- zone 3—between the South Fork of the Edisto River and the Salkehatchee River near Blackville, S.C.

In Georgia, recharge to eastward trans-river flow zones (located in South Carolina) occurred in similar locations for the predevelopment and modern-day conditions. Recharge in zones 2 and 3 occurred mostly in the vicinity of the interstream drainage divides between Brier Creek and the Ogeechee River and between Brier Creek and the Savannah River. In zone 1, recharge to layers A5–A7 originates near the Fall Line in Columbia and Richmond Counties, Ga.

Recharge areas respond very slowly to changes in ground-water-flow patterns and reflect the integrated effects of the movement of water through the system from the time and point at which the water entered the system to the time that it discharges (Franke and others, 1998). This slow response time suggests that recharge areas are largely insensitive to seasonal changes and are more likely to reflect longer term average flow patterns. Changes in the size of recharge areas to trans-river flow zones between predevelopment and modern-day conditions are shown in table 16.

**Table 16.** Recharge areas to trans-river flow zones by layer for predevelopment (pre-1953) and modern-day (1987–92) conditions [mi<sup>2</sup>, square mile]

Model layer	Recharge areas for trans-river flow zones			
	Predevelopment conditions (pre-1953)		Modern-day conditions (1987-92)	
	Number of cells	Area (mi <sup>2</sup> )	Number of cells	Area (mi <sup>2</sup> )
<b>Recharge originating in South Carolina</b>				
A2	63	14.8	44	16.7
A3	56	23.5	46	24.8
A4	60	27.5	53	29.1
A5	56	27.9	52	26.3
A6	68	13.7	71	13.8
A7	108	13.4	100	13.6
<b>Recharge originating in Georgia</b>				
A2	83	31.2	99	21.8
A3	48	32.8	55	26.8
A4	45	36.0	56	32.4
A5	60	31.7	70	26.1
A6	37	20.6	38	21.1
A7	42	29.4	45	23.6

During modern-day conditions, the number of model cells in South Carolina contributing recharge to westward trans-river flow zones decreased; whereas, the size of the area contributing recharge increased. This apparent discrepancy is due to shifting of recharge cells toward the outer edge of the simulated area, where model-cell sizes are appreciably larger. Conversely, in Georgia, the number of recharge cells during modern-day conditions increased; whereas, the size of recharge areas to eastward trans-river flow zones decreased. This apparent discrepancy is due to shifting of recharge cells eastward, toward the center of the simulated area, where model cell sizes are smaller. Changes in the position of recharge cells reflect changes in hydraulic gradients as a result of ground-water pumpage during 1953–92. Although the position of simulated recharge areas shifted slightly during the modern-day period, the simulated recharge areas were located in the same general areas as during predevelopment.

#### Simulated Time-of-Travel

Time-of-travel to trans-river flow areas from recharge locations or lateral boundaries was computed using MODPATH for both predevelopment (table 17) and modern-day conditions (table 18). The tables show the mean travel time categorized by aquifer and the three principal trans-river flow zones. These values represent the mean travel times for the particles of water in the active model area and do not include ground-water flow that occurred outside of the simulated area. Thus, travel times computed for water entering the ground-water

flow system at recharge areas within the active model area would be representative of the “true” age of the water; whereas water entering along lateral boundaries could be somewhat older, depending on the length of the flowpath outside of the simulated area.

Travel times are controlled by factors that influence the three-dimensional movement of a particle of water from its source area, including: (1) the transmissivity of aquifers; (2) vertical hydraulic conductivity of aquifers and confining units; (3) porosity of aquifers and confining units; and (4) lateral and vertical hydraulic gradients. For the MODPATH analysis, a uniform porosity of 30 percent was assigned to aquifer layers and 50 percent was assigned to confining units.

Within an individual cell, water may be derived from several contributing recharge areas, along several flowpaths. Thus, water in an individual cell is usually a mixture of waters of different ages, with a potentially wide range of ages. Changes in pumping rates can alter the flow regime and result in different ages of captured water.

During predevelopment, simulated mean travel times into trans-river flow zones ranged from 4,900 to 22,000 yr (table 17). Simulated mean time-of-travel toward westward trans-river flow areas ranged from 300 to 24,000 yr, and toward eastward trans-river flow areas ranged from 550 to 41,000 yr (table 17). Travel times were longest in a eastward direction in zones 1 and 3, and in a westward direction in zone 2.

**Table 17.** Mean time-of-travel for water particles in trans-river flow zones for simulated predevelopment conditions

[—, not applicable]

Layer	Trans-river flow zone, direction of flow, and simulated mean time-of-travel, in years						Mean time-of-travel for all zones
	Zone 1		Zone 2		Zone 3		
	Westward	Eastward	Westward	Eastward	Westward	Eastward	
A2	—	—	4,000	3,100	8,700	13,000	8,000
A3	—	—	8,000	3,700	12,000	23,000	12,000
A4	—	1,300	9,700	4,100	14,000	29,000	14,000
A5	780	680	6,100	4,300	24,000	41,000	22,000
A6	480	620	5,400	3,700	13,000	—	11,000
A7	300	550	4,800	3,800	6,900	—	4,900

**Table 18.** Mean time-of-travel for water particles in trans-river flow zones for simulated modern-day (1987-92) conditions  
[—, not applicable]

Layer	Trans-river flow zone, direction of flow, and simulated mean time-of-travel in years						Mean time-of-travel for all zones
	Zone 1		Zone 2		Zone 3		
	Westward	Eastward	Westward	Eastward	Westward	Eastward	
A2	—	—	3,900	3,100	12,000	20,000	11,000
A3	—	—	5,900	4,100	19,000	18,000	19,000
A4	—	1,200	7,700	4,400	30,000	15,000	29,000
A5	670	700	7,500	4,500	34,000	31,000	31,000
A6	480	620	6,500	3,900	13,000	—	11,000
A7	300	580	5,600	4,000	7,200	—	5,000

For the modern-day simulation, estimated mean travel times to trans-river flow areas were generally longer, ranging from 5,000 to 31,000 yr (table 18). Simulated mean time-of-travel toward westward trans-river flow areas ranged from 300 to 34,000 yr, and toward eastward trans-river flow areas ranged from 580 to 31,000 yr. As was the case for the predevelopment simulation, the time-of-travel was longest in a eastward direction in zone 1, and in a westward direction in zone 2. In zone 3, however, the simulated time-of-travel during the modern-day period was longer in a westward rather than eastward direction, which is the opposite case during predevelopment. Differences in travel times between the predevelopment and modern-day simulations result from changes in hydraulic gradients due to ground-water pumpage that alters flowpaths in the vicinity of the river.

For both the predevelopment and modern-day simulations, travel times to zone 3 are the longest, and to zone 1 are shortest, for all layers in trans-river flow areas on both sides of the river. The short travel times to zone 1 result from its proximity to aquifer recharge areas, shallow depth of ground-water flow, and relatively high vertical conductance of aquifers and confining units. Long travel times to zones 2 and 3 are the result of comparatively greater distances from recharge areas, greater depths of flow, and lower vertical conductance of aquifers and confining units.

Anomalies in estimated travel times demonstrate the complexity of ground-water flow in the vicinity of the SRS. Complex interrelations between horizontal and vertical-flow gradients and hydraulic properties result in distributions of travel times that often do not match the conceptual model of the flow system.

Conceptually, at a given location, ground-water particles in deep units would be expected to relate to the longest travel time, with progressively shorter times in shallower units. In the SRS area, however, MODPATH analyses indicate that water in deep units may have a shorter travel time than water in shallow units.

Anomalous vertical distributions of mean-estimated travel times are evident for both eastward and westward areas at all three trans-river flow zones for both the predevelopment and modern-day simulations. For example, the longest mean travel times at the three zones does not occur in the deepest model layers representing the Midville aquifer system (layers A6 and A7), but rather in shallower layers of the Dublin aquifer system (layers A3–A5).

In the Midville aquifer system, the mean travel time is shorter than in overlying layers in all three zones. These short mean travel times for layers A6 and A7 might be the result of: (1) close proximity to recharge areas (zone 1 only); (2) high transmissivity; (3) steep hydraulic gradients; (4) high vertical conductance; or (5) a combination of these factors when compared to the Dublin aquifer system. In addition, short travel times in layers A6 and A7 may be related to a large percentage of particles that originate from lateral-flow boundaries. Particles of water that originate from such boundaries laterally flow directly into the layer without flowing vertically through overlying units, as do particles that originate from recharge areas. Travel times for such particles would be expected to be shorter because lateral flow rates (controlled by transmissivity and lateral hydraulic gradients), generally are higher than vertical flow rates (controlled by vertical conductance and vertical hydraulic gradients).

*Trans-river flow, recharge areas, and time-of-travel  
at the Savannah River Site*

Delineation of ground-water flow originating on the SRS, toward westward trans-river flow zones is important because of the possibility of contaminated ground water from SRS moving beneath the Savannah River and into Georgia. Recharge originating on the SRS to Georgia trans-river flow zones was simulated for layers A2 and A4 during predevelopment (figs. 41 and 43), and in layer A2 during 1987-92 (figs. 41 and 47). The recharge originating on SRS was simulated in the interstream areas south of Four Mile Branch Creek (predevelopment and modern day) and near Parr Pond (predevelopment only).

For modern-day conditions, SRS recharge areas were delineated in 6 model cells that cover about 2 mi<sup>2</sup>. These recharge sites generally are located away from areas of ground-water contamination; however, two of the sites are located within about 0.5 mi of contaminated areas (fig. 47). All of the simulated recharge sites on SRS are located north of the Pen Branch Fault.

In the vicinity of recharge sites on SRS, ground water enters either the Upper Three Runs (layer A1) or Gordon (layer A2) aquifers, flows downward into units as deep as the lower Dublin aquifer (layer A5), laterally toward the river in one or more units, and finally moves upward to discharge from the Gordon aquifer into Savannah River alluvial sediments. The depth of penetration of recharge water appears to be related to the altitude of land surface and related head in the Upper Three Runs aquifer (layer A1)—where head in layer A1 is higher, there is deeper penetration of recharge water. Simulated aquifer discharge occurs in a 1 mi<sup>2</sup> marshy area immediately westward of the Savannah River that is distant from major pumping centers (locations shown on figure 7).

Simulated modern-day time-of-travel from recharge areas originating on SRS to westward trans-river flow zones ranges from about 90 yr to 2,900 yr. Selected flowpaths and travel times for the central part of SRS are shown in figure 47. In general, shorter simulated travel times occur where flowpaths have a shallower depth of penetration; longer travel times occur where the depth of penetration is deeper.

Results of the MODPATH analysis are representative of advective ground-water flow on a regional scale. To provide better definition of flowpaths on a more local scale at the SRS would require greater refinement of the MODFLOW simulations and

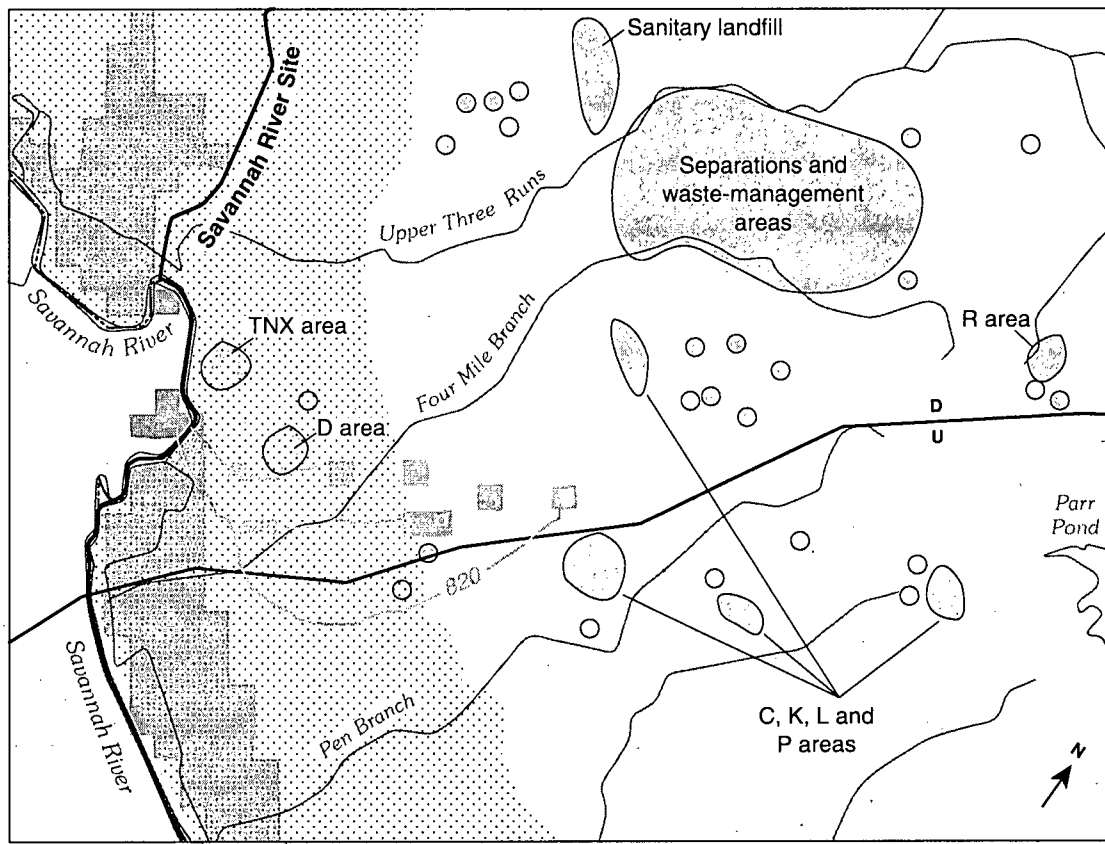
MODPATH analyses and additional hydraulic property data. Time-of-travel estimations would be improved by site-specific porosity data. To simulate movement of ground-water contaminants at SRS would require use of a solute-transport model to account for physical, chemical, and biological processes that attenuate chemical constituents in ground water, which are not built into either MODFLOW or MODPATH.

### **Sensitivity Analysis**

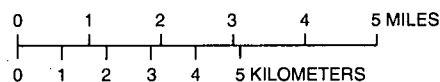
The effects of changing hydraulic characteristic values on computed ground-water levels, rates of ground-water discharge to streams, area of trans-river flow, area of recharge to trans-river flow zones, and time-of-travel from recharge areas to trans-river flow zones were determined in a sensitivity analysis conducted using the results of the calibrated steady-state model for modern-day conditions. The objective of this analysis was to determine which of the characteristic arrays, when changed from calibrated values, produced the most change in computed values in the six actively modeled layers (A2–A7).

The sensitivity analysis consisted of a series of simulations in which the value of a hydraulic characteristic or boundary condition was changed from calibrated values by a constant multiplier while keeping other input values constant. The change affected the hydrologic parameter in all layers simultaneously. Simulations were performed to evaluate the impact of changes in transmissivity, leakance, riverbed conductance, river head, recharge, specified head in the source sink layer, specified head in lateral boundaries, and pumpage. Storage coefficient also was tested as part of evaluating the transient response to pumpage (see section, "Testing of model for transient response to pumpage"). Porosity was adjusted to determine effects on time-of-travel from recharge areas to trans-river flow zones.

Values of transmissivity and leakance were changed by multiplying the calibrated values by factors of 0.1, 0.5, 2.0, and 10.0. The other parameters (riverbed conductance, river head, recharge, specified head in the source sink layer, specified head at lateral boundaries, pumpage, and porosity) were changed by multiplicative factors of 0.2, 0.4, 0.6, 0.8, 1.2, 1.4, and 1.6 times calibrated values. Model sensitivity to parameter changes was charted for changes in the root mean square (RMS) of the residuals (ground-water levels), ground-water discharge to the Savannah River, trans-river-flow



Base from U.S. Geological Survey digital files



### EXPLANATION

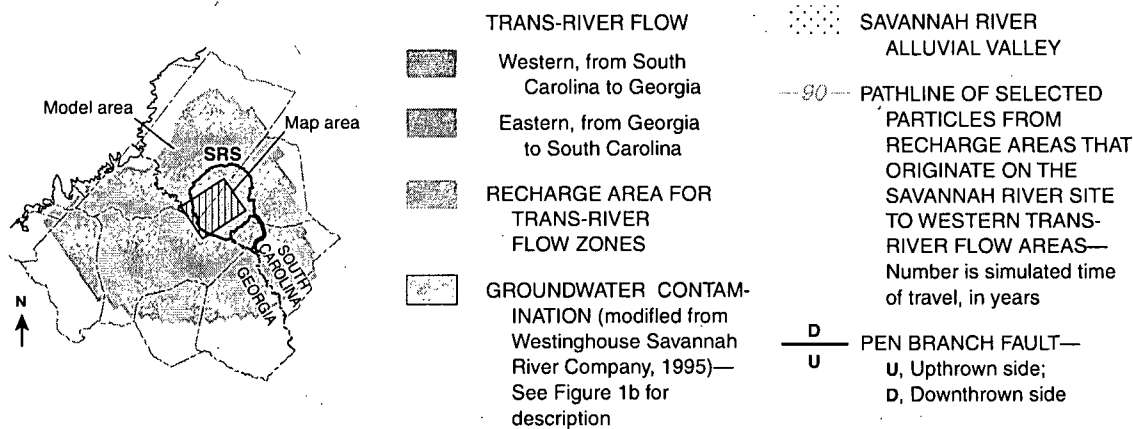


**Figure 47.** Simulated trans-river flow areas, associated recharge areas, and selected ground-water pathlines for the Gordon aquifer during the modern-day (1987–92) period, and ground-water contamination in the central part of the Savannah River Site.

area and recharge area, and time-of-travel from recharge areas to trans-river flow areas (figs. 48–52). Westward ground-water flow was used as a basis for sensitivity analysis of trans-river flow areas, associated recharge areas, and time-of-travel; results for eastward ground-water flow were assumed to be similar.

Simulated ground-water discharge to the Savannah River was highly sensitive to variations in river and source-sink layer specified head—discharge increased with higher source-sink head and lower river head, and decreased with lower source-sink head and higher river head (fig. 48). Discharge also was influenced by changes in lateral boundary specified heads, although to a lesser degree than river and source-sink layer heads. Discharge variations in response to specified heads largely reflect changes in hydraulic gradient at the river, whereby steeper gradients result in higher discharge rates. Ground-water discharge also was influenced by transmissivity and leakance variations—discharge increased in response to increased leakance and transmissivity, but showed only a minor decrease in response to decreased values. A somewhat unexpected result was that changes in riverbed conductance had only minor effect on rates of ground-water discharge.

Simulated ground-water levels were sensitive mostly to changes in specified heads in the source-sink layer, at lateral boundaries, and at the Savannah River (fig. 49). Variations in hydraulic parameters showed a less pronounced effect than specified heads, and variations in recharge and pumpage showed only minor effect on calibrated ground-water levels.

The size of westward trans-river flow zones was influenced mostly by changes in specified heads in the source-sink layer, at lateral boundaries, and at the river (fig. 50). The area of trans-river flow showed a pronounced increase in response to higher head at lateral boundaries and at the river, and to lower head in the source-sink layer. In addition, trans-river flow area for layers A5, A6, and A7 increased in response to decreased leakance and transmissivity. Recharge rates and riverbed conductance had very little effect on trans-river flow area. Pumpage generally had little effect on trans-river flow area, with some effect on layers A3 and A4.

Recharge area to westward trans-river flow zones also was influenced mostly by changes in specified heads that change flow gradients (fig. 51)—recharge area increased in response to higher lateral boundary head and decreased source-sink layer head; and

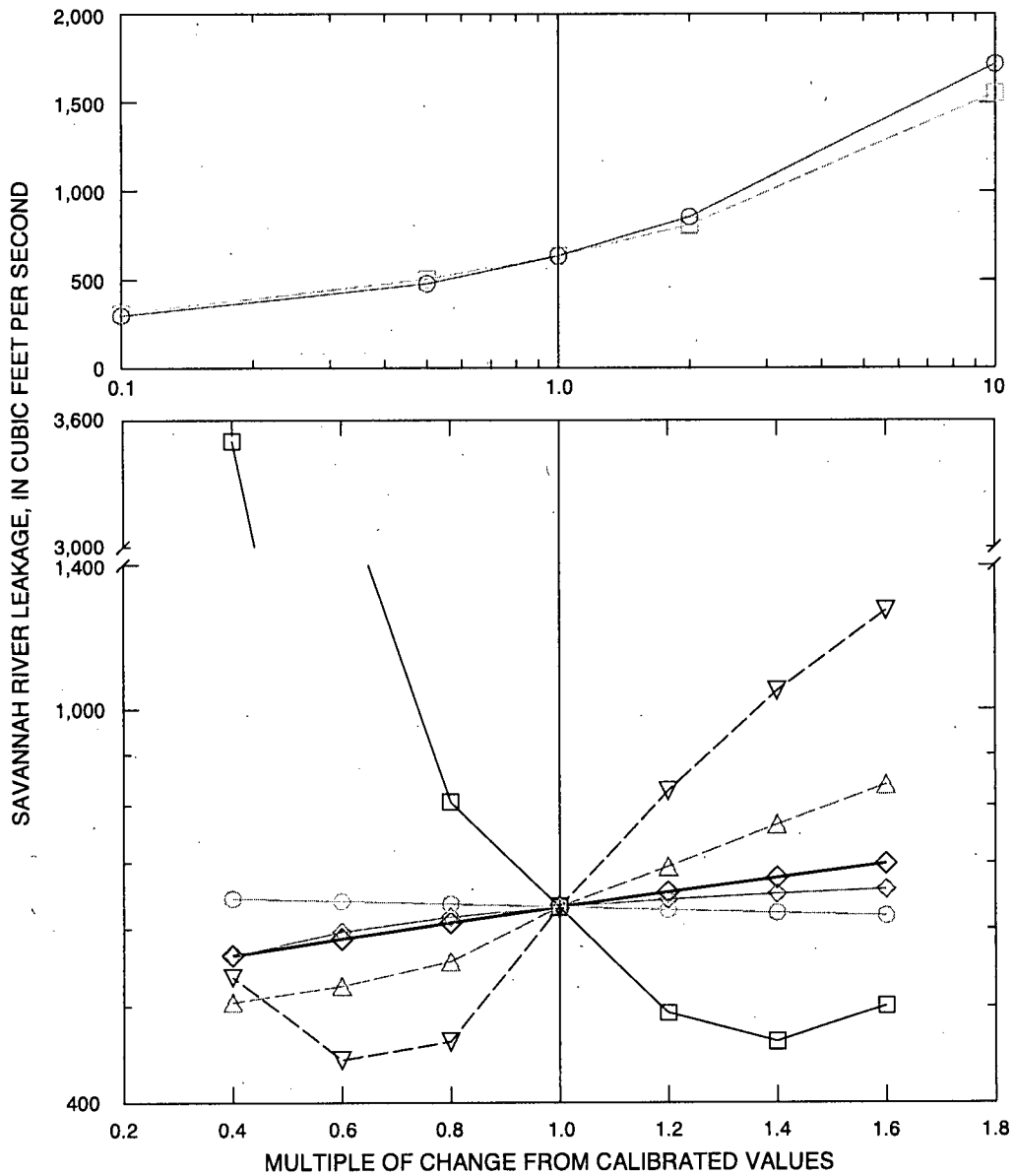
decreased in response to both higher and lower river head, to lower lateral boundary head, and to lower source-sink layer head. Size of recharge areas also increased in response to higher recharge rates, to lower riverbed conductance, and lower pumpage.

Time-of-travel from recharge areas to westward trans-river flow zones was influenced mostly by changes in specified head that control hydraulic gradients and related flow rates (fig. 52). Travel times decreased with decreased specified head in the river and at lateral boundaries, and with increased source-sink head. Recharge rates had little effect on time-of-travel. Increased transmissivity and leakance resulted in decreased time-of-travel; riverbed conductance and pumpage had little effect on time-of-travel. Porosity generally had little effect on travel times; however, in layers A2, A3, A4, and A5, decreased porosity resulted in somewhat shorter travel times, increased porosity resulted in longer travel times. In layers A6 and A7, there was no change in travel times in response to changes in porosity. This lack of response may indicate that flow to these deeper layers is dominantly horizontal in the aquifers, with little flow component affected by the higher porosity values of confining units.

### Limitations of Digital Simulation

The digital ground-water flow model developed for the study area addresses questions related to advective movement of ground water through a 7-layer aquifer system in the vicinity of the Savannah River Site on a regional scale, but cannot mimic the true system exactly. The model is limited by simplification of the conceptual model, lateral and vertical discretization effects, and difficulty in obtaining sufficient measurements to account for all of the spatial variation in hydraulic properties and boundary conditions throughout the model area. The relative importance of hydraulic properties and boundary conditions on the calibrated model results are presented in the section, "Sensitivity Analysis."

The conceptual model is believed to accurately represent flow-system dynamics at a regional scale; however, it is probable that some modification of system concepts would be required for more local scale studies. Lateral discretization of the model into a variably-spaced grid forced an averaging of hydraulic properties and boundary conditions for each model cell. In areas of finer grid resolution near the Savannah River and Savannah River Site, this averaging is believed to be



**EXPLANATION**

- ◇— RECHARGE
- ◇— RIVERBED CONDUCTANCE
- ▽— SOURCE SINK SPECIFIED
- RIVER HEADS
- △— LATERAL BOUNDARY SPECIFIED
- PUMPING
- TRANSMISSIVITY
- LEAKANCE

**Figure 48.** Sensitivity of simulated ground-water discharge to the Savannah River to selected parameters.

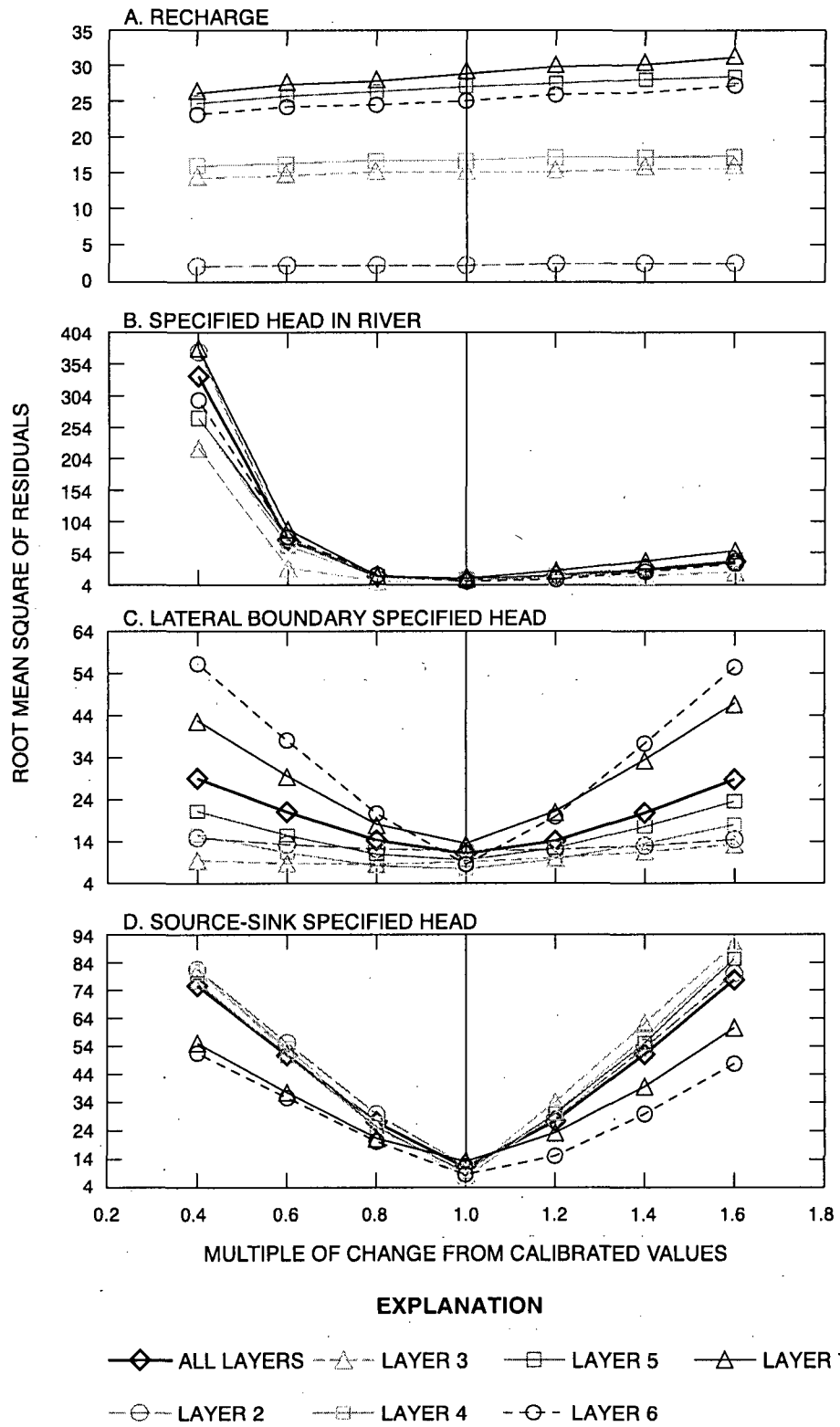


Figure 49. Sensitivity of simulated ground-water levels to selected parameters.

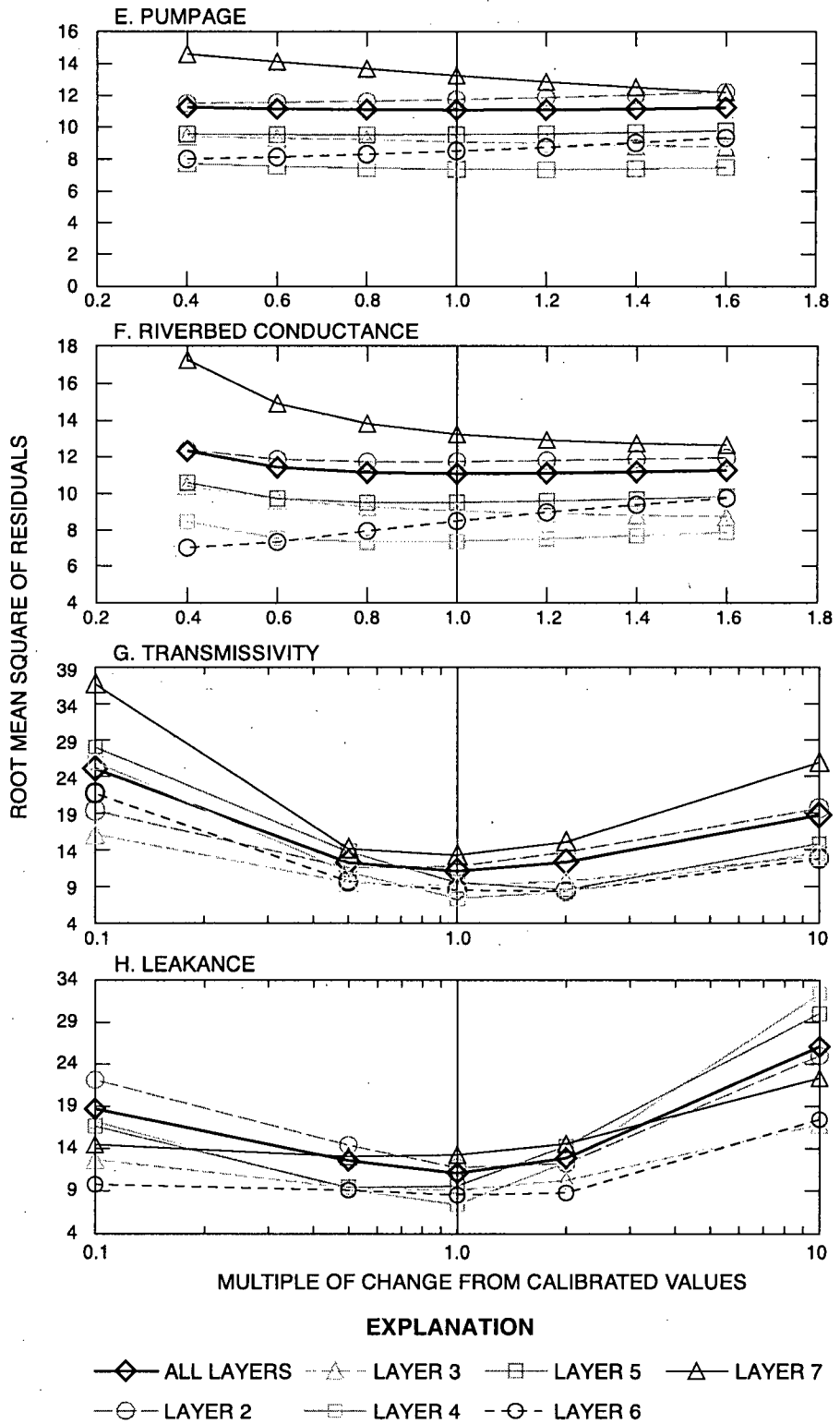
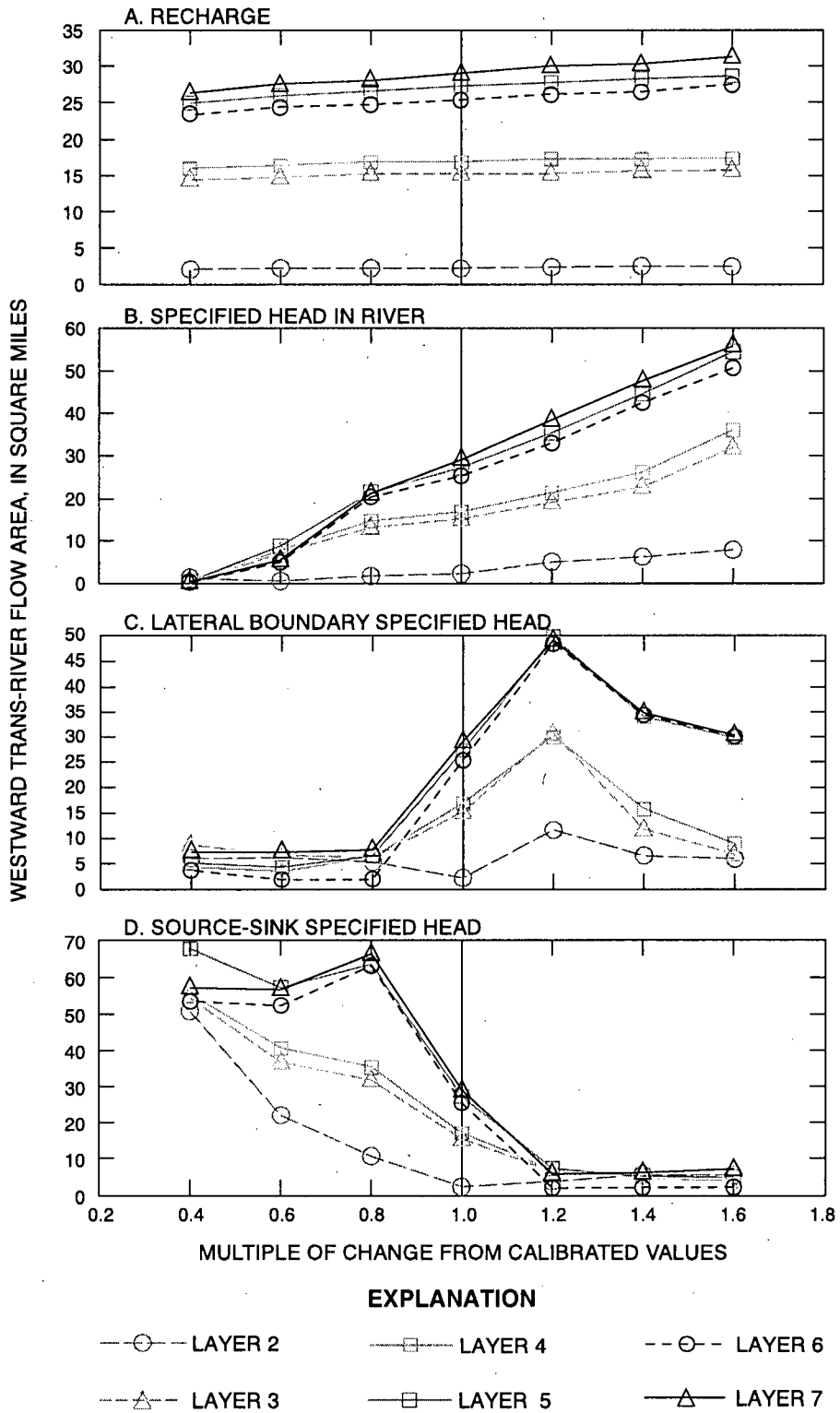


Figure 49. Sensitivity of simulated ground-water levels to selected parameters—continued.



**Figure 50.** Sensitivity of simulated westward trans-river flow area to changes in selected parameters.

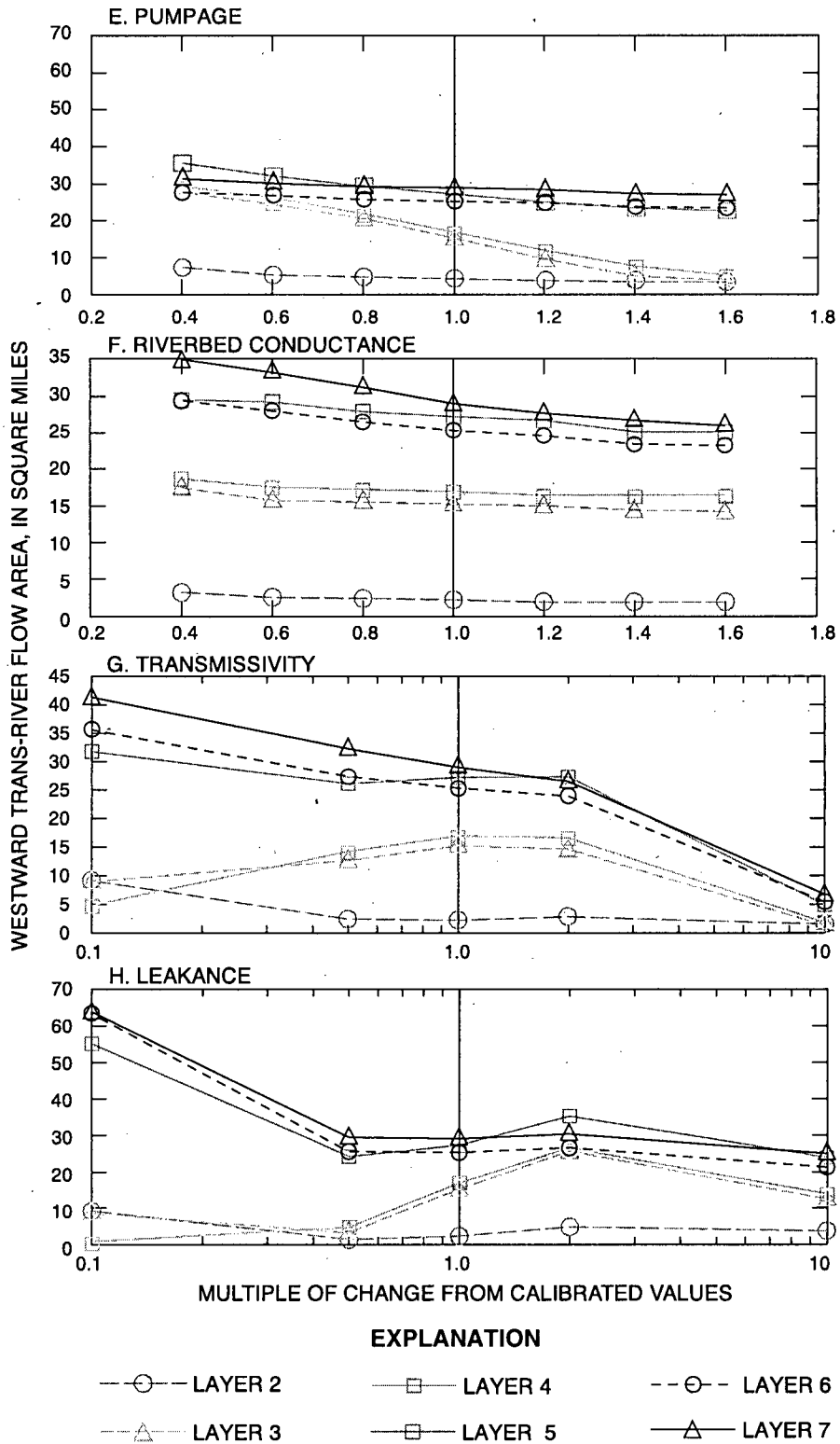
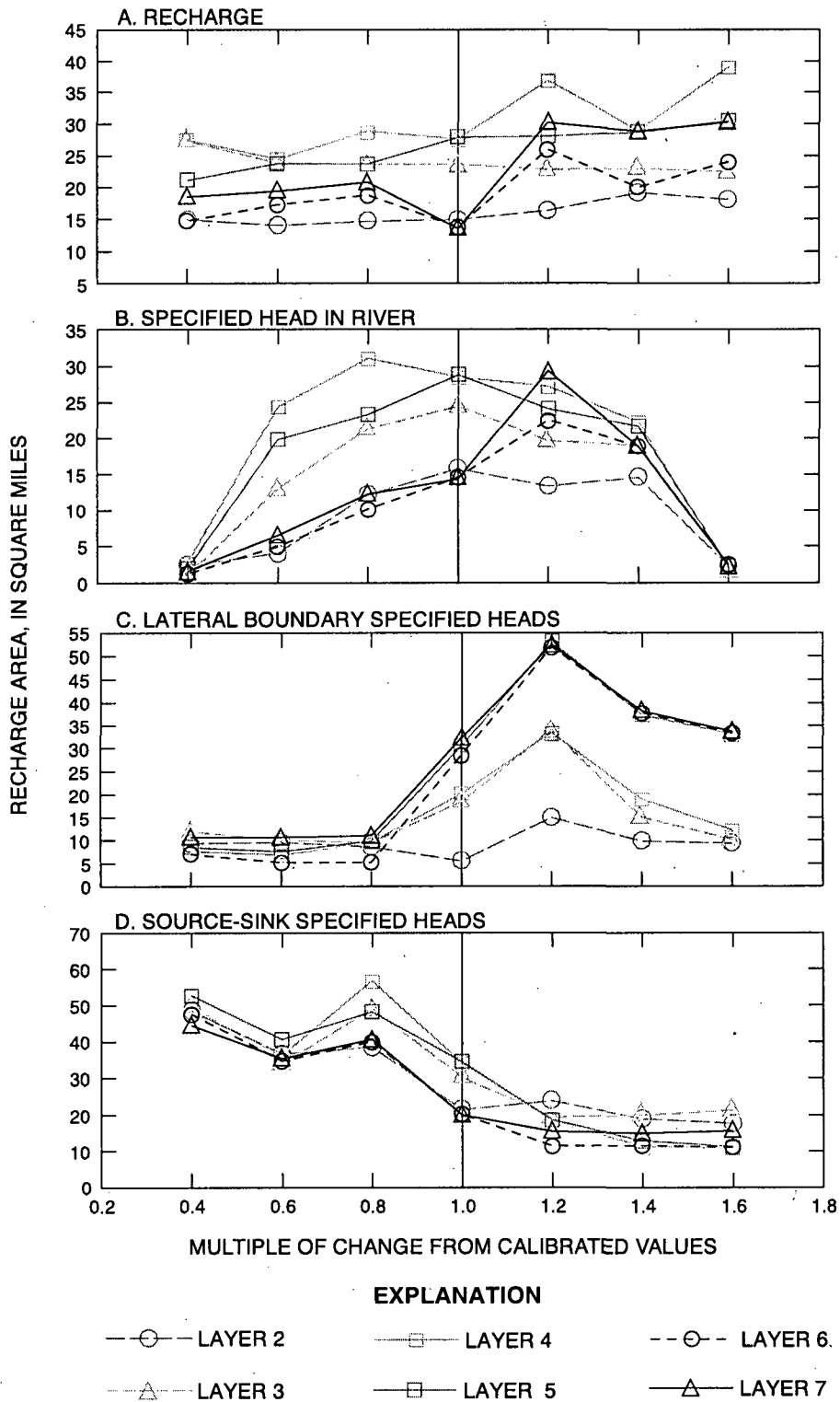


Figure 50. Sensitivity of simulated westward trans-river flow area to changes in selected parameters—continued.



**Figure 51.** Sensitivity of simulated recharge area to westward trans-river flow zones to changes in selected parameters.

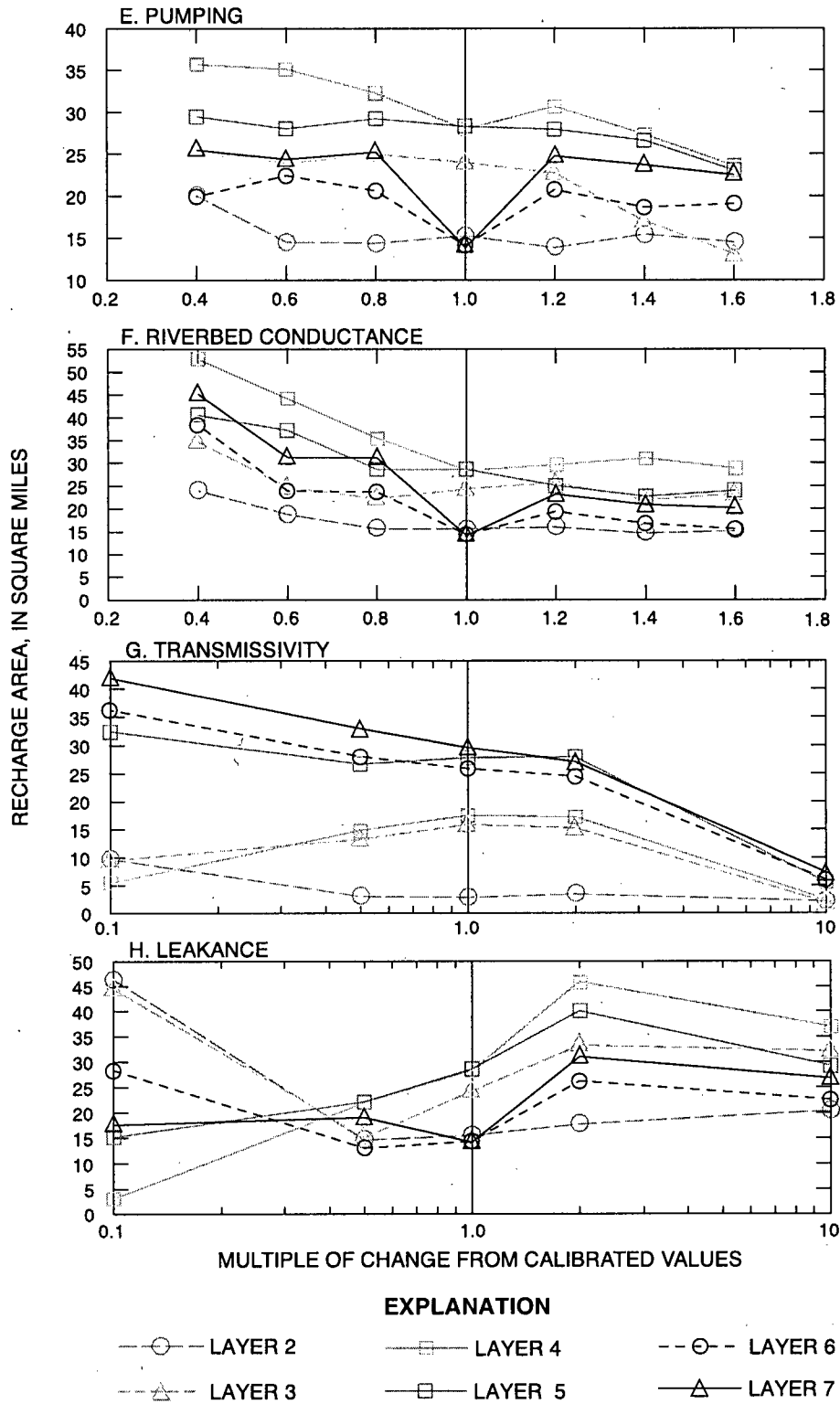
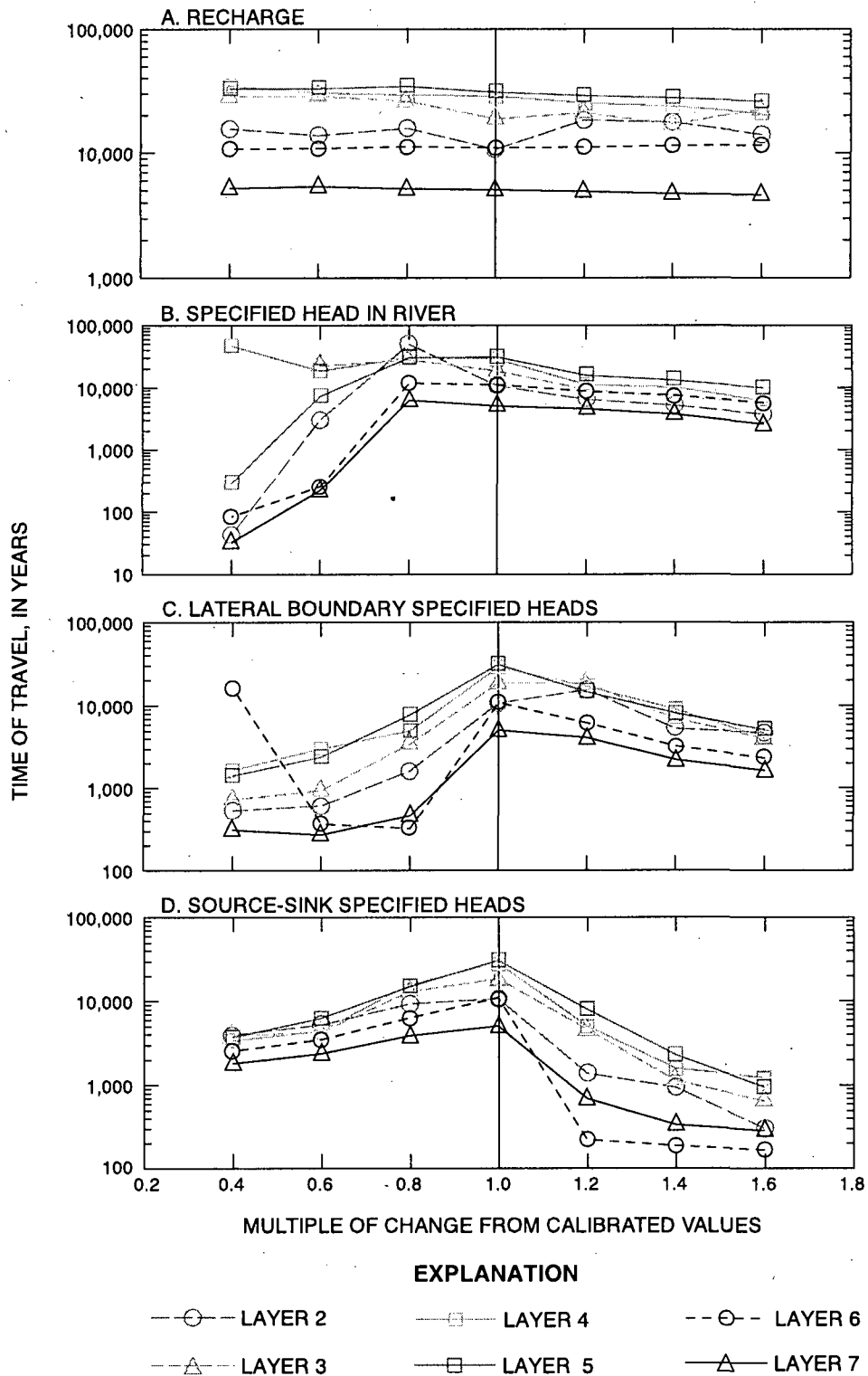
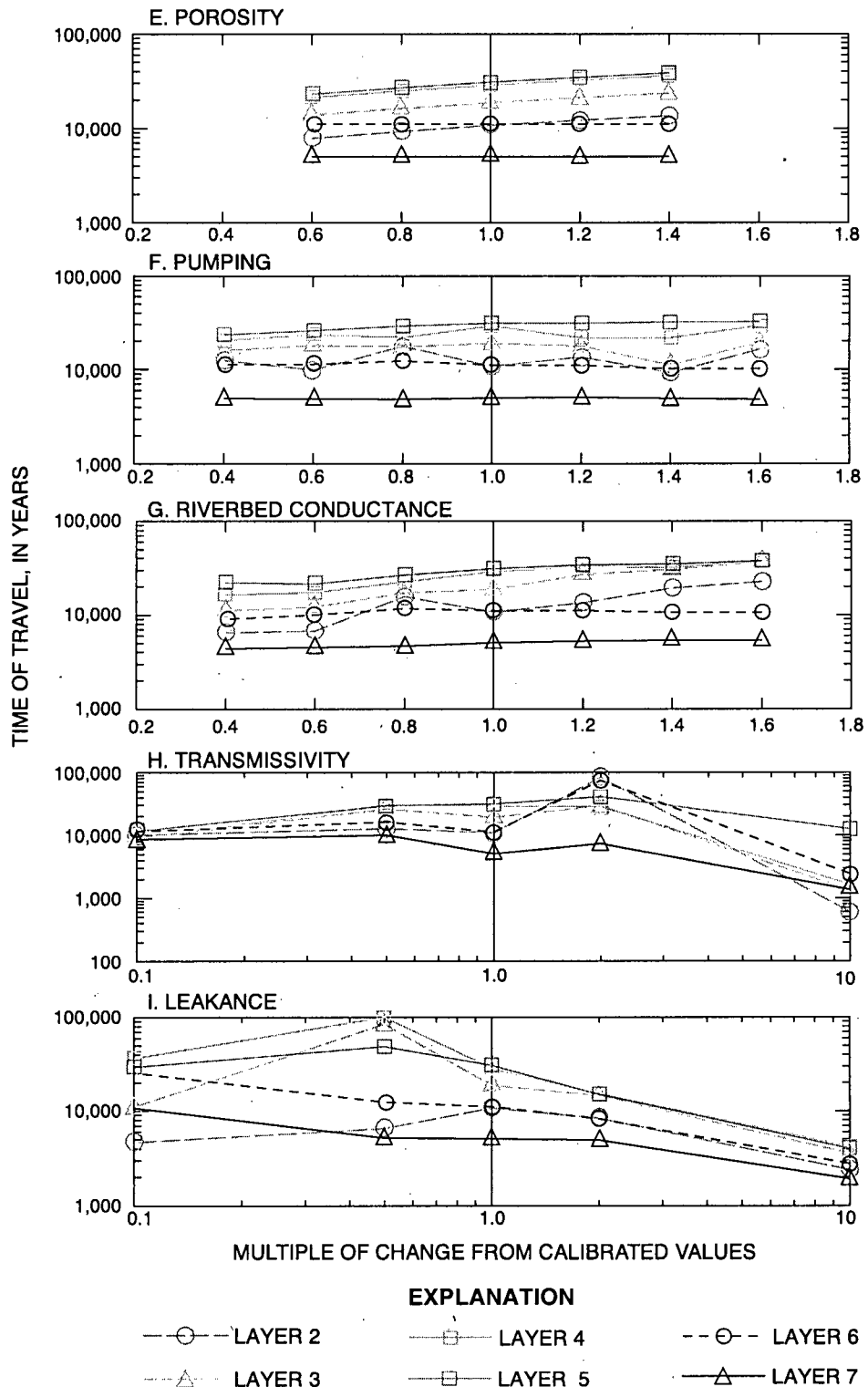


Figure 51. Sensitivity of simulated recharge area to westward trans-river flow zones to changes in selected parameters—continued.



**Figure 52.** Sensitivity of simulated time-of-travel from recharge areas to westward trans-river flow zones to changes in selected parameters.



**Figure 52.** Sensitivity of simulated time-of-travel from recharge areas to westward trans-river flow zones to changes in selected parameters—continued.

largely representative of field conditions for a regional-scale study; however, in outlying areas along the outer edge of the model, larger cell sizes forced greater generalization of field conditions. Additionally, some of the variations in horizontal hydraulic gradient, even in the finer-resolution cells, were not captured in the head values assigned to the source-sink layer (A1).

Vertical discretization of the model into 7 layers is believed adequate for representation of hydraulic variations on a regional-scale; however, for more local scale studies finer vertical resolution would probably be required to adequately represent these variations. In particular, simulation of flow in the uppermost layer (A1), the Upper Three Runs aquifer, was limited to a source-sink inactive layer. Active simulation of flow in this layer would probably require discretization into several active model layers, because of vertical heterogeneity of hydraulic properties and observed head separation within the unit.

The model was unable to account for all of the spatial variation in hydraulic properties due to a sparsity of field data on hydraulic properties, particularly vertical hydraulic conductivity and riverbed conductance, necessitating simplification. This simplification does not invalidate the model, but does mean model results should only be interpreted at scales the same size or smaller than the calibrated model.

### Limitations of Particle Tracking

Many uncertainties exist in estimating ground-water flowpaths, including pumping rates, areal recharge rates, and hydraulic properties of aquifers and confining units (Franke and others, 1998). In general, complexity of ground-water flow systems and uncertainty in quantifying properties that describe the flow system are related—greater complexity implies greater uncertainty. The complex hydrogeologic setting in the vicinity of the SRS implies some uncertainty regarding delineation of ground-water flowpaths; however, simulation results are believed representative of regional-scale flow. The relative importance of hydraulic properties and boundary conditions on particle-tracking results—trans-river flow and recharge areas, and time-of-travel are presented in the section, “Sensitivity Analysis.”

Hydraulic conductivities of aquifers and confining units help control the distribution of ground-water heads in the system. The three-dimensional distribution of head is, in turn, a major control on the configuration of flowpaths in the system (Franke and others, 1998).

Particularly in systems with low hydraulic gradients, small changes in the distribution of ground-water heads can have a significant influence on the configuration of ground-water flowpaths. Thus, uncertainty in quantifying the physical properties that describe the ground-water flow system results in uncertainty in delineating ground-water flowpaths. In the SRS area, sparse data are available on the vertical hydraulic conductivity of aquifers and confining units. Most data are from laboratory tests of core samples that are largely limited to clay-rich units in the immediate area of the SRS, with scattered data off site (see figures 36–38). Data on horizontal hydraulic conductivity in the vicinity of SRS are somewhat more abundant, with best coverage in the immediate area of the SRS and scattered data off site (see figures 33–35).

An additional limitation of particle tracking using MODPATH is its inability to determine whether a particle of water exits the system in a cell containing a weak sink. A weak sink can be described as a discharge well that does not remove all of the water entering a cell, thus allowing some of the water to continue to travel in the system. The solution to this limitation is further refinement of the finite difference grid to better depict flow around individual wells; however, such resolution was beyond the regional scope of this study. MODPATH results presented here do not account for weak sinks and are, thus, indicative of the worse-case scenario for trans-river flow—that which allows water to travel from one side of the river to another without being intercepted by wells that are weak sinks.

### SUMMARY AND CONCLUSIONS

Coastal Plain sediments in the 5,147-square mile (mi<sup>2</sup>) study area in the vicinity of the U.S. Department of Energy, Savannah River Site (SRS), Georgia and South Carolina consist of layers of sand, clay, and minor limestone that range in age from Late Cretaceous through Holocene. The sediments comprise three aquifer systems consisting of seven discrete aquifers: (1) the Floridan aquifer system, consisting of the Upper Three Runs and Gordon aquifers in sediments of Eocene age; (2) the Dublin aquifer system, consisting of the Millers Pond, and upper and lower Dublin aquifers in sediments of Paleocene and Late Cretaceous age; and (3) the Midville aquifer system, consisting of the upper and lower Midville aquifers in sediments of Late Cretaceous age.

A ground-water modeling investigation of ground-water flow and stream-aquifer relations described (1) directions and rates of ground-water flow and stream-aquifer relations prior to development (pre-1953); (2) modern-day (1987-92) ground-water flow and stream-aquifer relations and changes that have occurred as a result of development; and (3) evaluated the occurrence of trans-river flow beneath the Savannah River for predevelopment and modern-day conditions. Ground-water flow was simulated using the U.S. Geological Survey three-dimensional finite-difference ground-water flow model, MODFLOW. The flow system was modeled in seven layers—six active layers and an overlying source-sink layer that are separated to varying degrees by six confining units. The finite-difference grid for the model is aligned nearly parallel to the Savannah River and to the regional dip of the hydrogeologic units, and consisted of 130 rows and 102 columns with a variable grid spacing ranging in size from 0.33 mile x 0.33 mile, to 2 miles x 2.5 miles. The model covers an area of about 4,455 mi<sup>2</sup>, of which about 3,250 mi<sup>2</sup> contains the active simulated area.

In general, the ground-water flow system in the vicinity of the SRS is in a state of equilibrium, whereby rates of aquifer recharge and discharge are equal, and there is insignificant contribution of water from aquifer storage. Prior to pumpage (predevelopment), long-term average conditions prevailed, changes in ground-water levels were seasonal, and ground-water discharge was comprised solely of flow to streams and springs. After large-scale pumpage began in late 1952, ground-water levels in some areas declined and the quantity of water discharged to streams and springs was reduced. Because sensitivity analyses indicated that these responses resulted in insignificant changes in ground-water storage (less than  $1 \times 10^{-5}$  percent of the total water budget), the flow system was simulated with a series of six steady-state pumping periods; 1953-60, 1961-70, 1971-75, 1976-80, 1981-86, and 1987-92. Results were summarized for the predevelopment (pre-1953) and modern-day (1987-92) simulations, with hydrographs of selected wells presented for interim periods.

The predevelopment period was calibrated using data of observed head at 462 model cells, and ground-water discharge along 36 reaches of selected streams. For the predevelopment period, the model matched established error criteria for heads in 90 percent of the cells where observations were available, and simulated ground-water discharge was within 50 percent of estimated values. Over most of the model area simulated

directions of ground-water flow directions and of the distribution and quantity of recharge and discharge were consistent with the conceptual model.

Of the total simulated inflow of 1,023 million gallons per day (Mgal/d), 76 percent is contributed by leakage from constant-head cells in the source-sink layer, 15 percent is contributed by direct recharge to deeper layers, and 9 percent is contributed as inflow from lateral specified-head boundaries. Direct recharge of aquifer sediments by precipitation contributes only a small percentage of inflow because the area of exposed aquifer sediments is small and limited mostly to stream valleys that typically function as ground-water discharge areas. Because direct recharge of aquifers by precipitation is limited to a small percentage of the study area, vertical leakage from the source-sink layer is the largest contributor to ground-water inflow.

During predevelopment, of the total 1,022 Mgal/d outflow, ground-water discharge to streams accounts for 97 percent of the water leaving the model, with only 3 percent attributed to outflow at lateral specified head boundaries. Of the total simulated stream discharge of 988 Mgal/d, flow to the Savannah River accounts for 43 percent; Brier Creek, 28 percent; and Upper Three Runs Creek, 8 percent.

The model was calibrated to modern-day (1987-92) conditions using the average observed head during this time period at 313 model cells, and ground-water discharge along 36 reaches of selected streams. Individual error criteria were established for each model cell, based on topographic error, seasonal fluctuation, and cell size. For the modern-day period, the model matched established error criteria for heads in 88 percent of the cells where observations were available, and simulated ground-water discharge was within 50 percent of estimated values. Simulated ground-water flow directions and the distribution and quantity of recharge and discharge are consistent with the conceptual model over most of the model area.

The water budget for the modern-day period shows a similar distribution of flow as does the predevelopment period, with the exception that outflow from the modern-day simulation includes ground-water pumpage. Of the total simulated inflow of 1,041 Mgal/d, 76 percent is contributed by leakage from constant head cells in the source-sink layer, 15 percent is contributed by direct recharge to deeper layers, and 9 percent is contributed as inflow from lateral specified-head boundaries. Of the total 1,042 Mgal/d outflow, ground-

water discharge to streams accounts for 92 percent, lateral outflow at specified-head boundaries accounts for 3 percent, and discharge to wells accounts for 5 percent of the water leaving the model.

Throughout most of the study area, changes in ground-water level, ground-water discharge to streams, and water-budget components attributed to ground-water pumpage were small during 1953-92. In some areas, the model simulations did not match the magnitude of observed drawdowns; however, most water-level trends were matched. The addition of simulated pumpage to the modern-day water budget accounts for only minor changes to the simulated predevelopment water budget. The 52.6 Mgal/d of ground-water withdrawal by wells during 1987-92 accounts for: (1) 5 percent of the total ground-water outflow for the modern-day period; (2) a 3-percent decrease in ground-water discharge to streams; (3) a 2-percent increase in downward leakage from layer A1 (representing aquifer recharge); and (4) minor changes to ground-water inflow or outflow along lateral boundaries for the modern-day period. Contribution to ground-water withdrawal is provided mostly by intercepted recharge prior to discharge into streams (62 percent), with the remainder provided by increased leakage from the source-sink layer (30 percent) and increased lateral flow (7 percent).

Maps showing simulated drawdown between predevelopment and modern-day conditions indicate drawdown is small (less than 7 ft) and of limited areal extent, however these declines result in a change in the configuration of the simulated potentiometric surface and flowpaths near the river. The largest simulated declines (about 7 ft) are located in the upper and lower Dublin aquifers in the vicinity of the Sandoz site in South Carolina, that include a zone of influence extending beneath the Savannah River.

Trans-river flow is a term that describes a condition whereby ground water originating on one side of a river flows beneath the river floodplain to the other side of the river. Factors controlling the trans-river flow include: (1) vertical and horizontal hydraulic conductivity of aquifers and confining units; (2) thickness and areal extent of the confining units; and (3) hydraulic gradients. Hydraulic gradients and trans-river flow may be altered by ground-water pumpage, particularly at pumping centers located near the river. Pumped wells on one side of the river could intercept water originating from the other side prior to the water discharging to the

river. In general, greater trans-river flow occurs in areas where aquifers are hydraulically separated from the Savannah River than where they are well connected.

The U.S. Geological Survey particle-tracking code MODPATH was used to simulate flowpaths and evaluate the trans-river flow during predevelopment and modern-day conditions near the Savannah River. Particles of water in each active model layer were 'seeded' along a 6-mile wide corridor extending 3 miles into Georgia and 3 miles into South Carolina along the entire course of the Savannah River in the simulated area, and the particles were backtracked to determine their point of entry into the ground-water flow system. Model cells that had one or more particles entering from the opposite side of the river were mapped as zones of eastward or westward trans-river flow. Changing meander patterns of the Savannah River made it possible for a single flowpath to cross from one side of the river to the other side several times prior to discharging into the alluvial valley. Westward and eastward trans-river flow was simulated in three principal zones:

- zone 1—from the Fall Line southward to the confluence of Hollow Creek and the Savannah River;
- zone 2—from the zone 1 boundary southward to the southern border of the SRS (not including Lower Three Runs Creek section); and
- zone 3—from the zone 2 boundary, southward into the northern half of Screven County.

The areas of westward trans-river flow during predevelopment are larger than or equal to areas of eastern trans-river flow for all layers except the Gordon aquifer, which is larger in the eastern areas. During modern-day conditions, the largest area of trans-river flow in the Millers Pond and upper Dublin aquifers shifts from west to east, reflecting changes in hydraulic gradients due to ground-water pumpage:

The flowpath analysis indicated that during predevelopment, westward trans-river flow occurred in all active-model layers; the largest affected areas occurred in the Dublin aquifer system, and the smallest occurred in the Gordon aquifer. For each layer, the largest area of westward trans-river flow occurred in zone 3, where the Savannah River meanders eastward and is hydraulically separated from the aquifers.

For simulation of modern-day conditions, areas of westward trans-river flow zones are smaller than for the predevelopment simulations, but generally are coincident. In the Gordon aquifer and Dublin aquifer system, the area of westward trans-river flow during 1987–92 decreased from predevelopment by 32–60 percent, whereas the area in the Midville aquifer system decreased by only 7–8 percent. The decrease in westward trans-river-flow area during the modern-day simulation probably results from water-level declines and associated changes in hydraulic gradient due to ground-water pumpage.

During predevelopment, eastward trans-river flow occurred in all active model layers, with the largest affected areas occurring in the Dublin aquifer system. For each layer, the largest area of eastward trans-river flow occurred in zone 2, where the Savannah River meanders westward and is hydraulically separated from the aquifers. During the modern-day simulation, areas of eastward trans-river flow generally are in the same locations as in predevelopment. Areas of simulated eastward trans-river flow are the same or slightly larger for the modern-day simulation than for the predevelopment simulations in all layers except the lower Dublin aquifer, where these areas are slightly smaller.

Recharge areas to trans-river flow zones occur in both the uppermost unit and at lateral specified-head boundaries. Most recharge enters the water table in interstream drainage divides that are topographic highs, flows downward and laterally through one or more hydrogeologic units, and then flows upward and laterally through one or more hydrogeologic units to discharge into the Savannah River alluvial valley. The position of recharge cells shifted slightly during the modern-day period, but were located in the same general areas as during predevelopment.

Time-of-travel was computed by applying MODPATH to the same particles of water that defined the principal zones of westward and eastward trans-river flow in both predevelopment and modern-day simulations. During predevelopment, estimated mean travel times toward westward trans-river flow areas ranged from 300 to 24,000 years. These values represent the mean travel time for water particles in the simulated area and do not include ground water originating from outside of the simulated area. Travel times are controlled by factors that influence the three-dimensional movement of a water particle from the source area, including: (1) the transmissivity of aquifers;

(2) vertical conductance of confining units and aquifers; (3) porosity; and (4) lateral and vertical hydraulic gradients. Travel times toward eastward trans-river flow areas during predevelopment were somewhat longer than for westward areas, but were similarly distributed, ranging from 550 to 41,000 years.

For the modern-day simulation, estimated mean travel times changed from predevelopment in both eastern and western trans-river flow areas. Travel times for the modern-day simulation range from 300 to 34,000 years in westward trans-river flow areas, and from 580 to 31,000 years in eastward areas. The largest changes in travel times occurred in zone 3, where travel times for the modern-day simulation are longer for westward trans-river flow areas, and shorter for eastward areas than in predevelopment. Differences in travel times between the predevelopment and modern-day simulations result from changes in hydraulic gradients due to ground-water pumpage that altered flowpaths in the vicinity of the river.

Delineation of ground-water flow originating on the SRS, toward westward trans-river flow zones is important because of the possibility of contaminated ground water from SRS moving beneath the Savannah River and into Georgia. Recharge to Georgia trans-river flow zones originating on the SRS was simulated for the Gordon (layer A2) and upper Dublin aquifers (layer A4) during predevelopment, and in the Gordon aquifer during 1987–92. The recharge originating on SRS was simulated in the interstream areas south of Four Mile Branch Creek (predevelopment and modern day) and near Parr Pond (predevelopment only).

For the modern-day simulation, SRS recharge areas were delineated in 6 model cells that cover about 2 mi<sup>2</sup>. These recharge sites are generally located away from areas of ground-water contamination; however, two of the sites are located within about 0.5 mi of contaminated areas. In the vicinity of these recharge sites, simulated ground-water flow enters either the Upper Three Runs (layer A1) or Gordon (layer A2) aquifers, flows downward into units as deep as the lower Dublin aquifer (layer A5), laterally toward the river in one or more units, and finally moves upward to discharge from the Gordon aquifer into Savannah River alluvial sediments. Simulated aquifer discharge from the SRS recharge areas occurs in a 1 mi<sup>2</sup> marshy area immediately westward of the Savannah River that is distant from major pumping centers. Simulated modern-day time-of-travel from recharge areas originating on SRS to

westward trans-river flow zones ranges from about 90 to 2,900 years. Shorter simulated travel times occur where flowpaths have a shallower depth of penetration; longer travel times occur where the depth of penetration is deeper.

The complex hydrogeologic setting in the vicinity of the SRS implies some uncertainty regarding delineation of ground-water flowpaths, including pumping rates, areal recharge rates, and hydraulic properties of aquifers and confining units. The model is limited by simplification of the conceptual model, lateral and vertical discretization effects, and difficulty in obtaining sufficient measurements to account for all of the spatial variation in hydraulic properties and boundary conditions throughout the model area. Despite these limitations, simulation results are believed representative of regional-scale flow in the vicinity of the SRS. To provide better definition of flowpaths on a more-local scale would require greater refinement of the MODFLOW simulations and MODPATH analyses and additional hydraulic property data. Time-of-travel estimations would be improved by site-specific porosity data.

#### SELECTED REFERENCES

- Aadland, R.K., and Bledsoe, H.W., 1990, Classification of hydrostratigraphic units at the Savannah River Site, South Carolina: Aiken, S.C., Westinghouse Savannah River Company, WSRC-RP-90-987, 15 p.
- Aadland, R.K., Gellici, J.A., and Thayer, Paul, 1995, Hydrogeologic framework of west-central South Carolina: South Carolina Department of Natural Resources, Water Resources Division Report 5, 200 p.
- Aadland, R.K., Harris, M.K., Lewis, C.M., Gaughan, T.F., and Westbrook, T.M., 1991, Hydrostratigraphy of the General Separations Area, Savannah River Site (SRS), South Carolina: Aiken, S.C., U.S. Department of Energy Report WSRC-RP-91-13, Westinghouse Savannah River Company, 114 p.
- Aadland, R.K., Thayer, P.A., and Smits, A.D., 1992, Hydrostratigraphy of the Savannah River Site region, South Carolina and Georgia, *in* Price, Van, and Fallaw, Wallace, *eds.*, Geological investigations of the central Savannah River area, South Carolina and Georgia: Augusta, Ga., Carolina Geological Society fieldtrip guidebook, November 13–15, 1992, variously paged.
- Anderson, W.K. and Woessner, W.W., 1992, Applied groundwater modeling—simulation of flow and advective transport: San Diego, Ca., Academic Press, Inc., 381 p.
- Atkins, J.B., Journey, C.A., and Clarke, J.S., 1996, Estimation of ground-water discharge to streams in the central Savannah River basin of Georgia and South Carolina: U.S. Geological Survey Water-Resources Investigations Report 96-4179, 46 p.
- Aucott, W.R., 1988, The pre-development ground-water flow system and hydrologic characteristics of the Coastal Plain aquifers of South Carolina, U.S. Geological Survey Water-Resources Investigations Report 86-4347, 66 p.
- 1997, Hydrology of the Southeastern Coastal Plain Aquifer System in South Carolina and parts of Georgia and North Carolina: US Geological Survey Professional Paper 1410-E, 83 p.
- Aucott, W.R., Davis, M.E., and Speiran, G.K., 1987, Geologic framework of the Coastal Plain aquifers of South Carolina: U.S. Geological Survey Water-Resources Investigations Report 85-4271, 7 sheets.
- Aucott, W.R., Meadows, R.S., and Patterson, G.G., 1987, Regional ground-water discharge to large streams in the upper Coastal Plain of South Carolina and parts of North Carolina and Georgia: U.S. Geological Survey Water-Resources Investigations Report 86-4332, 28 p.
- Aucott, W.R., and Newcome, Roy, Jr., 1986, Selected aquifer-test information for the Coastal Plain aquifers of South Carolina: U.S. Geological Survey Water-Resources Investigations Report 86-4159, 30 p.
- Aucott, W.R., and Speiran, G.K., 1984, Water-level measurements for the Coastal Plain aquifers of South Carolina prior to development: U.S. Geological Survey Open-File Report 84-803, 36 p.
- 1985, Potentiometric surfaces of the Coastal Plain aquifers of South Carolina prior to development: U.S. Geological Survey Water-Resources Investigations Report 84-4208, 5 sheets.
- Baum, J.S., 1993, Three-dimensional modeling of ground-water flow in the vicinity of the Savannah River site, South Carolina and Georgia, *in* Abstracts with Programs, The Geological Society of America, Southeastern Section, March 1993: Boulder, Co., The Geological Society of America, v. 25, no. 4, p. 2.

- Baum, J.S., and Falls, W.F., 1995, Delineation of depositional environments and observed effects on ground-water flow properties near the Savannah River Site in South Carolina and Georgia, *in* Abstracts with Programs, The Geological Society of America, Southeastern Section, March 1995: Boulder, Co., The Geological Society of America, v. 27, no. 2, p. 36.
- Baum, J.S., Falls, W.F., and Edwards, L.E., 1993, Sedimentological techniques applied to the hydrology of the Atlantic Coastal Plain in South Carolina and Georgia near the Savannah River Site, *in* Proceedings, Society of Sedimentary Geology Symposium, June 12-15, 1994: Denver, Co., American Association of Petroleum Geologists annual meeting.
- Baum, J.S., McFadden, K.W., Flexner, N.M., Harrelson, L.G., and West, C.T., 1994, Management of geohydrologic data using a geographic information system for a three-dimensional ground-water flow model of the Savannah River Site area, South Carolina and Georgia, *in* Abstracts with Programs, The Geological Society of America, Southeastern Section, 43rd Annual Meeting, Blacksburg, Va., March 1994: Boulder, Co., The Geological Society of America, v. 26, no. 4, p. 3.
- Bechtel Corp., 1982, Studies of postulated Millett fault: Atlanta, Ga., unpublished report on file at the U.S. Geological Survey, Atlanta, Ga., variously paged.
- Benson, S.M., Moore, Jerry, Daggett, John, and Snipes, D.S., 1993, The influence of barometric pressure fluctuations, earth tides, and rainfall loading on fluid pressures in Coastal Plain aquifers, Burke County, Georgia, *in* Abstracts with Programs, The Geological Society of America, Southeastern Section, March 1993: Boulder, Co., The Geological Society of America, v. 25, no. 4, p. 3.
- Bledsoe, H.W., 1984, SRP baseline hydrogeologic investigation—Phase I: Aiken, S.C., E.I. duPont de Nemours & Co., Savannah River Laboratory, DPST-84-833, variously paged.
- \_\_\_\_\_, 1987, SRP baseline hydrogeologic investigation—Phase II: Aiken, S.C., E.I. duPont de Nemours & Co., Savannah River Laboratory, DPST-86-674, variously paged.
- \_\_\_\_\_, 1988, SRP baseline hydrogeologic investigation—Phase III: Aiken, S.C., E.I. duPont de Nemours & Co., Savannah River Laboratory, DPST-88-627, variously paged.
- Bledsoe, H.W., Aadland, R.K., and Sargent, K.A., 1990, SRS baseline hydrogeologic investigation—summary report: Aiken, S.C., Westinghouse Savannah River Company, Savannah River Site, WSRC-RP-90-1010, variously paged.
- Brooks, Rebekah, Clarke, J.S., and Faye R.E., 1985, Hydrogeology of the Gordon aquifer system of east-central Georgia: Georgia Geologic Survey Information Circular 75, 41 p.
- Bush, P.W., and Johnston, R.H., 1988, Ground-water hydraulics, regional flow, and ground-water development of the Floridan aquifer system in Florida and in parts of Georgia, South Carolina, and Alabama: U.S. Geological Survey Professional Paper 1403-C, 80 p.
- Buxton, H.T. and Reilly, T.E., 1986, A technique for analysis of ground-water systems at regional and subregional scales applied on Long Island, New York: *Ground Water*, v. 29, no. 1, p. 63–71.
- Cahill, J.M., 1982, Hydrology of the low-level radioactive solid-waste burial site and vicinity near Barnwell, South Carolina: U.S. Geological Survey Open-File Report 82-863, 101 p.
- Camp, Dresser, and McKee, Inc., 1992, Ground-water modeling for the nuclear weapons complex reconfiguration site at the Savannah River Site, Aiken, South Carolina—final report: Atlanta, Ga., by Camp, Dresser, McKee Federal Programs Corporation, *prepared for* Westinghouse Savannah River Company, document-no. 7901-003-RT-BBXZ, variously paged.
- Carter, R.F., and Stiles, H.R., 1983, Average annual rainfall and runoff in Georgia, 1941-70: Georgia Geologic Survey Hydrologic Atlas 9, 1 sheet.
- Chowns, T.M., and Williams, C.T., 1983, Pre-Cretaceous rocks beneath the Georgia Coastal Plain—Regional implications, *in* Gohn, G. S., *ed.*, Studies related to the Charleston, South Carolina earthquake of 1886—Tectonics and seismicity: U.S. Geological Survey Professional Paper 1313-L, p. L1–L42.
- Christl, R.J., 1964, Storage of radioactive wastes in basement rock beneath the Savannah River Plant: Aiken, S.C., U.S. Atomic Energy Commission Research and Development Report, DP-844, *prepared by* E.I. Dupont De Nemours and Company, under contract AT (07-2)-1, variously paged.

- Clark, W.Z., and Zisa, A.C., 1976, Physiographic map of Georgia: Georgia Geologic Survey, 1 sheet, scale 1: 2,000,000.
- Clarke, J.S., 1987, Potentiometric surface of the Upper Floridan aquifer in Georgia, 1985, and water-level trends, 1980–85: Georgia Geologic Survey Hydrologic Atlas 16, 1 sheet, scale 1:1,000,000.
- \_\_\_\_\_, 1992, Evaluation of ground-water flow and quality in the vicinity of the Savannah River Site, Georgia and South Carolina, *in* Abstracts with Programs, The Geological Society of America, Southeastern Section, annual meeting, March 1992: Boulder, Co., The Geological Society of America, v. 24, no. 2, March 1992, p. 47.
- \_\_\_\_\_, 1993, Conceptual models of possible stream–aquifer relations in the vicinity of the Savannah River Site, Georgia and South Carolina, *in* Abstracts with Programs, The Geological Society of America, Southeastern Section, March 1993: Boulder, Co., The Geological Society of America, v. 25, no. 4, March 1993, p. 8.
- \_\_\_\_\_, 1995, Use of a geographic information system to develop hydrogeologic unit outcrop and subcrop maps in the vicinity of the Savannah River Site, South Carolina and Georgia, *in* Abstracts with Programs, The Geological Society of America, Southeastern Section, March 1995: Boulder, Co., The Geological Society of America, v. 27, no. 2, p. 44.
- \_\_\_\_\_, 1997, Ground-water flow and stream–aquifer relations near the Savannah River Site, Georgia South Carolina, *in* Hatcher, K.J., *ed.*, Proceedings of the 1997 Georgia Water Resources Conference, March 20–22, 1997: Athens, Ga., The University of Georgia, Institute of Ecology, p. 452–456.
- Clarke, J.S., Brooks, Rebekah, and Faye, R.E., 1985, Hydrogeology of the Dublin and Midville aquifer systems of east central Georgia: Georgia Geologic Survey Information Circular 74, 62 p.
- Clarke, J.S., Falls, W.F., Edwards, L.E., Fredricksen, N.O., Bybell, L.M., Gibson, T.G., and Litwin, R.J., 1994, Geologic, hydrologic, and water-quality data for a multi-aquifer system in Coastal Plain sediments near Millers Pond, Burke County, Georgia: Georgia Geologic Survey Information Circular 96, 34 p.
- Clarke, J.S., Falls, W.F., Edwards, L.E., Fredricksen, N.O., Bybell, L.M., Gibson, T.G., Gohn, G.S., and Fleming, Farley, 1996, Hydrogeologic data and aquifer interconnection in a multiaquifer system in Coastal Plain sediments near Millhaven, Screven County, Georgia: Georgia Geologic Survey Information Circular 99, 43 p.
- Clarke, J.S., Hester, W.G., and O'Byrne, M.P., 1979, Ground-water data for Georgia, 1978: U.S. Geological Survey Open-File Report 79-1290.
- Clarke, J.S., Longworth, S.A., Joiner, C.N., Peck, M.F., McFadden, K.W., and Milby, B.J., 1987, Ground-water data for Georgia, 1986: U.S. Geological Survey Open-File Report 87-376, 177 p.
- Clarke, J.S., Joiner, C.N., Longworth, S.A., McFadden, K.W., and Peck, M.F., 1986, Ground-water data for Georgia, 1985: U.S. Geological Survey Open-File Report 86-304, 159 p.
- Clarke, J.S., Longworth, S.A., McFadden, K.W., and Peck, M.F., 1985, Ground-water data for Georgia, 1984: U.S. Geological Survey Open-File Report 85-331, 150 p.
- Clarke, J.S., Peck, M.F., Longworth, S.A., and McFadden, K.W., 1984, Ground-water data for Georgia, 1983: U.S. Geological Survey Open-File Report 84-605, 145 p.
- Clarke, J.S., and West, C.T., 1994, Development of water-table and potentiometric-surface maps for Coastal Plain aquifers in the vicinity of the Savannah River Site, South Carolina and Georgia, *in* Abstracts with Programs, The Geological Society of America, Southeastern Section, March 1994: Boulder, Co., The Geological Society of America, v. 26, no. 4, p. 8.
- \_\_\_\_\_, 1997, Ground-water levels, predevelopment ground-water flow, and stream–aquifer relations in the vicinity of the Savannah River Site, Georgia and South Carolina: U.S. Geological Survey Water-Resources Investigations Report 97-4197, 120 p., 1 plate.
- Colquhoun, D.J., 1981, Variation in sea level on the South Carolina Coastal Plain, *in* Colquhoun, D.J., *ed.*, Variation in sea level on the South Carolina Coastal Plain: I.G.C.P. no. 61, p. 1–44.

- Colquhoun, D.J., Woollen, I.D., Van Nieuwenhuise, D.S., Padgett, G.G., Oldham, R.W., Boylan, D.C., Bishop, J.W., and Howell, P.D., 1983, Surface and subsurface stratigraphy, structure, and aquifers of the South Carolina Coastal Plain: South Carolina Department of Health and Environmental Control Report ISBN 0-9613154-0-7, 78 p.
- Cook, J.R., 1986, Hydrogeologic data from Z area: Aiken, S.C., E.I. du Pont de Nemours and Co., Savannah River Laboratory, DPST-86-320, 113 p.
- Cooke, C.W., 1936, Geology of the Coastal Plain of South Carolina: U.S. Geological Survey Bulletin 867, 196 p.
- Cressler, A.M., 1996, Ground-water conditions in Georgia, 1995: U.S. Geological Survey Open-File Report 96-200, 102 p.
- Cressler, A.M., Jones, L.E., and Joiner, C.N., 1995, Ground-water conditions in Georgia, 1994: U.S. Geological Survey Open-File Report 95-302, 135 p.
- Delaimi, R.M., 1993, Development of a cross-sectional ground-water flow model for the Coastal Plain aquifers near the Savannah River Site, Georgia and South Carolina, *in* Abstracts with Programs, The Geological Society of America, Southeastern Section, March 1993: Boulder, Co., The Geological Society of America, v. 25, no. 4, p. 10.
- \_\_\_\_\_, 1996, Modeling ground-water flow in the vicinity of the Savannah River Site, South Carolina and Georgia: Athens, Ga., The University of Georgia, unpublished Ph.D. dissertation, University of Georgia, Athens, 344 p.
- Dennehy, K.F., and McMahon, P.B., 1987, Water movement in the unsaturated zone at a low-level radioactive-waste burial site near Barnwell, South Carolina: U.S. Geological Survey Open-File Report 87-46, 66 p.
- Dennehy, K.F., Prowell, D.C., and McMahon, P.B., 1989, Reconnaissance hydrogeologic investigation of the defense waste processing facility and vicinity, Savannah River Plant, South Carolina: U.S. Geological Survey Water-Resources Investigations Report 88-4221, 74 p.
- Dohrenwend, R.E., 1977, Evapotranspiration patterns in Florida: Florida Scientist, v. 40, no. 2, p. 184-192.
- Edwards, L.E., and Clarke, J.S., 1992, Biostratigraphic investigations help evaluation of the ground-water-flow system near the Savannah River Site, Georgia and South Carolina, *in* Lidgard, Scott and Crane, P.R., *eds.*, Abstracts and Program, Fifth North American Paleontological Convention, Field Museum of Natural History, Chicago, Il., June 28-July 1, 1992: The Paleontological Society, Special Publication no. 6, p.90.
- Fallow, W.C., and Price, Van, 1995, Stratigraphy of the Savannah River Site and vicinity: Southeastern Geology, v. 35, no. 1, March 1995, p. 21-58.
- Falls, W.F., and Baum, J.S., 1995, Recognition of the Millers Pond aquifer in the vicinity of Burke County, Georgia, *in* Abstracts with Programs, The Geological Society of America, Southeastern Section, March 1995: Boulder, Co., The Geological Society of America, v. 27 no. 2, p. 52.
- Falls, W.F., Baum, J.S., and Edwards, L.E., 1994, Sedimentological techniques applied to the hydrology of the Atlantic Coastal Plain in South Carolina and Georgia near the Savannah River Site, *in* Abstracts with Programs, The Geological Society of America, Southeastern Section, March 1994: Boulder, Co., The Geological Society of America, v. 26, no. 4, p. 13.
- Falls, W.F., Baum, J.S., and Prowell, D.C., 1997a, Physical stratigraphy and hydrostratigraphy of Upper Cretaceous and Paleocene sediments, Burke and Screven Counties, Georgia: Southeastern Geology, v. 36, no. 4, March 1997, p. 153-176.
- Falls, W.F., Baum, J.S., Harrelson, L.G., Brown, L.H., and Jreden, J.L., Jr., 1997b, Geology and hydrogeology of Cretaceous and Tertiary strata, and confinement in the vicinity of the U.S. Department of Energy Savannah River Site, South Carolina: U.S. Geological Survey Water-Resources Investigations Report 97-4245, 125 p.
- Falls, W.F., Prowell, D.C., Edwards, L.E., Frederiksen, N.O., Gibson, T.G., Bybell, L.M., and Gohn, G.S., 1993, Preliminary correlation of geologic units in three coreholes along the Savannah River in Burke and Screven Counties, Georgia, *in* Abstracts with Programs, The Geological Society of America, Southeastern Section, March 1993: Boulder, Co., The Geological Society of America, v. 25, no. 4, p. 14.

- Faye, R.E., and Mayer, G.C., 1990, Ground-water flow and stream-aquifer relations in the northern Coastal Plain of Georgia and adjacent parts of Alabama and South Carolina: U.S. Geological Water-Resources Investigations Report 88-4143, 83 p.
- \_\_\_\_\_, 1997, Digital model analysis of Southeastern Coastal Plain clastic aquifers in Georgia and adjacent parts of Alabama and South Carolina: U.S. Geological Survey Professional Paper 1410-F, 77 p., 16 plates.
- Faye, R.E., and McFadden, K.W., 1986, Hydraulic characteristics of Upper Cretaceous and lower Tertiary aquifers—eastern Alabama, Georgia, and western South Carolina: U.S. Geological Survey Water-Resources Investigations Report 86-4210, 22 p.
- Faye, R.E., and Prowell, D.C., 1982, Some effects of Late Cretaceous and Cenozoic faulting on the geology and hydrology of the Coastal Plain near the Savannah River, Georgia and South Carolina: U.S. Geological Survey Open-File Report 82-156, 73 p.
- Faye, R.E., and Smith, W.G., 1994, Relations of borehole resistivity to the horizontal hydraulic conductivity and dissolved-solids concentration in water of clastic Coastal Plain aquifers in the Southeastern United States: U.S. Geological Survey Water-Supply Paper 2414, 33 p.
- Franke, O.L., Reilly, T.E., Pollock, D.W., and LaBaugh, J.W., 1998, Estimating areas contributing recharge to wells—lessons from previous studies: U.S. Geological Survey Circular 1174, 14 p.
- Freeze, R.A., 1966, Theoretical analysis of regional groundwater flow: Berkeley, Calif., University of California at Berkeley, *unpublished* Ph.D. thesis, 304 p.
- Freeze, R.A., and Cherry, J.A., 1979, *Groundwater*: Englewood Cliffs, N.J., Prentice-Hall, Inc., 604 p.
- Freeze, R.A., and Witherspoon, P.A. 1966, Theoretical analysis of regional ground water flow: 1. Analytical and numerical solutions to the mathematical model: *Water Resources Research*, v. 1, no. 1, p. 641–656.
- \_\_\_\_\_, 1967, Theoretical analysis of regional ground water flow: 2. Effect of water-table configuration and subsurface permeability variation: *Water Resources Research*, v. 3, no. 2, p. 623–634.
- Garza, Reggina, and Krause, R.E., 1997, Water-supply potential of major streams and the Upper Floridan aquifer in the vicinity of Savannah, Georgia: U.S. Geological Survey Water-Supply Paper 2411, 38 p.
- Gellici, J.A., 1991, Hydrogeologic investigation and establishment of a permanent multi-observational well network in Aiken, Allendale, and Barnwell Counties, South Carolina—Phase IV: South Carolina Water Resources Commission Open-File Report No. 39, 35 p.
- Gorday, L.L., 1985, The hydrogeology of the Coastal Plain strata of Richmond and northern Burke Counties, Georgia: Georgia Geologic Survey Information Circular 61, 43 p.
- Harbaugh, A.W., 1990, A computer program for calculating subregional water budgets using results from the U.S. Geological Survey modular three-dimensional finite-difference ground-water flow model: U.S. Geological Survey Open-File Report 90-392.
- Harrelson, L.E., Falls, W.F., and Clarke, J.S., 1997, Selected well data in the vicinity of the Savannah River Site, South Carolina and Georgia: U.S. Geological Survey Open-File Report 97-657A, 215 p., 10 plates.
- Harris, W.B., and Zullo, V.A., 1990, Sequence stratigraphy of Paleocene and Eocene deposits in the Savannah River region, *in* Zullo, W.B., Price, Van, eds., *Savannah River Region—Transition between the Gulf and Atlantic Coastal Plains in proceedings of the second Bald Head Island Conference on Coastal Plain Geology*, November 6–11, 1990: Wilmington, N.C., The University of North Carolina, p. 134–142.
- Herrick, S.M., 1961, Well logs of the Coastal Plain of Georgia: Georgia Geologic Survey Bulletin 70, 462 p.
- Herrick, S.M., and Counts, H.B., 1968, Late Tertiary stratigraphy of eastern Georgia: Georgia Geologic Survey Guidebook, Third Annual Field Trip, 88 p.
- Herrick, S.M., and Vorhis, R.C., 1963, Subsurface geology of the Georgia Coastal Plain: Georgia Geologic Survey Information Circular 25, 80 p.
- Herrick, J.H., 1992, A geologic atlas of the Wrens-Augusta area: Georgia Geologic Survey Geologic Atlas 8, 3 sheets, scale 1:100,000.

- Hodges, R.A., Snipes, D.S., Benson, S.M., Daggett, J.S., Price, Van, Temples, Thomas, and Harrelson, L.E., 1994, Hydraulic properties of the Midville aquifer at the Savannah River Site, South Carolina, *in* Abstracts with Programs, The Geological Society of America, Southeastern Section, March 1994: Boulder, Co., The Geological Society of America, v. 26, no. 4, p. 20.
- Hoel, D.D., 1983, Climatology of the Savannah River Plant Site: Aiken, S.C., E.I. du Pont de Nemours and Co., Savannah River Laboratory, DPST-83-705, 315 p.
- Hubbard, J.E., Stephenson, D.E., Steele, J.L., and Gordon, D.E., 1988, Water resource management planning guide for Savannah River Plant: Aiken, S.C., E.I. du Pont de Nemours and Co., Savannah River Laboratory, DPST-88-835, 32 p.
- Huddlestun, P.F., Marsalis, W.E., and Pickering, S.M., Jr., 1974, Tertiary stratigraphy of the central Georgia Coastal Plain: Geological Society of America Guidebook 12, 35 p.
- Huddlestun, P.F., and Summerour, J.H., 1996, The lithostratigraphic framework of the uppermost Cretaceous and lower Tertiary of eastern Burke County, Georgia: Georgia Geologic Survey project report prepared for U.S. Geological Survey under cooperative agreement no. 1434-92-A-0959, 168 p.
- HydroGeoLogic, Inc., 1992, Ground-water flow and transport modeling of the TNX area at the Savannah River Site: Herndon, Va., by HydroGeoLogic, Inc., prepared for Westinghouse Savannah River Company, variously paged.
- Iman, R.L., and Conover, W.J., 1983, A modern approach to statistics: New York, John Wiley and Sons, 497 p.
- Joiner, C.N., Peck, M.F., Reynolds, M.S., and Stayton, W.L., 1989, Ground-water data for Georgia, 1988: U.S. Geological Survey Open-File Report 89-408, 176 p.
- Joiner, C.N., Reynolds, M.S., Stayton, W.L., and Boucher, F.G., 1988, Ground-water data for Georgia, 1987: U.S. Geological Survey Open-File Report 88-323, 172 p.
- Kidd, N.B., 1995, Hydraulic conductivities of Late Cretaceous Coastal Plain aquifers at Miller's Pond, east-central Georgia, *in* Abstracts with Programs, The Geological Society of America, Southeastern Section, March 1995: Boulder, Co., The Geological Society of America, v. 27 no. 2, p. 66.
- Krause, R.E., and Randolph, R.B., 1989, Hydrology of the Floridan aquifer system southeast Georgia and adjacent parts of Florida and South Carolina: U.S. Geological Survey Professional Paper 1403-D, 65 p.
- Kuntz, G.B., and Griffin, W.T., 1988, Hydrogeologic investigation and establishment of a permanent multi-observational well network in Aiken, Allendale, and Barnwell Counties South Carolina—Phase II: South Carolina Water Resources Commission Open-File Report No. 28, 92 p.
- Kuntz, G.B., Griffin, W.T., Greaney, T., and Gellici, J.A., 1989, Hydrogeologic investigation and establishment of a permanent multi-observational well network in Aiken, Allendale, and Barnwell Counties, South Carolina—Phase III: South Carolina Water Resources Commission Open-File Report No. 32, 54 p.
- LaForge, Lawrence, Cooke, C.W., Keith, Arthur, and Campbell, M.R., 1925, Physical geography of Georgia: Georgia Geologic Survey Bulletin 42, 189 p.
- Langley, T.M., and Marter, W.L., 1973, The Savannah River Site: Aiken, S.C., E.I. du Pont de Nemours & Company, Savannah River Laboratory, DP-1323, TID-4500, UC-2, prepared for Atomic Energy Commission contract AT(07-2)-I, p. 30–32.
- Leeth, D.C., and Nagle, D.D., 1994, Geomorphology and geologic characteristics of the Savannah River floodplain in the vicinity of the Savannah River Site, South Carolina and Georgia, *in* Abstracts with Programs, The Geological Society of America, Southeastern Section, March 1994: Boulder, Co., The Geological Society of America, v. 26, no. 4, p. 24.
- \_\_\_\_\_, 1996, Shallow subsurface geology of part of the Savannah River alluvial valley in the upper Coastal Plain of Georgia and South Carolina: Southeastern Geology, v. 36, no. 1, April 1996, p. 1–14.
- Leeth, D.C., Falls, W.F., Edwards, L.E., Frederiksen, N.O., and Fleming, R.F., 1996, Geologic, hydrologic, and water-quality data for a multi-aquifer system in Coastal Plain Sediments near Girard, Burke County, Georgia, 1993–1995: Georgia Geologic Survey Information Circular 100, 26 p.
- LeGrand, H.E., and Furcron, A.S., 1956, Geology and ground-water resources of central-east Georgia: Georgia Geologic Survey Bulletin 64, 174 p.

- LeGrand, H.E., and Pettyjohn, W.A., 1981, Regional hydrogeological concepts of homoclinal flanks: *Ground Water*, v. 19, no. 3, p. 303–310.
- Logan, W.R., 1987, Geohydrologic investigation and establishment of a permanent multi-observational well network in Aiken, Allendale, and Barnwell Counties South Carolina—Phase I: South Carolina Water-Resources Commission Open-File Report OF-23, 70 p.
- Logan, W.R., and Euler, G.M., 1989, Geology and ground-water resources of Allendale, Bamberg, and Barnwell Counties and part of Aiken County, South Carolina: South Carolina Water Resources Commission Report 155, 113 p.
- Looney, B.B., Haselow, J.S., Andersen, P.F., Spalding, C.P., and Davis, D.H., 1990, Ground-water modeling of the proposed new production reactor site, Savannah River Site, South Carolina: Aiken, S.C., Westinghouse Savannah River Company, *prepared for* U.S. Department of Energy, WSRC-RP-89-1010, 42 p.
- Lohman, S.W., 1972, Ground-water hydraulics: U.S. Geological Survey Professional Paper 708, 70 p.
- Mayer, G.C., and Jones, E.J., 1996, SWGW—A computer program for estimating ground-water discharge to a stream using streamflow data: U.S. Geological Water-Resources Investigations Report 96-4071, 20 p.
- Marine, I.W., 1966, Hydraulic correlation of fracture zones in buried crystalline rock at the Savannah River Plant near Aiken, South Carolina, *in* Geological Survey Research 1966: U.S. Geological Survey Professional Paper 550-D, p. D223–D227.
- \_\_\_\_\_, 1967a, The permeability of fractured crystalline rock at the Savannah River Plant near Aiken, South Carolina, *in* Geological Survey Research 1967: U.S. Geological Survey Professional Paper 575-B, p. B203–B211.
- \_\_\_\_\_, 1967b, The use of tracer test to verify an estimate of groundwater velocity in fractured crystalline rock at the Savannah River Plant near Aiken, South Carolina, *in* Stout, G.E., *ed.*, *Isotope techniques in the hydrologic cycle*: Washington, D.C., American Geophysical Union, Geophysical Monograph Series, v. 11, p. 171–178.
- \_\_\_\_\_, 1979, The use of naturally occurring helium to estimate groundwater velocities for studies of geologic storage of radioactive waste: *Water Resources Research*, v. 15, no. 5, p. 1,130–1,136.
- Marine, I.W., and Root, K.R., 1975, A ground-water model of the Tuscaloosa aquifer at the Savannah River Plant, Paper 14, *in* Crawford, T.V. (*compiler*), Savannah River Laboratory environmental transport and effects research annual report: Aiken, S.C., USERDA Report DP-1374, E.I. duPont de Nemours & Co., Savannah River Laboratory.
- \_\_\_\_\_, 1978, Geohydrology of deposits of Claiborne age at the Savannah River Plant: Aiken, S.C., Savannah River Laboratory environmental transport and effects research annual report DP-1489, p. 57–60.
- McDonald, B.B., 1984, General description of the geohydrology and burial trenches at the low-level radioactive waste burial facility near Barnwell, South Carolina: U.S. Geological Survey Open-File Report 84-806, 23 p.
- McDonald, M.G., and Harbaugh, A.W., 1988, A modular finite-difference ground-water flow model: U.S. Geological Survey Techniques of Water-Resources Investigations report, book 6, chap. A1, variously paged.
- Milby, B.J., Joiner, C.N., Cressler, A.M., and West, C.T., 1991, Ground-water conditions in Georgia, 1990: U.S. Geological Survey Open-File Report 91-486, 147 p.
- Miller, J.A., 1986, Hydrogeologic framework of the Floridan aquifer system in Florida, and in parts of Georgia, Alabama, and South Carolina: U.S. Geological Survey Professional Paper 1403-B, 91 p.
- Moore, Jerry, Benson S.M., Snipes, D.S., Daggett, John, James, April, Kroening, David, Price, Sarah, Price, Van, Jr., and Temples, Thomas, 1993, Characterization of aquifer properties in Coastal Plain sediments in Burke County, Georgia, *in* Abstracts with Programs, The Geological Society of America, Southeastern Section, March 1993: Boulder, Co., The Geological Society of America, v. 25, no. 4, p. 58.
- National Oceanic and Atmospheric Administration, 1995, Climatological data annual summary—Georgia, 1995: Asheville, N.C., National Oceanic and Atmospheric Administration, National Climatic Data Center, v. 99, no. 13, ISSN 0145-0492, 23 p.

- Newcome, Roy, Jr., 1993, Pumping tests of the Coastal Plain aquifers in South Carolina: South Carolina Water Resources Commission Report 174, 52 p.
- Nichols, R.L., Looney, B.B., and Huddleston, J.E., 1992, 3-D digital imaging: *Environmental Science and Technology*, v. 26, no. 4, p. 629-648.
- Nystrom, P.G., Jr., 1990, The original course of the Savannah River, South Carolina upper Coastal Plain, *in Geological Society of America, Abstracts with Programs: Boulder, Co., The Geological Society of America*, v. 22, no. 4, p. 53.
- Owens, J.P., and Gohn, G.S., 1984, Depositional history of the Cretaceous Series in the United States Coastal Plain: stratigraphy, paleoenvironments, and basin evolution: unpublished report on file at the U.S. Geological Survey, Reston, Va.
- Parizek, R.R., and Root, R.W., 1986, Development of a ground-water velocity model for the radioactive waste management facility, Savannah River Plant, Aiken, South Carolina: Aiken, S.C., U.S. Department of Energy Report DPST-86-658, E.I. duPont de Nemours & Co., Savannah River Plant, 31 p.
- Patterson, G.G., 1992, Localized ground-water discharge to the Savannah River near the Savannah River Site, South Carolina and Georgia, *in Abstracts with Programs, The Geological Society of America, Southeastern Section, March 1992: Boulder, Co., The Geological Society of America*, v. 24, no. 2, p. 45.
- Parizek, R.R., and Root, R.W., 1986, Development of a ground-water velocity model for the radioactive waste management facility, Savannah River Plant, Aiken, South Carolina: Aiken S.C., U.S. Department of Energy Report DPST-86-658, E.I. duPont de Nemours & Co., Savannah River Plant, 31 p.
- Peck, M.F., and Cressler, A.M., 1993, Ground-water conditions in Georgia, 1992: U.S. Geological Survey Open-File Report 93-358, 134 p.
- Peck, M.F., Joiner, C.N., Clarke, J.S., and Cressler, A.M., 1990, Ground-water data for Georgia, 1989: U.S. Geological Survey Open-File Report 90-706, 125 p.
- Peck, M.F., Joiner, C.N., and Cressler, A.M., 1992, Ground-water conditions in Georgia, 1991: U.S. Geological Survey Open-File Report 92-470, 137 p.
- P.E. LaMoreaux, Inc., 1980, Hydrology of the Georgia kaolin district: Atlanta, Ga., unpublished report on file at the U.S. Geological Survey, 139 p.
- Pollock, D.W., 1994, Users Guide for MODPATH/MODPATH-PLOT, Version 3: A particle tracking post-processing package for MODFLOW, the U.S. Geological Survey finite-difference ground-water flow model: U.S. Geological Survey Open-File Report 94-464, 188 p.
- Pollard, L.D., and Vorhis, R.C., 1980, The geohydrology of the Cretaceous aquifer system in Georgia: Georgia Geologic Survey Hydrologic Atlas 3, 5 sheets.
- Price, Van, Jr., Fallaw, W.C., and McKinney, J.B., 1991, Geologic setting of the new production reactor reference site within the Savannah River Site (U): Aiken, S.C., Westinghouse Savannah River Company, report no. WSRC-RP-91-96, ESH-EMS-90171, 80 p.
- Prowell, D.C., 1988, Cretaceous and Cenozoic tectonism on the Atlantic Coastal Plain margin, *in Sheridan, R.E., and Grow, J.A. eds., The Atlantic continental margin, United States: Boulder Co., The Geological Society of America, the Geology of North America*, v. I-2, p. 557-564.
- \_\_\_\_\_, 1994, Preliminary geologic map of the Barnwell 30' X 60' quadrangle, South Carolina and Georgia: U.S. Geological Survey Open-File Report 94-673, 38 p., 1 plate, scale 1:100,000.
- Prowell, D.C., Christopher, R.A., Edwards, L.E., Bybell, L.M., and Gill, H.E., 1985, Geologic section of the updip Coastal Plain from central Georgia and western South Carolina: U.S. Geological Survey Miscellaneous Field Studies Map MF-1737.
- Prowell, D.C., and O'Connor, B.J., 1978, Belair fault zone—Evidence of Tertiary fault displacement in eastern Georgia: *Geology*, v. 6, p. 681-684.
- Renken, R.A., Mahon, G.L., and Davis, M.E., 1989, Hydrogeology of clastic Tertiary and Cretaceous regional aquifers and confining units in the southeastern Coastal Plain aquifer system of the United States: U.S. Geological Survey Hydrologic Investigations Atlas HA-701, 3 sheets, scale 1:2,500,000.
- Root, R.W., Jr., 1980, Ground-water data from the H-area, Savannah River Plant, South Carolina: Savannah River Laboratory Report DPST-80-601, 34 p.

- \_\_\_ 1981, Results of drilling a well cluster near F-area at SRP: Aiken, S.C., Savannah River Laboratory Report DPST-81-503.
- \_\_\_ 1983, Numerical modeling of ground-water flow at the Savannah River Plant: U.S. Department of Energy Report DP-1638.
- Scott, J.C., 1990, A statistical processor for analyzing simulations made using the modular finite-difference ground-water flow model: U.S. Geological Survey Water-Resources Investigations Report 89-4159, 218 p.
- Siple, G.E., 1957, Geology and ground water in parts of Aiken, Barnwell, and Allendale Counties, South Carolina: U.S. Geological Survey, *prepared for Savannah River Operations Office of the Atomic Energy Commission*, copy on file with the U.S. Geological Survey, Columbia, S.C., 128 p.
- \_\_\_ 1960, Piezometric levels in the Cretaceous sand aquifer of the Savannah River Basin: Georgia Mineral Newsletter, v. 8, no. 4, winter 1960, p. 163-166.
- \_\_\_ 1967, Geology and ground water of the Savannah River Plant and vicinity, South Carolina: U.S. Geological Survey Water-Supply Paper 1841, 113 p.
- Sirrine Company, 1980, Groundwater resource study, Sirrine Job No. P-1550, DCN-001: Unpublished report on file at the U.S. Geological Survey, Atlanta, Ga., 26 p.
- Snipes, D.S., Benson, S.M., and Price, Van, Jr., 1995a, Hydrologic properties of aquifers in the central Savannah River area—volume 1: Clemson, S.C., Department of Geological Sciences, Clemson University, 353 p.
- \_\_\_ 1995b, Hydrologic properties of aquifers in the central Savannah River area—volume 2: Clemson, S.C., Department of Geological Sciences, Clemson University, 204 p.
- Snipes, D.S., Fallaw, W.C., Price, Van, Jr., and Cumbest, R.J., 1993, The Pen Branch Fault—Documentation of Late Cretaceous-Tertiary faulting in the Coastal Plain of South Carolina: Southeastern Geology, v. 33, no. 4, October 1993, p. 195-218.
- Sohl, N.F., and Owens, J.P., 1991, Cretaceous stratigraphy of the Carolina Coastal Plain, in Horton, J.W., Jr., and Zullo, V.A., eds., *The geology of the Carolinas: Knoxville, Tenn., Carolina Geological Society 50<sup>th</sup> Anniversary Volume*, University of Tennessee Press, p. 191-220.
- Speiran, G.K., and Aucott, W.R., 1991, Effects of sedimentary depositional environments and ground-water flow on quality and geochemistry of water in aquifers of sediments of Cretaceous age in the Coastal Plain of South Carolina: U.S. Geological Survey Open-File Report 91-102, 79 p.
- Stephenson, L.W., and Veatch, J.O., 1915, Underground waters of the Coastal Plain of Georgia, with a discussion of the quality of the waters by R. B. Dole: U.S. Geological Survey Water-Supply Paper 341, 539 p.
- Stevenson, A.E., 1982, Geomorphic history of a portion of the Savannah River floodplain, Barnwell County, South Carolina: Columbia, S.C., Department of Geological Sciences, University of South Carolina, *unpublished M.S. thesis*, 203 p.
- Stiles, H.R., and Matthews, S.E., 1983, Ground-water data for Georgia, 1982: U.S. Geological Survey Open-File Report 83-678, 147 p.
- Stokes, W.R., III, and McFarlane, R.D., 1996, Water resources data, Georgia—Water year 1995: U.S. Geological Survey Water-Data Report 95-1, 625 p.
- Stricker, V.A., 1983, Baseflow of streams in the outcrop area of southeastern sand aquifer—South Carolina, Georgia, Alabama, Mississippi: U.S. Geological Survey Water-Resources Investigations Report 83-4106, 17 p.
- Strom, R.N., 1992, Ground-water geochemistry and flow-path modeling, Savannah River Site, S.C., in *Abstracts with Programs*, The Geological Society of America, Southeastern Section, March 1992: Boulder, Co., The Geological Society of America, v. 24, no. 2, p. 69.
- Summerour, J.H., Shapiro, E.A., Lineback, J.A., Huddleston, P.F., and Hughes, A.C., 1994, An investigation of Tritium in the Gordon and other aquifers in Burke County, Georgia—Final Report: Georgia Geological Survey Information Circular 95, 93 p.

- Thomson, M.T., and Carter, R.F., 1955, Surface-water resources of Georgia during the drought of 1954—Part 1, Streamflow: Georgia Geologic Survey Information Circular 17, 79 p.
- Toth, J.A., 1962, A theory of ground-water motion in small drainage basins in central Alberta, Canada: *Journal of Geophysical Research*, v. 67, p. 4,795–4,812.
- \_\_\_\_ 1963, A theoretical analysis of ground-water flow in small drainage basins: *Journal of Geophysical Research*, v. 68, p. 4,795–4,812.
- U.S. Department of Commerce, 1991, Census data—Georgia and South Carolina, in *Census of Population and Housing, 1990 [machine readable data files]*: Washington, D.C., U.S. Department of Commerce, Bureau of the Census, Public Law (P.L.) 94–171.
- U.S. Department of Energy, 1990, Environmental data bases of the Savannah River Site (*Revision 2*): U.S. Department of Energy, Savannah River Operations Office, Environmental Division, 436 p.
- U.S. Geological Survey, 1978, Ground-water data for Georgia, 1977: Atlanta, Ga., U.S. Geological Survey unnumbered Open-File Report.
- \_\_\_\_ 1989, Digital line graphs from 1:100,000-scale maps—Data users guide 2: U.S. Geological Survey, National Mapping Division, Reston, Va., 88 p.
- Vincent, H.R., 1982, Geohydrology of the Jacksonian aquifer in central and east-central Georgia: *Georgia Geologic Survey Hydrologic Atlas 8*, 3 sheets.
- Wait, R.L., and Davis, M.E., 1986, Configuration and hydrology of the pre-Cretaceous rocks underlying the southeastern Coastal Plain aquifer system: U.S. Geological Survey Water-Resources Investigations Report 86-4010, 1 sheet, scale 1:2,000,000.
- West, C.T., 1995, Using a geographic information system to calibrate a ground-water flow model of the Savannah River Site, South Carolina and Georgia, in *Abstracts with Programs, The Geological Society of America, Southeastern Section, March 1995*: Boulder, Co., The Geological Society of America, v. 27, no. 2, March 1995, p. 96.
- Westinghouse Savannah River Company, 1991a, Savannah River Site environmental report for 1990: Aiken, S.C., Westinghouse Savannah River Company, WSRC-IM-91-28, prepared for U.S. Department of Energy contract no. DE-AC09-89SR18035, variously paged.
- \_\_\_\_ 1991b, Savannah River Site environmental report for 1991: Aiken, S.C., Westinghouse Savannah River Company, WSRC-TR-92-186, prepared for U.S. Department of Energy contract no. DE-AC09-89SR18035, variously paged.
- \_\_\_\_ 1992, Environmental Protection Department's well inventory (U) (through the fourth quarter of 1991): Aiken, S.C., Westinghouse Savannah River Company, report no. ESH-EMS-910092, 138 p.
- Winter, T.C., 1976, Numerical simulation analysis of the interaction of lakes and ground water: U.S. Geological Survey Professional Paper 1001, 45 p.
- Zheng, C., Bradbury, K.R., and Anderson, M.P., 1988a, Role of interceptor ditches in limiting the spread of contaminants in ground water: *Ground Water*, v. 26, no. 6, p. 734–742.
- Zheng, C., Wang, H.F., Anderson, M.P., and Bradbury, K.R., 1988b, Analysis of interceptor ditches for control of ground-water pollution: *Journal of Hydrology*, v. 98, p. 67–81.
- Zullo, V.A., Harris, W.B., and Price, Van, Jr., eds., 1990, Savannah River region—transition between the Gulf and Atlantic Coastal Plains, in *Proceedings of the Second Bald Head Island Conference on Coastal Plain Geology, November 6–11, 1990*: Wilmington, N.C., The University of North Carolina, 144 p.



Appendix A. Mean-annual ground-water discharge to streams estimated using hydrograph separation and simulated ground-water discharge for predevelopment (prior to 1953) and modern-day (1987-92) conditions

[mi<sup>2</sup>, square miles; ft<sup>3</sup>/s, cubic feet per second; in/yr, inches per year; —, not applicable; modified from Atkins and others (1996); Clarke and West (1997)]

Stream reach	Intermediate drainage area (mi <sup>2</sup> )	Years evaluated	Mean-annual gain in ground-water discharge							
			Estimated discharge				Simulated discharge			
			Period of record		1987-92		Predevelopment		1987-92	
			(ft <sup>3</sup> /s)	(in/yr)	(ft <sup>3</sup> /s)	(in/yr)	(ft <sup>3</sup> /s)	(in/yr)	(ft <sup>3</sup> /s)	(in/yr)
<b>Savannah River, Ga. and S.C.</b>										
Intermediate area between gages 02197000 and 02197500	1,142	1941, 1942, 1949	<sup>1/</sup> 1,220	14.5	—	—	635.8	7.7	???	7.5
<b>Upper Three Runs basin, S.C.</b>										
Intermediate area between stream headwaters and gage 02197300	87	1967-93	100	15.6	96	15	68.2	10.6	67.2	10.5
Intermediate area between gages 02197300 and 02197310	89	1967-93	94	14.3	82	12.5	47.9	7.3	45.6	6.9
Intermediate area between gages 02197310 and 02197315	27	1975-93	21	10.6	22	11	11.9	5.9	11.3	5.7
<b>Butler Creek basin, Ga.</b>										
Intermediate area between stream headwaters and gage 02196820	7.5	1969-90	1.4	2.5	1.4	2.5	1.9	3.4	1.8	3.3
<b>Brier Creek basin, Ga.</b>										
Intermediate area between the Fall Line and gage 02197830	418	1970-93	<sup>2/</sup> 284	<sup>3/</sup> 9.2	—	—	310.4	10.1	305.8	9.9
Intermediate area between gages 02197830 and 02198000	173	1970-93	126	9.9	75	5.9	114.2	8.9	112.9	8.9
<b>Brushy Creek basin, Ga.</b>										
Intermediate area between stream headwaters and gage 02197600	28	1959-93	14	6.8	14	6.8	10.3	4.9	9.9	4.8

<sup>1/</sup>Mean of 1941, 1942, and 1949 water years. Represents the difference between the net-annual stream-discharge gain between gages 02197000 and 02197500, and estimated ground-water discharge at gage 02197000 (from Faye and Mayer, 1990).

<sup>2/</sup>Mean-annual gain computed by multiplying the intermediate drainage area times the unit-area mean-annual discharge for gages 02197600 and 02197830.

<sup>3/</sup>Unit-area mean-annual ground-water discharge for gages 02197600 and 02197830.

Appendix B. Estimated ground-water discharge to streams during the 1954 and 1986 droughts and simulated ground-water discharge for predevelopment (prior to 1953) and modern-day (1987-92) conditions

[mi<sup>2</sup>, square mile; ft<sup>3</sup>/s, cubic feet per second; in/yr, inches per year; <, less than; —, not applicable; modified from Atkins and others (1996); Clarke and West (1997)]

Stream name and state	Stream reach	Intermediate drainage area (mi <sup>2</sup> )	Net gain in stream discharge									
			Estimated discharge						Simulated discharge			
			1954 drought			1986 drought			Predevelopment		1987-92	
			Date(s)	(ft <sup>3</sup> /s)	(in/yr)	Date(s)	(ft <sup>3</sup> /s)	(in/yr)	(ft <sup>3</sup> /s)	(in/yr)	(ft <sup>3</sup> /s)	(in/yr)
<b>Savannah River basin</b>												
Butler Creek, Ga.	intermediate area between stream headwaters and gage 02196820	7.5	—	—	—	07/24/86	<sup>1</sup> /0.28	0.5	1.9	3.4	1.8	3.3
Butler Creek, Ga.	intermediate area between stream headwaters and gage 02196840	13.5	10/05/54	<sup>2</sup> /0.58	58	—	—	—	7.9	7.9	7.8	7.8
Butler Creek, Ga.	intermediate area between gages 02196840 and 02196900	15.9	10/05/54, 10/06/54	<sup>2</sup> /8.7	7.4	—	—	—	8.2	7.0	7.4	6.3
Spirit Creek, Ga.	intermediate area between stream headwaters and gage 02197030	49.3	10/05/54	<sup>2</sup> /33.7	9.3	07/23/86	<sup>2</sup> /38	10.5	50.3	13.9	48.0	13.2
Spirit Creek, Ga.	intermediate area between stream headwaters and gage 02197020	18	10/05/54	<sup>2</sup> /12.7	9.6	—	—	—	26.7	20.1	26.5	19.9
Spirit Creek, Ga.	intermediate area between gages 02197020 and 02197030	32.3	10/05/54	<sup>2</sup> /21.7	9.1	—	—	—	11.3	4.7	11.1	4.7
Spirit Creek, Ga.	intermediate area between gages 02197030 and 02197045	20.8	10/05/54	<sup>2</sup> /0	0	—	—	—	12.3	8.03	10.5	6.9
Little Spirit Creek, Ga.	intermediate area between stream headwaters and gage 02197055	28.3	10/05/54	<sup>2</sup> /5.5	2.6	—	—	—	15.1	7.2	14.6	7.0
McBean Creek, Ga.	intermediate area between stream headwaters and gage 02197200	71.41	10/04/54	<sup>2</sup> /41.1	7.8	07/24/86	<sup>2</sup> /24	4.6	35.9	6.7	35.1	6.7
McBean Creek, Ga.	intermediate area between stream headwaters and gage 02197190	41.4	10/06/54	<sup>2</sup> /19.7	6.5	—	—	—	14.4	4.7	14.2	4.7
McBean Creek, Ga.	intermediate area between gages 02197190 and 02197200	30	10/04/54	<sup>2</sup> /21.7	9.8	—	—	—	21.5	9.7	20.9	9.5

Appendix B. Estimated ground-water discharge to streams during the 1954 and 1986 droughts and simulated ground-water discharge for predevelopment (prior to 1953) and modern-day (1987-92) conditions—Continued

[mi<sup>2</sup>, square mile; ft<sup>3</sup>/s, cubic feet per second; in/yr, inches per year; <, less than; —, not applicable; modified from Atkins and others (1996); Clarke and West (1997)]

Stream name and state	Stream reach	Intermediate drainage area (mi <sup>2</sup> )	Net gain in stream discharge									
			Estimated discharge						Simulated discharge			
			1954 drought			1986 drought			Predevelopment		1987-92	
			Date(s)	(ft <sup>3</sup> /s)	(in/yr)	Date(s)	(ft <sup>3</sup> /s)	(in/yr)	(ft <sup>3</sup> /s)	(in/yr)	(ft <sup>3</sup> /s)	(in/yr)
<b>Savannah River basin—continued</b>												
Upper Three Runs, S.C.	intermediate area between stream headwaters and gage 02197300	87	—	—	—	07/20/86			68.2	10.6	67.2	10.5
							<sup>1</sup> / <sub>67</sub>	10.4				
Upper Three Runs, S.C.	intermediate area between gages 02197300 and 02197310	89.0	—	—	—	07/20/86			47.9	7.3	45.6	6.9
							<sup>1</sup> / <sub>26</sub>	4.0				
Upper Three Runs, S.C.	intermediate area between gages 02197310 and 02197315	27	—	—	—	07/20/86			11.9	5.9	11.3	5.7
							0	0				
Brier Creek, S.C.	intermediate area between stream headwaters and gage 021975015	15.2	—	—	—	07/22/86			1.1	0.98	1.1	0.98
							<sup>2</sup> / <sub>23</sub>	.21				
Sandy Run Creek, Ga.	intermediate area between stream headwaters and gage 02197560	31.4	10/06/54	<sup>2</sup> / <sub>11.1</sub>	4.8	07/23/86			0	0	0	0
							<sup>2</sup> / <sub>11</sub>	4.8				
Brushy Creek, Ga.	intermediate area between stream headwaters and gage 02197600	28.0	—	—	—	07/24/86			10.3	4.9	9.9	4.8
							<sup>1</sup> / <sub>4.6</sub>	2.2				
Brushy Creek, Ga.	intermediate area between stream headwaters and gage 02197580	1.4	10/06/54	<sup>2</sup> / <sub>0</sub>	0	—	—	—	0	0	0	0
Brushy Creek, Ga.	intermediate area between gages 02197580 and 02197590	8	10/06/54	<sup>2</sup> / <sub>1.6</sub>	2.7	—	—	—	0.64	1.1	0.63	1.1
Brushy Creek, Ga.	intermediate area between gages 02197590 and 02197640	31.3	10/05/54	<sup>2</sup> / <sub>8.9</sub>	3.9	—	—	—	21.1	23.3	20.6	22.8
Brier Creek, Ga.	intermediate area between gages 02197557 and 02197830	302	10/04/54	86.2	3.9	—	—	—	310.4	14.0	305.8	13.7
Brier Creek, Ga.	intermediate area between gages 02197520 and 02197830	418	10/04/54 10/14/54	107.0	3.5	07/24/86	<sup>1</sup> / <sub>66.8</sub>	2.2	165.2	5.4	162.9	5.3

Appendix B. Estimated ground-water discharge to streams during the 1954 and 1986 droughts and simulated ground-water discharge for predevelopment (prior to 1953) and modern-day (1987-92) conditions—Continued

[mi<sup>2</sup>, square mile; ft<sup>3</sup>/s, cubic feet per second; in/yr, inches per year; <, less than; —, not applicable; modified from Atkins and others (1996); Clarke and West (1997)]

Stream name and state	Stream reach	Intermediate drainage area (mi <sup>2</sup> )	Net gain in stream discharge									
			Estimated discharge						Simulated discharge			
			1954 drought			1986 drought			Predevelopment		1987-92	
			Date(s)	(ft <sup>3</sup> /s)	(in/yr)	Date(s)	(ft <sup>3</sup> /s)	(in/yr)	(ft <sup>3</sup> /s)	(in/yr)	(ft <sup>3</sup> /s)	(in/yr)
<b>Savannah River basin—continued</b>												
Brier Creek, Ga.	intermediate area between gages 02197830 and 02198000	173	10/06/54	<sup>2</sup> /0	0	07/24/86	<sup>1</sup> /6.0	.5	114.2	8.9	112.9	8.9
McIntosh Creek, Ga.	intermediate area between stream headwaters and gage 02197890	131	10/05/54	<sup>2</sup> /0.9	.1	—	—	—	0	0	0	0
Beaverdam Creek, Ga.	intermediate area between stream headwaters and gage 02198120	85	07/29/54	<sup>2</sup> /1.3	.2	—	—	—	25.9	4.1	25.6	4.1
Beaverdam Creek, Ga.	intermediate area between gages 02198120 and 02198280	58	07/29/54	<sup>2</sup> /25.4	5.9	—	—	—	7.9	1.8	7.8	1.8
<b>Ogeechee River basin</b>												
Big Creek, Ga.	intermediate area between stream headwaters and gage 02200720	8.1	10/06/54	<sup>2</sup> /2.4	4.0	—	—	—	0.61	1.0	0.60	1.0
Big Creek, Ga.	intermediate area between gages 02200720 and 02200810	48.8	10/06/54	<sup>2</sup> /2.3	6.3	—	—	—	29.9	8.3	27.6	7.7
Big Creek tributary, Ga.	intermediate area between stream headwaters and gage 02200830	2.3	10/06/54	<sup>2</sup> /0.08	.5	—	—	—	9.1	53.7	9.0	53.1
Buckhead Creek, Ga.	intermediate area between stream headwaters and gage 02201350	63.7	10/05/54	<sup>2</sup> /0	0	—	—	—	15.9	3.4	15.8	3.4
Rocky Creek, Ga.	intermediate area between stream headwaters and gage 02201360	31.7	10/05/54	<sup>2</sup> /1.2	.1	—	—	—	0	0	0	0
Rocky Creek, Ga.	intermediate area between gages 02201360 and 02201365	3.1	10/05/54	<sup>2</sup> /0	0	—	—	—	0	0	0	0

Appendix B. Estimated ground-water discharge to streams during the 1954 and 1986 droughts and simulated ground-water discharge for predevelopment (prior to 1953) and modern-day (1987-92) conditions—Continued

[mi<sup>2</sup>, square mile; ft<sup>3</sup>/s, cubic feet per second; in/yr, inches per year; <, less than; —, not applicable; modified from Atkins and others (1996); Clarke and West (1997)]

Stream name and state	Stream reach	Intermediate drainage area (mi <sup>2</sup> )	Net gain in stream discharge									
			Estimated discharge						Simulated discharge			
			1954 drought			1986 drought			Predevelopment		1987-92	
			Date(s)	(ft <sup>3</sup> /s)	(in/yr)	Date(s)	(ft <sup>3</sup> /s)	(in/yr)	(ft <sup>3</sup> /s)	(in/yr)	(ft <sup>3</sup> /s)	(in/yr)
<b>Ogeechee River basin—Continued</b>												
Little Buckhead Creek, Ga.	intermediate area between stream headwaters and gage 02201400	29.7	09/10/54	<sup>2</sup> /0.02	<.1	—	—	—	1.9	0.87	1.8	0.82
Ogeechee Creek, Ga.	intermediate area between stream headwaters and gage 02202210	14.0	09/09/54	<sup>2</sup> /0	0	—	—	—	1.4	1.4	1.4	1.4
<b>Edisto River basin</b>												
South Fork Edisto River, S.C.	intermediate area between gage 02175000 and 02173000	522	09/10/54	<sup>1</sup> /129	3.4	—	—	—	77.8	2.0	77.4	2.0

<sup>1</sup>/Unit-area discharge computed using streamflow and drainage area.

<sup>2</sup>/Discharge measurement.

Appendix C. Measured heads, simulated predevelopment (prior to 1953) and modern-day (1987–92) heads, and error criteria in wells used for model calibration  
 [—, no data; do., ditto]

Well number or cell number <sup>1/</sup>	Model			Error criteria, in feet	Water-level altitudes, in feet						Wells used in averaging
					Predevelopment			Modern-day			
	Layer	Row	Column		Observed	Simulated	Difference	Observed	Simulated	Difference	
26AA101	7	22	3	43.0	313.0	344.9	31.9	—	—	—	not averaged
26AA103	7	17	3	40.8	318.2	354.0	35.8	318.2	350.9	32.7	do.
27AA02	7	13	7	26.5	383.0	367.9	-15.1	372.0	367.8	-4.2	do.
27AA16	6	22	4	23.4	310.0	325.0	15.0	—	—	—	do.
27AA17	7	23	4	23.9	313.0	323.2	10.2	—	—	—	do.
28AA06	5	35	10	14.2	281.0	265.1	-15.9	278.7	264.6	-14.1	do.
28AA09	7	22	12	19.0	258.3	267.2	8.9	—	—	—	do.
28AA10	7	20	13	14.5	233.0	243.8	10.8	—	—	—	do.
28BB12	7	17	13	18.0	267.3	273.1	5.8	257.2	72.5	15.3	do.
28BB21	7	8	16	31.7	304.4	298.7	-5.7	—	—	—	do.
28BB22	7	9	15	21.5	297.4	308.1	10.7	—	—	—	do.
28Z001	2	44	7	14.4	264.4	253.6	-10.8	241.0	253.4	12.4	do.
28Z003	2	50	7	13.0	257.0	248.3	-8.7	254.0	248.2	-5.8	do.
28Z004	2	63	7	14.7	230.0	254.8	24.8	—	—	—	do.
28Z005	4	38	7	13.3	259.4	267.8	8.4	255.4	267.7	12.3	do.
29AA01	4	34	13	13.7	256.0	242.5	-13.5	211.5	238.9	27.4	do.
29AA02	7	34	13	18.5	228.0	228.7	0.7	216.3	226.6	10.3	do.
29AA06	5	42	19	13.6	170.2	177.6	7.4	—	—	—	do.
29AA08	7	32	12	17.9	262.3	239.3	-22.9	240.4	237.4	-3.0	do.
29AA09	6	31	22	13.1	173.4	170.6	-2.8	173.4	167.9	-5.5	do.
29AA12	5	34	13	13.7	236.0	240.2	4.2	—	—	—	do.
29AA13	7	31	18	14.1	181.1	194.2	13.1	—	—	—	do.
29AA14	5	31	17	22.5	189.0	202.7	13.7	—	—	—	do.
29AA16	2	37	22	24.4	221.0	199.3	-21.7	—	—	—	do.
29AA17	2	33	17	10.9	267.0	227.2	-39.8	—	—	—	do.
29AA19	4	31	12	15.8	275.0	259.0	-16.0	—	—	—	do.
29BB01	7	20	29	15.7	—	—	—	116.6	133.2	16.6	29BB01,29BB59
29BB02	7	28	24	14.0	181.3	164.3	-17.0	176.1	160.7	-15.4	not averaged
29BB03	7	26	28	13.3	143.8	141.8	-2.0	—	—	—	do.
29BB05	7	23	27	15.6	140.7	153.0	12.3	131.3	145.5	14.2	do.
29BB06	7	24	27	15.4	155.6	152.1	-3.5	—	—	—	do.
29BB08	7	21	28	15.7	144.2	145.9	1.7	—	—	—	do.
29BB09	7	21	27	15.4	158.3	153.9	-4.4	—	—	—	do.
29BB10	7	22	29	15.6	147.2	140.9	-6.3	—	—	—	do.
29BB11	7	22	28	15.6	136.0	147.6	11.6	—	—	—	do.
29BB13	7	19	32	15.0	127.0	127.1	0.1	—	—	—	do.
29BB20	7	23	28	15.6	143.5	147.8	4.3	—	—	—	not averaged

Appendix C. Measured heads, simulated predevelopment (prior to 1953) and modern-day (1987–92) heads, and error criteria in wells used for model calibration—Continued  
 [—, no data; do., ditto]

Well number or cell number <sup>1/</sup>	Model			Error criteria, in feet	Water-level altitudes, in feet						Wells used in averaging
					Predevelopment			Modern-day			
	Layer	Row	Column		Observed	Simulated	Difference	Observed	Simulated	Difference	
29BB63	6	28	24	14.0	178.0	164.4	-13.6	—	—	—	do.
29Y003	4	82	10	13.4	203.0	220.6	17.6	195.3	217.9	22.6	do.
29Z001	2	67	11	13.7	195.0	205.1	10.1	—	—	—	do.
29Z003	2	67	12	10.9	207.6	205.0	-2.6	206.0	204.7	-1.3	do.
29Z004	2	70	11	11.3	198.1	203.8	5.7	197.2	203.5	6.3	do.
29Z008	3	63	8	15.7	242.5	237.6	-4.9	—	—	—	do.
29Z009	7	65	9	13.2	272.0	229.8	-42.2	—	—	—	do.
29Z010	2	63	9	13.6	216.4	220.2	3.8	—	—	—	do.
29Z011	2	50	11	16.2	213.6	222.4	8.8	—	—	—	do.
30AA02	7	39	33	12.4	112.0	107.4	-4.6	97.4	103.0	5.6	do.
30AA03	7	39	32	13.0	105.0	111.5	6.5	101.7	106.7	5.0	do.
30AA06	7	32	31	11.8	117.0	119.1	2.1	83.9	112.4	28.5	do.
30AA11	7	35	31	10.8	112.0	117.0	5.0	78.9	109.8	30.9	do.
30AA18	7	33	29	13.4	93.0	130.0	37.0	—	—	—	do.
30AA22	2	56	23	12.3	130.0	151.3	21.3	—	—	—	do.
30BB02	7	22	43	12.4	110.0	118.6	8.6	—	—	—	do.
30BB09	7	25	46	12.5	109.5	127.0	17.5	—	—	—	do.
30BB11	7	24	44	12.5	111.0	119.8	8.8	—	—	—	do.
30BB13	7	25	42	12.4	112.5	115.6	3.1	—	—	—	do.
30BB14	7	24	45	12.5	110.0	122.2	12.2	—	—	—	do.
30BB17	7	24	46	12.5	120.0	126.1	6.1	—	—	—	do.
30BB18	7	22	45	12.4	117.4	122.0	4.6	—	—	—	do.
30BB23	7	21	44	12.4	107.6	119.9	12.3	—	—	—	do.
30BB33	7	28	30	13.2	—	—	—	115.2	122.2	7.0	do.
30W007	2	116	8	13.4	164.3	171.6	7.3	164.3	171.5	7.2	do.
30W009	2	121	8	12.8	156.6	166.9	10.3	153.6	166.6	13.0	do.
30X004	2	113	9	12.5	196.0	203.0	7.0	181.9	202.4	20.5	do.
30X006	3	116	8	13.7	169.7	173.0	3.3	169.3	172.9	3.6	do.
30X007	2	115	9	14.0	182.0	196.0	14.0	174.5	195.5	21.0	do.
30Z006	2	68	32	10.9	131.9	142.8	10.9	122.1	142.4	20.3	do.
30Z007	4	58	23	11.6	141.5	149.0	7.5	—	—	—	do.
30Z009	2	63	27	12.9	163.9	151.8	-12.1	163.1	151.4	-11.7	do.
30Z019	2	69	16	12.5	198.9	193.6	-5.3	198.1	193.1	-5.0	do.
30Z020	2	72	22	11.8	189.2	177.9	-11.3	188.7	177.3	-11.4	do.
30Z023	6	66	33	11.4	157.2	150.7	-6.5	157.2	149.8	-7.4	do.
30Z028	3	66	33	11.3	135.0	138.7	3.7	135.0	138.3	3.3	not averaged

Appendix C. Measured heads, simulated predevelopment (prior to 1953) and modern-day (1987–92) heads, and error criteria in wells used for model calibration—Continued  
 [—, no data; do., ditto]

Well number or cell number <sup>1/</sup>	Model			Error criteria, in feet	Water-level altitudes, in feet						Wells used in averaging
					Predevelopment			Modern-day			
	Layer	Row	Column		Observed	Simulated	Difference	Observed	Simulated	Difference	
30Z036	2	57	16	14.6	170.2	177.2	7.0	—	—	—	do.
31Y007	3	94	37	12.6	152.9	156.1	3.2	151.5	154.8	3.3	do.
31Y019	2	96	38	12.2	149.3	152.0	2.8	148.0	151.0	3.0	do.
31Z009	2	91	43	15.1	148.0	128.9	-19.1	—	—	—	do.
31Z011	2	66	35	14.3	143.0	131.9	-11.1	—	—	—	do.
31Z015	2	91	45	14.6	116.0	114.3	-1.7	111.4	113.3	1.9	do.
31Z016	2	89	45	11.2	100.4	113.6	13.2	95.5	112.6	17.1	do.
31Z043	4	83	36	11.6	150.1	158.4	8.3	149.6	156.7	7.1	do.
31Z044	3	83	36	13.6	150.1	158.3	8.2	149.4	156.6	7.2	do.
31Z045	2	83	36	13.3	150.9	153.6	2.7	150.4	152.0	1.6	do.
31Z075	2	86	41	16.7	113.4	136.8	23.4	113.4	135.4	22.0	do.
31Z078	2	93	44	14.5	113.5	122.5	9.0	109.1	121.4	12.3	do.
31Z083	2	78	41	14.9	116.8	105.9	-10.9	116.0	105.5	-10.5	do.
31Z097	2	91	39	12.1	—	—	—	140.7	148.6	7.9	do.
31Z110	2	82	43	10.9	98.4	107.5	9.1	93.9	107.0	13.1	do.
31Z111	5	82	43	11.4	157.9	155.9	-2.0	157.0	153.7	-3.3	do.
31Z112	7	82	43	11.4	157.1	158.3	1.2	154.8	156.3	1.5	do.
32X023	2	120	47	12.1	125.8	132.0	6.2	—	—	—	do.
32Y016	5	107	54	10.8	165.3	158.3	-7.0	—	—	—	do.
32Y017	4	106	52	10.8	164.5	158.5	-6.0	—	—	—	do.
32Y018	5	104	50	10.8	171.0	161.3	-9.7	—	—	—	do.
32Y027	4	108	56	10.8	157.6	155.4	-2.2	—	—	—	do.
32Y028	2	103	48	13.0	128.4	132.0	3.6	—	—	—	do.
32Y029	5	106	43	11.4	164.1	163.6	-0.5	164.1	162.1	-2.0	do.
32Y030	7	106	56	10.8	175.0	180.5	5.5	175.0	179.0	4.0	do.
32Y031	5	106	56	10.8	154.2	157.1	2.9	154.2	155.2	1.0	do.
32Y032	7	106	43	11.5	180.1	182.2	2.1	180.1	180.9	0.8	do.
32Y033	2	106	56	11.2	121.0	124.1	3.1	121.0	123.6	2.6	do.
32Z004	2	92	46	14.0	84.8	110.9	26.1	73.5	110.1	36.6	do.
33W019	2	126	45	13.1	103.6	102.0	-1.6	98.1	101.6	3.5	do.
33W024	2	127	49	15.2	104.2	93.6	-10.6	—	—	—	do.
33X048	3	125	47	14.6	123.0	113.8	-9.2	—	—	—	do.
33X054	5	125	47	10.8	150.5	149.2	-1.3	150.5	148.1	-2.4	do.
33X055	7	125	47	12.9	189.1	188.3	-0.8	189.1	188.0	-1.1	do.
33Y008	2	110	58	11.0	128.0	133.7	5.7	—	—	—	do.
33Y011	2	115	62	10.9	121.0	114.6	-6.4	—	—	—	not averaged

Appendix C. Measured heads, simulated predevelopment (prior to 1953) and modern-day (1987–92) heads, and error criteria in wells used for model calibration—Continued  
 [—, no data; do., ditto]

Well number or cell number <sup>1/</sup>	Model			Error criteria, in feet	Water-level altitudes, in feet						Wells used in averaging
					Predevelopment			Modern-day			
	Layer	Row	Column		Observed	Simulated	Difference	Observed	Simulated	Difference	
AK-36	5	23	86	13.1	328.6	339.5	10.9	—	—	—	do.
AK-38	2	48	79	13.4	265.0	265.7	0.7	—	—	—	do.
AK-54	4	50	56	12.6	159.0	174.0	15.0	—	—	—	do.
AK-113	2	52	57	15.6	165.0	178.6	13.6	—	—	—	do.
AK-115	4	47	55	14.5	160.0	168.4	8.4	—	—	—	do.
AK-120	5	30	50	14.6	195.0	174.2	-20.8	—	—	—	do.
AK-121	6	29	50	13.4	180.0	154.2	-25.8	—	—	—	do.
AK-132	5	20	59	15.2	225.0	238.9	13.9	—	—	—	do.
AK-133	6	19	60	16.4	214.0	201.8	-12.2	—	—	—	do.
AK-141	5	27	54	18.1	240.0	223.5	-16.5	—	—	—	do.
AK-154	4	46	51	16.3	145.0	146.4	1.4	—	—	—	do.
AK-169	5	28	52	17.8	200.0	206.2	6.2	—	—	—	do.
AK-171	5	21	54	16.7	210.0	220.8	10.8	—	—	—	do.
AK-179	4	45	55	20.8	180.0	174.7	-5.3	—	—	—	do.
AK-180	5	31	47	16.0	140.0	133.7	-6.3	—	—	—	do.
AK-181	5	57	51	15.0	123.0	134.0	11.0	—	—	—	do.
AK-183	7	28	50	15.3	164.1	153.5	-10.6	—	—	—	do.
AK-184	2	49	78	12.6	260.0	263.9	3.9	—	—	—	do.
AK-202	7	8	93	10.8	333.0	338.6	5.6	—	—	—	do.
AK-220	6	19	62	13.5	222.0	215.3	-6.7	—	—	—	do.
AK-222	5	31	53	12.8	195.0	195.3	0.3	—	—	—	do.
AK-223	2	47	78	12.1	275.0	268.8	-6.2	—	—	—	do.
AK-225	5	27	57	14.7	234.0	232.5	-1.5	—	—	—	do.
AK-229	4	32	58	16.7	190.0	204.8	14.8	—	—	—	do.
AK-230	4	32	57	15.2	184.0	201.3	17.3	—	—	—	do.
AK-231	4	58	50	14.7	128.0	119.7	-8.3	—	—	—	do.
AK-236	7	23	86	13.1	336.0	331.0	-5.0	—	—	—	do.
AK-237	5	33	62	14.5	183.0	212.6	29.6	—	—	—	do.
AK-240	6	17	59	19.1	187.1	189.4	2.3	—	—	—	do.
AK-259	6	15	68	16.4	208.5	245.9	37.4	—	—	—	do.
AK-260	2	35	57	16.5	240.0	198.7	-41.3	—	—	—	do.
AK-265	5	27	100	14.6	270.0	284.2	14.2	—	—	—	do.
AK-274	5	21	97	12.0	320.0	310.6	-9.4	—	—	—	do.
AK-276	6	10	93	17.4	345.0	309.5	-35.5	—	—	—	do.
AK-290	5	45	80	10.8	258.4	261.7	3.3	255.1	260.6	5.5	do.
AK-291	5	26	58	15.6	245.0	237.4	-7.6	—	—	—	not averaged

Appendix C. Measured heads, simulated predevelopment (prior to 1953) and modern-day (1987–92) heads, and error criteria in wells used for model calibration—Continued  
 [—, no data; do., ditto]

Well number or cell number <sup>1/</sup>	Model			Error criteria, in feet	Water-level altitudes, in feet						Wells used in averaging
					Predevelopment			Modern-day			
	Layer	Row	Column		Observed	Simulated	Difference	Observed	Simulated	Difference	
AK-316	4	52	101	14.7	238.5	252.3	13.8	—	—	—	do.
AK-331	7	6	95	21.4	400.0	397.9	-2.1	—	—	—	do.
AK-351	2	55	55	12.9	188.3	164.4	-23.9	—	—	—	do.
AK-468	4	78	55	12.1	171.3	156.4	-14.9	—	—	—	do.
AK-476	7	16	63	13.7	200.6	205.8	5.2	200.3	204.4	4.1	do.
AK-483	5	40	97	12.1	280.4	285.2	4.8	279.8	284.9	5.1	do.
AK-508	4	75	50	15.1	124.0	123.4	-0.6	—	—	—	do.
AK-532	5	71	71	11.5	188.0	174.5	-13.5	—	—	—	do.
AK-544	7	73	75	10.8	185.0	183.8	-1.2	—	—	—	do.
AK-547	2	55	75	12.1	256.0	239.4	-16.6	—	—	—	do.
AK-582	7	73	74	10.8	184.3	182.0	-2.3	—	—	—	do.
AK-591	7	73	70	10.8	181.5	175.8	-5.7	—	—	—	do.
AK-600	5	73	74	11.6	184.5	181.0	-3.5	—	—	—	do.
AK-601	4	73	74	11.6	185.8	180.9	-4.9	—	—	—	do.
AK-623	2	70	69	14.6	144.6	155.7	11.1	—	—	—	do.
AK-643	7	56	83	12.0	219.0	215.6	-3.4	217.5	214.2	-3.3	do.
AK-681	2	59	61	14.3	212.0	203.9	-8.1	208.3	202.0	-6.3	do.
AK-748	5	35	96	14.1	294.3	293.6	-0.7	292.4	293.3	0.9	do.
AK-772	5	56	65	12.9	201.4	201.2	-0.2	199.1	192.1	-7.0	do.
AK-773	4	56	65	12.9	202.2	208.1	5.9	199.4	202.8	3.4	do.
AK-785	2	65	69	12.4	158.2	161.5	3.3	158.1	160.3	2.2	do.
AK-812	2	55	68	14.6	223.8	223.6	-0.2	222.0	220.3	-1.7	do.
AK-814	2	60	66	13.6	203.2	205.5	2.3	202.1	202.8	0.7	do.
AK-817	7	35	69	12.8	238.3	248.5	10.3	236.3	247.8	11.5	do.
AK-818	6	35	69	12.8	240.7	248.5	7.8	238.3	247.8	9.5	do.
AK-824	5	35	69	14.6	240.1	249.6	9.5	238.1	248.9	10.8	do.
AK-825	4	35	69	14.6	261.6	250.5	-11.1	239.9	249.8	9.9	do.
AK-833	5	23	92	13.1	320.0	344.0	24.0	320.0	342.1	22.1	do.
AK-845	6	36	100	14.8	273.0	267.6	-5.4	272.1	267.5	-4.6	do.
AK-847	5	36	100	14.7	271.8	261.3	-10.5	—	—	—	do.
AK-848	4	36	100	14.7	263.0	260.9	-2.1	262.6	260.8	-1.8	do.
AK-849	2	36	100	18.3	253.1	260.2	7.1	252.8	260.1	7.3	do.
AK-859	5	56	83	12.6	225.9	213.9	-12.0	221.7	213.0	-8.7	do.
AK-860	4	67	63	13.1	171.3	165.7	-5.6	168.6	163.0	-5.6	do.
AK-862	4	70	70	11.8	177.8	170.4	-7.4	175.0	165.4	-9.6	do.
AK-863	4	78	50	12.2	—	—	—	146.5	137.0	-9.5	not averaged

Appendix C. Measured heads, simulated predevelopment (prior to 1953) and modern-day (1987–92) heads, and error criteria in wells used for model calibration—Continued  
 [—, no data; do., ditto]

Well number or cell number <sup>1/</sup>	Model			Error criteria, in feet	Water-level altitudes, in feet						Wells used in averaging
					Predevelopment			Modern-day			
	Layer	Row	Column		Observed	Simulated	Difference	Observed	Simulated	Difference	
AK-864	6	70	70	10.8	177.5	174.4	-3.1	173.6	167.5	-6.1	do.
AK-865	7	67	63	11.5	173.0	166.3	-6.7	170.4	163.1	-7.3	do.
AK-866	6	58	69	12.3	203.2	197.4	-5.8	200.5	193.8	-6.7	do.
AK-870	4	56	83	12.6	220.9	213.9	-7.0	219.2	213.1	-6.1	do.
AK-871	6	56	83	12.0	223.5	215.4	-8.1	221.6	214.1	-7.5	do.
AK-872	7	78	50	11.4	165.6	154.0	-11.6	165.6	152.0	-13.6	do.
AK-873	6	78	50	11.4	165.1	154.0	-11.1	165.1	152.0	-13.1	do.
AK-874	5	78	50	12.2	155.8	151.9	-3.9	155.8	148.6	-7.2	do.
AK-878	7	70	70	10.8	177.3	175.2	-2.1	173.5	168.5	-5.0	do.
AK-880	5	70	71	11.5	177.3	172.9	-4.4	—	—	—	do.
AK-887	6	67	63	11.5	172.7	166.2	-6.5	170.4	163.1	-7.3	do.
AK-888	5	67	63	13.1	172.6	165.3	-7.3	170.4	162.5	-7.9	do.
AK-892	7	58	69	12.3	199.9	197.0	-2.9	192.2	193.4	1.2	do.
AK-893	5	58	69	13.1	208.9	204.3	-4.6	205.8	200.7	-5.1	do.
AK-901	6	71	70	10.8	184.0	174.8	-9.2	184.0	167.2	-16.8	do.
AK-902	7	48	55	13.1	172.5	163.2	-9.3	197.3	161.9	-35.4	do.
AK-905	6	5	90	16.8	391.4	383.1	-8.3	390.8	383.1	-7.7	do.
AK-906	4	44	68	14.1	231.8	231.9	0.1	231.7	230.9	-0.8	do.
AK-921	7	16	59	20.3	167.0	182.7	15.7	167.0	181.9	14.9	do.
AK-922	6	40	78	12.7	261.0	268.0	7.0	—	—	—	do.
AK-929	4	68	82	11.5	190.3	187.3	-3.0	188.2	185.7	-2.5	do.
AK-931	2	68	82	13.3	178.1	187.3	9.2	177.0	185.7	8.7	do.
AK-992	2	71	77	14.1	190.4	181.9	-8.5	179.3	178.6	-0.7	do.
AK-1202	2	72	73	15.4	169.8	176.0	6.2	167.9	171.7	3.8	do.
AK-1430	2	75	72	15.0	176.4	179.3	2.9	175.5	175.0	-0.5	do.
AK-1457	4	53	66	13.1	220.3	214.7	-5.6	218.8	211.3	-7.5	do.
AK-1458	2	53	65	14.2	230.4	219.8	-10.6	228.2	216.7	-11.5	do.
AK-1473	2	55	67	14.6	231.3	223.1	-8.2	224.0	218.5	-5.5	do.
AK-1483	2	56	68	15.2	220.2	220.3	0.1	218.6	217.0	-1.6	do.
AK-1485	4	56	67	13.0	202.3	211.9	9.6	198.1	207.8	9.7	do.
AK-1567	4	55	64	13.4	203.9	208.3	4.4	201.6	204.0	2.4	do.
AK-1584	4	56	66	13.0	206.7	210.0	3.3	204.4	205.2	0.8	do.
AK-1598	4	56	64	13.2	202.1	206.2	4.1	199.4	201.8	2.4	do.
AK-1638	2	60	67	14.2	205.6	206.3	0.7	204.0	203.6	-0.4	do.
AK-1655	4	58	65	12.9	195.0	202.9	7.9	192.8	198.9	6.1	do.
AK-1659	4	59	66	12.6	195.1	201.7	6.6	192.7	198.2	5.5	not averaged

Appendix C. Measured heads, simulated predevelopment (prior to 1953) and modern-day (1987–92) heads, and error criteria in wells used for model calibration—Continued  
 [—, no data; do., ditto]

Well number or cell number <sup>1/</sup>	Model			Error criteria, in feet	Water-level altitudes, in feet						Wells used in averaging
					Predevelopment			Modern-day			
	Layer	Row	Column		Observed	Simulated	Difference	Observed	Simulated	Difference	
AK-1672	4	60	65	12.7	190.0	196.0	6.0	186.8	192.8	6.0	do.
AK-1674	2	60	64	13.7	200.2	204.5	4.3	200.2	202.0	1.8	do.
AK-1675	2	61	65	13.6	200.7	201.4	0.7	198.6	198.9	0.3	do.
AK-1690	4	57	63	13.3	195.8	201.4	5.6	192.9	197.7	4.8	do.
AK-1765	5	58	63	13.3	192.6	190.1	-2.5	190.1	186.0	-4.1	do.
AK-1766	4	58	63	13.3	192.6	198.5	5.9	190.4	195.0	4.6	do.
AK-1783	4	58	64	13.0	193.2	200.6	7.4	191.2	196.8	5.6	do.
AK-1804	2	58	62	14.2	218.4	205.3	-13.1	216.5	202.6	-13.9	do.
AK-1809	4	59	63	13.0	197.9	195.2	-2.7	195.6	192.0	-3.6	do.
AK-1860	2	70	72	10.9	155.9	163.4	7.5	—	—	—	do.
AK-1960	2	67	65	15.0	160.7	155.1	-5.6	155.6	153.7	-1.9	do.
AK-2027	4	68	60	13.1	167.9	160.0	-7.9	166.5	157.7	-8.8	do.
AK-2028	2	68	60	13.5	158.8	162.7	3.9	155.8	160.4	4.6	do.
AK-2049	2	72	67	15.9	148.6	158.8	10.2	147.8	155.8	8.0	do.
AK-2222	2	73	69	13.5	158.7	168.7	10.0	158.2	165.0	6.8	do.
AK-2251	2	73	67	14.7	154.3	163.6	9.3	153.7	160.4	6.7	do.
AK-2263	2	74	64	17.6	150.8	157.1	6.3	—	—	—	do.
AK-2270	5	71	59	12.8	166.9	156.1	-10.8	165.1	153.7	-11.4	do.
AK-2352	2	78	49	14.3	95.9	83.1	-12.8	94.7	83.0	-11.7	do.
AK-2378	4	48	55	16.3	171.0	168.0	-3.0	184.2	167.0	-17.2	do.
AK-2379	5	48	55	16.3	170.8	166.8	-4.0	187.4	165.8	-21.6	do.
AK-2380	6	48	55	13.1	171.7	163.3	-8.4	192.9	161.9	-31.0	do.
AK-2382	7	7	94	19.7	370.0	366.9	-3.1	370.0	366.9	-3.1	do.
AK-2386	5	39	95	13.4	270.0	283.3	13.3	270.0	283.0	13.0	do.
AK-2389	5	32	63	14.0	202.0	218.3	16.3	202.0	217.8	15.8	do.
AK-2392	2	53	100	19.9	241.0	254.6	13.6	241.0	254.4	13.4	do.
AK-2393	2	47	99	15.0	270.0	267.6	-2.4	270.0	267.3	-2.7	do.
AK-2400	2	58	86	13.4	188.0	181.6	-6.4	—	—	—	do.
AK-2401	2	57	84	15.8	188.8	200.7	11.9	—	—	—	do.
AK-2429	4	71	55	12.8	159.5	143.8	-15.7	—	—	—	do.
AK-2430	4	71	50	10.8	95.0	93.0	-2.0	—	—	—	do.
AK-2437	5	79	56	11.5	165.0	159.5	-5.5	—	—	—	do.
AL-12	4	125	94	12.5	151.6	153.4	1.8	—	—	—	do.
AL-19	5	117	87	1.7	170.0	160.1	-9.9	—	—	—	do.
AL-24	4	125	95	10.9	156.5	153.6	-2.9	150.7	152.2	1.5	do.
AL-33	5	124	97	11.6	151.8	154.9	3.1	148.5	154.4	5.9	not averaged

Appendix C. Measured heads, simulated predevelopment (prior to 1953) and modern-day (1987–92) heads, and error criteria in wells used for model calibration—Continued  
 [—, no data; do., ditto]

Well number or cell number <sup>1/</sup>	Model			Error criteria, in feet	Water-level altitudes, in feet						Wells used in averaging
					Predevelopment			Modern-day			
	Layer	Row	Column		Observed	Simulated	Difference	Observed	Simulated	Difference	
AL-320	2	125	95	15.6	166.3	153.3	-12.9	—	—	—	do.
AL-329	2	108	75	12.0	124.4	146.6	22.2	—	—	—	do.
AL-344	2	107	70	12.1	135.0	141.0	6.0	—	—	—	do.
AL-345	4	109	71	10.8	163.7	160.0	-3.7	—	—	—	do.
AL-347	7	123	90	11.0	192.8	188.8	-3.9	191.7	188.5	-3.2	do.
AL-358	7	111	81	11.6	189.3	189.3	0.0	180.4	188.3	7.9	do.
AL-367	4	111	81	11.5	160.8	163.7	2.9	154.6	159.7	5.1	do.
AL-370	6	111	81	11.6	189.4	189.3	-0.1	182.5	188.3	5.8	do.
AL-377	6	123	90	11.0	192.5	188.8	-3.7	193.1	188.5	-4.6	do.
BW-41	2	82	101	13.0	231.6	233.4	1.8	—	—	—	do.
BW-42	2	81	101	13.1	234.9	234.9	0.0	—	—	—	do.
BW-44	6	68	100	11.6	242.0	237.3	-4.7	237.6	236.5	-1.1	do.
BW-45	2	101	98	13.0	—	—	—	205.9	175.9	-30.0	do.
BW-97	4	93	94	12.8	191.4	201.0	9.6	191.3	200.1	8.8	do.
BW-102	4	93	96	12.1	202.9	204.3	1.4	197.9	203.6	5.7	do.
BW-243	7	93	78	11.2	184.8	187.5	2.7	182.9	185.4	2.5	do.
BW-246	7	88	71	11.0	180.1	181.7	1.6	178.3	179.1	0.8	do.
BW-265	4	80	83	11.4	198.0	195.4	-2.6	—	—	—	do.
BW-274	7	73	76	11.6	184.8	185.5	0.7	—	—	—	do.
BW-279	5	79	71	11.4	189.0	180.0	-9.0	—	—	—	do.
BW-302	2	103	68	12.1	130.0	143.1	13.1	—	—	—	do.
BW-303	6	82	76	11.3	181.6	185.7	4.1	179.3	182.4	3.1	do.
BW-305	5	105	69	11.3	163.9	162.3	-1.6	—	—	—	do.
BW-308	7	71	83	12.1	192.2	196.9	4.7	188.7	193.6	4.9	do.
BW-312	7	72	95	12.5	217.4	217.8	0.4	215.4	216.5	1.1	do.
BW-314	7	100	87	11.4	194.8	193.4	-1.4	188.6	192.0	3.4	do.
BW-316	7	90	60	10.8	172.0	174.2	2.2	168.7	171.8	3.1	do.
BW-320	2	71	83	13.3	184.0	193.8	9.8	—	—	—	do.
BW-322	2	88	72	13.6	180.1	179.0	-1.1	177.8	176.4	-1.4	do.
BW-324	5	71	83	11.4	192.5	193.8	1.3	—	—	—	do.
BW-327	6	93	78	11.2	184.8	187.4	2.6	182.5	185.3	2.8	do.
BW-328	5	93	78	11.5	177.2	181.0	3.8	174.2	178.5	4.3	do.
BW-329	4	93	78	11.5	177.4	181.0	3.6	174.0	178.5	4.5	do.
BW-330	6	88	71	11.0	180.0	181.8	1.8	178.3	179.1	0.8	do.
BW-331	5	88	72	11.3	176.1	178.8	2.7	173.7	175.4	1.7	do.
BW-332	4	88	71	11.3	174.3	177.9	3.6	170.9	174.9	4.0	not averaged

Appendix C. Measured heads, simulated predevelopment (prior to 1953) and modern-day (1987–92) heads, and error criteria in wells used for model calibration—Continued  
 [—, no data; do., ditto]

Well number or cell number <sup>1/</sup>	Model			Error criteria, in feet	Water-level altitudes, in feet						Wells used in averaging
					Predevelopment			Modern-day			
	Layer	Row	Column		Observed	Simulated	Difference	Observed	Simulated	Difference	
BW-333	4	88	72	11.3	179.2	178.8	-0.4	176.6	175.5	-1.1	do.
BW-335	6	102	68	11.3	183.1	183.0	-0.1	180.7	181.3	0.6	do.
BW-349	7	111	99	14.4	198.8	199.5	0.7	195.4	199.3	3.9	do.
BW-353	4	111	99	12.1	188.5	169.9	-18.6	169.7	169.6	-0.1	do.
BW-355	5	111	99	12.1	170.9	171.1	0.2	169.8	170.7	0.9	do.
BW-356	6	111	99	14.4	196.5	199.5	3.0	192.6	199.3	6.7	do.
BW-358	7	84	98	11.6	214.7	213.6	-1.1	212.6	212.9	0.3	do.
BW-365	5	84	98	11.8	211.8	220.9	9.1	211.2	220.4	9.2	do.
BW-366	6	84	98	11.6	213.7	213.7	0.0	213.0	212.9	-0.1	do.
BW-368	4	84	98	11.8	210.2	220.9	10.7	209.9	220.4	10.5	do.
BW-370	6	74	76	11.5	181.3	185.4	4.1	178.8	179.6	0.8	do.
BW-372	4	82	76	11.4	181.1	186.4	5.3	178.3	183.4	5.1	do.
BW-374	4	72	95	12.0	217.7	228.0	10.3	215.7	227.3	11.6	do.
BW-375	4	80	85	11.4	191.2	197.8	6.6	189.2	195.8	6.6	do.
BW-376	4	102	68	11.5	168.8	165.0	-3.8	166.0	162.7	-3.3	do.
BW-378	4	88	80	11.5	182.9	187.0	4.1	177.6	184.3	6.7	do.
BW-380	4	74	76	11.4	182.5	185.2	2.7	179.4	180.8	1.4	do.
BW-382	6	72	95	12.5	217.8	217.9	0.1	215.8	216.6	0.8	do.
BW-383	6	100	87	11.4	190.3	193.3	3.0	188.1	191.9	3.8	do.
BW-384	6	90	60	10.8	171.4	174.2	2.8	168.0	171.8	3.8	do.
BW-385	6	89	80	11.3	185.7	189.2	3.5	183.6	186.8	3.2	do.
BW-386	4	99	97	12.1	197.0	190.8	-6.2	197.0	189.8	-7.2	do.
BW-389	5	72	95	12.0	216.6	228.1	11.6	214.6	227.4	12.8	do.
BW-391	7	77	67	11.1	174.6	173.4	-1.2	172.1	169.6	-2.5	do.
BW-395	2	82	76	10.9	272.2	191.1	-81.1	264.8	188.2	-76.6	do.
BW-398	2	80	85	14.1	196.9	198.8	1.9	195.1	196.9	1.8	do.
BW-402	5	102	68	11.5	168.8	165.0	-3.8	166.1	162.7	-3.4	do.
BW-403	3	102	68	12.9	136.6	151.1	14.5	134.9	149.9	15.0	do.
BW-404	2	102	68	12.6	135.8	144.3	8.6	133.9	143.7	9.8	do.
BW-407	3	100	87	11.8	155.8	173.3	17.5	154.0	172.8	18.8	do.
BW-408	2	100	87	11.0	155.1	172.3	17.2	153.2	171.9	18.7	do.
BW-413	4	90	60	11.4	166.0	165.1	-0.9	162.3	163.0	0.7	do.
BW-415	2	90	60	14.6	142.6	156.3	13.7	137.7	155.5	17.8	do.
BW-417	7	89	80	11.3	185.7	189.3	3.6	182.6	186.9	4.3	do.
BW-418	5	89	80	11.5	182.8	186.3	3.5	177.6	183.4	5.8	do.
BW-419	2	88	80	13.0	193.6	187.6	-6.0	191.4	185.2	-6.2	not averaged

Appendix C. Measured heads, simulated predevelopment (prior to 1953) and modern-day (1987–92) heads, and error criteria in wells used for model calibration—Continued  
 [—, no data; do., ditto]

Well number or cell number <sup>1/</sup>	Model			Error criteria, in feet	Water-level altitudes, in feet						Wells used in averaging
					Predevelopment			Modern-day			
	Layer	Row	Column		Observed	Simulated	Difference	Observed	Simulated	Difference	
BW-423	6	86	66	11.3	175.6	176.6	1.0	172.4	173.8	1.4	do.
BW-426	3	86	66	13.8	174.9	176.3	1.4	172.4	173.5	1.1	do.
BW-427	2	86	66	13.5	190.5	181.8	-8.7	178.3	179.9	1.6	do.
BW-430	7	74	76	11.5	181.0	185.4	4.4	177.3	179.2	1.9	do.
BW-433	2	74	76	14.5	181.5	185.5	4.0	179.6	181.2	1.6	do.
BW-438	6	77	67	11.1	174.2	173.4	-0.8	171.5	169.6	-1.9	do.
BW-440	4	91	94	12.6	192.9	204.0	11.1	192.9	203.1	10.2	do.
BW-456	3	91	94	12.6	213.6	204.8	-8.8	211.9	204.0	-7.9	do.
BW-459	3	92	94	11.9	203.7	203.2	-0.5	202.5	202.3	-0.2	do.
BW-464	4	86	66	11.4	171.9	175.8	3.9	168.5	172.9	4.4	do.
BW-538	2	73	83	11.2	191.0	195.8	4.8	190.9	193.6	2.7	do.
BW-590	2	78	73	16.4	188.5	183.3	-5.2	188.0	179.5	-8.5	do.
BW-604	2	80	73	18.5	187.3	184.1	-3.2	187.2	180.6	-6.6	do.
BW-674	2	89	72	13.6	178.6	178.4	-0.2	178.5	175.8	-2.7	do.
BW-676	4	89	72	11.3	172.8	178.1	5.3	—	—	—	do.
BW-693	2	89	71	13.6	176.4	177.8	1.4	176.4	175.4	-1.0	do.
BW-695	3	89	71	13.9	172.7	177.5	4.8	—	—	—	do.
BW-863	5	80	70	11.1	189.0	179.0	-10.0	—	—	—	do.
BW-871	2	98	61	13.9	121.0	127.7	6.7	—	—	—	do.
BW-877	2	103	61	13.0	120.4	126.5	6.1	—	—	—	do.
BW-882	4	85	54	11.9	158.1	159.3	1.2	—	—	—	do.
BW-885	2	100	57	12.8	108.2	109.3	1.1	—	—	—	do.
LA-8	6	67	62	11.5	180.0	164.2	-15.8	—	—	—	do.
M17-63-7	7	17	63	14.9	206.8	210.7	3.9	205.2	209.2	4.0	AK-440, AK-477
M20-29-7	7	20	29	15.7	129.8	141.4	11.6	—	—	—	29BB01,29BB59
M20-30-7	7	20	30	15.4	123.0	130.5	7.5	—	—	—	29BB07,29BB57
M22-44-7	7	22	44	12.4	116.3	119.9	3.6	—	—	—	30BB20,30BB21,30BB22
M23-43-7	7	23	43	12.4	119.7	118.2	-1.5	—	—	—	not averaged
M24-43-7	7	24	43	12.4	113.0	117.9	4.9	—	—	—	30BB12, 30BB15, 30BB16
M25-44-7	7	25	44	12.5	114.5	119.0	4.5	—	—	—	30BB05,30BB10
M25-45-7	7	25	45	12.5	111.3	122.5	11.2	—	—	—	30BB06,30BB07,30BB08
M26-25-7	7	26	25	14.4	152.1	161.1	9.0	149.3	157.0	7.7	29BB04,29BB19,29BB58
M28-30-7	7	28	30	13.2	129.0	127.6	-1.4	—	—	—	30BB32, 30BB33

Appendix C. Measured heads, simulated predevelopment (prior to 1953) and modern-day (1987–92) heads, and error criteria in wells used for model calibration—Continued  
 [—, no data; do., ditto]

Well number or cell number <sup>1/</sup>	Model			Error criteria, in feet	Water-level altitudes, in feet						Wells used in averaging
					Predevelopment			Modern-day			
	Layer	Row	Column		Observed	Simulated	Difference	Observed	Simulated	Difference	
M33-31-7	7	33	31	10.8	117.1	118.1	1.0	—	—	—	30AA07,30AA08
M34-30-7	7	34	30	12.9	121.3	123.4	2.1	73.0	113.3	40.3	30AA09, 30AA10
M36-100-5	5	36	100	14.7	—	—	—	270.9	261.2	-9.7	AK-846, AK-847
M53-66-2	2	53	66	13.9	225.4	220.8	-4.6	223.9	217.6	-6.3	AK-145, AK-1455, AK-1456
M54-6-4	4	54	67	12.9	222.6	214.8	-7.8	221.0	211.0	-10.0	AK-1453,AK-1468
M54-65-2	2	54	65	14.1	227.6	219.0	-8.6	224.8	215.1	-9.7	AK-1463,AK-1464, AK-1551,AK-1552, AK-1553
M54-65-4	4	54	65	13.0	215.2	211.7	-3.5	212.1	207.4	-4.7	AK-1549, AK-1466
M54-66-2	2	54	66	14.1	226.2	219.9	-6.3	223.5	215.4	-8.1	AK-153, AK-774, AK-1459, AK-1460, AK-1526, AK-1527, AK-1532,AK-1533, AK-1540,AK-1545, AK-1554, AK-1555
M54-66-4	4	54	66	13.0	217.9	212.8	-5.1	215.9	208.6	-7.3	AK-787,AK-1461, AK-1529, AK-1530, AK-1536
M54-67-2	2	54	67	14.4	224.0	222.3	-1.7	222.2	218.7	-3.5	AK-813, AK-1451, AK-1452, AK-1454, AK-1469, AK-1470, AK-1472
M55-64-2	2	55	64	14.6	234.5	215.9	-18.6	229.8	212.1	-17.7	AK-1566, AK-1568
M55-65-2	2	55	65	14.4	227.7	218.5	-9.2	224.1	213.5	-10.6	AK-1571,AK-1573, AK-1575, AK-1576
M55-65-4	4	55	65	13.1	222.9	210.3	-12.6	205.8	205.1	-0.7	AK-507,AK-1574, AK-1577,AK-1578
M55-66-2	2	55	66	14.4	224.4	221.5	-2.9	222.8	211.8	-11.0	AK-1475, AK-1477, AK-1479,AK-1542, AK-1543, AK-1546, AK-1561
M55-66-4	4	55	66	12.8	217.8	211.7	-6.1	215.4	206.9	-8.5	AK-1541,AK-1544, AK-1559, AK-1564
M56-60-2	2	56	60	15.0	215.5	216.2	0.7	213.1	214.9	1.8	AK-680,AK-2372
M56-63-2	2	56	63	16.0	223.6	211.8	-11.8	223.4	208.6	-14.8	AK-679, AK-1608, AK-1610,AK-2417
M56-63-4	4	56	63	13.2	212.3	203.7	-8.6	210.0	199.9	-10.1	AK-1606, AK-1607

Appendix C. Measured heads, simulated predevelopment (prior to 1953) and modern-day (1987–92) heads, and error criteria in wells used for model calibration—Continued  
 [—, no data; do., ditto]

Well number or cell number <sup>1/</sup>	Model			Error criteria, in feet	Water-level altitudes, in feet						Wells used in averaging
					Predevelopment			Modern-day			
	Layer	Row	Column		Observed	Simulated	Difference	Observed	Simulated	Difference	
M56-64-2	2	56	64	16.2	224.6	214.6	-10.0	222.1	210.9	-11.2	AK-677,AK-678, AK-1595,AK-1596, AK-1613,AK-1614, AK-1616
M56-65-2	2	56	65	15.2	222.1	218.9	-3.2	219.4	214.5	-4.9	AK-675,AK-745, AK-789,AK-1590, AK-1599,AK-1602, AK-1603, AK-1605
M56-66-2	2	56	66	14.7	225.6	221.5	-4.1	223.5	216.4	-7.1	AK-1491, AK-1492, AK-1581,AK-1582, AK-1583,AK-1585, AK-1586
M56-67-2	2	56	67	15.1	226.4	221.6	-4.8	218.9	217.7	-1.2	AK-1481,AK-1482, AK-1487
M56-83-2	2	56	83	17.1	215.1	214.3	-0.8	212.4	213.4	1.0	AK-868,AK-869
M57-6-22	2	57	62	15.4	219.6	208.4	-11.2	218.0	205.6	-12.4	AK-1777,AK-2291
M57-60-2	2	57	60	14.8	213.0	210.6	-2.4	208.0	209.0	1.0	AK-2296, AK-2297, AK-2298, AK-2300
M57-61-2	2	57	61	14.8	222.0	209.5	-12.5	214.0	207.4	-6.6	AK-2292, AK-2293
M57-63-2	2	57	63	16.1	223.5	209.8	-13.7	219.4	206.7	-12.7	AK-667, AK-668, AK-1691
M57-64-2	2	57	64	16.4	220.9	213.5	-7.4	216.9	210.1	-6.8	AK-655,AK-656, AK-657, AK-658, AK-659, AK-673, AK-1630,AK-1676, AK-1679, AK-1719, AK-1721,AK-1727, AK-1728
M57-65-2	2	57	65	17.2	219.3	217.1	-2.2	216.4	213.5	-2.9	AK-671,AK-1508, AK-1509,AK-1623, AK-1626,AK-1628, AK-1634,AK-1636, AK-1641
M57-65-4	4	57	65	12.9	198.3	205.6	7.3	195.2	201.0	5.8	AK-452,AK-534, AK-691,AK-1523, AK-1632
M57-66-2	2	57	66	16.5	220.2	218.1	-2.1	219.3	214.4	-4.9	AK-1500,AK-1503, AK-1504,AK-1510, AK-1521, AK-1522
M57-67-2	2	57	67	15.7	217.6	217.9	0.3	216.0	214.5	-1.5	AK-1495, AK-1497
M57-67-4	4	57	67	13.1	212.0	209.7	-2.3	209.9	205.8	-4.1	AK-1498,AK-1499

Appendix C. Measured heads, simulated predevelopment (prior to 1953) and modern-day (1987–92) heads, and error criteria in wells used for model calibration—Continued  
 [—, no data; do., ditto]

Well number or cell number <sup>1/</sup>	Model			Error criteria, in feet	Water-level altitudes, in feet						Wells used in averaging	
					Predevelopment			Modern-day				
	Layer	Row	Column		Observed	Simulated	Difference	Observed	Simulated	Difference		
M58-59-2	2	58	59	2	14.7	01.0	192.5	-8.5	195.5	190.9	-4.6	AK-2317,AK-2318, AK-2319,AK-2320, AK-2321,AK-2322
M58-60-2	2	58	60	14.8	211.1	202.7	-8.4	205.4	201.0	-4.4	AK-2303,AK-2310, AK-2311,AK-2315, AK-2316	
M58-63-2	2	58	63	14.7	218.8	206.9	-11.9	215.5	203.9	-11.6	AK-660,AK-661, AK-665,AK-1764, AK-1772,AK-1773, AK-1786, AK-1787, AK-1788, AK-1790, AK-1795, AK-1796	
M58-64-2	2	58	64	15.8	215.2	211.3	-3.9	211.5	208.2	-3.3	AK-662,AK-663, AK-664, AK-1735, AK-1736,AK-1745, AK-1748, AK-1749, AK-1750, AK-1752, AK-1753,AK-1757, AK-1761,AK-1762, AK-1767,AK-1769, AK-1774,AK-1776, AK-1779,AK-1780, AK-1782, AK-1793, AK-1794	
M58-65-2	2	58	65	17.0	214.3	213.3	-1.0	212.0	210.1	-1.9	AK-1651, AK-1653, AK-1654	
M58-66-2	2	58	66	17.5	215.2	214.1	-1.1	214.0	210.9	-3.1	AK-669, AK-670,	
M58-69-2	2	58	69	15.7	211.0	215.4	4.4	209.3	212.7	3.4	AK-895, AK-896	
M58-69-4	4	58	69	13.1	209.0	210.0	1.0	206.1	206.9	0.8	AK-861, AK-894	
M59-63-2	2	59	63	13.9	215.8	204.1	-11.7	210.0	201.4	-8.6	AK-666,AK-1811, AK-1802,AK-1800, AK-1805, AK-816	
M59-64-2	2	59	64	13.8	208.9	208.5	-0.4	206.9	205.7	-1.2	AK-1807,AK-1808	
M59-65-2	2	59	65	14.3	209.9	209.4	-0.5	208.4	206.5	-1.9	AK-1664, AK-1665	
M59-66-2	2	59	66	15.4	211.1	210.1	-1.0	208.2	207.2	-1.0	AK-1656,AK-1657, AK-1660,AK-1661, AK-1662	
M60-62-2	2	60	62	14.1	202.0	200.2	-1.8	195.4	198.0	2.6	AK-1826, AK-1819	
M60-65-2	2	60	65	13.6	204.9	205.6	0.7	203.5	202.9	-0.6	AK-1668, AK-1669, AK-1670	
M61-63-2	2	61	63	13.6	196.0	199.3	3.3	193.3	197.0	3.7	AK-1817, AK-1824, AK-1835	
M66-33-5	5	66	33	12.8	157.2	149.2	-8.0	157.2	148.3	-8.9	30Z025,30Z026	

Appendix C. Measured heads, simulated predevelopment (prior to 1953) and modern-day (1987–92) heads, and error criteria in wells used for model calibration—Continued  
 [—, no data; do., ditto]

Well number or cell number <sup>1/</sup>	Model			Error criteria, in feet	Water-level altitudes, in feet						Wells used in averaging
					Predevelopment			Modern-day			
	Layer	Row	Column		Observed	Simulated	Difference	Observed	Simulated	Difference	
M66-33-7	7	66	33	11.4	158.2	150.7	-7.5	158.1	149.8	-8.3	30Z017, 30Z021
M67-62-2	2	67	62	14.0	169.5	168.1	-1.4	—	—	—	AK-441, AK-743
M67-63-2	2	67	63	12.9	169.8	167.0	-2.8	166.2	164.6	-1.6	AK-889, AK-890
M67-64-2	2	67	64	13.6	164.9	164.1	-0.8	161.6	162.2	0.6	AK-1951, AK-1952, AK-1953, AK-1955, AK-1956, AK-1958, AK-1959, AK-1961, AK-1957, AK-1963, AK-1965, AK-1966, AK-1967
M68-64-2	2	68	64	15.6	152.0	159.2	7.2	149.8	157.4	7.6	AK-1972, AK-1976, AK-1977, AK-1978, AK-1979, AK-1981, AK-1982, AK-1984, AK-1985, AK-1987, AK-1988, AK-1990, AK-1991, AK-1992, AK-1996, AK-2001, AK-2002, AK-2006, AK-2010, AK-2011, AK-2012
M68-65-2	2	68	65	15.7	150.1	148.7	-1.4	146.3	147.4	1.1	AK-1964, AK-1968, AK-1969, AK-1970, AK-1971, AK-1973, AK-1974, AK-1975, AK-1980, AK-1983, AK-1986, AK-1989, AK-1993, AK-1994, AK-1995, AK-1998, AK-1999, AK-2003, AK-2004, AK-2005, AK-2007
M69-65-2	2	69	65	15.6	142.7	140.6	-2.1	141.8	139.5	-2.3	AK-2040, AK-2014, AK-2009, AK-2008, AK-2013
M69-76-2	2	69	76	16.6	163.5	167.4	3.9	162.3	165.2	2.9	AK-939, AK-942
M70-72-2	2	70	72	10.9	—	—	—	184.6	160.2	-24.4	AK-1144, AK-1860
M70-70-2	2	70	70	12.3	147.5	159.4	11.9	146.5	156.3	9.8	AK-881, AK-882, AK-883
M70-71-5	5	70	71	11.5	—	—	—	174.7	167.6	-7.1	AK-879, AK-880, AK-898
M71-59-2	2	71	59	14.0	141.7	149.3	7.6	138.0	147.8	9.8	AK-2269, AK-2271

Appendix C. Measured heads, simulated predevelopment (prior to 1953) and modern-day (1987–92) heads, and error criteria in wells used for model calibration—Continued  
 [—, no data; do., ditto]

Well number or cell number <sup>1/</sup>	Model			Error criteria, in feet	Water-level altitudes, in feet						Wells used in averaging
					Predevelopment			Modern-day			
	Layer	Row	Column		Observed	Simulated	Difference	Observed	Simulated	Difference	
M71-71-2	2	71	71	12.8	162.6	166.5	3.9	161.0	162.8	1.8	AAK-1197,K-1879, AK-1882, AK-1895, AK-1896,AK-1909, AK-1915,AK-1917, AK-1921, AK-1929
M71-72-2	2	71	72	13.9	164.3	168.9	4.6	161.0	165.2	4.2	AK-1148, AK-1158, AK-1168,AK-1171, AK-1178,AK-1179, AK-1193
M71-83-5	5	71	83	11.4	—	—	—	189.5	191.9	2.4	BW-324, BW-325
M72-68-2	2	72	68	14.8	153.3	162.1	8.8	150.9	158.9	8.0	AK-2155, AK-2164, AK-2171,AK-2180, AK-2182, AK-2191, AK-2208
M72-69-2	2	72	69	14.1	155.4	165.0	9.6	153.6	161.5	7.9	AK-2140,AK-2143, AK-2146
M72-70-2	2	72	70	13.9	160.8	167.7	6.9	160.1	164.0	3.9	AK-2108, AK-2129, AK-2073
M72-71-2	2	72	71	14.1	164.2	170.5	6.3	164.2	166.5	2.3	AK-2123, AK-1305
M72-95-2	2	72	95	13.1	230.3	228.9	-1.4	228.0	228.2	0.2	BW-387, BW-388
M73-68-2	2	73	68	13.4	157.4	166.3	8.9	154.6	162.8	8.2	AK-2220,AK-2226, AK-2227,AK-2247, AK-2249
M73-71-2	2	73	71	13.9	168.2	174.0	5.8	177.5	169.7	-7.8	AK-1339, AK-1361, AK-1364,AK-1392
M73-72-2	2	73	72	14.5	170.7	176.5	5.8	168.7	172.0	3.3	AK-1319, AK-1325, AK-1343
M73-73-2	2	73	73	14.5	178.2	178.7	0.5	176.0	174.1	-1.9	AK-1298, AK-1316, AK-1308,AK-1327
M73-82-2	2	73	82	13.0	190.0	194.1	4.1	189.9	191.7	1.8	BW-793,BW-796
M74-72-2	2	74	72	14.1	173.1	178.3	5.2	171.1	173.8	2.7	AK-1402, AK-1395, AK-1397,AK-1410, AK-1413
M74-73-2	2	74	73	15.0	175.4	180.2	4.8	175.1	175.6	0.5	AK-1444,AK-1448
M74-76-5	5	74	76	11.4	182.2	185.1	2.9	179.4	180.6	1.2	BW-431, BW-432
M77-67-2	2	77	67	13.2	171.0	172.4	1.4	168.7	168.7	0.0	BW-313, BW-436
M77-67-5	5	77	67	11.4	175.2	172.4	-2.8	171.2	168.5	-2.7	BW-371,BW-437
M78-38-2	2	78	38	15.1	135.4	117.8	-17.6	134.7	117.2	-17.5	31Z030, 31Z037

Appendix C. Measured heads, simulated predevelopment (prior to 1953) and modern-day (1987–92) heads, and error criteria in wells used for model calibration—Continued  
 [—, no data; do., ditto]

Well number or cell number <sup>1/</sup>	Model			Error criteria, in feet	Water-level altitudes, in feet						Wells used in averaging
					Predevelopment			Modern-day			
	Layer	Row	Column		Observed	Simulated	Difference	Observed	Simulated	Difference	
M78-50-2	2	78	50	14.3	89.9	83.2	-6.7	93.5	85.7	-7.8	AK-875,AK-876, AK-2336,AK-2340, AK-2341,AK-2344, AK-2350,AK-2353, AK-2354
M78-50-4	4	78	50	12.2	155.3	139.1	-16.2	—	—	—	AK-529,AK-863
M78-51-2	2	78	51	14.6	117.2	85.8	-31.4	—	—	—	AK-875, AK-876
M78-55-2	2	78	55	16.3	146.3	153.5	7.2	—	—	—	AK-2424, AK-2425, AK-2438
M78-67-5	5	78	67	11.4	165.8	173.6	7.8	—	—	—	BW-247, BW-248
M79-50-2	2	79	50	14.0	86.0	83.1	-2.9	84.5	83.1	-1.4	AK-2356, AK-2359
M81-52-7	7	81	52	11.4	166.9	160.0	-6.9	—	—	—	BW-813, BW814
M82-76-5	5	82	76	11.4	181.1	186.3	5.2	178.6	183.3	4.7	BW-392, BW-393
M84-98-2	2	84	98	11.9	218.0	225.2	7.2	217.0	224.8	7.8	BW-359, BW-367
M86-66-5	5	86	66	11.4	173.3	175.4	2.1	168.5	172.4	3.9	BW-424,BW-425
M89-71-4	4	89	71	11.3	170.1	177.1	7.0	—	—	—	BW-692,BW-694, BW-696
M90-43-2	2	90	43	15.3	111.8	127.6	15.8	—	—	—	31Z021,31Z074
M90-44-2	2	90	44	15.3	109.1	120.2	11.1	106.5	118.8	12.3	31Z071,31Z077
M90-60-5	5	90	60	11.4	167.9	166.0	-1.9	164.4	163.7	-0.7	BW-377,BW-412
M90-71-2	2	90	71	13.6	175.4	176.6	1.2	—	—	—	BW-699,BW-700
M91-39-2	2	91	39	12.1	141.0	150.3	9.3	—	—	—	31Z09, 31Z109
M91-94-2	2	91	94	12.3	216.7	205.4	-11.3	214.5	204.6	-9.9	BW-454,BW-455
M92-94-2	2	92	94	11.6	201.0	203.8	2.8	200.3	203.0	2.7	BW-443, BW-458
M93-45-2	2	93	45	14.4	108.9	116.1	7.2	103.3	115.2	11.9	31Z076,32Z003
M93-78-2	2	93	78	12.8	176.3	181.0	4.7	174.2	179.3	5.1	BW-321,BW-323
M94-94-2	2	94	94	11.1	202.4	200.4	-2.0	202.2	199.7	-2.5	BW-450,BW-451
M100-87-5	5	100	87	11.7	177.6	181.8	4.2	175.2	179.7	4.5	BW-373,BW-406
M101-98-2	2	101	98	13.0	195.0	180.0	-15.0	—	—	—	BW-22, BW-45
M102-99-2	2	102	99	13.8	201.9	189.6	-12.3	—	—	—	BW-67, BW-3,BW-2
M111-99-2	2	111	99	14.6	163.9	166.6	2.7	165.3	166.5	1.2	BW-352,BW-354
M111-81-2	2	111	81	12.8	154.4	146.1	-8.3	124.2	145.9	21.7	AL-365, AL-366
M111-81-5	5	111	81	11.5	161.1	163.7	2.6	153.4	159.7	6.3	AL-368, AL-369
M123-90-2	2	123	90	13.6	135.2	144.8	9.6	136.1	144.5	8.4	AL-374, AL-375
M125-95-5	5	125	95	10.9	168.0	153.6	-14.4	—	—	—	AL-2, AL-605

<sup>1/</sup>Cell number—cells containing multiple wells are designated with the prefix “M,” followed by row, column, and model layer number.